Table des matières

Liste des figures

Liste des abbrévations

5-HIAA	Acide 5-hydroxyindolacétique
5-HT	Sérotonine
6-OHDA	6-hydroxydopamine
AADC	Acide L-aminé décarboxylase
ACh	Acétylcholine
AMPc	Adénosine monophosphate cyclique
ATV	Aire tegmentaire ventrale
BDNF	Facteur neurotrophique issu du cerveau
CLHP	Chromatographie en phase liquide à haute performance
CM	Noyaux centromédian du thalamus
COMT	Cathécol-O-méthyltransférase
D_1	Récepteur dopaminergique type 1
D_2	Récepteur dopaminergique type 2
DA	Dopamine
DAT	Transporteur de la dopamine
DIL	Dyskinésie induite par la L-DOPA
GABA	Acide γ -aminobutyrique
GP	Globus pallidus
GPe	Globus pallidus externe
GPi	Globus pallidus interne
ICh	Interneurone cholinergique
LCR	Liquide céphalo-rachidien
L-DOPA	3,4-dihydroxyphénylalanine
MDMA	3,4-méthylènedioxy-N-méthylamphétamine
MPTP	1-méthyl-4-phényl-1,2,3,6-tétrahydropyridine
NPS	Neurone de projection du striatum
NRD	Noyau Raphé dorsal
NRM	Noyau Raphé médian

NST	Noyau subthalamique
Pf	Noyaux parafasciculaires du thalamus
SERT	Transporteur de la sérotonine
SNc	Substantia nigra *pars compacta*
SNr	Substantia nigra *pars reticulata*
TEP	Tomographie par émission de positrons
VGLUT1	Transporteur vésiculaire du glutamate de type 1
VGLUT2	Transporteur vésiculaire du glutamate de type 2
VGLUT3	Transporteur vésiculaire du glutamate de type 3

Remerciements

Cette thèse est l'aboutissement de plusieurs années de travail acharné. Ce doctorat fut une épopée d'introspection remplie d'embuches. Ce chemin m'a permis de grandir comme personne ainsi que comme scientifique. J'ai découvert une ténacité insoupçonnée et une curiosité sans borne.

Je voudrais profiter de ces quelques lignes pour remercier toutes les personnes qui sans leur aide auraient rendu ce projet impossible. Tout d'abord, mon superviseur Martin merci de m'avoir accueilli dans ton laboratoire. Ta patience et tes conseils m'ont permis de faire de moi une meilleure personne et d'affuter mon esprit scientifique à un niveau que je n'avais même pas cru possible. Je voudrais aussi remercier son père André Parent pour les conversations instructives et les conseils. Votre rôle de mentor m'a permis d'apprendre énormément sur le domaine des neurosciences et surtout sur son histoire.

Ensuite, je voudrais remercier tous les étudiants présents et passés et personnel de soutien du laboratoire ainsi tous mes amis du centre de recherche. Merci de vos encouragements et de nos conservations complètement farfelues sans lesquels j'aurais sans doute perdu une partie de ma santé mentale dans les passages à vide de mes projets. Merci plus particulièrement à Marie-Josée de m'avoir ramassé les nombreuses fois où mon esprit s'égarait pendant mes expériences.

Je voudrais aussi remercier mes parents de toujours m'avoir encouragé dans mes projets académiques et de toujours m'appuyer quand j'en ai le plus besoin, vous êtes mes fondations qui me permettent encore à ce jour de me tenir debout.

Merci à ma merveilleuse femme, Carolane, de m'avoir accompagné tout au long de ce parcours. Ton soutien dans les moments heureux comme dans les

plus difficiles m’a permis de surmonter les nombreux obstacles de ce parcours. Merci de partager ma vie, merci d’être aussi parfaite et compréhensive. Merci à mes deux merveilleux enfants qui sont nés pendant ma formation de doctorat. Vous êtes la lumière qui ensoleille mes journées, la vie serait tout simplement plus sombre sans vous.

Avant-propos

Les travaux présentés dans cette thèse jettent un éclairage nouveau sur notre connaissance de la microcircuiterie des ganglions de la base ainsi que sur la réorganisation de celle-ci dans la maladie de Parkinson. Mes résultats auront permis d'identifier de nouveaux phénomènes compensatoires reliés aux axones dopaminergiques et sérotoninergiques dans la maladie de Parkinson ajoutant ainsi à la complexité de sa physiopathologie. Ma contribution permettra de mieux comprendre cette maladie neurodégénérative ainsi que le développement de symptômes moteurs et non-moteurs reliés à celle-ci.

Les études présentées dans cette thèse de doctorat ont toutes fait l'objet d'articles originaux publiés ou soumis dans des revues scientifiques renommées. Chacune de ces publications a été révisée scrupuleusement par un comité de lecture afin de s'assurer de leur valeur scientifique. Je suis premier auteur sur 4 des 5 articles qui vous seront présentés dans cette thèse, j'ai donc réalisé la majeure partie des travaux scientifiques, l'analyse des résultats et de rédaction pour chacun de ses projets. Il est important de mentionner que mon directeur de recherche, le Dr Martin Parent, a joué un rôle essentiel dans l'élaboration des projets de recherche et dans les conseils qu'il m'a fournis pour chaque étape ainsi que dans la révision des manuscrits des études publiées.

En premier lieu, cette thèse s'ouvrira sur une introduction générale vous permettant d'apprécier l'état des connaissances actuelles sur les ganglions de la base, le système sérotoninergique et la maladie de Parkinson.

Le deuxième chapitre de cette thèse contient un article publié dans *European Journal of Neuroscience* où je suis deuxième auteur. Les expériences que j'ai réalisées dans le cadre de ce projet se sont montrées essentielles afin de pouvoir répondre aux questions du comité de révision dans le but de publier cet article.

Le troisième chapitre est constitué d'un article publié dans *PlosOne* dans lequel je suis premier auteur. J'ai effectué toutes les expérimentations, fait l'analyse de résultats ainsi que l'écriture de l'article.

Le chapitre 4 de la thèse présente un article publié dans *Brain Structure and Function* où je suis premier auteur. Dans cet article, j'ai aussi effectué toutes les expérimentations ainsi que l'analyse des résultats et la rédaction du manuscrit.

Le chapitre 5 de la thèse consiste à un article présentement sous-presse dans le journal *Frontiers in Neuroanatomy.* Dans le cadre de ce projet, j'ai effectué la majorité des expérimentations, l'analyse des résultats et l'écriture de l'article. Il est important de mentionner le travail important de mes coauteurs dans ce projet : Lara Eid, Carl Whissel et Dymka Coudé. Sans leur aide précieuse, ce projet n'aurait certainement pas eu la même ampleur.

Le chapitre 6 présente un article publié dans *Scientific Report* pour lequel mon nom figure comme premier auteur. J'ai fait la quasi-totalité des expériences et toute l'analyse des résultats pour cet article ainsi que la rédaction du manuscrit.

CHAPITRE 1 :

INTRODUCTION GÉNÉRALE

CHAPITRE 1 – INTRODUCTION GÉNÉRALE

1.1. Préambule

Pendant les nombreuses années que j'ai passées au centre de recherche de l'Institut en santé mentale de Québec (CR-IUSMQ), maintenant CERVO, j'ai pu étudier les ganglions de la base sous plusieurs aspects. J'ai porté une attention particulière à la complexité avec laquelle des neuromodulateurs comme la dopamine (DA) et sérotonine (5-HT) interagissent avec cet ensemble de structures. Le dérèglement d'une seule de ces composantes libérant de la DA, est en mesure de complètement déséquilibrer les fonctions normales des ganglions de la base et ainsi causer des symptômes moteurs importants et handicapants. Ce genre de dysfonctions amène une multitude de changements morphologiques chez pratiquement tous les acteurs importants du contrôle moteur. Les travaux présentés dans cette thèse visent à décrire, à l'aide de techniques neuroanatomiques de pointes, ces changements morphologiques en contexte pathologique ainsi que l'interaction de ces composantes des ganglions de la base avec leur environnement en condition normale. La quantification et la caractérisation de la morphologie dans ces deux contextes sont primordiales à la compréhension du fonctionnement des ganglions de la base en condition normale et pathologique.

L'histoire de la neuroscience a été marquée par une multitude de grands neuroanatomistes. Le plus célèbre d'entre eux fut sans doute Camillo Golgi (1843 – 1926) qui mit au point une technique d'imprégnation des tissus nerveux avec des sels d'argent. Cette technique qui porte actuellement son nom (méthode de Golgi) fut pendant des années l'étalon-or pour l'étude du tissu nerveux. Elle permit pour la toute première fois aux neuroscientifiques de visualiser des neurones ainsi que leur domaine somatodendritique complet. Les descriptions effectuées à cette époque furent d'une précision exceptionnelle décrivant même pour la toute première fois les axones. Les travaux les plus remarquables réalisés à l'aide de la méthode de Golgi furent sans doute ceux

réalisés par le célèbre Santiago Ramón y Cajal (1852 – 1934) avec la publication de *Histologie du système nerveux de l'homme et des vertébrés* (1909 – 1911), une œuvre en deux volumes qui s'attarde à la morphologie d'une grande partie des neurones composants le système nerveux central. L'utilisation de l'imprégnation à l'argent fut très répandue jusqu'au milieu du 20e siècle, alors que l'on découvrait l'existence de traceurs axonaux antérogrades et rétrogrades. Ces traceurs permirent pour la première fois d'étudier les projections axonales de populations neuronales spécifiques. Cette période de l'histoire fut aussi marquée par l'émergence d'autres techniques de visualisation de tissus nerveux, par exemple, l'immunohistochimie. Le principe de cette technique existait depuis les années 30, mais ce ne fut pas avant 1941 que le premier article sur le sujet fut publié (Coons *et al.*, 1941). L'arrivée de l'immunohistochimie révolutionnera littéralement la neuroanatomie permettant de marquer spécifiquement certains éléments neuronaux, d'après leur contenu en diverse molécules reliées à la transmission nerveuse. Le ciblage d'antigènes permis, pour la toute première fois, d'avoir une idée générale de la distribution régionale de plusieurs innervations chimiospécifiques. Les publications de l'époque réalisées avec cette approche méthodologique contenaient généralement des évaluations qualitatives de l'innervation dans différentes structures. Le besoin d'une approche quantitative précise s'est rapidement fait sentir, ce à quoi l'arrivée de la stéréologie répondit. Le principe de la stéréologie tel que l'on le connait aujourd'hui fut publié dans les années 80 (Gundersen, 1986; Gundersen *et al.*, 1988). Cette technique d'échantillonnage permit d'évaluer pour la première fois la quantité d'un objet donné dans une structure donnée. Le développement d'autres sondes stéréologiques a permis, ultérieurement, de quantifier d'autres aspects neuromorphologiques comme la longueur d'axones avec une sonde appelée *spaceballs* (Mouton et al., 2002).

Les travaux présentés dans le cadre de cette thèse de doctorat sont une suite logique des travaux de neuroanatomistes qui m'ont précédés. Le raffinement des techniques d'injection de traceur antérograde, de marquage

somatodendritique fluorescent, d'immunohistochimie et de stéréologie m'ont permis de quantifier et de documenter avec une précision inédite l'interaction de l'innervation 5-HT avec son milieu ainsi que sa capacité à s'adapter à une insulte neurodégénérative majeure. Les résultats générés par ces travaux permettront de mieux comprendre le fonctionnement des ganglions de la base et les phénomènes de plasticité qui se produisent dans un contexte parkinsonien.

1.1.1. Présentation des chapitres

La première partie de mon doctorat fut consacrée à l'étude des projections axonales provenant du noyau raphé dorsal. Ces données ont fait l'objet de deux articles publiés et qui correspondent aux chapitres 2 et 3 de cette thèse. Cette population de neurones du tronc cérébral est composée majoritairement de neurones 5-HT qui innervent majoritairement le prosencéphale. Le chapitre 2 traitera d'une étude immuhistochimique du système 5-HT réalisée sur du tissu *post-mortem* humain en condition normale. Ces données ont permis de cartographier et de tracer les principales voies qu'empruntent les axones 5-HT ainsi que de décrire leur innervation dans les différentes composantes des ganglions de la base. Au chapitre 3, il sera question de l'étude, au niveau neuronal unitaire, des axones provenant du noyau raphé dorsal chez le rat. Ces données ont été obtenues par l'injection de traceurs antérogrades permettant ainsi la reconstruction entière et unitaire d'arborisations axonales. Ces injections ont mis en évidence la grande hétérogénéité des projections 5-HT ascendantes, permis de caractériser le contenu neurochimique de ces axones et d'aborder le phénomène de co-transmission 5-HT et glutamate.

Le troisième volet de cette thèse sera composé de deux articles publiés traitant de l'innervation DA et 5-HT du striatum et du globus pallidus (GP), deux composantes majeures des ganglions de la base. Une combinaison d'approches immunohistochimiques et stéréologiques ainsi que l'utilisation de la microscopie électronique ont permis de dresser un portrait de l'innervation DA

et 5-HT avec une précision inédite dans ces deux structures, dans un contexte normal et parkinsonien. Ces 2 études nous permettent de constater que les systèmes DA et 5-HT sont très plastiques dans le GP et le striatum après une lésion DA de la substance noire *pars compacta* (SNc). Ces changements se traduisent principalement par des augmentations importantes de la densité des varicosités (terminaisons) axonales et des axones visant probablement à compenser pour le déficit DA. Ces deux articles feront l'objet des chapitres 4 et 5 de cette thèse.

Finalement, le troisième volet de ma thèse de doctorat qui sera présenté dans le chapitre 6 contient une étude anatomique de neurones de projection du striatum (NPS). Ces travaux ont été réalisés à l'aide d'injections intracellulaires sur tranches fixées, une approche qui présente plusieurs avantages comparativement à la technique de Golgi entre autres d'analyser le domaine somatodendritique des neurones ainsi leur contenu neurochimique. En combinaison avec un modèle transgénique de souris, il est possible, contrairement à l'imprégnation à l'argent, de sélectionner spécifiquement la population neuronale à étudier. Cette technique d'injection nous a donc permis d'élucider, de manière distincte, la morphologie des différents sous-types de NPS ainsi que les changements neuroadaptatifs qu'ils présentent suite à une dénervation DA, grâce à l'utilisation d'un modèle murin de la maladie de Parkinson.

1.2. Les ganglions de la base

1.2.1. Historique

La première description des structures sous-corticales qui forment aujourd'hui les ganglions de la base fut effectuée par Thomas Willis (1621 – 1675) dans son œuvre *Cerebri Anatome*. Alors appelés *corpus striatum*, les ganglions de la base étaient considérés comme le centre de toutes les modalités sensorielles. Ce rôle prépondérant dans la hiérarchie fonctionnelle du système nerveux fut

longtemps maintenu, jusqu'à être détrôné par le cortex cérébral au cours du 18e et 19e siècle. Le désintérêt pour les ganglions de la base se termina à la fin du 19e siècle et début du 20e siècle, alors que des descriptions plus étoffées furent apportées (Luys, 1865; Meynert, 1872; Dejerine & Dejerine-Klumpke, 1895; Cajal, 1909, 1911; Wilson, 1914; Vogt & Vogt, 1920; Foix & Nicolesco, 1925). À ce moment, l'arrivée de nouvelles techniques en neuroanatomie aura permis de décrire, dans toute sa complexité, l'organisation de ces structures sous-corticales. L'implication des ganglions de la base dans le contrôle du mouvement fut aussi mise en lumière au début du 20e siècle (Vogt, 1911; Wilson, 1912; Vogt & Vogt, 1919; 1920). Ces différents chercheurs furent donc les premiers à établir un lien entre une lésion survenant au sein de ce regroupement de structures sous-corticales et différents troubles du mouvement. Plus tard, la popularisation des techniques d'imprégnation à l'argent permit à des scientifiques comme (Nauta & Mehler, 1966) d'établir les principales connexions entre les différentes composantes des ganglions de la base. L'arrivée des traceurs neuronaux, quelques décennies plus tard, a permis à la communauté scientifique de présenter un modèle de l'organisation anatomique et fonctionnelle des ganglions de la base qui vous sera présenté en détails plus loin.

1.2.2. Organisation anatomique

Les ganglions de la base sont principalement composés du striatum (noyau caudé et putamen) et du globus pallidus (GP) aussi divisé en segment interne (GPi) et segment externe (GPe). Ensemble, le striatum et le GP forment le noyau lenticulaire. Pour certains auteurs, les ganglions de la base englobent également le noyau subthalamique (NST) ainsi que la substance noire qui se divise également en *pars compacta* (SNc) et en *pars reticulata* (SNr)(Penney & Young, 1983; Alexander *et al.*, 1986; Albin *et al.*, 1989; Parent & Hazrati, 1995b).

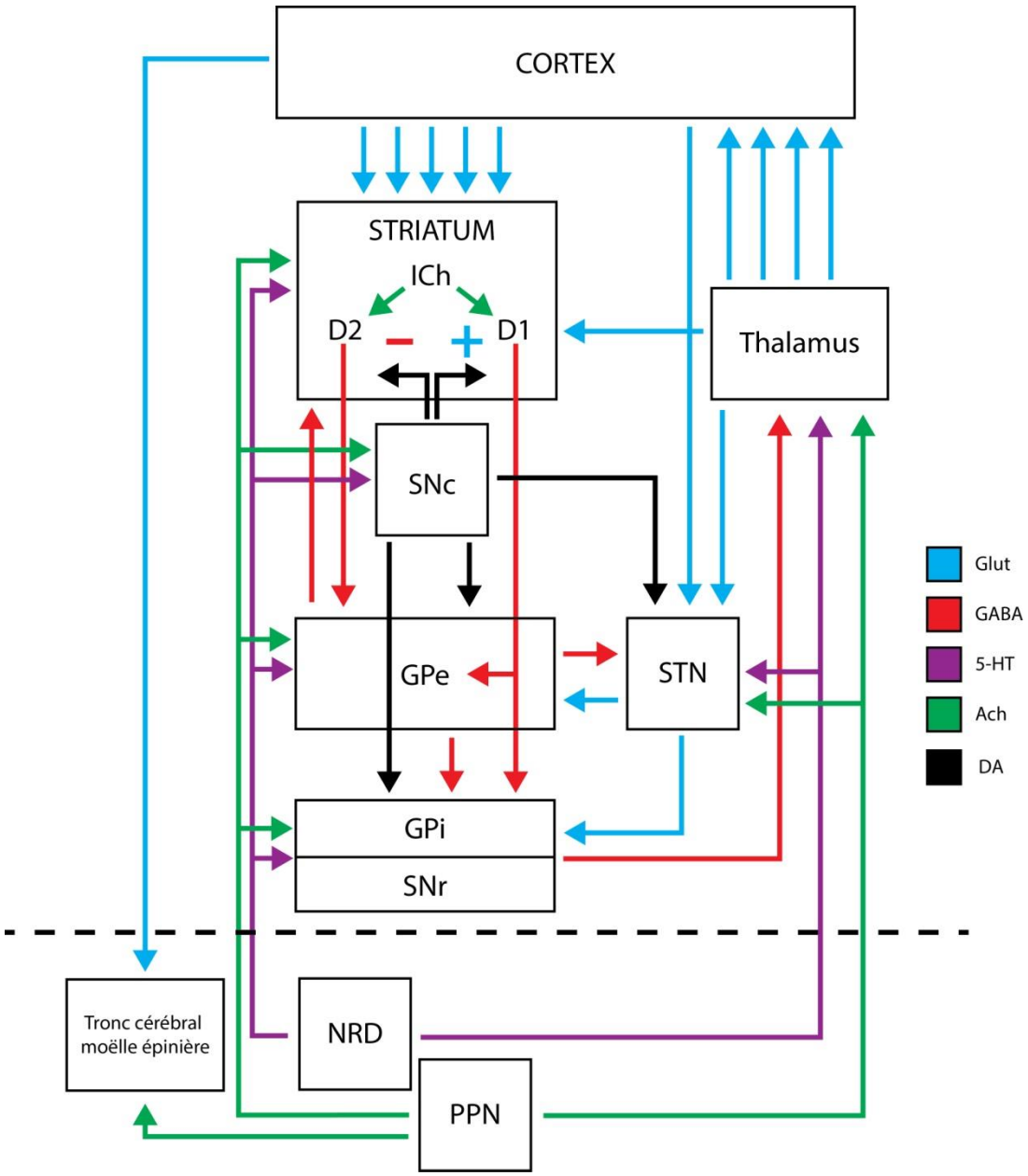

FIGURE 1.1. – Représentation graphique de la circuiterie des ganglions de la base.

1.2.3. Le striatum

Le striatum est la principale structure intégratrice des ganglions de la base. Il est composé, chez le primate, du putamen et du noyau caudé. Le putamen est délimité par la capsule externe à l'extrémité latérale, le corps calleux à l'extrémité dorsale et la capsule interne l'extrémité médiale. Le noyau caudé a

une forme tridimensionnelle complexe et borde le ventricule latéral. Le striatum est facilement reconnaissable par les nombreuses stries de substance blanche qui le traversent, ce qui lui a d'ailleurs valu son nom. Il joue un rôle crucial dans le fonctionnement des ganglions de la base étant considéré comme la principale porte d'entrée de l'information neuronale en provenance de l'ensemble du cortex cérébral ainsi que du principal site d'intégration de l'information provenant d'afférences hétérogènes et variées. Ces informations sont par la suite redistribuées de manière structurée via des efférences striatales GABAergiques projetant vers d'autres composantes des ganglions de la base.

Afférences

Extrinsèques

Considéré comme la principale porte d'entrée des ganglions de la base, le striatum reçoit des signaux provenant de sources multiples et hétérogènes. Il reçoit des innervations glutamatergiques provenant de la plupart des aires corticales (Spencer, 1976; McGeer *et al.*, 1977a) ainsi que des noyaux intralaminaires du thalamus (Powell & Cowan, 1956; Berendse & Groenewegen, 1990; Francois *et al.*, 1991). Les afférences provenant du cortex interagissent principalement avec les neurones épineux moyens qui composent majoritairement le striatum (voir Smith & Bolam, 1990a). Ces axones corticostriés expriment le transporteur vésiculaire du glutamate de type 1 (VGLUT1) contrairement aux axones thalamostriés qui contiennent le transporteur vésiculaire du glutamate de type 2 (VGLUT2) (Fujiyama *et al.*, 2004; Wouterlood *et al.*, 2012).

Les travaux du Dr André Parent dans les années 90 (Parent, 1990) ont permis de diviser le striatum en 3 territoires fonctionnels différents soit en territoires sensorimoteur, associatif et limbique (voir figure 1.2). Cette division fonctionnelle du striatum repose sur la ségrégation des afférences corticales. Le territoire sensorimoteur du striatum correspond principalement à la partie postcommissurale et dorsale du noyau caudé et du putamen puisque cette

région striatale reçoit du cortex sensorimoteur. Le territoire associatif est composé de la partie précommissurale et plus ventrale du striatum qui reçoit une information massive en provenance du cortex associatif. Pour ce qui est du territoire limbique, il correspond à la partie ventrale du striatum, aussi appelée noyau accumbens. Il est donc possible de diviser le striatum en plusieurs régions fonctionnelles distinctes, mettant ainsi en évidence le caractère parallèle du traitement des informations sensorimotrices, associatives ou limbiques. Par contre, il est important de mentionner que ces territoires fonctionnels ne sont pas mutuellement exclusifs et qu'il existe un chevauchement partiel entre ceux-ci, démontrant le rôle intégrateur que le striatum joue dans le traitement des signaux provenant des aires corticales (voir Parent & Hazrati, 1995b).Le noyau caudé et le putamen sont également innervés par des axones à sérotonine (5-HT) provenant principalement du noyau du raphé dorsal (NRD) ainsi que par des axones à dopamine (DA) qui proviennent de la SNc (Beckstead *et al.*, 1993). Ces projections seront amplement décrites dans les sections subséquentes.

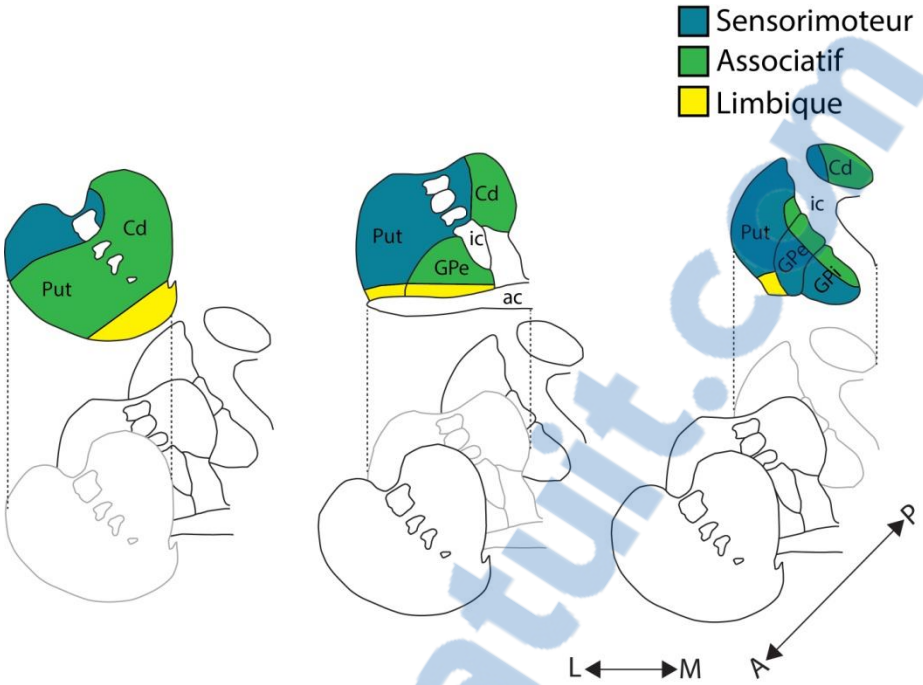

FIGURE 1.2. – Représentation graphique des territoires fonctionnels du noyau caudé (Cd), du putamen (Put), du globus pallidus externe (GPe) et interne (GPi). Les territoires sensorimoteurs (bleu), associatifs (vert) et limbiques sont représentés dans l'axe antéropostérieur (gauche à droite). Abréviation : ic = capsule interne.

Intrinsèques

L'activité du striatum n'est pas seulement influencée par des projections axonales afférentes, mais également par des interneurones intrinsèques qui influencent de manières significatives l'intégration des signaux corticostriés. L'une des populations d'interneurones la plus étudiée dans le striatum est formée par des neurones cholinergiques (ACh). Cette population neuronale représente approximativement 1% de tous les neurones striataux chez le rongeur, ce nombre étant plus important chez les primates (Graveland & DiFiglia, 1985). Ces neurones furent tout d'abord identifiés grâce à leur activité électrophysiologique tonique sous anesthésie, ce qui leur valut le nom de neurones toniquement actifs (voir Bennett & Wilson, 2003). Ils possèdent un soma qui peut dépasser les 40 µm de diamètre et forment de longs et denses plexus axonaux qui limitent leur étendue aux délimitations du striatum (Bolam

et al., 1984; DiFiglia & Carey, 1986). Cette caractéristique morphologique leur permet d'étendre leur influence sur de grands volumes et d'interagir à la fois avec un nombre important de neurones striataux. Les interneurones ACh reçoivent leurs informations principalement des neurones DA nigrostriés ainsi que des neurones glutamatergiques du thalamus et, de manière plus limitée, du cortex cérébral (Lapper & Bolam, 1992; Dimova *et al.*, 1993; Doig *et al.*, 2014). Finalement, l'activité des neurones ACh est aussi régulée de manière intrinsèque par les collatérales récurrentes des NPS GABAergiques (Gonzales *et al.*, 2013).

Les principales cibles des interneurones ACh sont les NPS sur lesquels ils exercent leur influence par l'entremise de récepteurs nicotiniques et muscariniques se situant sur la membrane postsynaptique du soma et des dendrites proximales des NPS. Ces récepteurs sont également présents sur la membrane présynaptique de certaines afférences striatales (voir Smith & Bolam, 1990a). L'activité des interneurones ACh du striatum est étroitement reliée à celle des neurones DA de la SNc. De façon réciproque, les interneurones ACh semblent être en mesure d'influencer la relâche de DA dans le striatum (Jones *et al.*, 2001; Zhou *et al.*, 2001; Rice & Cragg, 2004; Zhang & Sulzer, 2004; Threlfell *et al.*, 2010). Par exemple, une activation des neurones ACh par une entrée glutamatergique a pour effet de stimuler la libération de DA via l'activation de récepteurs nicotiniques présents à la surface des axones DA (Nelson *et al.*, 2014b). Cette activité ACh sera inhibée à son tour par cette libération de DA grâce à la présence de récepteur D_2 sur les interneurones cholinergiques. L'activité des neurones ACh peut également être régulée par la libération de GABA provenant des NPS ainsi que par les autorécepteurs muscariniques qui sont capables de fortement inhiber la libération d'ACh (Nelson *et al.*, 2014b). En somme, les neurones cholinergiques sont capables d'influencer de manière significative l'activité des NPS et ainsi réguler l'information neuronale émergeant du striatum.

D'autres types d'interneurones font aussi partie du striatum et sont présents en plus grand nombre que les neurones ACh (3 – 4 % des neurones striataux) (Luk & Sadikot, 2001; Rymar *et al.*, 2004; Tepper *et al.*, 2010). Il s'agit de la grande famille des interneurones GABAergiques. Elle se divise en 3 types d'interneurones différents basés sur l'expression de protéines qui lient le calcium soit la parvalbumine ou la calrétinine, ou encore par l'expression de la somatostatine, du neuropeptide Y, ou de l'oxyde nitrique synthase (voir Tepper *et al.*, 2010). Leur implication dans la microcircuiterie du striatum dépasse la portée de cette thèse, mais je vous invite à lire la thèse d'une de mes collègues (Petryszyn, 2016) pour une revue de la littérature récente à ce sujet.

Efférences

Les NPS ont été caractérisés au cours du 20^{e} siècle (Cajal, 1909, 1911). Des reconstructions neuronales élaborées à l'aide la méthode de Golgi ont permis d'identifier six sous-types morphologiques de neurones striataux (Cajal, 1909, 1911; Kemp & Powell, 1971; DiFiglia *et al.*, 1976). De ces sous-types, seulement deux présentent des dendrites épineuses et correspondent à la description des NPS que l'on connait aujourd'hui. C'est-à-dire qu'ils possèdent un corps cellulaire relativement petit (14 – 20 µm) et plusieurs dendrites montrant une grande quantité d'épines. Ces neurones de projections du striatum utilisent l'acide γ-aminobutyrique (GABA) comme neurotransmetteur et représentent approximativement 90 – 95% des neurones striataux (Graveland & DiFiglia, 1985).

Malgré des caractéristiques morphologiques similaires, les NPS peuvent être divisés en deux populations distinctes en fonction de leur contenu neurochimique ainsi que par leurs sites projections. Approximativement la moitié des NPS exprime le récepteur DA de type 1 (D_1) ainsi que la substance P et la dynorphine. Les axones de ces neurones ciblent principalement la SNr et le globus pallidus interne (GPi) ou son homologue chez le rongeur, c'est-à-dire, le noyau entopédonculaire. Cette efférence striatale forme la voie

directem dont l'activation facilite le mouvement. L'autre moitié des NPS forme quant à eux la voie indirecte. Ces neurones expriment le récepteur D_2 ainsi que le neuropeptide enképhaline. Les axones de ces NPS innervent principalement le globus pallidus externe (GPe), ou GP chez le rongeur, formant ainsi la voie indirecte qui, à l'opposé de la voie directe, induit principalement une inhibition du mouvement (Gerfen *et al.*, 1990; Albin *et al.*, 1995; Le Moine & Bloch, 1995; Wichmann & DeLong, 1998).

C'est sur ces deux types d'efférences striatales que repose le schéma classique de l'organisation anatomique et fonctionnelle des ganglions de la base (Voir figure 1.1.). Cependant, des études par traçage axonal unitaire ont jeté un doute sur la validité de ce modèle organisationnel (Wu *et al.*, 2000; Levesque & Parent, 2005). En effet, les auteurs ont pu mettre en évidence un important degré de collatéralisation concernant l'axone des NPS. En effet, tous les axones reconstruits innervaient le GPe, ce qui va à l'encontre de l'idée voulant que les projections striatofuges soient ségrégées en voies directe et indirecte. Cette caractéristique morphologique a été également présentée par une étude fonctionnelle démontrant que l'activation simultanée des types de neurones NPS (D_1 et D_2) soit nécessaire pour l'initiation du mouvement (Cui *et al.*, 2013) ainsi que par la découverte de NPS montrant des caractéristiques neurochimiques appartenant aux deux voies (voir Perreault *et al.*, 2011). Cette population de NPS, qui sera décrite en détail dans le chapitre 6 de cette thèse, exprime simultanément les récepteurs D_1 et D_2 (Aizman *et al.*, 2000). Ces neurones sont plus rares que les autres types de NPS représentant environ 1 – 5%. Ils se retrouvent cependant en plus grand nombre dans le noyau accumbens (Shuen *et al.*, 2008; Thibault *et al.*, 2013). La morphologie somatodendritique de ces neurones ainsi que leur contenu neurochimique sont cependant mal connus. De plus, les sites de projections de leur axone restent à être établis, mais certains groupes supposent déjà la possibilité d'une troisième voie d'efférence striatale (Perreault *et al.*, 2011).

1.2.4. Le globus pallidus

Chez les primates, le globus pallidus (GP) se divise en deux segments soit le segment interne (GPi) et le segment externe (GPe). L'organisation de cette structure est différente chez le rongeur où l'homologue du GPe se dénomme GP et l'homologue du GPi est une structure plus postérieure appelée le noyau entopédonculaire. Bien que les neurones du GPi et du GPe possèdent des caractéristiques somatodendritiques similaires, les deux segments du GP se distinguent de par leurs afférences et efférences. Ainsi, ces deux structures occupent des positions différentes dans l'organisation anatomo-fonctionnelle des ganglions de la base, le GPi étant considéré comme la principale porte de sortie des ganglions de la base et le GPe comme une structure intégratrice clé.

Afférences

Les principales afférences pallidales proviennent, tel que mentionné plus haut, des NPS du striatum. En effet, selon le modèle couramment utilisé des ganglions de la base, les neurones GABAergiques de la voie directe projettent leur axone sur le GPi et tandis que ceux de la voie indirecte projettent plutôt sur le GPe (Alexander *et al.*, 1986; Parent & Hazrati, 1995b). Le cortex ainsi que le NST amènent, quant à eux, une innervation glutamatergique moins dense sur les 2 segments du GP (Leichnetz & Astruc, 1977; Naito & Kita, 1994). Contrairement au GPe, le GPi reçoit une innervation glutamatergique thalamique provenant des noyaux centromédian (CM) et parafasciculaire (Pf) (Royce & Mourey, 1985; Kincaid *et al.*, 1991; Deschênes *et al.*, 1996; Parent & Parent, 2005). Les 2 segments du GP reçoivent également des afférences provenant du tronc cérébral soit (1) des projections 5-HT provenant du NRD (DeVito *et al.*, 1980; Vertes, 1991a; Charara & Parent, 1994), (2) une innervation cholinergique provenant du noyau pédonculopontin (DeVito *et al.*, 1980; Charara & Parent, 1994; Lavoie & Parent, 1994b) et (3) des axones DA provenant de la SNc (Charara & Parent, 1994; Gauthier *et al.*, 1999). Ces projections sont décrites plus en détail dans une publication de notre laboratoire (voir Eid & Parent, 2016) et seront décrites plus en profondeur dans le chapitre 5 de cette thèse.

Efférences

Les neurones du GPi et du GPe présentent une morphologie somatodendritique similaire. En effet, ils possèdent un corps cellulaire de grande taille avec un diamètre allant de 20 à 60 µm et utilisent le GABA comme neurotransmetteur. Bien que leur domaine somatodendritique soit peu ramifié, celui-ci est composé de très longues dendrites en mesure de couvrir une distance pouvant atteindre jusqu'à 1 mm permettant aux neurones pallidaux d'intégrer une quantité importante de signaux en provenance du striatum (DiFiglia *et al.*, 1982). L'arborisation dendritique des neurones du GP est décrite comme discoïdale avec un ratio largeur / hauteur élevé (Yelnik *et al.*, 1984). Ces dendrites sont d'ailleurs dépourvues d'épines, contrairement aux NPS du striatum décrits plus haut. La densité neuronale ainsi que le nombre de neurones au sein des deux segments du pallidum est relativement faible comparativement au striatum (Schroder, 1975). Cette caractéristique indique l'existence d'une convergence importante des afférences striatales sur les neurones pallidaux (Hazrati & Parent, 1992a; Eid & Parent, 2016). Cela se traduit par une transposition seulement partielle des territoires fonctionnels du striatum au sein du GP. En effet, les NPS localisés dans les trois différents territoires fonctionnels décrits plus haut (sensorimoteur, associatif et limbique) voient leurs projections respecter en partie, cette organisation (Hazrati & Parent, 1992b).

Tout comme le striatum, le rôle du GPi et du GPe au sein des ganglions de la base est principalement défini par leurs efférences. À cet égard, le GPi est considéré comme la principale porte de sortie des ganglions de la base et le GPe comme une structure intégratrice clé (Parent & Hazrati, 1995b). Les neurones du GPe projettent de façon massive vers le NST. Cette projection est réciproque et forme une boucle appelée boucle de Nauta-Mehler qui a longtemps été considérée comme fermée (voir Parent & Hazrati, 1995a). Cependant, des études par traçage neuronal unitaire ont permis de démontrer une diversité des efférences du GPe beaucoup plus grande (Kim *et al.*, 1976; Shink *et al.*, 1996; Sato *et al.*, 2000). En effet, il a été possible de montrer que

certains axones en provenance du GPe étaient non seulement hautement collatéralisés, mais également en mesure d'innerver les structures de sorties des ganglions de la base soit le GPi et la SNr. Il est aussi nécessaire de mentionner l'existence d'une efférence réciproque vers le striatum (Beckstead, 1983b; Sato *et al.*, 2000; Kita & Kita, 2001) qui ajoute à l'éventail hétérogène d'efférences du GPe. Les projections efférentes du GPi sont également fortement collatéralisées permettant à ces neurones d'envoyer une copie de l'information neuronale non seulement vers les noyaux moteurs du thalamus (VA/VL), mais également vers les noyaux intralaminaires du thalamus ainsi que vers le noyau pédonculopontin du tegmentum mésencéphalique (Kuo & Carpenter, 1973; Kim *et al.*, 1976; DeVito & Anderson, 1982; Schell & Strick, 1984; Parent *et al.*, 2001).

1.2.5. Le noyau subthalamique

Afférences

Le noyau subthalamique (NST), le seul regroupement de neurones glutamatergiques des ganglions de la base, joue un rôle crucial dans le contrôle moteur, tel que le démontre l'hémibalisme causé par une lésion unilatérale de cette structure (Whittier, 1947; Dewey & Jankovic, 1989; Absher *et al.*, 2000). Ce noyau sous-cortical se situe entre la *zona incerta,* la capsule interne et la SN. Le NST est considéré comme un noyau fermé, car il est encapsulé entre des faisceaux de fibres myélinisées. Sa principale afférence est GABAergique et provient du GPe (Nauta & Mehler, 1966; Carpenter *et al.*, 1968; Carter & Fibiger, 1978; Carpenter *et al.*, 1981; Van Der Kooy *et al.*, 1981; Alexander & DeLong, 1985). Celle-ci joue d'ailleurs un rôle majeur dans la modulation de l'activité de neurones du NST. Ces neurones reçoivent également des afférences glutamatergiques provenant de plusieurs régions du cortex primaire. Cette voie, appelée hyperdirecte, contourne le traitement du signal par le striatum afin d'influencer directement le NST (Künzle & Akert, 1977; Künzle, 1978; Monakow *et al.*, 1978; Carpenter *et al.*, 1981; Kitai & Deniau, 1981; Jürgens, 1984; Afsharpour, 1985; Canteras *et al.*, 1990). Le

NST est aussi innervé par des axones glutamatergiques provenant du thalamus, plus précisément du complexe intralaminaire CM/Pf (Sugimoto & Hattori, 1983; Sugimoto *et al.*, 1983; Sadikot *et al.*, 1992). Le NST reçoit, tout comme le GP, des afférences provenant des principaux noyaux neuromodulateurs du tronc cérébral. Il est donc innervé par la 5-HT du NRD, la DA de la SNc et l'ACh du noyau pédonculopontin (Campbell *et al.*, 1985; Woolf & Butcher, 1986; Canteras *et al.*, 1990; Spann & Grofova, 1992).

Efférences

Le NST est composé majoritairement de neurones de projection qui utilisent le glutamate comme neurotransmetteur, faisant ainsi du NST le seul noyau glutamatergique des ganglions de la base. Les neurones du NST possèdent un soma qui mesure entre 25 et 50 µm de diamètre. Leurs dendrites, quant à elles, montrent peu d'épines et peuvent s'étendre sur plus de 750 µm de distance chez les primates (Rafols & Fox, 1976). Puisque le NST reçoit d'importantes afférences en provenance du cortex cérébral via la voie hyperdirecte, il est intéressant de mentionner que les territoires fonctionnels se transposent sur le NST avec les neurones de la partie dorsale traitant principalement des informations sensorimotrices, la partie ventrale des informations associatives et la pointe médiale des informations limbiques (Nauta & Cole, 1978; Smith *et al.*, 1990). Les principaux sites de projection des neurones du NST sont la SNr et le GPi. Cependant, des projections vers le striatum, la SNc et le GP ont aussi été décrites chez le rongeur et le primate (Kita & Kitai, 1987; Smith *et al.*, 1990). Ainsi, le NST est en mesure d'influencer l'activité des principales structures de sortie des ganglions de la base, grâce à son activité excitatrice sur les neurones du GPi et de la SNr, ce qui a pour effet d'augmenter la contrainte inhibitrice qu'exercent les portes de sortie (GPi et SNr) sur les neurones prémoteurs thalamocorticaux et ainsi diminuer l'activité du cortex moteur. Les projections du NST innervent aussi le GPe dans une proportion relativement équivalente au GPi (Smith *et al.*, 1990). Cependant, en ce qui concerne la SN, les neurones du NST projettent davantage à la SNc comparativement à la SNr (Kita & Kitai, 1987; Smith *et al.*,

1990). Des efférences vers le striatum ont été décrites, mais semblent plus faibles lorsqu'on les compare aux autres cibles à l'intérieur des ganglions de la base (Kita & Kitai, 1987; Smith *et al.*, 1990).

1.2.6. La substance noire

La SN se situe dans le tronc cérébral plus précisément dans le tegmentum mésencéphalique antérieur au noyau rouge. Elle est facilement identifiable par sa pigmentation noire distinctive due au contenu neuronal en neuromélanine (Foley & Banter, 1958; Van Woert & Ambani, 1974; Barden, 1975). Cette structure se divise en deux parties distinctes soit la SNc et la SNr. Ces deux parties jouent des rôles différents dans le fonctionnement des ganglions de la base. Cette différence fonctionnelle s'explique par des afférences et des efférences distinctes, mais aussi par l'utilisation de neurotransmetteurs différents.

Substance noire pars compacta

Afférences

La SNc est la partie la plus dorsale de la SN. Ce segment reçoit des afférences provenant de plusieurs sources. Les plus documentées sont, sans aucun doute, les projections glutamatergiques en provenance du NST (Hammond *et al.*, 1978; Smith & Grace, 1992) et du cortex préfrontal (Carter, 1982; Kornhuber *et al.*, 1984; Gariano & Groves, 1988; Naito & Kita, 1994; Tong *et al.*, 1996). La libération de glutamate par ces axones a pour effet de provoquer des trains de potentiels d'action par les neurones de la SNc (Grace & Bunney, 1984; Smith & Grace, 1992). La SNc reçoit également des afférences excitatrices en provenance du noyau pédonculopontin (Clarke *et al.*, 1987; Futami *et al.*, 1995). Celles-ci se présentent sous deux formes, soit par une innervation glutamatergique et cholinergique (Lavoie & Parent, 1994a). Les projections cholinergiques en provenance du noyau pédonculopontin exercent un effet excitateur sur les neurones de la SNc. Cette relation complexe implique les

récepteurs nicotiniques et muscariniques sur les différentes afférences présentes dans la SNc ainsi que sur sa population neuronales (Forster & Blaha, 2003). Les afférences GABAergiques, qui sont particulièrement affectées par la relâche d'ACh, proviennent d'ailleurs principalement du striatum, du GP et de la SNr (Grofová & Rinvik, 1970; Ribak *et al.*, 1980; Smith & Bolam, 1989; Bolam & Smith, 1990). La SNc est l'une des structures recevant l'innervation 5-HT provenant du NRD la plus dense (Vertes, 1991a).

Efférences

Les neurones qui composent la SNc sont majoritairement DA (Björklund & Lindvall, 1984). Ils forment une population composée d'environ 30 000 neurones chez la souris, 300 000 chez le primate non humain et 450 000 chez l'humain (voir Björklund & Dunnett, 2007). Ces neurones ont des corps cellulaires mesurant environ 20 µm de diamètre chez le rongeur et 35 µm chez les primates non-humains (Poirier *et al.*, 1983). Ils sont dotés de 2 à 6 dendrites primaires non épineuses pouvant s'étendre jusqu'à 1200 µm chez le rongeur (Grace & Onn, 1989) et sur plusieurs millimètres chez le singe (François *et al.*, 1987). La morphologie de leur domaine somatodendritique est d'ailleurs souvent décrite comme semblable à celle des neurones du NST (Parent & Hazrati, 1995a). Leur activité électrophysiologique est caractérisée par un grand éventail de patron d'activité qui va de trains de potentiel d'actions à des patrons de décharges toniques simples (Bunney *et al.*, 1973; Grace & Bunney, 1983; Grace & Bunney, 1984; Shepard & Bunney, 1988). Les changements d'activités sont fréquents et souvent reliés au système de la récompense qui permet de favoriser l'apprentissage moteur (Schultz *et al.*, 1995; Kimura & Matsumoto, 1997).

Les efférences de la SNc se divisent principalement en trois groupes. Les neurones de la partie dorsale de la SNc projettent vers le striatum ventral, tandis ceux situés dans la partie ventrale innervent les territoires sensorimoteur et associatif du striatum (Haber & Fudge, 1997; Smith & Kieval, 2000; Prensa & Parent, 2001; Smith & Villalba, 2008). Ces neurones sont

dotés d'axones d'une longueur remarquable (Gauthier *et al.*, 1999; Prensa & Parent, 2001; Matsuda *et al.*, 2009), ce qui les rendrait d'ailleurs plus vulnérables face à certains processus neurodégénératifs (Parent & Parent, 2006b; Bolam & Pissadaki, 2012b; Pacelli *et al.*, 2015). L'innervation DA de la partie limbique du striatum provient principalement des neurones de l'aire tegmentaire ventrale (ATV) (Gerfen *et al.*, 1987). Le striatum présente également deux territoires neurochimiques distincts dénommés striosomes et matrice (Graybiel & Ragsdale, 1983; Gerfen *et al.*, 1987). Non seulement les NPS qui appartiennent à ces divisions montrent des efférences spécifiques, mais ils reçoivent aussi des afférences distinctes. Les neurones de la partie ventrale de la SNc semblent innerver préférentiellement les striosomes alors que les neurones de la partie dorsale de la SNc projettent leur axone principalement sur la matrice striatale (Gerfen *et al.*, 1987; Prensa & Parent, 2001).

L'influence qu'exerce la DA sur les neurones du striatum est essentielle au bon fonctionnement des ganglions de la base. Ce fonctionnement harmonieux repose sur un équilibre fragile entre l'activité des deux principaux types de NPS. Ainsi, la DA influence l'activité des NPS par l'entremise des récepteurs D_1 et D_2. Ces récepteurs métabotropiques ont des rôles antagonistes. Le récepteur D_1 est un récepteur couplé à la protéine G_s. Lorsqu'activé, il est en mesure de déclencher une cascade de réponses intracellulaires qui mènent à une activation des NPS. D'un autre côté, le récepteur D_2 est couplé à la protéine G_i qui, lorsqu'activée provoque une inhibition des NPS (Beaulieu & Gainetdinov, 2011; Beaulieu *et al.*, 2015). Il est aussi important de rappeler que les interneurones cholinergiques expriment aussi le récepteur D_2 et que l'inhibition de ces neurones par la DA est aussi un facteur majeur dans le fonctionnement du striatum. Nous avons également mentionné l'existence de NPS exprimant à la fois D_1 et D_2. L'expression de ces deux récepteurs mène supposément à une dimérisation de ceux-ci capable d'activer une toute nouvelle voie de signalisation par le recrutement de G_q et de la phospholipase C menant à une excitation des NPS (Lee *et al.*, 2004; Perreault *et al.*, 2010;

Perreault *et al.*, 2011; Perreault *et al.*, 2012; Perreault *et al.*, 2016). L'existence de ces dimères demeure toutefois controversée (Biezonski *et al.*, 2015; Frederick *et al.*, 2015). Par l'entremise de ces différents récepteurs, la DA est en mesure de favoriser l'initiation et l'exécution du mouvement en activant les NPS de la voie directe (qui favorisent le mouvement) et en inhibant ceux de la voie indirecte (qui entravent le mouvement). Dans la maladie de Parkinson, une diminution de la concentration intrastriatale en DA est donc en mesure de provoquer un important déséquilibre entre la voie directe et indirecte et de conduire à d'importants dérèglements dans le fonctionnement des ganglions de la base.

Les projections provenant de la SNc ne se limitent pas au striatum, mais sont aussi en mesure d'influencer d'autres éléments des ganglions de la base. Ces projections extrastriatales ont trop souvent été négligées. Elles sont très importantes pour le fonctionnement des ganglions de la base. En effet, la SNc fournit une innervation DA aux deux segments du GP, bien que beaucoup moins dense que celle du striatum (Parent & Smith, 1987; Lavoie *et al.*, 1989; Smith *et al.*, 1989; Charara & Parent, 1994; Cossette *et al.*, 1999; Hedreen, 1999; Jan *et al.*, 2000b; Prensa *et al.*, 2000; Smith & Villalba, 2008). Celle-ci est significativement plus importante dans le GPi que dans le GPe (Eid & Parent, 2015a). Cette innervation affecte principalement l'activité des neurones pallidaux par son action présynaptique sur les autres afférences pallidales (Kliem *et al.*, 2007b; Kliem *et al.*, 2010b; Hadipour-Niktarash *et al.*, 2012b) ainsi que de manière postsynaptique sur les dendrites et le soma de neurones pallidaux (Eid & Parent, 2015a) via l'activation d'une multitude de récepteurs DA (voir Eid & Parent, 2016). Les projections DA de la SNc ciblent également le NST (Campbell *et al.*, 1985; Hassani *et al.*, 1997; François *et al.*, 2000). Il a été possible d'identifier des collatérales locales qui s'arborisent à l'intérieur de la SNr (Prensa & Parent, 2001). Les axones DA sont en mesure de libérer leur neurotransmetteur de deux manières; par transmission synaptique ou volumique. Cette dernière suppose que la varicosité axonale (site de libération des neurotransmetteurs) ne possède pas de spécialisation membranaire

postsynaptique, donc ne forme pas de synapse. Des données en microscopie électronique indiquent que seulement 40% des terminaisons DA présentent une synapse dans le cortex et le striatum (Descarries *et al.*, 1996). Cette proportion est très variable d'une structure à l'autre avec des incidences synaptiques, par exemple, qui s'établissent entre 15 à 17% dans le GP (Eid & Parent, 2015a). Ainsi, une proportion importante de terminaisons axonales DA libère de la DA de manière volumique (Arluison *et al.*, 1984; Descarries *et al.*, 1996; Bérubé-Carrière *et al.*, 2012; Martin & Spühler, 2013). Cette caractéristique permettrait aux axones DA d'influencer un plus grand nombre de neurones grâce à la diffusion du neurotransmetteur qui se ferait sur plusieurs micromètres. Ce mode diffus de communication neuronale permettrait de maintenir un niveau de neurotransmetteur ambiant relativement constant dans les différentes structures cibles.

Substance noire pars reticulata

Afférences

De par ses projections vers les neurones prémoteurs du thalamus, la SNr est, avec le GPi, une des principales portes de sortie des ganglions de la base avec le GPi. Elle consiste en la partie plus ventrale de la SN et occupe un volume important de la structure. Tout comme le GPi, la SNr reçoit des afférences en provenance de plusieurs composantes des ganglions de la base. Celles-ci sont plutôt similaires à celles de la SNc. Des fibres GABAergiques innervent la SNr en provenance principalement du striatum (Deniau *et al.*, 1976; Chevalier *et al.*, 1985; Deniau & Chevalier, 1985) et du GP (Smith & Bolam, 1989; Smith & Bolam, 1990b; 1991). La SNr reçoit également une forte innervation glutamatergique en provenance du NST (Kita & Kitai, 1987). La SNr reçoit également des afférences en provenance du tronc cérébral, mais l'innervation cholinergiques du noyau pédonculopontin et 5-HT du NRD, est beaucoup moins importante que celle observée dans la SNc (Vertes, 1991a; Lavoie & Parent, 1994b).

Efférences

La SNr est majoritairement composée de neurones de projections qui présentent une morphologie somatodendritique similaire aux neurones de la SNc (Tepper *et al.*, 1987). Les corps cellulaires des neurones qui composent la SNr sont de 2 tailles différentes. Les neurones de tailles moyennes montrent un corps cellulaire de forme ovoïde ou fusiforme et leur axe le plus long mesure environ 30 µm. Les neurones de grande taille présentent une forme polygonale ou triangulaire avec un diamètre d'environ 45 µm (Gulley & Wood, 1971; Juraska *et al.*, 1977; Grofova *et al.*, 1982). Leurs arborisations dendritiques sont relativement semblables avec de 2 à 5 dendrites primaires couvrant entre 250 et 400 µm avec des dendrites tertiaires d'un diamètre très fin (Grofova *et al.*, 1982). Contrairement aux neurones de la SNc qui contiennent de la DA, les neurones de la SNr utilisent le GABA comme neurotransmetteur (Mugnaini & Oertel, 1985). Les axones de ces neurones innervent principalement le thalamus plus précisément le noyau médiodorsal, ventromédian et le noyau parafasciculaire chez le rat (Di Chiara *et al.*, 1979; Beckstead *et al.*, 1993). Les projections chez le primate sont un peu différentes avec une innervation thalamique spécifique des noyaux paralaminaires médiodorsal et ventroantérieur (Ilinsky *et al.*, 1985). Il est aussi possible d'observer des projections vers les collicules supérieurs et le noyau pédonculopontin (Gerfen *et al.*, 1982; Beckstead, 1983a; Deniau & Chevalier, 1992). Les projections de la SNr vers le thalamus moteur permettent à cette structure d'acheminer l'information neuronale ayant été traitée par les ganglions de la base vers le cortex cérébral.

En somme, les ganglions de la base forment un ensemble de structures sous-corticales qui sont reliées par une microcircuiterie extrêmement complexe. Cette organisation, caractérisée par des neurones dont l'axone est fortement collatéralisé, contraste fortement avec le modèle simple de l'organisation anatomique et fonctionnelle présenté à la figure 1.1. Dans les précédents paragraphes, vous avez été en mesure de constater à quel point les relations qu'entretiennent les différentes composantes des ganglions de la base sont

fragiles. Ceci fait en sorte que le dérèglement d'une seule de ces structures est en mesure de conduire à des déficits moteurs et cognitifs importants. La prochaine partie de cette thèse traite d'ailleurs la pathologie la plus commune reliée aux ganglions de la base, la maladie de Parkinson.

1.3. Innervation sérotoninergique des ganglions de la base

1.3.1. La sérotonine

La 5-HT a été isolée pour la première fois dans les plaquettes sanguines (Rapport *et al.*, 1946; Rapport *et al.*, 1948). Cette substance chimique qui provoquait la vasoconstriction lors de la coagulation fut alors appelée sérotonine. Parallèlement, un autre groupe isola le même composé dans les cellules entérochromaffines de l'intestin et lui donna le nom d'entéramine (Erspamer & Asero, 1952). Quelque temps après, ils conclurent qu'il s'agissait de la même molécule (voir Sjoerdsma & Palfreyman, 1990). La première détection de la 5-HT dans le système nerveux central a été faite par Twarog and Page (1953). Comme les autres monoamines soient la DA et la noradrénaline, la synthèse de la 5-HT est dérivée d'un acide aminé. La 5-HT étant dérivée du tryptophane, elle se classe comme indolamine tandis que la DA et la noradrénaline font partie des catécholamines qui sont dérivées de la tyrosine (voir figure 1.3.). L'importance de ce neurotransmetteur dans le bon fonctionnement du système nerveux central a rapidement été mise en évidence par la démonstration de son implication dans le sommeil (voir Ursin, 2002), le mouvement (voir Fox *et al.*, 2009) et l'humeur (voir Young, 2013).

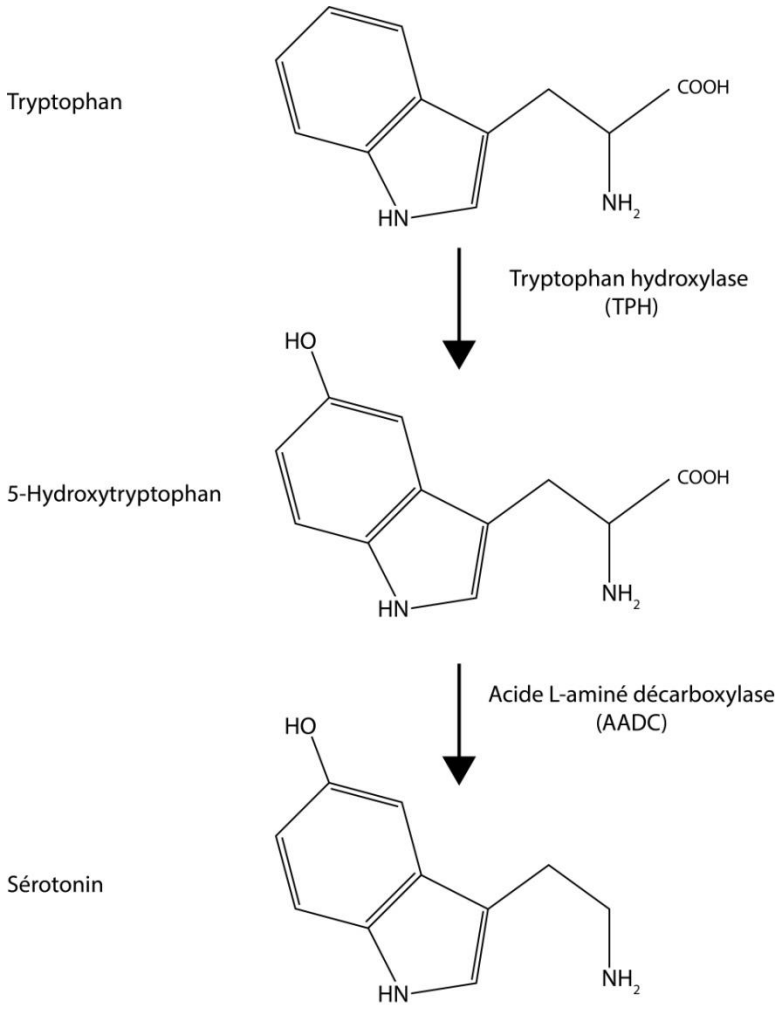

FIGURE 1.3. – Voie de synthèse de la sérotonine à partir de l'acide aminé tryptophane.

1.3.2. Morphologie générale

Les neurones 5-HT sont confinés principalement dans les noyaux du raphé situés dans le tronc cérébral. Les noyaux du raphé ont été décrits au début du 20^{e} siècle (Cajal, 1904). Ces noyaux se divisent en 9 entités (Dahlstroem & Fuxe, 1964b) avec une partie caudale projetant principalement vers la moelle épinière et une partie rostrale qui projette principalement vers le prosencéphale. Le groupe rostral comprend le noyau raphé médian (NRM) et dorsal (NRD). Ce dernier procure 85% de l'innervation 5-HT du prosencéphale

(Vertes, 1991a; Vertes & Kocsis, 1994; Vertes *et al.*, 1999b; Hornung, 2003). Des injections de traceurs antérogrades ont aussi permis de confirmer que le système 5-HT possède des ramifications qui s'étendent dans tout le système nerveux central (Azmitia & Segal, 1978; Vertes, 1991a; Morin & Meyer-Bernstein, 1999b; Vertes *et al.*, 1999b). Plusieurs travaux ont également tenté de répertorier l'importance et l'étendue de la collatéralisation axonale des neurones 5-HT du NRD en utilisant des injections de traceurs rétrogrades. Les limitations de la méthode ont fait en sorte qu'il a été impossible d'observer l'étendue totale de l'arborisation axonale d'un seul neurone 5-HT (Van Der Kooy & Hattori, 1980; Kohler *et al.*, 1982; Kohler & Steinbusch, 1982; Sarter & Markowitsch, 1984; Imai *et al.*, 1986; Li *et al.*, 2001a). De par ces travaux, on a quand même été en mesure de conclure qu'il s'agissait d'un système fortement collatéralisé (voir Waselus *et al.*, 2011). Ces travaux, ont permis de récolter une quantité importante de données neuroanatomiques, mais n'ont pas permis d'apprécier l'étendue de l'arborisation axonale d'un neurone unitaire.

Les noyaux du raphé sont composés de plusieurs types neuronaux (Descarries *et al.*, 1982). Tout dépendant du noyau, le nombre de neurones 5-HT peut représenter près du tiers de la population neuronale totale de ce noyau (Descarries *et al.*, 1982). De plus, dans cette population, environ 40% des neurones co-expriment également la substance P (Baker *et al.*, 1991b). La grande majorité des neurones du raphé co-expriment également le transporteur vésiculaire du glutamate de type 3 (VGLUT3) (Fremeau *et al.*, 2002; Gras *et al.*, 2002). Il est possible d'observer l'expression de VGLUT3 dans le NRD ainsi que dans le NRM (Gras *et al.*, 2002). Chez le rat, 95.3% des neurones 5-HT du NRD et du NRM montrent aussi une immunoréactivité pour VGLUT3 (Hioki *et al.*, 2004). Malgré cette expression répandue dans la population neuronale 5-HT, seulement un sous-groupe d'axone composant l'innervation 5-HT semble contenir le VGLUT3 (Gras *et al.*, 2002; Schafer *et al.*, 2002; Hioki *et al.*, 2004; Amilhon *et al.*, 2010). Cette observation suggère fortement la possibilité d'une colibération de glutamate et de 5-HT par les

neurones 5-HT du raphé tel que déjà rapporté pour les interneurones Ach du striatum exprimant également le VGLUT3 (Gras *et al.*, 2008). La colibération de glutamate et de 5-HT serait particulièrement importante dans la régulation de la transmission 5-HT ainsi que de l'anxiété (Amilhon *et al.*, 2010). Cependant, encore à ce jour, le rôle exact et la distribution exacte du VGLUT3 à l'intérieur d'un neurone 5-HT reste à être élucidé. Il est aussi intéressant de noter qu'une portion significative (environ 10%) des neurones du NRD contenant VGLUT3 n'exprime pas la 5-HT et serait considérée comme des neurones exclusivement glutamatergiques (Gras *et al.*, 2002; Mintz & Scott, 2006; Commons, 2009; Jackson *et al.*, 2009). Cette population neuronale bien spécifique se concentre plus particulièrement dans la partie médiane NRM et du NRD (Hioki *et al.*, 2010). Les autres neurones non-5-HT, quant à eux, utilisent l'oxyde nitrique (Nakamura *et al.*, 1991; Pasqualotto *et al.*, 1991), le GABA (Stamp & Semba, 1995) et la DA comme neurotransmetteur (Lindvall & Björklund, 1974; Trulson *et al.*, 1985). Il y a relativement peu d'informations sur ces populations neuronales sauf pour les neurones GABAergiques qui formeraient un circuit GABAergique local capable de réguler l'activité neuronale des noyaux du raphé (Allers & Sharp, 2003; Day *et al.*, 2004). Ces autres neurones seraient distribués à l'écart des populations de neurones 5-HT, dans les parties latérales de ces structures (Allers & Sharp, 2003; Day *et al.*, 2004; Fu *et al.*, 2010).

Les différentes composantes des ganglions de la base, tout comme les autres régions du cerveau, reçoivent une innervation 5-HT plutôt hétérogène. L'innervation 5-HT du striatum est relativement dense et irrégulière. Elle fut décrite pour la première fois par Fuxe and Jonsson (1967). Les études par traceurs rétrogrades et antérogrades ont permis d'identifier le NRD comme étant la source principale de l'innervation 5-HT du striatum (Lorens & Guldberg, 1974; Kellar *et al.*, 1977; Azmitia & Segal, 1978; Moore *et al.*, 1978; Parent *et al.*, 1981; Vertes & Kocsis, 1994). Le GP, quant à lui, reçoit une innervation forte en 5-HT relativement semblable à celle du striatum (Palkovits *et al.*, 1974; Pasik *et al.*, 1984a). Tout comme le striatum, cette

innervation provient majoritairement du NRD (DeVito *et al.*, 1980; Vertes, 1991a). D'un autre côté, le NST reçoit la plus faible innervation 5-HT de toutes les composantes des ganglions de la base (Mori *et al.*, 1985a; Descarries & Mechawar, 2008; Parent *et al.*, 2010), celle-ci provient également du NRD (Vertes, 1991a; Charara & Parent, 1994). Malgré cette faible densité, on sait que la 5-HT est en mesure d'influencer de manière significative l'activité des neurones du NST (Flores *et al.*, 1995). Finalement, les deux segments de la SN reçoivent l'innervation 5-HT la plus dense des ganglions de la base (Steinbusch, 1981; Wallman *et al.*, 2011), celle-ci étant plus intense dans la SNr que dans la SNc (Pasik *et al.*, 1984a; Moukhles *et al.*, 1997).

Les axones 5-HT présentent deux types de morphologies distinctes. Certains axones sont de faible calibre avec des varicosités axonales ovoïdes alors que d'autres présentent un plus fort diamètre et présentent des varicosités en forme de billes (Lidov *et al.*, 1980; Köhler *et al.*, 1981). Il a été suggéré que les varicosités axonales présentées par les deux types d'axones proviennent de deux sources différentes. En effet, il a été hypothétisé chez les rongeurs que les axones fins proviendrait principalement du NRD tandis que l'autre type du NRM (Kosofsky & Molliver, 1987; Mamounas *et al.*, 1991). Cette découverte semble aussi s'appliquer chez les primates où les axones fins sont plus sensibles à une lésion induite par l'administration de 3,4-méthylènedioxy-N-méthylamphétamine (MDMA) que les axones dotés de varicosités en forme de billes (Wilson *et al.*, 1989). Le système 5-HT est capable, tout comme le système DA, de libérer ses neurotransmetteurs de deux manières distinctes. Le premier mode de libération est le classique, c'est-à-dire, un relâche synaptique, où les sites de libération comportent des spécialisations membranaires présynaptiques. Dans cette situation, le neurotransmetteur se retrouve relativement confiné dans la fente synaptique suite à sa libération et rapidement dégradé ou recyclé par les neurones présynaptiques via l'action des transporteurs membranaires. Typiquement, ce mode de transmission est toujours utilisé par les neurotransmetteurs classiques tels que le GABA et le glutamate. Le deuxième mode de libération se fait par transmission diffuse ou

volumique. En effet, les travaux du Dr Laurent Descarries en microscopie électronique ont permis de démontrer que la plupart des varicosités axonales 5-HT étaient dépourvues de synapses. Les incidences synaptiques rapportées dans le striatum, par exemple, sont plutôt basses avec des valeurs se situant entre 6% à 13% (voir Descarries *et al.*, 2010b). De cette façon, la transmission volumique pourrait permettre à la 5-HT d'influencer un plus grand nombre de neurones avec une diffusion du neurotransmetteur pouvant se faire sur plusieurs centaines de micromètres. Cette hypothèse implique également que la libération par diffusion de la 5-HT puisse permettre de maintenir un niveau de neurotransmetteur ambiant dans les différentes structures cibles, permettant ainsi de moduler l'excitation ou l'inhibition d'une grande quantité de neurones. De plus, il a été montré que la libération de 5-HT par le soma et les dendrites des neurones 5-HT du raphé est possible, permettant d'autoréguler leur activité via l'activation des autorécepteurs 5-HT_{1A} présents sur leur domaine somatodendritique (Hery *et al.*, 1982). Il semble que ce genre de libération locale existe également pour d'autres types de neurones tels que les neurones DA de la SNc et de l'ATV (Bjorklund & Lindvall, 1975; Cheramy *et al.*, 1981).

D'un autre côté, les noyaux du raphé, plus particulièrement le NRD, reçoivent des afférences provenant d'une multitude de sources. Tout d'abord, le NRD reçoit des projections corticales, cette innervation provient principalement des parties limbiques du cortex, c'est-à-dire, le cortex orbital (Peyron *et al.*, 1997), le cortex insulaire (Peyron *et al.*, 1997; Jasmin *et al.*, 2004) ainsi que plusieurs régions du cortex préfrontal (Sesack *et al.*, 1989b; Hurley *et al.*, 1991; Takagishi & Chiba, 1991; Peyron *et al.*, 1997; Hajós *et al.*, 1998; Lee *et al.*, 2003; Vertes, 2004; Gabbott *et al.*, 2005). Ces projections permettent à ces régions corticales limbiques de contrôler la relâche de 5-HT dans une grande partie du système nerveux central et ainsi d'altérer significativement la neuromodulation de celle-ci (Arnsten & Goldman-Rakic, 1984).

Les neurones du NRD reçoit également des projections provenant du prosencéphale basal, plus spécifiquement, de l'aire préoptique latérale et médiale, du septum latéral, du noyau du lit de la strie terminale, du pallidum ventral, de la *substantia innominata* et du claustrum (Aghajanian & Wang, 1977; Kalén *et al.*, 1985; Peyron *et al.*, 1997; Steininger *et al.*, 2001; Lee *et al.*, 2003; Dong & Swanson, 2006b; a).

L'activité des neurones 5-HT du NRD peut aussi être influencé par des projections provenant du diencéphale. Les neurones du noyau tubéromamillaire, noyau dorsomédial et de l'hypothalamus latéral projettent leurs axones vers le NRD (Aghajanian & Wang, 1977; Saper *et al.*, 1979; Peschanski & Besson, 1984; Kalén *et al.*, 1985; Thompson *et al.*, 1996; Peyron *et al.*, 1997; Lee *et al.*, 2003; Lee *et al.*, 2005a; Lee *et al.*, 2005b). Les projections vers le NRD provenant de l'hypothalamus latéral sont principalement hypocrétinergiques (Peschanski & Besson, 1984; Peyron *et al.*, 1998; Lee *et al.*, 2003; Lee *et al.*, 2005b; Wang *et al.*, 2005). Cette innervation a un effet excitateur sur les neurones 5-HT du NRD permettant principalement de supporter l'état d'éveil (Brown *et al.*, 2001; Takahashi *et al.*, 2005; Tao *et al.*, 2006). Des projections provenant de l'amygdale sont aussi rapportées et sont aussi impliqués dans le cycle éveil/sommeil (Canteras *et al.*, 1995; Peyron *et al.*, 1997).

Les neurones glutamatergiques de l'habenula innervent aussi les neurones du NRD (Aghajanian & Wang, 1977; Herkenham & Nauta, 1979; Peschanski & Besson, 1984; Kalén *et al.*, 1985; Peyron *et al.*, 1997; Lee *et al.*, 2003; Klemm, 2004). Cette innervation aura un effet inhibiteur sur les neurones 5-HT en activant principalement les interneurones GABA du NRD (Ferraro *et al.*, 1996). Une suractivation de l'habenula peut d'ailleurs reproduire des symptômes dépressifs chez la souris (Shumake *et al.*, 2003; Yang *et al.*, 2008). La relation habenula – NRD est aussi en mesure d'influencer le cognition, le cycle circadien, les phénomènes de récompense et la perception de la douleur (voir Zhao *et al.*, 2015).

Les neurones du NRD reçoivent également une innervation de certains noyaux du tronc cérébral, comme par exemple, des axones DA de la SNc et de la ATV (Aghajanian & Wang, 1977; Kalén *et al.*, 1985; Peyron *et al.*, 1995; Peyron *et al.*, 1996; Lee *et al.*, 2003; Klemm, 2004) ainsi que des axones 5-HT du NRM (Vertes, 1991b; Vertes & Kocsis, 1994; Morin & Meyer-Bernstein, 1999a; Vertes *et al.*, 1999a; Tischler & Morin, 2003).

En somme, plusieurs détails morphologiques concernant l'innervation 5-HT du système nerveux central sont encore à ce jour peu connus. Tel que mentionné précédemment, cette innervation semble impliquée dans une multitude de fonctions qui reflètent bien l'étendu de l'arborisation axonale de ces neurones et l'hétérogénéité des afférences qu'ils reçoivent. C'est ce manque d'information et le rôle crucial que la 5-HT joue dans le fonctionnement du cerveau qui nous a poussé à en faire une description anatomique précise que vous pourrez appréciée dans les chapitres 2 et 3 de cette thèse de doctorat.

1.4. La maladie de Parkinson

1.4.1. Historique

Il y a 200 ans, James Parkinson publiait « *Essay on the Shaking Palsy ».* Dans cette publication, il décrivait pour la toute première fois des symptômes d'une pathologie qui sera appelée plus tard, maladie de Parkinson (Parkinson, 1817). Cette première description était plutôt sommaire, comme le suggère le Professeur Jean-Martin Charcot dans sa publication « De la paralysie agitante » (Charcot & Vulpian, 1862):

> « Comme le tableau symptomatologique présenté par ce médecin, bien que très succinct, indique cependant avec précision les principaux traits de la maladie (…) »

Jean-Martin Charcot fit d'ailleurs une description beaucoup plus complète des principaux symptômes de la maladie de Parkinson dans ses nombreuses publications ainsi que pendant ses célèbres cours du mardi donnés à l'hôpital de la Pitié-Salpêtrière. Tout d'abord, il a quantifié la fréquence des tremblements et a établi qu'il s'agissait de tremblements lents (4 – 6 oscillations par seconde). Il a aussi établi que les tremblements présentés par les patients parkinsoniens étaient présents surtout au repos, ce qui permettait de différencier la maladie de Parkinson des autres pathologies neurologiques causant des tremblements comme la sclérose en plaques ou le tremblement essentiel. Il fut aussi le premier clinicien à faire la distinction entre la rigidité et la bradykinésie dans l'évolution de la pathologie. Charcot fut aussi en mesure de caractériser les problèmes posturaux et de la marche qui affectent les patients parkinsoniens (voir figure 1.4.). Encore à ce jour, les principaux symptômes décrits à cette époque par le Professeur Charcot sont toujours utilisés afin de poser un diagnostic clinique de la maladie.

Aujourd'hui, on estime que le diagnostic posé par les neurologues suite à l'évaluation symptomatologique des patients conduit, dans environ 90% des cas, à un bon diagnostic (Jankovic *et al.*, 2000). Dans les cas de tableaux symptomatologiques atypiques, le diagnostic final s'établit bien souvent par des analyses neuropathologiques en post-mortem avec deux signes bien distinctifs : une dégénérescence des neurones pigmentés de la SNc et la présence de corps de Lewy (Oppenheimer, 1992). La première description des corps de Lewy fut effectuée par Fritz Jakob Heinrich Lewy (Lewy, 1912). Il observa chez des patients parkinsoniens la présence d'agrégats, mais dans des structures autres que la SNc. La première mention de corps de Lewy dans la SNc et la description complète de ces agrégats intracytoplasmiques se fit quelques années plus tard (Tretiakoff, 1919).

Figure 1.4. – Illustration des problèmes posturaux chez un patient parkinsonien typique. Illustration de Gowers (1886)

1.4.2. Étiologie

La maladie de Parkinson est la 2e maladie neurodégénérative la plus fréquente après la maladie d'Alzheimer avec une incidence de 2% chez les personnes âgées de plus de 60 ans (Mayeux, 2003). Encore à ce jour, les causes exactes de la maladie de Parkinson demeurent inconnues. La grande majorité (75%) des cas diagnostiqués sont de nature idiopathique. Ils sont caractérisés par une apparition tardive des symptômes moteurs avec des caractéristiques neuropathologiques bien définies telles que la présence de corps de Lewy et la dégénérescence des neurones de la SNc (Jellinger, 2010). Les causes de la maladie de Parkinson idiopathique sont considérées comme étant multifactorielles incluant des facteurs environnementaux, des prédispositions génétiques ainsi que des causes liées au vieillissement du cerveau. Bien que plus rares, certaines formes familiales ou génétiques de la maladie de Parkinson peuvent aussi se présenter. La première mutation causant la maladie de Parkinson a avoir été identifié en 1997 (Polymeropoulos *et al.*, 1997) porte l'acronyme PARK1 et se retrouve sur le gène de l'α-synucléine (SNCA). Cette mutation est de nature autosomale dominante et sa découverte

a conduit, peu de temps après, à l'identification de la protéine α-synucléine comme faisant partie des corps de Lewy (Spillantini *et al.*, 1997). Au cours des années suivantes, plusieurs autres formes génétiques de la maladie de Parkinson affectant les gènes *Parkin*, *PINK1*, *DJ-1*, *LRRK2* et ATP13A2 ont été identifiées (voir Klein & Schlossmacher, 2007).

D'un autre côté, plusieurs facteurs environnementaux ont pu être identifiés comme ayant un lien avec le développement de la maladie de Parkinson (voir Sherer *et al.*, 2007). Le lien le plus direct qui a pu être établi est le contact avec le produit chimique 1-méthyl-4-phényl-1,2,3,6-tétrahydropyridine (MPTP). La découverte fortuite de cette neurotoxine a été faite dans les années 80 alors qu'un groupe d'héroïnomanes se sont injecté cette drogue. Ce groupe s'est rapidement présenté en clinique avec des symptômes semblables à ceux de la maladie de Parkinson (Ballard *et al.*, 1985). Des études plus approfondies du mécanisme d'action de ce composé (voir figure 1.4.) ont permis d'observer que le MPTP dans sa forme non-métabolisée est capable de traverser la barrière hématoencéphalique (Markey *et al.*, 1984). Une fois entré dans le système nerveux le MPTP est métabolisé par les cellules gliales en MPDP+ et finalement en MPP+. Cette dernière molécule est ensuite transportée dans le milieu extracellulaire avant d'être captée spécifiquement par les neurones DA par le transporteur de la DA (DAT) (Javitch *et al.*, 1985; Bezard *et al.*, 1999). Une fois dans le cytosol des neurones DA le MPTP induit son effet neurotoxique principalement en bloquant le complexe I mitochondrial de la chaine respiratoire (Nicklas *et al.*, 1985). Cette inhibition mène à des réductions drastiques des niveaux d'ATP et éventuellement à la mort des cellules DA (Chan *et al.*, 1991; Fabre *et al.*, 1999). La découverte de ces mécanismes d'actions permit d'ailleurs de mettre en lumière des dysfonctions mitochondriales chez des patients parkinsoniens (Schapira *et al.*, 1990).

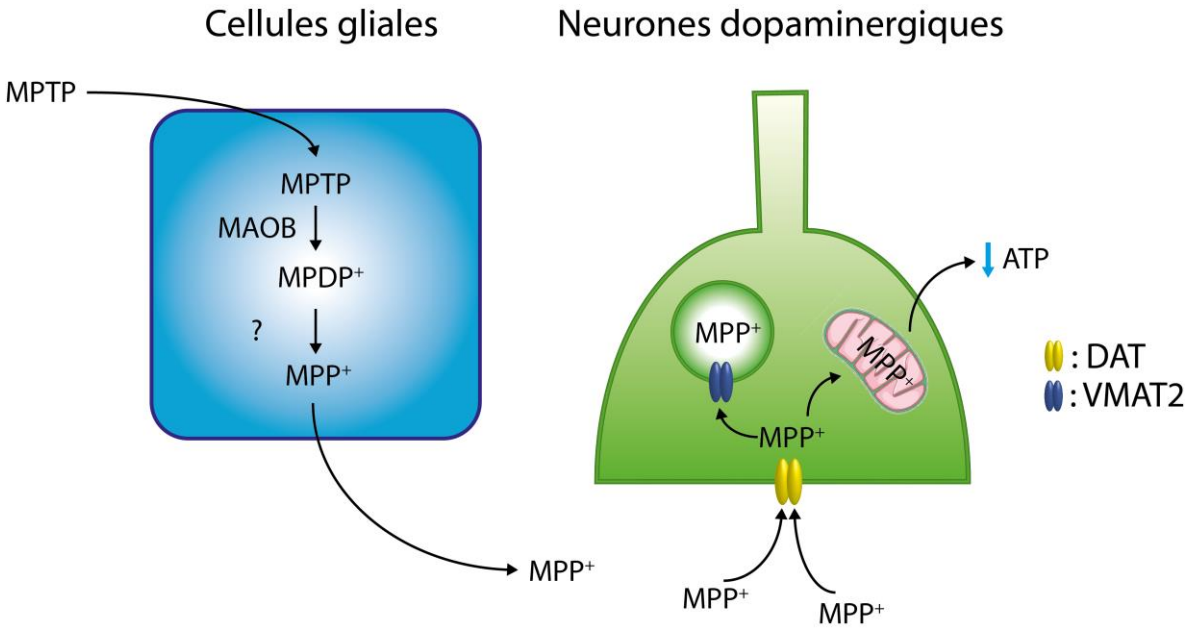

Figure 1.5.: Schématisation du mécanisme d'action de la neurotoxine MPTP. Adaptée de Brauer, 2003.

1.4.3. Pathologie

La substance noire

On retrouve environ 450 000 neurones DA dans la SNc chez une personne adulte. Chez un individu âgé de plus de 60 ans, ce nombre tombe à 270 000. Cette perte neuronale fait partie du processus de vieillissement normal du cerveau. En effet, une perte normale d'environ 5% des neurones DA par décennie a été estimée (Fearnley & Lees, 1991). Cependant, chez les personnes atteintes de la maladie de Parkinson, on observe une réduction de plus de 45% de la population neuronale DAergique dans les dix premières années suivant le diagnostic (McGeer *et al.*, 1988), le nombre de neurones DA se situant à environ 140 000 dans la SNc (McGeer *et al.*, 1977b). Cette perte neuronale est très hétérogène. Des réductions allant jusqu'à 90% ont été rapportées dans les stades avancés de la maladie (German *et al.*, 1989).

Les causes exactes de la dégénérescence des neurones DA de la SNc sont encore inconnues. Les neurones situés dans l'ATV, un regroupement de

neurones DA adjacents à la SNc, semblent être plus résistants aux mécanismes neuropathologiques de la maladie de Parkinson, enregistrant une perte neuronale qui se situe entre 36% et 55% (Uhl *et al.*, 1985). La dégénérescence de la SNc est plus prononcée dans sa partie ventrale (Hassler, 1938; German *et al.*, 1989; Fearnley & Lees, 1991). Les neurones épargnés sont davantage situés dans la partie dorsale de la SNc et contribuent surtout à l'innervation DA du striatum ventral aussi appelé noyau accumbens (Haber & Fudge, 1997; Smith & Kieval, 2000; Prensa & Parent, 2001; Smith & Villalba, 2008). La présence de la protéine liant le calcium calbindin D28K semble offrir une résistance accrue à ces neurones DA face aux processus neurodégénératifs associés à la maladie (Lavoie & Parent, 1991b; German *et al.*, 1992b; Iacopino *et al.*, 1992; Damier *et al.*, 1999). Ainsi, la voie nigrostriée est, sans aucun doute, la voie DA la plus affectée dans la maladie de Parkinson. Il a été suggéré qu'une arborisation axonale plus étendue puisse rendre les neurones DAergiques nigrostriés vulnérables à la dégénérescence étant donné la forte demande énergétique et l'importante quantité de protéines qui doivent être synthétisées afin d'assurer l'intégrité des membranes neuronales nécessaires au maintien d'axones fortement collatéralisé (Pacelli *et al.*, 2015). Typiquement, lors du diagnostic, un patient aura perdu environ 80% de son innervation DA striatale, selon des estimations *post-mortem* (Bernheimer *et al.*, 1973a). Les études *in vivo* rapportent des pertes d'activité DA allant de 40% à 70% (Brooks *et al.*, 1990; Leenders *et al.*, 1990; Morrish *et al.*, 1995; Piccini *et al.*, 1997; Rakshi *et al.*, 1999; Lee *et al.*, 2000; Nurmi *et al.*, 2001; Ito *et al.*, 2002). Ce déficit DA s'accentue avec l'évolution de la maladie et avec la sévérité des symptômes moteurs (Brooks *et al.*, 1990; Leenders *et al.*, 1990; Antonini *et al.*, 1995; Morrish *et al.*, 1995; Nurmi *et al.*, 2001; Nandhagopal *et al.*, 2009). Les études effectuées à partir de tissus *post-mortem* montrent une dénervation encore plus prononcée avec des pertes allant de 85 à 95% par rapport aux cerveaux contrôles (Bernheimer *et al.*, 1973a; Scherman *et al.*, 1989; Gerlach *et al.*, 1996). Ces différences entre les études *in vivo* et *post-mortem* peuvent probablement être expliquées par une forme de compensation des fibres restantes DA qui vont accroitre l'activité de

l'acide L-aminé décarboxylase (AADC) *in vivo* augmentant ainsi les niveaux d'activités DA mesurés chez les patients parkinsoniens (Lee *et al.*, 2000). De manière intéressante, la voie nigropallidale semble relativement conservée dans les modèles de la maladie de Parkinson (Parent *et al.*, 1989; Gash *et al.*, 1996a) ou même augmentée chez certains patients (Whone *et al.*, 2003b). Ce phénomène s'explique en partie par le fait que les axones de la voie nigrostriée et nigropallidale semblent provenir de régions différentes de la SNc (Smith *et al.*, 1989). D'ailleurs, le chapitre 5 de cette thèse traitera de cette question plus en détail. On y présente également la quantification stéréologique d'une plasticité importante concernant les projections DA nigropallidales retrouvées dans le GPe et le GPi.

Tel que mentionné plus haut, la dégénérescence de la SNc est la seule façon de confirmer le diagnostic de la maladie de Parkinson. La dégénérescence neuronale au sein de cette région pigmentée du tronc cérébral s'accompagne souvent, comme mentionné auparavant, d'inclusions cytoplasmiques que l'on nomme corps de Lewy dans les neurones de la SNc. La présence de la protéine α-synucléine dans ces agrégats a permis rapidement de classer la maladie de Parkinson comme une synucléinopathie. Des études plus récentes des corps de Lewy ont mis en lumière un caractère évolutif de cette synucléinopathie (Braak *et al.*, 2003a; Braak *et al.*, 2004). L'hypothèse de Braak divise la progression en six stades. Les premiers stades affectent principalement les noyaux du tronc cérébral pour ensuite progresser vers le prosencéphale. Cela suggère que, lors des stades I et II, les noyaux du raphé et le PPN montrent des inclusions d'α-synucléine. La SNc, quant à elle, présenterait des corps de Lewy plus tard dans l'évolution de la pathologie. C'est à ce moment qu'il serait possible de constater une neurodégénérescence des neurones DA. Je tiens à souligner qu'à ce jour il s'agit encore d'une hypothèse qui attire son lot de critiques (Burke *et al.*, 2008; Surmeier *et al.*, 2017). La présence de corps de Lewy chez un nombre significatif de patients asymptomatiques laisse croire que l'apparition de ces agrégats pourrait être le signe d'un vieillissement normal du cerveau, plutôt qu'un marqueur spécifique de la maladie de

Parkinson (Gibb & Lees, 1988; Hansen *et al.*, 1990; Parkkinen *et al.*, 2003; Parkkinen *et al.*, 2005; Markesbery *et al.*, 2009). Certains cas présentent des corps de Lewy dans le mésencéphale alors que ces agrégats semblent absents des structures inférieures du tronc cérébral tel que, par exemple, le locus cœruleus (Parkkinen *et al.*, 2005). De plus, de nombreux cas de démences à corps de Lewy montrent une évolution de synucléinopathie incompatible avec le modèle proposé par Braak (Parkkinen *et al.*, 2008). Par ailleurs, à ce jour, aucune corrélation entre la présence d'agrégat d'α-synucléine et la sévérité de la pathologie n'a pu être établie (Braak *et al.*, 2005). Ces évidences tendent à démontrer que la maladie de Parkinson n'est pas simplement une synucléinopathie, mais que les processus neurodégénératifs dépendent aussi d'une variété d'autres facteurs qui restent à être identifiés.

Le striatum

Les axones appartenant aux neurones DA situés dans la SNc ciblent préférentiellement le striatum. La dégénérescence des neurones de la SNc conduit donc à une dénervation DA massive du striatum. Ce phénomène pourrait être en mesure de conduire à une réorganisation importante des autres afférences ainsi que des efférences striatales. L'une des plus notables est certainement les changements que subissent les domaines somatodendritiques des NPS. Il est possible d'observer une perte de près de 50% des épines dendritiques chez les neurones de projections striataux dans la maladie de Parkinson (McNeill *et al.*, 1988; Stephens *et al.*, 2005; Zaja-Milatovic *et al.*, 2005) et chez les modèles animaux (Ingham *et al.*, 1993; Villalba *et al.*, 2009b; Nishijima *et al.*, 2014). À cette perte d'épines s'ajoute une diminution significative de l'arborisation dendritique (McNeill *et al.*, 1988; Zaja-Milatovic *et al.*, 2005; Deutch *et al.*, 2007). Récemment, il a été rapporté dans un modèle murin de la maladie de Parkinson que seulement les NPS qui expriment D_2 présenteraient une perte d'épines dendritiques (Day *et al.*, 2006). Ces résultats contredisent les études chez les patients parkinsoniens (McNeill *et al.*, 1988; Stephens *et al.*, 2005; Zaja-Milatovic *et al.*, 2005) et

chez un modèle simien de la maladie (Villalba *et al.*, 2009a; Villalba *et al.*, 2009b) qui montrent une perte d'épines dendritiques uniforme entre ces deux populations de NPS. Une restauration des épines dendritiques avec un traitement chronique à la L-DOPA a pu être observée uniquement chez les rongeurs après une lésion DA (Zhang *et al.*, 2013; Fieblinger *et al.*, 2014; Nishijima *et al.*, 2014; Suarez *et al.*, 2014). La perte d'épines dendritiques correspond probablement à une diminution du nombre de synapses glutamatergiques corticostriées et laisse croire à une baisse de l'excitabilité des NPS par les neurones du cortex (Surmeier *et al.*, 2007). Le chapitre 6 traitera plus en profondeur du sujet en présentant les changements induits par une lésion DA chez la souris en ce qui concerne les NPS exprimant à la fois les récepteurs D_1 et D_2.

Les interneurones cholinergiques du striatum jouent aussi un rôle majeur dans la physiopathologie de la maladie de Parkinson. Les récepteurs cholinergiques furent l'une des premières cibles de traitement dans le but de réduire les tremblements chez les patients parkinsoniens (Sethy & Van Woert, 1973). C'est à ce moment que l'interaction DA-acétylcholine a commencé à être étudiée plus en détail. Les premières hypothèses suggéraient que ces 2 neurotransmetteurs jouaient un rôle opposé dans les symptômes extrapyramidaux (McGeer *et al.*, 1961). Cette hypothèse suggère que le maintien d'un équilibre fragile entre les niveaux de DA et d'ACh est nécessaire afin d'avoir un comportement moteur approprié. Le tonus DA constant permet de réguler la libération d'ACh via le récepteur $D_{2,}$, ce qui explique que, lors d'une dénervation DA, les interneurones cholinergiques se retrouvent hyperactifs (Barbeau, 1962). Ce changement d'activité, dû à la diminution de l'activation du récepteur D_2 par la DA a pour effet d'augmenter la libération d'ACh dans le striatum (Maurice *et al.*, 2004). La diminution de DA dans le milieu extracellulaire mène à une plus grande excitabilité (Fino *et al.*, 2007) et à une synchronisation de la décharge des interneurones ACh (Raz *et al.*, 1996). La synchronisation de l'activité de ceux-ci est cependant étonnante, puisque ces neurones sont distancés dans le striatum et qu'ils ne montrent que

très peu d'interactions (Raz *et al.*, 1996). Il a aussi été proposé que ces oscillations puissent correspondre à la fréquence des tremblements, ce qui impliquerait que les interneurones ACh seraient directement impliqués dans l'apparition de ce symptôme moteur chez les patients parkinsoniens (Raz *et al.*, 2001).

En somme, la dénervation DA du striatum cause de grands changements d'activité des neurones striataux (voir figure 1.6.). Les interneurones ACh se retrouvent suractivés causant une hypercholinergie dans le striatum influençant directement l'activité des NPS. Les NPS D_1 et D_2 se retrouvent, respectivement, sous-activés et suractivés causant une disinhibition des structures de sortie des ganglions de la base (GPi et SNr). Ce dérèglement du fonctionnement des ganglions de la base cause une inhibition du mouvement chez les patients atteints de la maladie de Parkinson causant des symptômes moteurs handicapants. Dans la prochaine partie il sera question des traitements actuellement disponibles visent à rétablir une activité normale des ganglions de la base de manière pharmacologique ou chirurgicale.

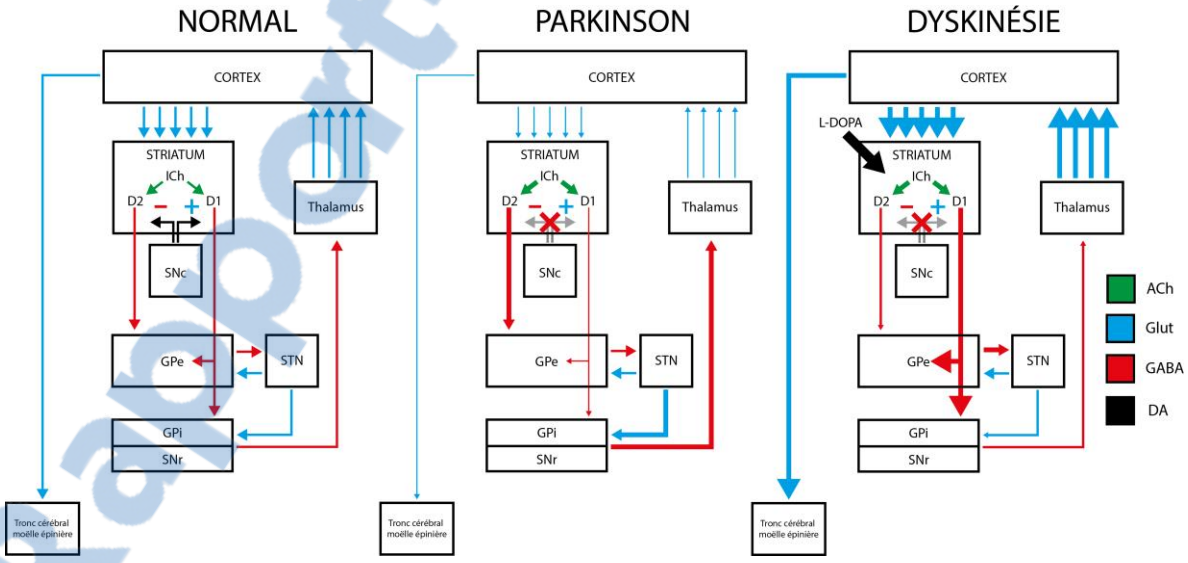

FIGURE 1.6. – Représentation graphique simplifiée des changements d'activité des composantes des ganglions dans la maladie de Parkinson et lorsque le patient présente des dyskinésies induites par la L-DOPA. Adapté de Smith *et al.* (2012).

1.4.4. Traitements

Les traitements pharmacologiques

La L-DOPA

Le médicament le plus utilisé pour traiter les symptômes moteurs de la maladie de Parkinson est la L-3,4-dihydroxyphenylalanine (L-DOPA), qui constitue le précurseur métabolique de la DA. La première utilisation de cette molécule pour traiter la maladie de Parkinson remonte au début des années 60 alors que Birkmayer et Hornykiewicz remarquèrent une amélioration temporaire des symptômes moteurs suite à l'administration d'une faible dose de L-DOPA (Birkmayer & Hornykiewicz, 1962). Ces résultats suscitèrent immédiatement un très grand intérêt pour cette pharmacothérapie de remplacement DA. La L-DOPA est rapidement métabolisée par l'AADC exprimée par les neurones DA et 5-HT et transformée en DA. Plusieurs expérimentations avec différentes doses de L-DOPA furent effectuées dans les années suivant la découverte initiale de Birkmayer et Hornykiewicz. Cependant, ces études se sont avérées peu fructueuses, les fortes doses nécessaires afin de produire un effet thérapeutique étant mal tolérées par les patients (McGeer & Zeldowicz, 1964). Un protocole d'administration progressive de L-DOPA a permis aux patients de mieux tolérer des doses élevées. Ce genre de protocole est d'ailleurs toujours utilisé en clinique (Cotzias *et al.*, 1967; Cotzias *et al.*, 1969; Yahr *et al.*, 1969). Ultérieurement, l'utilisation conjointe d'inhibiteurs de l'AADC et de la catéchol-*O*-méthyltransférase (COMT) périphériques ont permis de baisser les doses orales en augmentant la quantité de L-DOPA étant acheminée et métabolisée dans le système nerveux central (voir Nagatsu & Sawada, 2009). Ces essais cliniques ont sonné le début de l'ère de la DOPAthérapie dans laquelle nous sommes toujours plongés actuellement. Par contre, des complications importantes suite à un traitement chronique à la L-DOPA ont rapidement été observées.

Ces complications comprennent des dyskinésies induites par le traitement ainsi que d'autres effets secondaires handicapants (Cotzias *et al.*, 1969; Yahr *et al.*,

1969; McDowell *et al.*, 1970; Schwarz & Fahn, 1970). L'apparition de dyskinésies et les fluctuations motrices sont les effets secondaires moteurs les plus fréquents de la DOPAthérapie chronique avec près de 75% des patients qui en développent après 15 ans de traitement (Rajput *et al.*, 2002a). Les dyskinésies induites par la L-DOPA (DILs) peuvent être classées en 3 types; (1) dyskinésies de pics de doses, c'est-à-dire, des mouvements anormaux qui se présentent lors de la phase efficace de la L-DOPA, (2) dyskinésies diphasiques qui apparaissent typiquement avant et après l'effet thérapeutique de la prise de L-DOPA et (3) dystonie OFF qui surviennent lorsque les patients sont sans L-DOPA. Les manifestations motrices les plus communes de ces dyskinésies sont la chorée, les dystonies et le ballisme. Typiquement, les chorées sont caractérisées par des mouvements involontaires, anormaux et incontrôlables qui semblent progresser d'un membre à l'autre. Les mouvements choréiques sont la manifestation la plus commune des DILs et peuvent varier dans leur intensité passant de mouvements à peine perceptibles à des mouvements involontaires de grandes amplitudes nuisant considérablement à la qualité de vie du patient. Les chorées sont typiquement associées aux dyskinésies de pic de doses (Davie, 2008). D'un autre côté, la dystonie est la seconde forme de DILs la plus commune. Elle se manifeste par une contraction soutenue des muscles agonistes et antagonistes de certains membres. Les dystonies peuvent être observées comme dyskinésies de pic de doses, des dyskinésies diphasiques ou des dystonies OFF. La dystonie se présente normalement comme des mouvements de coup de pied tandis que les dystonies en période OFF se manifestent tôt le matin sous la forme de contractions douloureuses des orteils ou d'un pied. Finalement, le ballisme se traduit par des mouvements de grande amplitude de la partie proximale des membres affectés et est souvent associé à des mouvements choréiques.

La prise chronique de L-DOPA peut aussi conduire à d'autres effets secondaires appelés fluctuations motrices. Celles-ci peuvent se manifester sous la forme de *freezing* moteur ou de mouvement paradoxal (court soulagement du parkinsonisme dû à un stress ou un stimulus externe) (Quinn, 1998). Les

fluctuations motrices peuvent apparaitre pendant les périodes *OFF* ou à la fin de la période *ON* de la prise de L-DOPA (*wearing-off*). Les fluctuations motrices apparaissent normalement quelques années après le début de la DOPAthérapie. La perception de ce phénomène est probablement due à une plus grande amplitude de la différence entre les périodes ON et les périodes OFF qui accompagne l'évolution des processus neurodégénératifs (Kempster *et al.*, 1989). Ces périodes de motricité anormale peuvent durer de plusieurs minutes à plusieurs heures (Quinn, 1998). Il est aussi possible d'observer une variété d'effets secondaires non-moteurs liés au traitement tels que des hallucinations ou des dépressions, et ce chez, plus de 50% des personnes traitées chroniquement à la L-DOPA (Hely *et al.*, 2005b).

Les agonistes dopaminergiques

Bien que moins efficaces que la L-DOPA (Rascol *et al.*, 2000), les agonistes DA (pramipexole, ropinirole et apomorphine) sont également utilisés en clinique afin d'atténuer les symptômes moteurs de la maladie de Parkinson. Ces agonistes DA se lient aux récepteurs D_2 localisés sur les NPS du striatum. Cette action permet ainsi de rétablir un niveau d'activité relativement normal des neurones striatofuges et ainsi soulager les symptômes moteurs des patients (voir Surmeier *et al.*, 2007). Ces molécules sont principalement utilisées afin de retarder l'administration de la L-DOPA chez des patients souvent plus jeunes et à un stade précoce de la maladie. En effet, il a été souligné que l'utilisation d'agonistes DA à cette étape de la maladie permet de retarder l'utilisation de L-DOPA et donc, les effets secondaires qui y sont associés (Rinne *et al.*, 1998a; Rascol *et al.*, 2000; Whone *et al.*, 2003c; Parkinson-Study-Group, 2004). Par contre, l'utilisation d'agonistes DA se montre moins efficace pour soulager les symptômes moteurs de la maladie de Parkinson que la DOPAthérapie (Stowe *et al.*, 2008) bien que certains les patients qui utilisent la pramipexole en monothérapie ont montré des mesures de qualité de vie semblables à ceux directement traités à la L-DOPA pendant une étude longitudinale (Holloway *et al.*, 2004). Le profil d'effets secondaires des agonistes DA est relativement semblable à la L-DOPA avec des fluctuations motrices apparaissant graduellement au cours d'un traitement à long terme.

Par contre la confusion et les hallucinations sont plus souvent présentes lors de l'utilisation d'agonistes DA (Davie, 2008).

Gestion des complications d'un traitement à la L-DOPA

Les cliniciens ont actuellement plusieurs molécules disponibles afin de gérer les complications motrices liées à la prise de L-DOPA. L'amantadine est un antagoniste des récepteurs NMDA développé initialement comme un agent antiviral. L'utilisation de cette molécule pourrait réduire le *freezing*, ainsi que les périodes OFF et les dyskinésies en limitant l'hyperactivité de la transmission glutamatergique dans les ganglions de la base (voir figure 1.6.) (Metman *et al.*, 1998; Luginger *et al.*, 2000). Par contre, l'utilisation d'amantadine s'accompagne d'une incidence élevée d'effets secondaires tels que des confusions, hallucinations, enflure des chevilles et livedo reticularis (problème vasculaire de la peau) (Davie, 2008). L'efficacité d'un tel traitement semble donc relativement limitée, en accord avec une métaanalyse (Crosby *et al.*, 2003). Actuellement, la modulation allostérique de récepteurs glutamatergiques métabotropiques de type 4 (mGluR4) et de type 7 (mGluR7) semble un futur traitement prometteur des DILs avec une bonne efficacité dans les modèles animaux en réduisant, hypothétiquement, la transmission glutamatergique corticostriée tout en limitant les effets secondaires observés avec l'amantadine (Johnson *et al.*, 2009; Jones *et al.*, 2011; Bennouar *et al.*, 2013).

L'utilisation d'apomorphine, un agoniste DA, s'est également montrée bénéfique afin réduire les périodes OFF des patients traités à la L-DOPA (Poewe & Wenning, 2000). L'infusion duodénale de L-DOPA permet aussi d'améliorer la durée d'efficacité de la DOPAthérapie sans augmenter les dyskinésies chez les patients (Nyholm *et al.*, 2005).

Les inhibiteurs de la COMT périphérique (entacapone et tolcapone) sont généralement utilisés en combinaison avec un inhibiteur de l'AADC périphérique (carbidopa). Leurs effets combinés font en sorte d'augmenter la quantité de L-DOPA qui traverse la barrière hématoencéphalique en inhibant

les principales enzymes qui métabolisent cette molécule en DA au niveau périphérique. Leur utilisation permet d'augmenter la demi-vie de la L-DOPA dans le plasma sanguin de plus de 45% pour chaque dose (Davie, 2008). Cet effet fait en sorte que les inhibiteurs de la COMT et de l'AADC sont une médicamentation efficace afin de réduire les fluctuations motrices sous L-DOPA qui apparaissent dans les stades avancés de la maladie de Parkinson. Ils permettent de réduire les périodes OFF, d'allonger les périodes ON en réduisant de réduire les doses de L-DOPA (Rinne *et al.*, 1998b).

L'intérêt pour l'implication des interneurones ACh dans les DILs est assez récent. En effet, ce n'est qu'en 2011 qu'un lien direct entre l'augmentation de l'ACh dans le striatum et l'expression des DILs a été fait (Ding *et al.*, 2011). Le désintéressement face aux traitements ACh des dyskinésies est principalement dû aux échecs des essais cliniques (voir Won *et al.*, 2014). En effet, l'étude des traitements anticholinergiques dans le but de soulager les DILs s'est soldée par des améliorations minimes et parfois même à une exacerbation des symptômes parkinsoniens chez les patients (Birket-Smith, 1975; Pourcher *et al.*, 1989). Ce n'est qu'avec des résultats récents et encourageants obtenus à partir de modèles animaux que l'intérêt pour les traitements ACh a resurgi. L'étude par le groupe de Kang chez la souris (Won *et al.*, 2014) a apporté des résultats intéressants concernant le rôle des interneurones ACh dans l'expression des DILs. L'ablation spécifique de ces interneurones dans le striatum avant l'injection de L-DOPA diminue significativement la sévérité des DILs subséquentes. De plus, cette lésion n'interfère pas avec l'effet antiparkinsonien de la L-DOPA. Ces résultats démontrent que, lors d'un traitement à la L-DOPA, les interneurones ACh constituent fort probablement un joueur clé dans le développement et l'expression des DILs chez les patients parkinsoniens. De plus, l'utilisation de molécules plus spécifiques aux récepteurs muscariniques a permis d'obtenir une atténuation des DILs (Bordia *et al.*, 2010; Ding *et al.*, 2011).

Les traitements chirurgicaux

L'intérêt pour les traitements chirurgicaux de la maladie de Parkinson a principalement commencé bien avant l'utilisation de la L-DOPA, soit avec l'apparition de la stéréotaxie à la fin des années 40. À ce moment, une électrocoagulation bilatérale du GPi (Fenelon, 1950; Guiot & Brion, 1953; Cooper & Bravo, 1958) ou du noyau ventral intermédiaire du thalamus (Hassler & Riechert, 1954; Cooper & Bravo, 1958) semblait la meilleure option afin de traiter les tremblements au repos. Par contre, puisqu'irréversible, cette intervention pouvait parfois être mal tolérée, avec de nombreux effets secondaires incommodants. L'utilisation de courant électrique afin de moduler certaines fonctions du cerveau a fait son apparition dans les années 50. Subséquemment, les stimulations hautes fréquences (SHF) ont rapidement été identifiées comme une méthode efficace, modulable et réversible pour traiter certains désordres neurologiques (Hassler *et al.*, 1960). Avec l'apparition de la L-DOPA, à la fin des années 60, l'intérêt pour les traitements chirurgicaux pour la maladie de Parkinson a grandement diminué, les traitements pharmacologiques étant moins invasifs et moins risqués. Malgré cette défaveur, plusieurs groupes ont identifié de nouvelles cibles chirurgicales afin de traiter une variété grandissante de problèmes neurologiques avec l'aide de stimulations électriques. L'apparition de stimulateurs implantables est venue changer la donne dans les années 80 en donnant réellement naissance à la stimulation cérébrale profonde telle qu'on la connait aujourd'hui. À partir de ce moment, l'utilisation de la SHF s'imposait réellement comme thérapie alternative, pouvant remplacer les chirurgies lésionnelles dans le traitement des tremblements parkinsoniens (Benabid *et al.*, 1987). Au départ, les stimulations bilatérales du thalamus étaient favorisées pour atténuer les tremblements. Elles ont peu à peu laissé leur place à la stimulation du NST (Pollak *et al.*, 1993) et du GPi (Siegfried & Lippitz, 1994) qui permettent de traiter plus efficacement les autres symptômes moteurs de la maladie de Parkinson tels que la rigidité et la bradykinésie (The Deep-Brain Stimulation for Parkinson's Disease Study Group, 2001). Les études chez l'animal ont permis de déterminer que la dénervation DA striatale qui caractérise la maladie de

Parkinson conduit à l'hyperactivité du NST (Filion & Tremblay, 1991; Parent *et al.*, 2000)(voir figure 1.6.). Le retour à une activité normale de cette structure lors d'un traitement à la L-DOPA (Benazzouz *et al.*, 1996) ou suite à une lésion permet d'atténuer les symptômes moteurs de la maladie de Parkinson (Bergman *et al.*, 1990). Le même genre de phénomène se produit lors de la SHF des NST, l'effet de celle-ci conduit à une inhibition des neurones du NST s'apparentant à l'effet d'une lésion de cette structure (Vitek, 2008). Par contre, la simple inhibition des NST ne peut expliquer tous les effets bénéfiques observés lors d'une SHF chez les patients parkinsoniens (Gradinaru *et al.*, 2009). D'ailleurs, les connaissances actuelles n'arrivent pas à expliquer tous les mécanismes cellulaires et moléculaires impliqués dans les effets thérapeutiques de la stimulation cérébrale profonde du NST.

En somme, la maladie de Parkinson est une pathologie qui se caractérise principalement par une neurodégénérescence des neurones DA de la SNc. Cette dégénérescence du système DA affecte principalement la voie nigrostriée. La perte de DA striatale qui s'en suit affecte grandement le fonctionnement de cette structure (Voir figure 1.6.). Ces changements d'activité nous laissent croire que l'on pourrait voir apparaitre des phénomènes de plasticité adaptative et compensatoire dans le striatum ainsi que dans les autres composantes des ganglions de la base, plus particulièrement en ce qui concerne leur innervation 5-HT. La prochaine partie de cette introduction traitera de quelles manières les neurones 5-HT sont affectés par la maladie de Parkinson ainsi que les changements observés par en ce qui concerne leurs axones.

1.5. Le système sérotoninergique dans un contexte parkinsonien

1.5.1. La sérotonine dans la maladie de Parkinson

Les noyaux du raphé constituent un ensemble de structures situées dans le tronc cérébral. Ces noyaux referment des neurones qui synthétisent et libèrent de la 5-HT et ce, dans pratiquement toutes les régions du système nerveux central, incluant les différentes composantes des ganglions de la base. Les études menées par Braak *et al.* (2003) suggèrent la présence de corps de Lewy dans le cytoplasme des neurones 5-HT du tronc cérébral et ce, dès les premiers stades de la maladie de Parkinson. L'hypothèse de Braak suggère donc une implication hâtive des systèmes 5-HT qui pourrait se traduire par une variété de symptômes non-moteurs qui précèdent souvent de plusieurs années l'expression des symptômes moteurs (voir Poewe, 2008). Ces symptômes non-moteurs de la maladie de Parkinson peuvent prendre la forme de problèmes de sommeil, d'olfaction, de constipation ou de dépression majeure et peuvent, dans bien des cas, se montrer plus handicapants que les symptômes moteurs. Des études épidémiologiques ont pu démontrer que les patients parkinsoniens sont beaucoup plus à risque de développer une maladie mentale avec près de 50% des patients qui présentent des symptômes de dépression au cours de leur suivi (Hely *et al.*, 2005b; Poewe, 2008). Ces chiffres plutôt alarmant expliquent en grande partie les raisons pour lesquelles autant d'importance est accordée à la composante non-motrice des symptômes de la maladie de Parkinson. Dans les paragraphes qui suivent, il sera question de l'altération de l'innervation 5-HT des ganglions de la base dans la maladie de Parkinson.

Études in vivo

L'état des systèmes 5-HT peut être mesuré *in vivo* à l'aide de plusieurs techniques d'imagerie. La plus connue est surement la tomographie par

émission de positrons (TEP). Cette technique permet d'imager en trois dimensions la distribution d'une molécule radioactive présente à l'intérieur du cerveau d'un patient, et ce, en temps réel. Cette approche permet ainsi d'obtenir une mesure quantitative de la distribution régionale de cette molécule. Dans le cas qui nous intéresse, la molécule la plus utilisée pour quantifier l'état de l'innervation 5-HT est le 3-amino-4-(2-dimethylaminomethylphenylsulfanyl)-benzonitrile (^{11}C-DASB). Cette molécule se lie spécifiquement au transporteur membranaire de la 5-HT (SERT) et est considérée comme l'un des meilleurs marqueurs afin d'évaluer la disponibilité *in vivo* de ce transporteur, donnant ainsi une indication indirecte de l'état de la transmission 5-HT (Brust *et al.*, 2006).

Les noyaux du raphé

La seule étude disponible effectuée pendant la phase pré-symptomatique de la maladie de Parkinson montre une augmentation de la liaison de C-DASB dans les noyaux du raphé (Wile *et al.*, 2017). Lors des stades précoces, il est possible de constater une conservation de la disponibilité de SERT dans ces noyaux (Haapaniemi *et al.*, 2001; Kim *et al.*, 2003; Albin *et al.*, 2008; Politis *et al.*, 2010a; Roselli *et al.*, 2010; Beucke *et al.*, 2011; Strecker *et al.*, 2011; Wile *et al.*, 2017) ou une légère baisse (Politis *et al.*, 2010b; Qamhawi *et al.*, 2015). D'un autre côté, la littérature rapporte généralement une baisse de la biodisponibilité du SERT à l'intérieur des noyaux du raphé dans les stades avancés de la maladie de Parkinson (Berding *et al.*, 2003; Guttman *et al.*, 2007; Politis *et al.*, 2010a). Un autre groupe a même rapporté une conservation du signal dans les noyaux du raphé chez des patients se trouvant aussi en stade avancé de la maladie (Pavese *et al.*, 2010). En somme, les études concernant l'état des neurones 5-HT des noyaux du raphé chez les patients parkinsoniens montrent des résultats inconsistants. Ces différences peuvent être expliquées par le stade de la maladie auquel les patients sont imagés. La phase pré-motrice de la maladie de Parkinson suggère la présence de phénomènes compensatoires qui augmenteraient l'activité de SERT dans les noyaux raphé. Ces mêmes niveaux reviendraient à la normale pendant les

stades précoces de la maladie avec l'apparition de symptômes moteurs et la prise de L-DOPA (Wile *et al.*, 2017) pour ensuite diminuer légèrement dans les stades avancés de la pathologie.

Les ganglions de la base

Les études par imagerie TEP indiquent que les projections 5-HT semblent soit dégénérer assez tôt dans la maladie (Politis *et al.*, 2010a; Politis *et al.*, 2010b; Roselli *et al.*, 2010; Strecker *et al.*, 2011) ou encore être relativement conservées (Boileau *et al.*, 2008). Une métaanalyse en TEP de l'innervation 5-HT striatale a permis de corréler une baisse des niveaux de liaison de C-DASB avec la durée de la maladie de Parkinson (Pagano *et al.*, 2017). Cette baisse de l'innervation 5-HT des ganglions de la base semble précéder une perte éventuelle d'activité dans les noyaux du raphé (Kim *et al.*, 2003; Politis *et al.*, 2010a). Une étude en TEP récente effectuée sur des patients porteurs de la mutation LRRK2 fait la démonstration que les niveaux d'activités des axones 5-HT présents dans le striatum semblent être augmentés avant l'apparition des symptômes moteurs de la maladie de Parkinson (Wile *et al.*, 2017). Tout comme les noyaux du raphé, cette activité 5-HT revient à un niveau normal lors de l'apparition des déficits moteurs et lors d'un début de traitement à la L-DOPA (Wile *et al.*, 2017). La biodisponibilité de SERT est généralement abaissée dans les autres composantes des ganglions de la base (Guttman *et al.*, 2007; Politis *et al.*, 2010a).

En somme, les changements d'activité 5-HT dans les ganglions de la base semblent calqués sur ceux des noyaux du raphé. Ces phénomènes plastiques sont mal compris et leur ampleur inconnue. Le rôle exact qu'ils jouent dans la physiopathologie de la maladie de Parkinson reste à être élucider. Il a cependant été possible de démontrer l'implication de ces changements dans certaines complications motrices et non-motrices. Des études en TEP ont pu identifier qu'une préservation de l'innervation 5-HT dans le GP est associée au développement de DILs. Une baisse de l'innervation 5-HT pallidale serait quant

à elle associée à une réponse normale à un traitement à la L-DOPA (Smith *et al.*, 2015).

La baisse de l'innervation 5-HT striatale ne semble pas influencer le développement de symptômes dépressifs chez le patient (Kim *et al.*, 2003; Politis *et al.*, 2010b), mais pourrait être reliée à des symptômes de fatigue (Pavese *et al.*, 2010). Les patients montrant des signes dépressifs auraient plutôt une augmentation de la liaison à SERT dans l'amygdale, l'hypothalamus, le noyau raphé caudal et le cortex cingulaire postérieur comparativement au groupe contrôle (Boileau *et al.*, 2008; Politis *et al.*, 2010b). L'augmentation de l'activité de SERT pourrait contribuer à la baisse de 5-HT extracellulaire en haussant la capacité de recapturer ce neurotransmetteur, favorisant ainsi l'apparition de symptômes dépressifs chez les patients (Boileau *et al.*, 2008). Il est encore impossible à ce jour de savoir si ces phénomènes compensatoires sont dus à une vulnérabilité inhérente des patients ou à une réponse compensatoire à la maladie de Parkinson. L'altération de l'innervation 5-HT combinée avec des incidences plus élevées de dépression et de symptômes de fatigue chez les patients parkinsoniens suggèrent que la 5-HT est probablement impliqués dans la manifestation des symptômes non-moteurs de la maladie.

Le liquide céphalorachidien

Une autre méthode permettant de mesurer indirectement l'état de la transmission 5-HT dans le système nerveux central est le dosage, par chromatographie en phase liquide à haute performance (CLHP) de la 5-HT et de son principal métabolite, l'acide 5-hydroxyindolacétique (5-HIAA), obtenu dans le liquide céphalorachidien (LCR). En général, ce genre de mesures indiquent des baisses d'environ 20% des concentrations de ces molécules dans le LCR de patients parkinsoniens (Granerus *et al.*, 1974; Mayeux *et al.*, 1984; Tohgi *et al.*, 1993). L'administration de L-DOPA provoque une chute de l'ordre de 50% de la concentration de 5-HT dans le LCR (Tohgi *et al.*, 1993). Contrairement aux indices de neurotransmission 5-HT obtenus indirectement

dans le striatum par TEP, il semble que la baisse de concentration de 5-HIAA puisse corréler avec la dépression chez les patients (Mayeux *et al.*, 1984), bien que l'absence de corrélation ait aussi été rapportée (Granerus *et al.*, 1974). La baisse de 5-HT et de 5-HIAA dans le LCR peut indiquer une diminution de la transmission 5-HT dans le système nerveux central. Les conclusions que l'on peut tirer de ces mesures sont cependant limitées vu l'impossibilité d'identifier les structures affectées. Il est cependant possible d'affirmer que l'administration de L-DOPA est en mesure d'affecter significativement la transmission 5-HT dans le système nerveux central.

Études post-mortem

Les résultats *in vivo* sont très intéressants, mais les approches utilisées possèdent certaines limitations. Tout d'abord, les images obtenues en TEP sont de faible résolution, ce qui laisse un certain degré d'incertitude en ce qui concerne la délimitation de structures de petites tailles comme les segments du GP, le NST et les noyaux du raphé. De plus, il est impossible d'établir s'il s'agit d'une dénervation ou seulement d'une baisse d'activité des neurones étudiés. En effet, il serait possible que les axones restants suite à une dégénérescence DAergique expriment plus ou moins certains marqueurs (dont le SERT) montrant alors des mesures d'activités plus ou moins élevées donnant alors un portrait erroné de l'état de l'innervation étudiée. Par contre, ils permettent de faire un suivi longitudinal de l'évolution de la maladie, ce qui est impossible à faire à partir de tissus *post-mortem*. En contrepartie, l'analyse *post-mortem* de ce type de tissu permet de faire des quantifications d'axones et de mort cellulaire d'une précision inégalée, mais à un temps donné dans l'évolution de la maladie. Il est aussi possible d'observer la présence ou non de corps de Lewy, ce qui est présentement impossible en imagerie TEP puisqu'il n'existe aucun marqueur spécifique de ces agrégats.

L'analyse *post-mortem* des noyaux du raphé des patients parkinsoniens nous permet de constater une perte de neurones dans ces noyaux qui semble

surtout présents dans les noyaux du raphé appartenant au groupe postérieur qui projette principalement vers la moelle épinière (Halliday *et al.*, 1990). Cette mort cellulaire semble être exacerbée chez les patients parkinsoniens montrant des symptômes de dépression (Paulus & Jellinger, 1991), malgré que cette affirmation fut mise en doute dans une étude suggérant une implication plus importante des systèmes DA et noradrénergique dans cette co-morbidité (Frisina *et al.*, 2009). Des corps de Lewy ont également été observés dans le NRD (Ohama & Ikuta, 1976; Mann & Yates, 1983b; Sawada *et al.*, 1985; Halliday *et al.*, 1990).

Le tissu *post-mortem* peut également être utilisé afin de quantifier directement les niveaux de 5-HT et de ses métabolites par CLHP. Cette technique a permis de mettre en lumière une baisse de la 5-HT dans pratiquement toutes les composantes des ganglions de la base, incluant le striatum qui présente la baisse la plus marquée (60%) (Bernheimer *et al.*, 1961; Fahn *et al.*, 1971; Scatton *et al.*, 1983; Shannak *et al.*, 1994; Wilson *et al.*, 1996; Calon *et al.*, 2003; Kish *et al.*, 2008). Contrairement à ce qui est observé pour la DA (Fahn *et al.*, 1971), le noyau caudé montre des niveaux 5-HT beaucoup plus réduits que ce qui est observé dans le putamen (Kish *et al.*, 2008). D'autres baisses de 5-HT ont également été rapportées dans le thalamus et l'hypothalamus (Shannak *et al.*, 1994). Il est aussi possible d'observer ce phénomène dans différentes aires corticales (Scatton *et al.*, 1983).

Cette baisse marquée de 5-HT striatale a aussi été observée lors d'études *post-mortem* par liaison sur SERT, mais il est intéressant de noter que les niveaux de liaison semblent être conservés seulement dans les noyaux du raphé (Cash *et al.*, 1985; Raisman *et al.*, 1986; Chinaglia *et al.*, 1993; Rylander *et al.*, 2010). Des baisses de liaison au SERT dans le GP ont aussi pu être observées chez des patients présentant une réponse normale à la L-DOPA, comparativement aux patients ayant des DILs qui montrent une conservation de ces niveaux (Rylander *et al.*, 2010). Par contre, une étude par liaisons du neurotransmetteur 5-HT tritié a aussi permis d'observer une conservation des

niveaux dans le striatum et le GP (Reisine *et al.*, 1977). Une autre étude plus récente a rapportée une augmentation de l'immunomarquage dirigé contre SERT dans le striatum de patients parkinsoniens ainsi qu'une augmentation de la quantité de terminaisons axonales 5-HT dans cette structure (Bédard *et al.*, 2011). Cette dernière étude suggère, contrairement aux autres, que le nombre d'axones 5-HT se retrouvent augmenté dans le striatum. Par contre, cette augmentation n'impliquerait pas nécessairement une hausse des niveaux et de la transmission de 5-HT. Il est suggéré par les auteurs que les niveaux abaissés de liaison sur SERT observés *post-mortem* chez les patients parkinsoniens seraient dues à un état dépressif des patients parkinsoniens plutôt qu'à une perte modérée des axones 5-HT.

En somme, dans les phases précoces dans la maladie de Parkinson, il n'y aurait pas de mort cellulaire dans les noyaux du raphé. La présence de corps de Lewy dans ces structures, tel que décrit par Braak *et al.* (2003), ne serait donc pas nécessairement synonyme de neurodégénérescence. Les études *in vivo* et *post-mortem* des axones 5-HT quant à elles nous démontrent que, dans les phases précoces de la pathologie, il est possible d'observer une conservation, voir même, une augmentation de l'innervation 5-HT dans le striatum et le GP. Encore à ce jour, les mécanismes exacts et l'amplitude de ces phénomènes de bourgeonnement 5-HT sont méconnus. Les stades avancés de la maladie de Parkinson montrent, par contre, un tout autre portrait de l'état des systèmes 5-HT. Les études *post-mortem* et *in vivo* indiquent sans équivoque une mort cellulaire dans les différents noyaux du raphé plus particulièrement dans le NRD qui se soldent par la perte des axones 5-HT et donc une diminution de la disponibilité de SERT présent sur ces axones. L'innervation 5-HT des ganglions de la base semble également diminuée chez les patients avec une pathologie avancée. Ces données suggèrent fortement que la présence de corps de Lewy n'affecte pas directement les neurones du raphé, mais que le traitement chronique à la L-DOPA pourrait être en partie responsable de ce dérèglement majeur de la transmission 5-HT.

1.5.2. La sérotonine et les dyskinésies induites par la L-DOPA

La maladie de Parkinson est surtout connue pour sa composante DA. Cette dénervation striatale DA cause une multitude de changements neuroadaptatifs dans le système nerveux central. Les axones 5-HT sont capables d'une grande plasticité (Michelsen *et al.*, 2008) démontrée par la réorganisation massive qu'ils peuvent démontrer suite à une injure neurodégénérative majeure ou une greffe de neurones 5-HT (Berger *et al.*, 1985; Zhou *et al.*, 1991; Descarries *et al.*, 1992). Ces axones sont capables de conserver, chez l'adulte, la capacité de bourgeonner et de former de nouvelles connexions. De plus, les neurones 5-HT sont capable de libérer la DA *in vivo* (Hollister *et al.*, 1979b; Tanaka *et al.*, 1999b; Navailles *et al.*, 2010) et *in vitro* (Ng *et al.*, 1970a; 1972; Arai *et al.*, 1994; Arai *et al.*, 1995b; Arai *et al.*, 1996; Maeda *et al.*, 2005b). L'expression de l'AADC par ces neurones leur donne la capacité de métaboliser la L-DOPA en DA (Ng *et al.*, 1970a; Hollister *et al.*, 1979b; Arai *et al.*, 1995b). Cette synthèse est aussi accompagnée par la capacité d'emmagasiner la DA nouvellement synthétisée dans des vésicules synaptiques via le transporteur vésiculaire des monoamines de type 2 (VMAT2) exprimé par les neurones DA mais aussi par les neurones 5-HT (Miller & Abercrombie, 1999). Les preuves les plus convaincantes de la métabolisation de la L-DOPA exogène par les neurones 5-HT en contexte parkinsonien proviennent de modèles animaux qui implique une lésion DA ainsi qu'une lésion subséquente du système 5-HT te dans lesquels on observe une diminution significative de l'efficacité de la L-DOPA accompagnée d'une absence de changement en ce qui concerne les niveaux de DA dans le striatum (Tanaka *et al.*, 1999b; Navailles *et al.*, 2010). Il est aussi intéressant d'ajouter qu'une inhibition pharmacologique des neurones 5-HT avec des agonistes 5-HT_{1A} et 5-HT_{1B} produisent relativement le même effet, c'est-à-dire, une diminution de l'efficacité du traitement à la L-DOPA (Kannari *et al.*, 2001; Carta *et al.*, 2007b; Eskow *et al.*, 2007). Les

neurones 5-HT peuvent aussi participer à la recapture de la DA dans un striatum lourdement dénervé en DA (Kannari *et al.*, 2006).

Ces mécanismes et l'implication de la 5-HT dans la métabolisation de la L-DOPA en DA suggèrent fortement que ce système puisse être impliqué dans le développement des DILs. Ces mouvements anormaux chez les patients arrivent plus tardivement dans l'évolution de la maladie de Parkinson où la dénervation DA est la plus importante (Rajput *et al.*, 2002a). D'ailleurs, le degré de dénervation DA est l'un des premiers facteurs de développement des LIDs chez l'humain. Contrairement aux patients atteints de la maladie de Parkinson, des patients intoxiqués au MPTP ont développé presqu'immédiatement des DILs après un traitement à la L-DOPA (Langston *et al.*, 1984). Le même phénomène peut être observé chez des patients atteints d'une maladie génétique affectant la synthèse de DA indiquant du même coup que l'absence de DA endogène est un facteur important du développement des LIDs (Pons *et al.*, 2013). De plus, une autre étude a pu comparer 2 groupes de patients parkinsoniens au même stade symptomatologique de la maladie ; l'un des 2 avec un historique de traitement plus long à la L-DOPA. Les patients des 2 groupes ont développé des LIDs renforçant ainsi l'hypothèse que la progression de la maladie est un facteur important impliqué dans le développement des LIDs (Cilia *et al.*, 2014).

Il a pu être confirmé que la libération de DA par les neurones 5-HT est l'un des principaux facteurs présynaptiques du développement et du maintien des dyskinésies (Carta *et al.*, 2007b). Il est donc possible d'obtenir l'abolition complète des DILs après l'inhibition ou la lésion du système 5-HT (Carta *et al.*, 2007b; Eskow *et al.*, 2007). Ces affirmations sont appuyées par l'exacerbation des DILs dans les modèles animaux de la maladie de Parkinson après une greffe de neurones 5-HT dans le striatum créant ainsi une hyperinnervation 5-HT striatale (Carlsson *et al.*, 2007). Les hypothèses sur les mécanismes cellulaires et moléculaires en lien avec le développement des DILs sont nombreuses, mais la principale repose sur une libération non contrôlée de la

DA par les neurones 5-HT (voir Carta *et al.*, 2008b). Cette hypothèse soutient que, tant que des axones DA sont encore présents dans le striatum, la L-DOPA peut être métabolisée en DA par les axones DA et ensuite libérée de manière physiologique et contrôlée. La présence d'autorécepteur D_2 et de transporteur membranaire de la DA (DAT) assurant, respectivement, une rétroaction négative de la libération de DA et sa recapture. Lors d'une dénervation DA importante, le système 5-HT prend le relais de la conversion de la L-DOPA exogène en DA grâce à l'expression de l'AADC et de VMAT2 au sein des neurones 5-HT. Les axones 5-HT sont, cependant, dépourvus du transporteur membranaire DAT et de l'autorécepteur D_2, relâchant ainsi la DA nouvellement synthétisée, mais de manière non contrôlée (Voir figure 1.7.). Cette libération non contrôlée et ectopique pourrait même être amplifiée par le fait que la L-DOPA exogène est capable de significativement altérer à la baisse les niveaux de 5-HT dans les tissus striataux. Les autorécepteurs 5-HT inhibiteurs se retrouvent alors sous-activés augmentant du même coup la libération de DA par les neurones 5-HT qui présentent une activité augmentée (Everett & Borcherding, 1970; Carta *et al.*, 2007b). Ce phénomène serait l'un de déterminant présynaptique majeur du développement des DILs.

La relâche de DA par les neurones 5-HT affecte grandement les signaux de sorties du striatum. La relâche de DA exogène facilite les activités motrices en activant le NPS D_1 et en inhibant les NPS D_2. Le modèle actuel suppose que la réponse hyperkinétique à la L-DOPA est causée par une suractivation des récepteurs D_1 qui est considéré comme un des facteurs postsynaptiques les plus importants dans le développement des LIDs (Bastide *et al.*, 2015) (Voir figure1.6.). Il est d'ailleurs possible de réduire les LIDs dans des modèles animaux en faisant l'ablation des NPS D_1 (Révy *et al.*, 2014) ou en en réduisant leur activité pharmacologiquement (Engeln *et al.*, 2016).

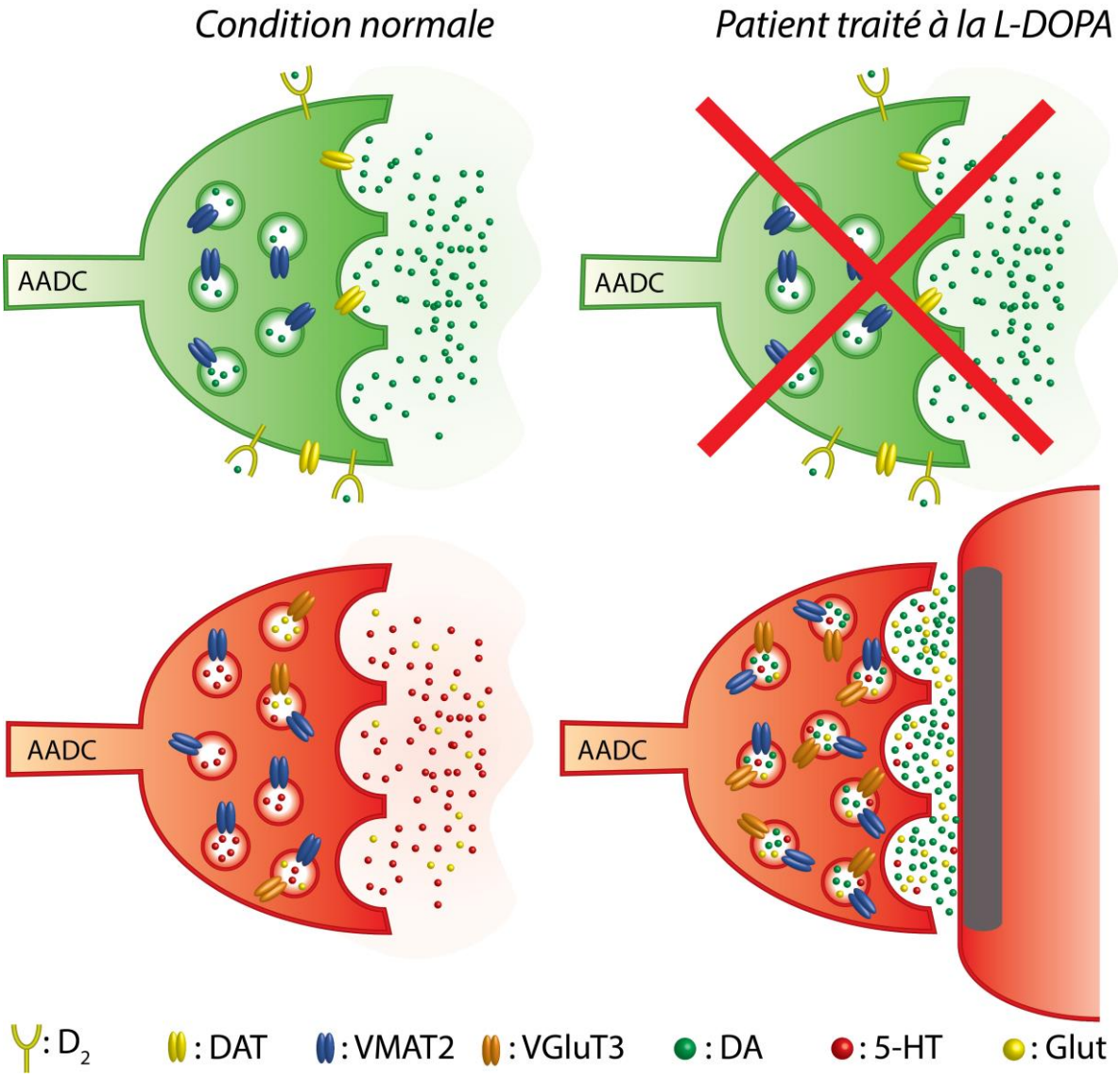

FIGURE 1.7. – Schématisation de la libération de DA et 5-HT striatale dans un contexte normal et parkinsonien lors d'un traitement à la L-DOPA.

1.5.3. Les changements du système sérotoninergique dans les modèles parkinsoniens

Innervation

L'étude de la plupart des maladies neurodégénératives passe souvent par le développement de modèles animaux permettant d'obtenir des résultats *in vivo* et ainsi, de mieux comprendre les différents mécanismes sous-jacents. La maladie de Parkinson a été étudiée par l'entremise d'une multitude de ces modèles qui sont d'ailleurs toujours utilisés à ce jour. La grande majorité de ceux-ci reposent sur une lésion DA induite par une neurotoxine spécifique aux neurones DA. Une grande partie de nos connaissances actuelles des différents mécanismes de la maladie de Parkinson s'appuient principalement sur ces modèles. La découverte du MPTP dans les années 80 a permis de révolutionner la recherche sur cette maladie et de populariser d'autres toxines comme la 6-hydroxydopamine (6-OHDA) (Langston *et al.*, 1984; Langston, 2017).

La dénervation DA induite par ces toxines permet de reproduire la plupart des symptômes moteurs de la maladie de Parkinson. Dans ce contexte, des changements concernant l'innervation 5-HT des ganglions de la base ont été rapportés. L'effet d'une importante perte de DA striatale sur l'innervation 5-HT semble varier d'une structure à l'autre et même d'un modèle animal à l'autre.

Typiquement, les lésions DA ne semblent pas affecter le nombre de neurones 5-HT dans les noyaux du raphé autant chez les rongeurs (Gupta *et al.*, 1984; Rylander *et al.*, 2010) que chez les primates (Langston *et al.*, 1984; Gaspar *et al.*, 1993a), malgré quelques indications contraires (Jaunarajs *et al.*, 2012), tout particulièrement après un traitement chronique à la L-DOPA (Stansley & Yamamoto, 2014). La littérature actuelle montre en général un effet plutôt modéré des différentes neurotoxines DA sur les neurones 5-HT (Friedman & Mytilineou, 1990). Cette toxicité spécifique des neurones DA est d'ailleurs une

caractéristique essentielle au développement de modèles animaux adéquats permettant de répliquer la principale caractéristique neuropathologique de la maladie de Parkinson. Une dénervation DA semble, par contre, altérer l'activité électrophysiologique des neurones 5-HT du NRD avec une augmentation marquée du taux de décharge. Ces changements sont très probablement secondaires à la diminution de l'innervation DA plutôt qu'à un effet direct des neurotoxines sur les neurones 5-HT (Zhang *et al.*, 2007; Wang *et al.*, 2009). Cette altération de l'activité électrophysiologique des neurones du NRD suggérerait une plus grande relâche de ce neurotransmetteur qui pourrait être aussi impliquée dans la plasticité que montre l'innervation 5-HT striatales et pallidales dont il sera question dans les prochains paragraphes.

Le sort des projections axonales 5-HT dans les modèles animaux est beaucoup plus controversé. Tel que mentionné plus haut, les axones 5-HT se projettent pratiquement sur toutes les structures importantes du système nerveux central. Le chamboulement causé par une dégénérescence importante du système DA affecte l'état de l'innervation 5-HT causant, très probablement, l'apparition de complications comme les DILs et les symptômes non-moteurs observés chez les patients parkinsoniens. Les modèles de rongeurs montrent en grande majorité un maintien de la densité des axones 5-HT. Les lésions à la 6-OHDA chez de jeunes rongeurs, plus particulièrement, induisent un bourgeonnement des axones 5-HT notamment dans le striatum, une observation qui n'a pu être répliquée chez les rats adultes (Breese *et al.*, 1984; Stachowiak *et al.*, 1984; Erinoff & Snodgrass, 1986; Snyder *et al.*, 1986; Luthman *et al.*, 1987; Towle *et al.*, 1989; Dewar *et al.*, 1990; Descarries *et al.*, 1992). La L-DOPA est aussi capable d'induire une augmentation du nombre de varicosités 5-HT dans le striatum chez le rat intoxiqué au MPTP. Cet effet s'est montré dose-dépendant (Rylander *et al.*, 2010). Ces résultats sont aussi appuyés par une augmentation des niveaux de 5-HIAA striatale chez les rats 6-OHDA dyskinétiques (Lindgren *et al.*, 2010). L'intoxication au MPTP a aussi pu générer un phénomène de bourgeonnement des axones 5-HT dans le striatum chez des souris (Rozas *et al.*, 1998).

Les modèles simiens de la maladie de Parkinson, quant à eux, montrent une plus grande variabilité des résultats en ce qui concerne l'innervation 5-HT du striatum. Après une intoxication au MPTP, il est possible d'observer chez ces animaux soit une baisse sévère des niveaux de 5-HT et de ses métabolites (Perez-Otano *et al.*, 1991; Russ *et al.*, 1991; Van Vliet *et al.*, 2006) ou plus légère (Riahi *et al.*, 2011). Il est aussi possible de constater une augmentation du nombre d'axones et de varicosités 5-HT striatales après une dénervation DA (Gaspar *et al.*, 1993a; Zeng *et al.*, 2010) aussi accompagnée par une hausse des concentrations de 5-HT (Schneider, 1990; Pifl *et al.*, 1991; Boulet *et al.*, 2008). Plusieurs autres groupes n'ont rapporté aucun changement de l'innervation 5-HT après une lésion DA chez les primates (Burns *et al.*, 1983; Di Paolo *et al.*, 1986; Huot *et al.*, 2012b). Il est intéressant de mentionner qu'un bourgeonnement des fibres 5-HT est le plus souvent associé à une récupération post-lésionnelle, comme il a pu être démontré par immunohistochimie (Mounayar *et al.*, 2007b) et par des mesures biochimiques (Boulet *et al.*, 2008). Ces variations de résultats peuvent être dues à des différences interspécifiques ainsi qu'à des régimes d'injection des neurotoxines DA différents. Il est intéressant de noter que la plupart de ces articles utilisent différentes approches afin de quantifier l'état du système 5-HT, ce qui peut expliquer une certaine variabilité des données obtenues.

De plus en plus d'intérêt est porté à l'innervation 5-HT du pallidum. En général, une conservation des axones 5-HT pallidaux est observée chez les singes intoxiqués au MPTP (Pifl *et al.*, 1991; Zeng *et al.*, 2010). Cette conservation se traduit par une augmentation du nombre de varicosités 5-HT avec un traitement chronique à la L-DOPA (Zeng *et al.*, 2010). D'un autre côté, des niveaux abaissés de liaison de citalopram ont été rapportés dans le GP de singes MPTP, ces mêmes niveaux revenant à la normale chez les singes présentant des DILs (Rylander *et al.*, 2010). L'innervation 5-HT du GP est importante dans l'expression de symptômes de rigidité chez le singe parkinsonien. Une lésion des axones 5-HT du GP chez le singe intoxiqué au

MPTP mène à l'apparition d'une rigidité plus importante, laissant croire qu'une libération pallidale de 5-HT puisse être impliquée dans des phénomènes compensatoires post-lésionnels (Beaudoin-Gobert *et al.*, 2015).

L'innervation du cortex par le système 5-HT est très étendue et diffuse. Cette innervation subit également des changements lors d'une dénervation DA. Chez les rongeurs, les résultats sont plutôt mitigés. Chez la souris MPTP, il semble y avoir une baisse de l'innervation 5-HT du cortex (Nayyar *et al.*, 2009). Chez le jeune rat, par contre, il est possible d'observer un bourgeonnement après une lésion 6-OHDA qui se traduit par une augmentation des métabolites de la 5-HT (Dewar *et al.*, 1990). Des résultats qui ne peuvent être reproduits chez le rat adulte (Jaunarajs *et al.*, 2010) ou même chez le rat néonatal lésé à la 6-OHDA (Erinoff & Snodgrass, 1986; Luthman *et al.*, 1987).

Il y a peu de données concernant les projections 5-HT corticales chez des modèles simiens de la maladie de Parkinson. Les articles disponibles semblent suggérer qu'il y a une réduction de l'immunoréactivité 5-HT (Masilamoni *et al.*, 2011) et des niveaux de métabolites de la 5-HT (Pifl *et al.*, 1991) dans le cortex cérébral.

En somme, l'innervation 5-HT du système nerveux central se retrouve grandement altérée dans les ganglions de la base après une lésion DA. Cette altération peut se présenter comme une baisse ou une augmentation de l'innervation 5-HT autant chez le patient parkinsonien que chez les modèles animaux de la maladie de Parkinson. Ces observations permettent de conclure que les systèmes 5-HT sont hautement plastiques et sont aptes à réagir rapidement à des changements fonctionnels des structures qu'ils innervent. Le rôle exact de ces modifications de l'arborisation axonale 5-HT dans la physiopathologie de la maladie de Parkinson reste toujours à élucider. L'ampleur de la réorganisation de la microcircuiterie 5-HT des ganglions de la base sera le sujet principal des chapitres 4 et 5.

Les récepteurs 5-HT

À ce jour, 14 sous-types de récepteurs 5-HT ont été identifiés appartenant à 7 classes distinctes (voir Nichols & Nichols, 2008). On identifie ces classes de récepteurs par une numérotation allant de 5-HT_1 à 5-HT_7. À l'exception des récepteurs 5-HT_3, tous les récepteurs 5-HT sont couplés à une protéine G. L'altération de l'innervation 5-HT tel qu'observée dans un contexte pathologique provoque d'importants changements concernant les récepteurs 5-HT distribués un peu partout dans le système nerveux central. Ces variations de l'expression et la localisation de ces récepteurs influencent très probablement le développement des symptômes moteurs et non-moteurs de la maladie de Parkinson.

5-HT_{1A}

Le récepteur 5-HT_{1A} fut l'un des premiers récepteurs 5-HT à avoir été caractérisé (voir Glennon, 1987). Ce récepteur est couplé à la protéine $G_{i/o}$ qui cause l'inhibition de l'adénylate cyclase, ce qui entraine une baisse de la production de l'adénosine monophosphate cyclique (AMPc). Ce récepteur est impliqué dans une grande variété de fonctions et de pathologies du système nerveux central. Il a été possible d'établir son rôle, par exemple, dans l'anxiété (Heisler *et al.*, 1998; Blier & Ward, 2003; Toth, 2003), la dépression (Drevets *et al.*, 1999; Blier & Ward, 2003; Overstreet *et al.*, 2003), la schizophrénie (Burnet *et al.*, 1996) et la dépendance aux drogues (Müller *et al.*, 2007).

Comme le suggère la pluralité de ses rôles, le récepteur 5-HT_{1A} est vastement distribué dans le système nerveux central. Les concentrations les plus élevées sont retrouvées dans l'hippocampe, le septum, l'amygdale, le cortex ainsi que dans les noyaux du raphé (Hoyer *et al.*, 1985; Pazos & Palacios, 1985; Köhler *et al.*, 1986; Pazos *et al.*, 1987b; Waeber *et al.*, 1989). Dans le NRD, ces récepteurs sont surtout localisés sur le domaine somatodendritique des neurones 5-HT. En tant qu'autorécepteur, ils agissent afin de produire une rétroaction négative suite à la libération de 5-HT (Verge *et al.*, 1985; Vergé *et*

al., 1986; Sotelo *et al.*, 1990). Ainsi, l'activation de ce récepteur par la 5-HT mène à la diminution de l'activité électrophysiologique des neurones des noyaux du raphé (Van der Maelen *et al.*, 1986; Sprouse & Aghajanian, 1987; Sprouse & Aghajanian, 1988). Cette inhibition des neurones du NRD provoque une baisse des niveaux de 5-HT dans les différentes cibles (Kreiss & Lucki, 1994; Knobelman *et al.*, 2000). Ailleurs que dans les noyaux du raphé, leurs récepteurs 5-HT_{1A} se présentent comme hétérorécepteurs et leur activation conduit aussi à une diminution de l'activité électrophysiologique des neurones postsynaptiques qui l'expriment (Kia *et al.*, 1996a; Kia *et al.*, 1996b).

L'expression du récepteur 5-HT_{1A} se retrouve particulièrement affectée dans un contexte parkinsonien. La littérature actuelle montre très peu de changement du récepteur 5-HT_{1A} chez des rongeurs néonataux lésés à la 6-OHDA dans les ganglions de la base (Radja *et al.*, 1993; Numan *et al.*, 1995). Par contre, l'expression de ce récepteur change de manière importante lors d'une dénervation DA chez les primates non-humains. Sans aucune thérapie de remplacement DA, les augmentations de l'expression du récepteur 5-HT_{1A} se font dans les striosomes du noyau caudé (Frechilla *et al.*, 2001; Huot *et al.*, 2012a) et dans les couches médianes du cortex moteur (Huot *et al.*, 2012a). Une baisse d'expression de 5-HT_{1A} a aussi été observée dans le cortex cingulé antérieur (Sanchez *et al.*, 2011) ainsi que dans les couches superficielles du cortex moteur (Huot *et al.*, 2012a). Suite à un traitement chronique à la L-DOPA, des augmentations d'expression de ce récepteur dans la matrice du noyau caudé ont aussi été rapportées (Huot *et al.*, 2012a).

L'expression de ce récepteur varie aussi chez les patients parkinsoniens. Plusieurs études semblent démontrer que ces variations se produisent surtout dans le cortex cérébral (Ballanger *et al.*, 2012). Il est toutefois important de mentionner que le niveau d'expression de ce récepteur semble diminuer dans les noyaux du raphé (Doder *et al.*, 2003). Par contre, les études *in vivo* et *post-mortem* sont contradictoires sur l'élévation ou la baisse de l'expression du récepteur 5-HT_{1A} (Sharp *et al.*, 2008).

Les variations d'expression de ce récepteur dans la maladie de Parkinson laissent croire que le récepteur 5-HT_{1A} est très probablement impliqué dans l'expression des troubles moteurs de la maladie de Parkinson et des DILs. L'influence que le récepteur 5-HT_{1A} peut avoir sur la libération de différents neurotransmetteurs impliqués dans la pathophysiologie de la maladie a conduit plusieurs laboratoires à le considérer comme une cible thérapeutique de choix pour traiter les symptômes de la maladie de Parkinson.

Une étude complète à partir d'agonistes 5-HT_{1A} n'a pas pu être convenablement effectuée puisque la plupart des molécules disponibles sont peu spécifiques et affectent donc plusieurs autres sous-types de récepteurs (voir Huot *et al.*, 2011a). Par exemple, l'injection de l'agoniste 8-OH-DPAT de manière systémique, dans le striatum (Bishop *et al.*, 2009) et les noyaux du Raphé (Eskow *et al.*, 2009) conduit à une réduction des dyskinésies dans un modèle de rongeurs de la maladie de Parkinson, sans diminuer l'action antiparkinsonien de la L-DOPA. Les mécanismes par lesquels les récepteurs 5-HT_{1A} pourraient jouer ce rôle sont nombreux. Tout d'abord, il a été montré que l'administration systémique d'un agoniste 5-HT_{1A} serait en mesure de diminuer la libération de DA par les neurones 5-HT lors d'un traitement à la L-DOPA (Kannari *et al.*, 2001). Ce phénomène peut être expliqué par l'activation des autorécepteurs inhibiteurs 5-HT_{1A} dans les noyaux du raphé. Il a ensuite été montré que l'administration locale d'agonistes dans les noyaux du raphé est suffisante pour réduire les DILs (Eskow *et al.*, 2009). D'un autre côté, l'administration d'un antagoniste 5-HT_{1A} augmente la sévérité des dyskinésies (Eskow *et al.*, 2009). La baisse de l'excitabilité des corps cellulaires 5-HT pourrait ainsi venir réduire la quantité de DA relâchée dans le striatum lors d'un traitement de remplacement DA. Cette particularité pourrait expliquer, en partie, pourquoi plusieurs drogues antidyskinétiques, lorsque co-administrée avec la L-DOPA, diminue l'action antiparkinsonienne de la L-DOPA.

L'administration locale d'un agoniste 5-HT_{1A} dans le striatum permet d'atténuer à la fois les DILs et les symptômes parkinsoniens (Bishop *et al.*, 2009). Par exemple, on pense que l'administration de 8-OH-DPAT dans le striatum permet d'atténuer les effets des signaux glutamatergiques pathologiques en provenance du cortex cérébral (Mignon & Wolf, 2005). L'effet exercé par l'activation des récepteurs 5-HT_{1A} est donc très probablement dû à une activité sur les récepteurs présynaptiques, localisés sur les terminaisons glutamatergiques, ainsi qu'à une activité sur les récepteurs postsynaptiques (Bishop *et al.*, 2009). Il a été montré dans plusieurs études que la signalisation glutamatergique est hyperactive lors de l'expression des DILs (voir Bezard *et al.*, 2001a). Il serait alors possible que la stimulation du récepteur 5-HT_{1A} dans le striatum vienne régulariser la libération de glutamate provenant du cortex cérébral. Cette normalisation des entrées striatales glutamatergiques pourrait expliquer l'amélioration des dyskinésies lors d'un traitement avec un agoniste 5-HT_{1A}.

En somme, la stimulation du récepteur 5-HT_{1A} provoque une multitude de changements physiologiques dans le cerveau. L'utilisation d'agonistes dans le but d'atténuer les DILs s'est montrée encourageante lors d'essais précliniques. Par contre, nous sommes actuellement dans l'incapacité de reproduire ces effets bénéfiques dans les études cliniques (voir Huot & Fox, 2013) dû probablement aux différences inhérentes entre les modèles animaux et la maladie de Parkinson. Le récepteur 5-HT_{1A} reste quand même une cible thérapeutique des plus intéressantes dans le traitement des DILs. Malheureusement, à l'heure actuelle, le manque de spécificité des molécules disponibles fait en sorte que nous ne sommes pas en mesure de conclure de façon définitive à son efficacité.

5-HT_{1B}

Le récepteur 5-HT_{1B} fait partie de la même famille que 5-HT_{1A}. Il est aussi lié à une protéine $G_{i/o}$, ce qui lui permet d'inhiber la production d'AMPc. Ce récepteur est impliqué dans une grande variété de comportements tels que la

satiété (Lee & Simansky, 1997), l'apprentissage (Malleret *et al.*, 1999; Åhlander-Lüttgen *et al.*, 2003), l'impulsivité (Saudou *et al.*, 1994; Ramboz *et al.*, 1995) et la locomotion (Oberlander *et al.*, 1986; Oberlander *et al.*, 1987; Ramboz *et al.*, 1995). Le récepteur 5-HT_{1B} se retrouve en plus grande quantité dans le GP, le striatum ventral et le cortex occipital. Il est aussi possible d'observer sa présence en moins grande concentration dans le cortex frontal ainsi que temporal et dans le striatum dorsal (Bonaventure *et al.*, 1997; Bonaventure *et al.*, 1998a; Castro *et al.*, 1998; Riad *et al.*, 2000; Varnäs *et al.*, 2001; Sari, 2004b; Mostany *et al.*, 2005a; Varnäs *et al.*, 2011). Le récepteur 5-HT_{1B} peut se présenter comme un autorécepteur particulièrement présent sur les terminaisons 5-HT, au niveau présynaptique. L'activation de celui-ci est en mesure d'inhiber significativement la libération de 5-HT (Middlemiss, 1984; Engel *et al.*, 1986; Martin *et al.*, 1992; Knobelman *et al.*, 2000; Rutz *et al.*, 2006). Le récepteur 5-HT_{1B} peut aussi se présenter comme un hétérorécepteur sur les axones GABAergiques innervant les ganglions de la base (Tanaka & North, 1993; Sari *et al.*, 1999). D'ailleurs, les interactions du récepteur 5-HT_{1B} avec les ganglions de la base sont nombreuses. Son influence sur le striatum est importante puisqu'il module l'activité des neurones DA de la SNc (Benloucif *et al.*, 1993; Sarhan *et al.*, 2000)

Actuellement, le rôle du récepteur 5-HT_{1B} dans la physiopathologie de la maladie de Parkinson n'est pas très bien connu. Aucune augmentation n'a été révélée chez le rongeur après une déplétion DA seule (Zhang *et al.*, 2008). Contrairement, une lésion effectuée chez des rats néonataux provoque une augmentation significative de l'expression de ce récepteur dans le striatum, le GP et la SNr (Radja *et al.*, 1993). De plus, un traitement à la L-DOPA chez le rongeur adulte va mener à une surexpression de 5-HT_{1B} par les NPS striatonigraux (Zhang *et al.*, 2008).

La stimulation du récepteur 5-HT_{1B} a sans aucun doute un effet antidyskinétique chez les rongeurs (Carta *et al.*, 2007b; Zhang *et al.*, 2008). L'inhibition présynaptique des axones 5-HT striatales fait en sorte que la DA

nouvellement synthétisée par les neurones 5-HT pourrait être relâchée de façon moins importante dans le striatum. Ainsi, les agonistes 5-HT_{1B} influencent les niveaux de DA striatale, un peu de la même manière que le font les agonistes 5-HT_{1A}, c'est-à-dire en réduisant la relâche de neurotransmetteur par les axones 5-HT. Il est intéressant de mentionner que l'utilisation de faibles doses d'agonistes pour 5-HT_{1A} et 5-HT_{1B} semble procurer un effet synergique dans le traitement des DILs (Carta *et al.*, 2007b). Cette synergie s'expliquerait par la distribution complémentaire des deux autorécepteurs sur les neurones 5-HT. Selon l'auteur, les effets antidyskinétiques s'expliqueraient seulement par l'inhibition de la libération de DA par les neurones 5-HT. D'un autre côté, le groupe de Svenningsson ajoute que l'utilisation d'agonistes 5-HT_{1B} pourrait aussi inhiber l'activité des NPS striatonigraux ce qui pourrait expliquer en partie les effets antidyskinétiques induits par l'activation de ce récepteur (Zhang *et al.*, 2008).

5-HT_{2A}

Le récepteur 5-HT_{2A} est un récepteur associé à $G\alpha_q$. L'activation de celui-ci mène à une augmentation de l'activité de la phospholipase C initiant une cascade signalétique stimulant l'activité de la protéine kinase C et la libération de calcium (voir Barnes & Sharp, 1999).Ce récepteur est particulièrement impliqué dans des fonctions comme la cognition (de Quervain *et al.*, 2003; Lai *et al.*, 2005; Landolt & Wehrle, 2009) et le mouvement (Halberstadt *et al.*, 2009) ou des pathologies comme la dépression (Arias *et al.*, 2001), l'anxiété (Weisstaub *et al.*, 2006) et l'hyperactivité (Quist *et al.*, 2000). Ce récepteur est vastement distribué dans le système nerveux central. La plus haute concentration se trouve dans plusieurs aires corticales, surtout dans la couche V qui contient une densité importante d'axones 5-HT (Pazos *et al.*, 1987a; Blue *et al.*, 1988). Les concentrations retrouvées dans les ganglions de la base sont plus faibles que celles retrouvées dans le cortex cérébral (Wong *et al.*, 1987; Varnäs *et al.*, 2004). On retrouve des densités de récepteurs 5-HT_{2A} relativement hétérogènes dans les différentes composantes des ganglions de la base. Le GP et le NST montrent des concentrations de récepteurs 5-HT_{2A} les

plus faibles, tandis que le striatum et la SN présentent les concentrations les plus élevés chez le singe macaque et chez l'humain (Varnäs *et al.*, 2004; Riahi *et al.*, 2011; Huot *et al.*, 2012b). Le récepteur 5-HT_{2A} est principalement considéré comme étant un hétérorécepteur postsynaptique qui se retrouve sur les dendrites et sur le soma des neurones (Cornea-Hébert *et al.*, 1999). Cependant, il est également possible de le retrouver sur les axones corticostriés (Bubser *et al.*, 2001).

Les changements d'expression du récepteur 5-HT_{2A} lors d'une dénervation DA sans traitement à la L-DOPA sont différents selon le modèle animal utilisé. Plusieurs études ont été faites chez les rongeurs. Les auteurs ont pu observer une surexpression du récepteur 5-HT_{2A} dans le striatum ainsi que dans le cortex cérébral chez des modèles parkinsoniens (Résumé dans Huot *et al.*, 2011a). Par contre, chez le singe aucune différence n'a pu être observée (Riahi *et al.*, 2011; Huot *et al.*, 2012b).

Les résultats se montrent plus intéressants lorsqu'il y a une thérapie de remplacement DA. Les niveaux de récepteurs 5-HT_{2A} augmentent significativement dans les couches médianes du cortex moteur ainsi que dans le noyau caudé et le putamen chez les singes MPTP (Huot *et al.*, 2012b). Par contre, une autre étude montre des élévations seulement dans le cortex cérébral et dans le noyau caudé, chez des singes dyskinétiques (Riahi *et al.*, 2011).

Ces changements dans l'expression du récepteur 5-HT_{2A} peuvent nous laisser croire qu'il puisse être impliqué dans l'expression des DILs. Les dyskinésies, tel que mentionné plus haut, sont caractérisées par une hyperactivité des projections corticostriées glutamatergiques. Le rôle facilitateur qu'exerce le récepteur 5-HT_{2A} sur la libération de glutamate fait en sorte qu'il soit probablement important dans l'hyperactivité de ces afférences. Il est alors probable que l'inhibition de ce récepteur à l'aide d'un antagoniste spécifique soit en mesure de normaliser l'activité des afférences corticostriées

glutamatergiques. Le groupe de Brotchie soulève aussi une hypothèse intéressante stipulant que l'augmentation des niveaux de 5-HT_{2A} dans la SNc puisse signifier une transmission nigrostriée DA anormale chez les primates non-humains dyskinétiques menant à exacerbation de la stimulation pulsative des récepteurs DA striataux, un mécanisme important dans la pathophysiologie des dyskinésies (Huot *et al.*, 2011b; Huot *et al.*, 2012b).

L'inhibition de l'activité du récepteur 5-HT_{2A} pourrait aussi représenter une cible thérapeutique intéressante pour diminuer les DILs. Par contre, ce genre de traitement aurait probablement comme effet de réduire la libération de DA par les axones nigrostriés restants, en agissant sur les récepteurs 5-HT_{2A} localisés sur les neurones de la SNc, réduisant ainsi l'effet antiparkinsonien de la L-DOPA. D'un autre côté, un antagoniste 5-HT_{2A} permettrait de régulariser l'activité des projections glutamatergiques corticostriées, réduisant ainsi les dyskinésies.

5-HT_4

Le récepteur 5-HT_4 est lié à la protéine G_S. Son activation mène donc à une augmentation de la concentration d'AMPc intracellulaire (Dumuis *et al.*, 1988). Il est impliqué dans la mémoire (Terry Jr *et al.*, 1998; Lamirault & Simon, 2001; Lelong *et al.*, 2001), les fonctions gastro-intestinales (voir Gershon, 2005) et joue un rôle important dans la vulnérabilité face aux crises d'épilepsie (Compan *et al.*, 2004). Les plus hautes concentrations de ce récepteur, telles que mesurées en radio-liaison, se trouvent dans les ganglions de la base (Bonaventure *et al.*, 2000). Cette distribution est relativement semblable chez le rat et l'humain (Ullmer *et al.*, 1996; Vilaró *et al.*, 1996). Des études par lésions ont permis de montrer que le récepteur 5-HT_4 est principalement un hétérorécepteur qui se situe préférentiellement sur les neurones de projections GABAergiques du striatum (Patel *et al.*, 1995; Compan *et al.*, 1996).

Le récepteur 5-HT_4 est surement un des récepteurs 5-HT les moins étudiés dans la maladie de Parkinson. Deux études chez les rongeurs ont permis

d'obtenir des résultats bien différents. Premièrement, une lésion 6-OHDA chez le rongeur n'a démontré aucun changement significatif en ce qui concerne l'expression du récepteur 5-HT_4 dans les ganglions de la base (Patel *et al.*, 1995). Lors de la deuxième étude réalisée avec le même modèle animal, il a été possible de mettre en lumière des augmentations de l'expression du récepteur 5-HT_4 dans le striatum caudal et dans le GP ipsilatéral à la lésion (Compan *et al.*, 1996). Les études *post-mortem* chez les patients parkinsoniens n'ont pu démontrer de changement significatif par rapport au groupe contrôle en ce qui concerne la densité de récepteur 5-HT_4 (Reynolds *et al.*, 1995; Wong *et al.*, 1995).

Le récepteur 5-HT_4 a été longtemps considéré comme une cible de choix pour atténuer les DILs. Son influence sur le comportement moteur a été mis en évidence par l'effet d'un antagoniste 5-HT_4 diminuant significativement l'hyperactivité induite par la cocaïne (McMahon & Cunningham, 1999). Par contre, aucune étude clinique à ce jour n'a pu montrer un effet bénéfique sur les symptômes moteurs de la maladie de Parkinson, la prise d'agonistes 5-HT_4 amplifiant même les tremblements chez certains patients (Sempere *et al.*, 1995). Dans les études cliniques qui ont été réalisées jusqu'à présent, on a surtout utilisé les agonistes 5-HT_4 pour leur capacité à stimuler la motilité intestinale afin de soulager les problèmes de constipation dont souffrent les patients parkinsoniens (Jost & Schimrigk, 1993; 1997). De plus, on s'est aperçu que l'amélioration du transit intestinal avec un agoniste 5-HT_4 s'accompagnait d'une réduction des fluctuations motrices inhérentes à un traitement chronique à la L-DOPA (Asai *et al.*, 2005). Par contre, les principaux agents prokinétiques de l'intestin agissant sur 5-HT_4, le cisapride et mosapride, ont été retirés du marché aux États-Unis dû à une cardiotoxicité (voir Cloud & Greene, 2011).

1.5.4. La sérotonine et les symptômes non moteurs

La 5-HT est un neuromodulateur qui est impliqué dans une multitude de fonctions. Lors d'une insulte neurodégénérative majeure comme dans la maladie de Parkinson, le fonctionnement du système 5-HT est altéré. L'un des symptômes non-moteurs potentiellement lié à l'activité des neurones 5-HT dans le maladie de Parkinson est la dépression majeure. La prévalence des dépressions majeures est de 17% alors que celle des dépressions mineures est de 22% chez les patients parkinsoniens (Reijnders *et al.*, 2008). De manière intéressante, il semble que les personnes ayant reçu un diagnostic de dépression au cours de leur vie sont plus susceptibles de développer la maladie de Parkinson (Nilsson *et al.*, 2001; Schuurman *et al.*, 2002). Certains auteurs supposent l'implication d'un phénomène de neurodégénérescence dans les noyaux du raphé qui précède l'expression des symptômes moteurs, tel que le suggère l'hypothèse de Braak (Braak *et al.*, 2003a). Les mécanismes exacts du développement de la dépression chez les patients parkinsoniens sont encore relativement méconnus et la littérature actuelle ne s'entend pas sur l'implication de la 5-HT. Les études *in vivo* n'ont pu établir une corrélation directe entre les niveaux d'activité de SERT et la dépression dans la maladie de Parkinson (Kim *et al.*, 2003; Politis *et al.*, 2010b). Par contre, ces conclusions sont réfutées par des études *post-mortem* qui voient un lien entre l'état général du système 5-HT et la dépression chez les patients (Mayeux *et al.*, 1984; Paulus & Jellinger, 1991). De plus, une quantité significative de dépression chez ces patients semble résister aux antidépresseurs normaux ce qui pourrait suggérer un rôle limité de la 5-HT dans la pathophysiologie de la dépression majeure chez les patients parkinsoniens (Weintraub *et al.*, 2005).

Les patients parkinsoniens sont aussi plus susceptibles de développer des psychoses avec près de 40% des patients qui présenteront des hallucinations visuelles (Fénelon *et al.*, 2000; voir Ravina *et al.*, 2007). L'implication de la 5-HT pourrait se faire via une interaction entre les processus neuropathologiques et l'effet de la médication antiparkinsonienne (voir Fox *et al.*, 2009). La 5-HT est souvent impliquée dans les hallucinations visuelles dans la prise de drogue

comme le LSD (Bennett & Aghajanian, 1974) ou dans des pathologies comme la schizophrénie (Joyce *et al.*, 1993; Breier, 1995; Burnet *et al.*, 1996). Dans le cadre de la maladie de Parkinson, il semble que le récepteur 5-HT_{2A} dans le cortex cérébral soit particulièrement impliqué dans le développement des hallucinations visuelles (Ballanger *et al.*, 2010). Il est aussi intéressant de mentionner que l'expression de ce récepteur se retrouve augmentée dans le cortex orbitofrontal et temporal chez les patients parkinsoniens (Chen *et al.*, 1998).

Il est connu que les personnes souffrant de la maladie de Parkinson ont une motilité gastro-intestinale réduite menant à des complications qui mènent le plus souvent à la constipation. Actuellement, il est supposé que la cause de ces constipations serait principalement la perte de l'innervation parasympathique du tract gastro-intestinal provenant du noyau moteur du nerf vague (Wakabayashi *et al.*, 1990). Il est d'ailleurs suggéré que le système 5-HT périphérique se retrouverait impliqué dans ce phénomène et que l'innervation 5-HT pourrait se retrouvé altéré dans le système nerveux entérique (voir Fox *et al.*, 2009). L'action d'un agoniste 5-HT_4 permet de palier à ces symptômes en stimulant directement la relâche d'ACh dans le système nerveux entérique (Inui *et al.*, 2002).

Ces quelques exemples des symptômes non-moteurs de la maladie de Parkinson permettent de démontrer l'implication des axones 5-HT dans l'apparition de ceux-ci. Les mécanismes exacts par lesquels l'innervation 5-HT est capable d'influencer ces manifestations de la maladie sont, par contre, encore inconnus d'où l'importance d'étudier en détail la réorganisation que subissent ces axones dans un contexte parkinsonien.

1.6. Problématique de recherche

Les ganglions de la base jouent un rôle primordial dans le contrôle du mouvement. Au centre de cette circuiterie, la DA permet de moduler l'activation du mouvement. La dégénérescence de l'innervation DA dans la maladie de Parkinson perturbe un équilibre fragile rendant l'initiation des actions motrices beaucoup plus laborieuse. Le cerveau est un organe plastique, capable de se réorganiser et de répondre à une insulte majeure comme une dégénérescence telle qu'observée dans la maladie de Parkinson. Les études disponibles ont permis d'établir un portrait général des phénomènes compensatoires par, en grande partie, des immunomarquages et des quantifications biochimiques *in vivo* et *in vitro*. Cependant, peu d'études morphologiques fines et stéréologiques sont actuellement disponibles, autant chez les primates et que chez les rongeurs. De telles études permettent de dresser un portrait juste et précis de l'état de la microcircuiterie des ganglions de la base. Elles permettent également d'obtenir une vision détaillée de l'organisation neuroanatomique des neurones en identifiant les cibles ainsi que le degré de collatéralisation des axones et en décrivant avec précision l'état de l'organisation somatodendritiques. Ces observations permettent, du même coup, de mettre en lumière le rôle de ces neurones dans la physiopathologie de la maladie de Parkinson.

1.7. Objectifs de recherche

1.7.1. Objectifs généraux

Cette thèse de doctorat a pour but de mieux comprendre l'organisation anatomique des ganglions de la base et de caractériser les changements morphologiques qui affectent cette microcircuiterie dans la maladie de Parkinson. Les objectifs généraux de ces projets étaient : (1) Décrire de manière précise l'innervation 5-HT des ganglions de la base chez l'humain et le singe en condition normative, (2) d'établir un portrait complet de l'arborisation axonale des projections efférentes des neurones du NRD chez le rat, (3) de caractériser les changements morphologiques des axones 5-HT innervant le striatum et le GP chez le singe parkinsonien, (4) et de caractériser la réorganisation du domaine somatodendritiques des NPS du striatum après une lésion DA.

1.7.2. Objectifs spécifiques

Les objectifs spécifiques de mon projet de doctorat sont multiples. Tout d'abord, il était question de décrire l'innervation à 5-HT des ganglions de la base chez l'humain par l'utilisation de marquages immunohistochimiques. Ceux-ci ont permis de (1) décrire les différentes voies empruntées par le système 5-HT et de (2) caractériser l'innervation 5-HT des différentes structures composant les ganglions de la base chez l'humain.

Ensuite, cette thèse avait pour but de reconstruire l'arborisation axonale des neurones du NRD en mode neuronal unitaire. L'hypothèse de départ stipulait que les neurones 5-HT seraient munis d'un axone fortement arborisé dans lequel se distribue de manière hétérogène le VGLUT3. Ces reconstructions ont permis (1) d'apporter la première description détaillée des projections efférentes du NRD et de (2) caractériser la distribution du transporteur VGLUT3 au sein de ses axones fortement collatéralisés.

Une partie de cette thèse de doctorat avait pour but de quantifier l'innervation 5-HT et DA dans le striatum et le GP chez le singe contrôle et parkinsonien. La littérature antérieure nous permettait de formuler l'hypothèse que ces innervations subissaient probablement une réorganisation massive suite à une dénervation DA sous la forme d'un bourgeonnement axonal et de changements majeures de leur morphologie ultrastructurelle. La quantification de l'innervation 5-HT nous a permis de (1) présenter un modèle précis de l'organisation chimioanatomique des projections 5-HT striatales ainsi que pallidales chez le singe, (2) de caractériser la réorganisation des systèmes 5-HT suites à la dégénérescence des axones DA et (3) déterminer l'influence de ces phénomènes compensatoires sur l'ultrastructure des varicosités axonales.

La dernière partie de cette thèse a pour objectif de reconstruire le domaine somatodendritique de NPS du striatum et d'observer les changements suite à une lésion DA chez la souris. Notre hypothèse de départ était que les NPS qui expriment à la fois les récepteurs D_1 et D_2 forment probablement une population distincte de NPS par rapport à leur morphologie ainsi que par leur distribution. Il était aussi supposé que ces neurones pouvaient subir des changements morphologiques après une dénervation DA du striatum. Ces reconstructions ont conduit à (1) décrire la distribution et la morphologie de cette nouvelle sous-population de NPS, et (2) décrire l'effet d'une lésion DA sur l'arborisation dendritique et sur la distribution de ces neurones.

1.8. Approches méthodologiques

Les données présentées dans cette thèse ont été obtenues grâce à l'utilisation d'une grande variété de techniques neuroanatomiques. Une grande partie des résultats présentés repose sur l'immunohistochimie seule ou en combinaison avec d'autres approches morphologiques, comme le traçage unitaire des projections axonales. Cette technique nous permet de marquer précisément certaines protéines à l'aide d'anticorps spécifiques. Dans le cas échéant, elle nous a aidé à identifier la localisation de certaines protéines comme le VGLUT3

à l'intérieur d'axones. L'identification du type de neurotransmetteur libéré par les axones est cruciale afin de pouvoir étudier spécifiquement une innervation, comme par exemple, la 5-HT ou DA. L'immunohistochimie nous a aussi permis, comme dans le cas de l'article présenté dans le chapitre 2, de décrire les différentes voies qu'empruntent les axones 5-HT dans le cerveau humain afin d'innerver les ganglions de la base.

L'article qui vous sera présenté dans le chapitre 3 contient des données qui ont été obtenues suite à l'injection par microiontophorèse d'un traceur antérograde (Biotine dextran amine). L'injection se fait *in vivo* et est guidée par des enregistrements électrophysiologiques qui augmentent grandement la précision des injections. Cette technique nous permet d'injecter des volumes infimes de traceur marquant ainsi seulement un nombre limité de neurones et leurs axones. Contrairement à des injections par pression de traceurs qui marquent un plus grand nombre de neurones, les injections par microiontophorèse rendent possible le traçage de manière unitaire des axones marqués. Ces reconstructions axonales tridimensionnelles apportent une description avec un niveau de détail inédit des projections de certaines structures du système nerveux central.

L'observation au microscope optique seule de ce genre d'immunomarquage ne nous permet pas de quantifier avec précision l'innervation de certains axones dans une structure donnée. La stéréologie, d'un autre côté, pallie à cet obstacle en nous permettant de quantifier à la fois les longueurs d'axones et le nombre de sites de libération (varicosités ou terminaisons axonales) à l'intérieur d'une région cérébrale donnée, avec une très grande précision. Cette technique d'estimation consiste à effectuer un échantillonnage non-biaisé de la structure et d'une identification à la main des éléments neuronaux à quantifier. Les résultats générés sont reproductibles et d'une fiabilité quantifiable (coefficient d'erreur calculable) lorsque l'expérimentation est bien planifiée.

Dans le cadre de mes travaux, l'immunohistochimie a aussi été combinée avec la microscopie électronique. Cette approche nous permet de faire une description détaillée de l'ultrastructure des varicosités axonales d'un sous-type d'axones donné. Les paramètres mesurés sont l'aire, le diamètre, le nombre de mitochondries ainsi que la présence de synapses et la longueur de celles-ci. Ces mesures nous permettent, par la suite, d'estimer l'incidence synaptique. Cette mesure est particulièrement importante dans le cadre d'étude sur des neuromodulateurs comme la 5-HT et la DA qui utilisent en grande partie un mode de libération volumique (sans spécialisation membranaire pré ou postsynaptique). Une étude complète en microscopie électronique permet d'identifier les changements morphologiques fins concernant une innervation identifiée chimiquement, en comparant différentes structures ou conditions expérimentales.

D'autres approches ont aussi été utilisées afin de visualiser des populations spécifiques de neurones. Tout d'abord, des injections intracellulaires de traceurs fluorescents sur tranches fixées m'ont permis de marquer le domaine somatodendritique de NPS du striatum. Cette technique combinée à l'utilisation d'une souris transgénique exprimant des protéines fluorescentes a rendu possible le marquage de sous-populations spécifiques de neurones de projections du striatum et d'observer les changements morphologiques qu'ils subissent dans un modèle expérimental de la maladie de Parkinson.

Afin de pouvoir étudier en détails les conséquences d'une dénervation DA sur l'organisation anatomique et neurochimique de la microcircuiterie des ganglions de la base, nous avons utilisé des modèles animaux. Ces modèles reposent principalement sur des lésions spécifiques des neurones DA dans le but de reproduire certains déficits moteurs. Ces modèles expérimentaux ont été présentés plus haut. Les deux toxines utilisées dans le cadre de mes travaux sont la 6-OHDA et le MPTP. L'injection *in vivo* de la 6-OHDA chez la souris s'est faite dans le faisceau prosencéphalique médian manière unilatérale provoquant ainsi une lésion ipsilatérale des projections DA striatales. Chez les

singes, le syndrome parkinsonien a été induit par l'administration systémique de MPTP, produisant ainsi une mort cellulaire des neurones DA. La dégénérescence obtenue reproduit fidèlement les patrons de dégénérescence observés chez les patients atteints de la maladie de Parkinson.

CHAPITRE 2:

SEROTONIN INNERVATION OF HUMAN BASAL GANGLIA

CHAPITRE 2- *SEROTONIN INNERVATION OF HUMAN BASAL GANGLIA*

Marie-Josée Wallman, Dave Gagnon, Martin Parent

Centre de recherche CERVO
2601, Ch. de la Canardière, Québec, Québec
Canada G1J 2G3

European Journal of Neuroscience (2011) 33: 1519-1532

2.1. Résumé

Cette étude procure la toute première description détaillée de l'innervation sérotoninergique (5-HT) des ganglions de la base chez l'humain, en condition normale. Nous avons utilisé une approche immunohistochimique sur du tissu *post-mortem* avec des anticorps dirigés contre le transporteur de la sérotonine et l'enzyme de synthèse de la 5-HT (tryptophane hydoxylase) afin de visualiser respectivement les axones et les corps cellulaires 5-HT. Des sections adjacentes ont été immunomarquées à la tyrosine hydroxylase dans le but de pouvoir comparer la distribution des axones 5-HT avec celle des axones dopaminergiques. Les ganglions de la base chez l'humain sont innervés par des axones 5-HT qui proviennent principalement du noyau raphé dorsal et, de manière moins abondante, du noyau raphé médian. Ces axones forment des faisceaux larges ascendants qui se fragmentent en pénétrant dans la décussation supérieure des pédoncules cérébelleux. Ils se regroupent ensuite au sein de l'aire tegmentaire ventrale et montent le long du faisceau prosencéphalique médian, immédiatement sous les fibres dopaminergiques ascendantes. À des intervalles réguliers, les axones 5-HT se détachent du faisceau prosencéphalique médian et se déplacent latéralement pour s'arboriser à l'intérieur de toutes les composantes des ganglions de la base, où ils montrent des densités et des patrons d'innervations des plus variables. La substance noire est la composante des ganglions de la base la plus densément innervée, tandis que le noyau caudé reçoit une innervation plus hétérogène que le putamen et le globus pallidus. Le noyau subthalamique arbore des fibres immunoréactives 5-HT qui montrent un gradient décroissant mediolatéral. Le fait que toutes les composantes des ganglions de la base reçoivent une innervation 5-HT dense indique que, de concert avec la dopamine, la 5-HT joue un rôle crucial dans l'organisation fonctionnelle de ces structures.

2.2. Abstract

This study aimed at providing a first detailed description of the serotonin (5-hydroxytryptamine, 5-HT) innervation of the human basal ganglia under nonpathological conditions. We have applied an immunohistochemical approach to postmortem human brain material, with antibodies directed against the 5-HT transporter and the 5-HT synthesizing enzyme (tryptophane hydroxylase) to visualize 5-HT axons and cell bodies, respectively. Adjacent sections were immunostained for tyrosine hydroxylase to compare the distribution of 5-HT axons with that of dopamine axons. Human basal ganglia are innervated by 5-HT axons that emerge chiefly from the dorsal and, less abundantly, from the median raphe nuclei. These axons form thick ascending fascicles that fragment themselves as they penetrate the decussation of the superior cerebellar peduncle. They regroup within the ventral tegmental area and ascend along the medial forebrain bundle, immediately beneath the dopamine ascending fibers. At regular intervals along their course, 5-HT axons detach themselves from the medial forebrain bundle and sweep laterally to arborize within all basal ganglia components, where they display highly variable densities and patterns of innervation. The substantia nigra is the most densely innervated component of the basal ganglia, whereas the caudate nucleus is more heterogeneously innervated than the putamen and pallidum. The subthalamic nucleus harbors 5-HT immunoreactive fibers that display a mediolateral-decreasing gradient. The fact that all components of human basal ganglia receive a dense 5-HT input indicates that, in concert with dopamine, 5-HT plays a crucial role in the functional organization of these motor-related structures, which are often targeted in neurodegenerative diseases.

2.3. Introduction

Serotonin (5-hydroxytryptamine, 5-HT) is involved in multitudinous functions, such as the regulation of sleep-waking cycle (Steriade, 2004; Jones, 2005; Monti & Jantos, 2008), the modulation of pain signals (Sommer, 2004) and the pathogenesis of mood disorders (Owens & Nemeroff, 1994; Cools *et al.*, 2008). Such a multifaceted role of 5-HT is possible because this monoamine is produced and released by a widely distributed neuronal system that reaches virtually all major brain structures (Parent, 1996). Endowed with a markedly collateralized axon, 5-HT neurons have their cell body confined to the raphe nuclei, which occur in all vertebrate species (Parent *et al.*, 1984; Parent, 1986). Originally divided into nine entities (groups B1-B9 of Dahlstroem & Fuxe, 1964a), they are actually considered to form a small caudal and a large rostral group having distinct efferent projections (Tork, 1990; Hornung, 2003; Monti & Jantos, 2008). The caudal group comprises medullary raphe nuclei, which project to the spinal cord whereas the rostral group, scattered along the pons and midbrain, contains the dorsal (DRN, B6 and B7) and median (MRN, B8) raphe nuclei, which supply about 85% of the 5-HT forebrain innervation (Parent, 1996; Hornung, 2003; Monti & Jantos, 2008).

Among the various forebrain structures that receive a particularly dense 5-HT innervation are the basal ganglia, which play a crucial role in the control of motor behavior (Di Matteo *et al.*, 2008). The density and distributional pattern of 5-HT axons vary significantly from one basal ganglia component to the other. This has been clearly established by various mapping studies undertaken in rats (Moore *et al.*, 1978; Parent *et al.*, 1981; Steinbusch, 1981; Mori *et al.*, 1985a; Mori *et al.*, 1985b; Mori *et al.*, 1987; Harding *et al.*, 2004; Parent *et al.*, 2010) and monkeys (Schofield & Everitt, 1981; Mori *et al.*, 1985a; Mori *et al.*, 1985b; Azmitia & Gannon, 1986; Mori *et al.*, 1987; Lavoie & Parent, 1990; Parent *et al.*, 2010). In humans, morphological studies of the 5-HT neuronal system have focused principally on the raphe nuclei (Baker *et al.*, 1991a; Baker *et al.*, 1991b; Hornung, 2003). Some biochemical studies have provided useful information on the 5-HT content of human basal ganglia

in both health and disease conditions (Lloyd *et al.*, 1974; Walsh *et al.*, 1982; Hornykiewicz, 1998; Kish *et al.*, 2008). However, except for pioneering data on ascending 5-HT axons gathered from embryonic brain tissue (Olson *et al.*, 1973), little information is available on the morphological aspect of the 5-HT innervation of the basal ganglia in man.

This lack of knowledge has prompted us to undertake a detailed immunohistochemical study of the organization of the 5-HT innervation of human basal ganglia using antibodies against the 5-HT transporter (SERT) and tryptophan hydroxylase (TPH), the rate-limiting enzyme in 5-HT synthesis. These antibodies were applied to human postmortem material obtained from healthy adult individuals. Such knowledge will hopefully help us comprehend the role of 5-HT at basal ganglia level and better interpret the complex neurochemical changes that occur within these nuclei in neurodegenerative diseases.

2.4. Materials and Methods

2.4.1. Tissue preparation

Morphological descriptions are based on the analysis of postmortem material obtained from 8 men and 1 woman with no clinical or pathological evidence of neurological or psychiatric disorders. The mean age and postmortem delays are 47.1 ± 8.2 years and 11.6 ± 0.7 h, respectively (Table 1). The material was taken from the brain bank established at the Centre de Recherche Université Laval Robert-Giffard (CRULRG). Brain banking and postmortem tissue handling procedures were approved by the Ethic Committee of the Centre Hospitalier Robert-Giffard and by Université Laval. The brains were obtained with written consents and the analyses were performed in conformity with the Code of Ethics of the World Medical Association (Declaration of Helsinki).

The nine brains were sliced in half along the midline; the right side of the brain served for neuropathological examination, while the left side was used for immunohistochemical investigation. The latter hemi-brains were sliced unfixed into 2 cm-thick slabs along the coronal or sagittal plane and the slabs were fixed by immersion in 4% paraformaldehyde at 4°C for 3 days. They were then stored at 4°C in a 0.1M phosphate-buffered saline (PBS, pH 7.4) solution containing 15% sucrose and 0.1% sodium azide. The slabs containing the basal ganglia and adjacent structures were cut with a freezing microtome into 50 µm-thick sections that were serially collected in PBS and stored at –20°C in a solution containing glycerol and ethanediol until immunostaining.

A detailed view of the overall pattern of the 5-HT innervation of the human basal ganglia was obtained by examining serial coronal sections taken at four different caudorostral levels: through the mid portion of the subthalamic nucleus (STN, level 1); through the maximally developed pallidal complex (level 2); through the anterior commissure (level 3); and through the pre-commissural portion of the striatum (level 4). These four levels correspond respectively to levels 21, 27, 35 and 39 of the human brain atlas of Mai and colleagues (Mai *et al.*, 2008). Sagittal sections covering the rostral portion of the pons, the entire midbrain and the caudal portion of the forebrain were also examined to visualize the 5-HT cell bodies of the DRN and MRN and to obtain an overall view of the initial trajectory of the 5-HT ascending axons. Complete sets of coronal sections taken at three caudorostral levels of STN were also used to provide a detailed picture of the 5-HT innervation of this basal ganglia key component.

2.4.2. Antibodies

Antibodies raised against 5-HT itself have been successfully used to study the 5-HT system in the brain of rats (Steinbusch, 1981) and monkeys (Lavoie & Parent, 1990), but this approach cannot be applied to human postmortem tissue because 5-HT is rapidly dissipated from neurons after death.

Morphological studies of the human 5-HT system have to rely on the detection of various 5-HT-associated proteins, which are preserved in their natural state and location for many hours after death and are thus much more easily detectable with immunohistochemical procedures than 5-HT (Tork *et al.*, 1992). In the present study, the human 5-HT neuronal system was visualized with the help of two complementary markers: (a) the 5-HT biosynthetic enzyme tryptophan hydroxylase (TPH), which predominates in the somatodendritic domain of 5-HT neurons, and (b) the 5-HT transporter (SERT), which abound in 5-HT axons and axon varicosities (terminals) (Qian *et al.*, 1995). More specifically, we used a mouse monoclonal antibody against TPH (catalog # 10678; Sigma, St-Louis, MO, USA) and a goat polyclonal SERT antiserum (catalog # sc-1458; Santa Cruz Biotechnology, Santa Cruz, CA, USA). The preparation and characterization of the TPH antibody, including the demonstration of its specificity by preabsorption and Western blot, have been described elsewhere (Haycock *et al.*, 2002). The distribution of the immunostaining with this antibody matched that of 5-HT neurons, without any cross-reactivity with midbrain dopamine (DA) neurons (Haycock *et al.*, 2002). The SERT antiserum was raised against 20 amino acids in the C-terminal of the human SERT. It was affinity-purified and characterized by Western blot in brain tissue (Santa Cruz Biotechnology). This anti-SERT is considered a faithful marker of 5-HT neurons at both light and electron microscopic levels (Pickel & Chan, 1999; Huang *et al.*, 2004), and its production and characterization have been reported in detail elsewhere (Zhou *et al.*, 1996). Complementary studies were performed with antibodies against either the enzyme tyrosine hydroxylase (TH, catalog # 22941; ImmunoStar, Hudson, WI, USA), the neuroactive peptide enkephalin (ENK, provided by Dr. Claudio Cuello, McGill University) or the dopamine-β-hydroxylase (DBH, catalog # AB1538; Chemicon, Temecula, CA, USA). The monoclonal antibody against TH was used principally to determine the relative position of the 5-HT and DA axons as they ascend towards the basal ganglia. Because TH, the rate-limiting enzyme in the synthesis of catecholamines, is also expressed by noradrenergic neurons, immunohistochemistry for DBH, the enzyme that transforms DA into

noradrenalin, was used to label noradrenergic axons in the human basal ganglia. The rabbit polyclonal antibody against the N-terminal 18 amino acid of the human DBH has been previously well characterized (Nagatsu *et al.*, 1990). The monoclonal antibody against ENK served essentially to visualize the striosomal compartment of the human striatum. This antibody did not distinguish between Met- and Leu-enkephalin and details about its production and characterization can be found elsewhere (Cuello *et al.*, 1984). The TH, DBH and ENK antibodies were routinely used in previous studies of the human basal ganglia (see Prensa *et al.*, 1999; Prensa *et al.*, 2000; Huot *et al.*, 2007).

2.4.3. Immunohistochemistry

Complete series of coronal sections taken at 300 µm interval and covering the entire caudorostral extent of the basal ganglia (levels 1 to 4) of brains 1, 2 and 5-9, were processed for the demonstration of SERT immunoreactivity. After three rinses in PBS, the sections were placed for 30 min at room temperature in hydrogen peroxide (3% H_2O_2 in ethanol) to eliminate endogenous peroxidase activity. The free-floating sections were then preincubated for 30min at room temperature in a PBS solution containing 2% normal rabbit serum (NRS) and 0.1% Triton X-100, and incubated overnight at 4°C in the same solution to which the goat anti-SERT antibody was added (Santa Cruz Biotechnology; 1:500). The sections were then rinsed, reincubated for 1 h at room temperature with a rabbit anti-goat biotinylated IgG (catalog # BA-5000; Vector Labs, Burlingame, CA, USA; 1:500). After three rinses in PBS, the sections were reincubated for 1 h at room temperature in 2% avidin-biotin-peroxidase complex (catalog # PK-4000; Vector Labs). The bound peroxidase was revealed by placing the sections in a medium containing 0.05% 3,3'-diaminobenzidine tetrahydrochloride (DAB, catalog # D5637; Sigma) and 0.005% H_2O_2 in 0.05 M Tris buffer, pH 7.6. The reaction was stopped after 4 min by several washes in Tris buffer and PBS. The mapping of 5-HT neuronal profiles was complemented by incubating complete sets of sagittal sections taken from brains 3 and 4 alternatively with either goat anti-SERT or mouse

anti-TPH (Sigma; 1:250). The procedure was the same as above except that normal horse serum (NHS) and a horse anti-mouse biotinylated IgG (catalog # BA-1300; Vector Labs; 1:250) were used in cases of sections immunostained for TPH. Furthermore, coronal sections taken through the entire caudorostral extent of the striatum (levels 3 and 4) of brain 1 were incubated with the anti-SERT antibody (same as above), while the adjacent sections were incubated with the mouse anti-ENK antibody (Cuello; 1:50). This set of experiments was designed to compare the density of the 5-HT innervation between the ENK-rich striosomes and the ENK-poor extrastriosomal matrix of the striatum. Coronal sections taken from brain 6 at the locus coeruleus and the post-commissural striatal levels were incubated with the rabbit anti-DBH antibody (Chemicon; 1:250) to label noradrenergic cell bodies and axons, respectively. All immunostained sections were mounted on gelatine-coated slides. Those that were incubated without the primary antibodies remained unstained.

2.4.4. Immunofluorescence

A double immunofluorescence labeling approach was used to compare, on single coronal sections, the location of the SERT and TH immunoreactive axons that both ascend towards the basal ganglia by coursing along the same forebrain pathways. Hence, serial sections from brains 1, 2 and 5, were remove from their storage medium and rinsed in PBS. They were preincubated for 1 h in a PBS solution containing 2% NHS and 0.1% Triton X-100 at room temperature and then incubated overnight at 4°C in the same solution to which two primary antibodies were added, one directed against SERT (goat anti-SERT, Santa Cruz Biotechnology; 1:250) and the other against TH (mouse anti-TH, ImmunoStar; 1:500). After rinses in PBS, sections were incubated at room temperature in a solution containing a rabbit anti-goat biotinylated IgG (Vector Labs; 1:250). After additional rinses in PBS, sections were incubated for 2 h at room temperature in the dark, in a PBS solution containing Alexa 488-conjugated streptavidin (cataolog # S-11223; Molecular Probes, Eugene, OR, USA; 1:200) and Alexa 555-conjugated rabbit anti-mouse (catalog # A-

21427; Molecular Probes; 1:200). The sections were finally rinsed three times in PBS and mounted on gelatine-coated slides. Once dried, sections were treated with an autofluorescence eliminator reagent (catalog # 2160; Chemicon). They were then cover slipped with a fluorescent mounting medium (catalog # S3023; DAKO Corporation, Carpinteria, CA, USA). Sections incubated without the primary antibodies remained virtually free of immunofluorescence.

2.4.5. Material analysis

The immunostained sections were observed and photographed under both bright and darkfield illuminations with a microscope equipped with a digital camera and a camera lucida (Leitz DM RB; Leica, Onrario, Canada). The location of the 5-HT axons and terminals in each of the various components of the human basal ganglia were precisely mapped on four drawings (levels 1-4) derived from the atlas of Mai and colleagues (Mai *et al.*, 2008). The location of the 5-HT cell bodies in DRN and MRN and the initial trajectory of their ascending axons were further studied by analyzing serial parasagittal sections covering 1,800 µm on each side of the midline. We generated a composite picture of it by drawing a typical section extending from the upper pons to the lower forebrain upon which the distribution of the 5-HT neurons was mapped out following observations made on alternate sections immunostained for either SERT or TPH. The location of the 5-HT cells bodies in the DRN and MRN nuclei and their ascending axonal projections were drawn with the help of a camera lucida. A particularly detailed analysis of the 5-HT innervation of STN was undertaken by examining serial SERT-immunostained coronal sections from brain 1 taken at caudal, middle and rostral thirds of the STN. A camera lucida was used to delineate the STN contours and to draw the 5-HT axonal arborization within this basal ganglia component. All diagrams derived from the analysis of coronal or sagittal sections were generated using Canvas X Software (ACDSystems International Inc,Victoria, Canada). Darkfield photomicrographs of SERT-immunolabeled sections were used to examine the

density of 5-HT innervation in striosomes after being delineated on ENK-immunostained adjacent sections. Immunofluorescence sections used to compare the relative distribution of SERT and TH immunoreactive axons were observed with a confocal laser-scanning microscope LSM 5 PASCAL (Zeiss, Oberkochen, Germany). The emission signals of Alexa 488 (SERT) and Alexa 555 (TH) were assigned to green and red, respectively. Photomicrographs were handled with the Adobe Photoshop CS4 software (Adobe, San Jose, CA, USA).

2.5. Results

2.5.1. Ascending serotonin pathways

The origin and initial trajectory of the ascending 5-HT fibers were particularly well outlined on human brainstem sections cut along the sagittal plane (Fig. 1). These thick and nonvaricose SERT-immunopositive (+) fibers (Fig. 1B, C) emerge from the cell bodies of the DRN and, less abundantly, from those of the MRN (Fig. 1D, E). They arch rostroventrally and traverse the central portion of the midbrain tegmentum. As they penetrate the decussation of the superior cerebellar peduncles they break out into a multitude of small and compact fascicles that form a strikingly intricate network. More rostrally, these fibers collected themselves dorsomedially to the substantia nigra in the form of a rather diffuse bundle that passes partly through the ventral tegmental area and ascends within the lateral hypothalamic area along the medial forebrain bundle (Figs. 1A, 2A). Despite its overall diffuseness, the core of this bundle is nevertheless composed of two smaller fascicles located one above the other and which are particularly visible in the caudal portion of the bundle (Fig. 3C), as it courses lateral to the mammillary bodies. The bundle of SERT+ fibers tapers as it ascends within the lateral hypothalamic area because several immunoreactive fascicles detach themselves from it at different caudorostral levels. These fascicles sweep laterally to innervate various components of the basal ganglia, such as the STN, globus pallidus and putamen, where both thin

and varicose, and thick and beaded SERT+ fibers can be found in unequal number (Fig. 4).

2.5.2. Substantia nigra

The substantia nigra is by far the most densely innervated component of the human basal ganglia (Fig. 2A). The nigral 5-HT innervation derives from axons that reach the structure mainly from its caudal border and arborize profusely immediately upon entering the susbtantia nigra. In fact, very few thick and poorly beaded SERT+ axons occur within the confines of the substantia nigra, although some immunoreactive fiber fascicles course along its dorsolateral surface. Within the substantia nigra, SERT+ axons and terminals are rather uniformly distributed throughout the caudorostral and mediolateral extent of the structure. No significant difference could be noted between the pars compacta and the pars reticulata of the substantia nigra in regards to the density of the 5-HT innervation (Fig. 2A). The 5-HT innervation of the substantia nigra derives principally from thin and varicose axons, which outnumber the thick and poorly beaded axons. Some SERT+ axon varicosities were seen in close apposition to the cell bodies of pars compacta neurons, which could easily be delineated by virtue of their neuromelanine content (Fig. 4E, F).

2.5.3. Subthalamic nucleus

The SERT+ axons observed in STN derive chiefly from one fiber fascicle that detaches itself from the main bundle coursing in the lateral hypothalamic area, to run along the dorsal surface of STN (Fig. 2A). A smaller immunoreactive fascicle that courses along the ventral surface of STN appears also to contribute, albeit less importantly, to the STN 5-HT innervation (Fig. 3). The STN contains a small number of thick and beaded SERT+ varicose fibers and only a few thin and varicose fibers (Fig. 4D). These immunoreactive fibers are

distributed according to a clear mediolateral decreasing gradient, whereas the isolated SERT+ axon varicosities present within the nucleus appear equally distributed throughout the structure (Fig. 3). Overall, the density of the 5-HT innervation of STN is about half of that of the substantia nigra (Fig. 2A).

2.5.4. Pallidum

The human pallidal complex receives a moderate 5-HT innervation that derives from several fascicles leaving the main SERT+ fiber bundle at various points along its courses within the lateral hypothalamic area. At caudal pallidal levels, some of the SERT+ fibers that run along the dorsal surface of STN continue their route laterally and pierce the internal capsule to reach the pallidum along its dorsal border (Fig. 2). At more rostral levels, other fascicles sweep laterally and penetrate the pallidum by piercing its ventromedial aspect (Fig. 2B). Other ventrally coursing fibers turn dorsally and invade the various medullary laminae that separate the different components of the lenticular nucleus (Fig. 2B). Some of these medullary SERT+ fibers continue their course dorsally through the internal capsule to finally reach the caudate nucleus, whereas others turn perpendicularly to enter the putamen.

Overall, SERT+ fibers reaching the pallidum arborize more profusely in the internal segment than in the external segment, although much variation exists along the caudorostral axis. In the caudal third of the pallidum (Fig. 2A), the number of SERT+ fibers is similar than in the STN and they appear rather uniformly distributed throughout the structure. Thick and beaded fibers occur as frequently as thin and varicose fibers at this level (Fig. 4B). The medial third of the pallidal complex (Fig. 2B) harbors a much larger number of SERT+ fibers than its caudal third. These fibers are mostly thick and beaded (Fig. 4C) and abound preferentially within the internal segment of the pallidum, where they do not display any preferential orientation. A relatively small number of isolated SERT+ axon varicosities are uniformly distributed throughout the two pallidal segments (Fig. 2B). By comparison, the rostral third of the pallidal

complex contains a much smaller number of SERT+ fibers, which are mostly of the thick and weakly varicose type, and only scarce and uniformly distributed isolated axon varicosities.

2.5.5. Striatum

The striatum is by far the most heterogeneously innervated component of the basal ganglia.Overall, the 5-HT innervation of the caudate nucleus is slightly weaker than that of the putamen, but these two components of the striatum share a similar degree of heterogeneity in regard to the distribution of SERT+ fibers and axon varicosities. At caudal levels (Fig. 2A), SERT+ fibers and axon terminals are distributed within the putamen according to a clear dorsoventral gradient, the immunopositive axon profiles being much more abundant ventrally than dorsally in the structure. The tail of the caudate nucleus at the same level harbors a few SERT+ fibers and a moderate number of uniformly distributed SERT+ axon terminals, except for a densely innervated zone at the ventral border of the structure (Fig. 2A). At post-commissural levels (Fig. 2B), SERT+ fibers and axon terminals are much more uniformly distributed within the striatum, except for the dorsal border of the body of the caudate nucleus, where immunopositive axon terminals are less abundant than in the rest of the striatum. The two types of SERT+ fibers occur in about equal proportion in the post-commissural striatum (Fig. 4A). At commissural levels (Fig. 2C), the putamen harbors a large number of rather uniformly distributed SERT+ fibers of both thick/beaded and thin/varicose types. In contrast, isolated SERT+ axon varicosities abound preferentially in the dorsal two-thirds of the putamen. By comparison, the caudate nucleus displays a smaller number of uniformly distributed SERT+ axon varicosities, except for two small zones located within its ventral aspect that are densely innervated (Fig. 2C). At pre-commissural levels (Fig. 2D), only a few SERT+ fibers are homogeneously distributed throughout the striatum, whereas innumerable SERT+ axon varicosities are heterogeneously scattered throughout the structure. These axon terminals abound principally in the dorsal two-thirds of both the putamen and the head

of the caudate nucleus, leaving the ventral striatum, including the nucleus accumbens, comparatively less densely innervated (Fig. 2D).

Apart from the striatum, several long, thick and beaded SERT+ fibers also occur throughout the entire caudorostral extent of the basal ganglia within the external medullary lamina that separates the putamen from the claustrum (Fig. 2). They course ventrodorsally in a rather linear fashion within the lamina (Fig. 2C[2]), spread out in the white matter above the claustrum and finally arborize within the various layers of the cerebral cortex. On the other hand, the detailed examination of adjacent sections stained for enkephalin, a faithful marker of the striosomal compartment of the striatum, and SERT, revealed that the striatal 5-HT innervation do not obey the striosomal-matrix compartmentalization in human. The density and morphological characteristics of SERT+ fibers and axon varicosities are strikingly similar in the two striatal compartments, the striosomes and the extrastriosomal matrix (Fig. 5).

2.5.6. Ascending SERT and TH immunoreactive axons

The double-immunofluorescence approach has enabled us to compare the course of the SERT and TH-immunolabeled axons that ascend towards the human basal ganglia on single sections taken through two distinct caudorostral levels. The first caudal level corresponds to the region where STN is maximally developed, defined above as level 1 (Fig. 6A), whereas the rostral level corresponds and to the region where the pallidal complex is maximally developed, defined above as level 2 (Fig. 6E). The more rostral levels, corresponding to that of the anterior commissure (level 3) and the pre-commissural portion of the striatum (level 4), were not analyzed because the SERT+ and TH+ fibers in these rostral regions had already broke out into a multitude of isolated immunostained axon varicosities, the remaining fibers being short, scarce and difficult to trace individually.

The detailed examination of sections taken though the caudal level (Fig. 6A) reveals that the SERT+ and TH+ fibers ascend within the medial forebrain bundle and, in fact, constitute the essential fibrillary component of this weakly myelinated bundle. Within this bundle, the SERT+ fibers tend to be more diffusely distributed then the TH+ fibers, which form a compact entity lying upon the dorsal surface of the substantia nigra (Fig. 6A, B). Both SERT+ and TH+ fiber bundles that ascend within the lateral hypothalamic area give rise to fiber fascicles that sweep laterally to course along the dorsal surface of STN (Fig. 6A, C). More laterally, the immunostained fibers traverse the strongly myelinated internal capsule by coursing in a typical sinuous fashion (Fig. 6A, D) until they reach the caudal portion of the pallidal complex. As they travel dorsal to STN and within the internal capsule, the SERT+ and TH+ fibers are closely intermingled with one another.

At the more rostral level (Fig. 6E), the SERT+ and TH+ fibers still occupy much of the mediolateral and dorsoventral extent of the medial forebrain bundle, in the lateral hypothalamic area. In contrast to the more caudal level, however, SERT+ and TH+ fiber bundles are clearly separated from one another, the former being more ventrally and medially located than the latter (Fig. 6E, F). Here again, the bundles of the SERT+ and TH+ fibers give rise to fascicles that sweep laterally beneath the pallidum and invade the internal and external medullary laminae that separate respectively the internal from the external pallidum and the external pallidum from the putamen (Fig. 6E). Beneath the globus pallidus, SERT+ fibers are again more diffusely distributed than TH+ fibers that tend to closely follow the trajectory of the ansa lenticularis (Fig. 6E, G). Within the internal and external medullary laminae, however, both types of fibers are intimately intermingled (Fig. 6E, H). In summary, as they course within the lateral hypothalamic area, the SERT+ fibers are more diffusely distributed than the TH+ fibers, whereas as they approach the basal ganglia through different routes, both types of fibers tend to be more closely intermingled.

2.6. Discussion

2.6.1. Methodological considerations

Since the brains analyzed in the present study belonged to individuals whose age ranged from 20 to 80 years, we looked for possible age-dependent variations in the pattern of basal ganglia 5-HT innervation. A comparison of SERT-immunostained sections from the brains of the older (54-80 years-old) and the younger (20-25 years-old) age group in our sample revealed interesting differences. These included a greater inter-individual variation in the overall immunostaining intensity and a larger number of lipofuscin pigments in the old versus young individuals. Furthermore, SERT immunostaining was generally more intense and less diffuse in the younger individuals. Except for these differences, however, there was no significant variation between the two groups in regards to the density and pattern of distribution of SERT imunoreactive axons and axon terminals in the various basal ganglia components.

In addition to age, other factors inherent to the investigation of postmortem human material, such as variations in postmortem delay and agonal status, might explain inter-individual variability in the quality of the immunostaining. In the present discussion, the 5-HT innervation of the basal ganglia in human is compared with that in other species, particularly nonhuman primates, as reported in the literature. Such a comparison must take into account the superior quality of brain tissue from monkeys that have been fixed by systemic perfusion under ideal conditions. Hence, some of the differences between human and nonhuman primates regarding basal ganglia 5-HT innervation reported in the present study might, at least in part, reflect methodological variations due to tissue fixation. However, a careful comparison of the present human data with materials from a previous study of the 5-HT innervation of the basal ganglia in the squirrel monkey (*Saimiri sciureus*) (Lavoie & Parent, 1990) has revealed that the density and patterns of distribution of the 5-HT fibers and terminals were fairly similar in both groups. Furthermore, the two

morphological types of 5-HT axons encountered in the basal ganglia of squirrel monkeys could be clearly delineated in the present human study. The latter finding reveals that the postmortem material used here was of sufficient quality to allow meaningful comparisons between human and nonhuman primates. The major similarities and differences between human and nonhuman primates in regard to the 5-HT innervation will be dealt with below in the various sections devoted to each basal ganglia component.

Antibodies against TH were used in a set of double (TH/SERT) immunofluorescence experiments designed to compare, on single sections, the location of 5-HT and DA axons innervating the human basal ganglia. Although TH is recognized as a faithful marker of DA, this catecholamine-synthesizing enzyme is also present in fibers using noradrenalin as a transmitter. An antibody raised against DBH was thus used to detect the presence of noradrenalin-producing fibers in human basal ganglia. The clear and intense immunolabeling of neurons of the human locus cœruleus obtained with this antibody (see supporting document) served as a positive control for its immunoreactivity. In sections incubated with this anti-DBH antibody, a small number of immunoreactive fibers and axon terminals were noted particularly in the ventral portion of the striatum (see supporting document), but the bulk of the fibers and axon terminals that pervaded the basal ganglia, as visualized in TH-immunostained sections, remained totally immunonegative for DBH. These results, which are perfectly congruent with the data gathered previously in a different series of human individuals (see Prensa *et al.*, 2000), indicate that the basal ganglia in human do not receive a significant noradrenergic innervation and that TH is a reliable DA marker in the different components of human basal ganglia. However, the possibility that a certain proportion of the TH immunoreactive axons ascending in the lateral hypothalamic area might be noradrenergic instead of DA cannot be ruled out.

2.6.2. Serotonin pathways innervating the human basal ganglia

The organization of the 5-HT afferents to human basal ganglia, as revealed in the present study, shared many similarities with that described previously in rats (Parent *et al.*, 1981; Steinbusch, 1981) and monkeys (Azmitia & Segal, 1978; Azmitia & Gannon, 1986; Lavoie & Parent, 1990). In human, multitudinous immunoreactive fibers originating from 5-HT neurons located in the DRN and less abundantly from those in the MRN formed several small and intertwined fascicles that appeared along the sagittal plane as a complex reticulum occupying much of the core of the midbrain tegmentum. The bulk of these fibers arched ventrally, invade the ventral tegmental area, and ascend to the forebrain by coursing along the medial forebrain bundle in the lateral hypothalamic area. Our double immunofluorescent analysis has revealed that SERT immunoreactive fibers were more diffusely organized and slightly more ventrally located in the lateral hypothalamus than TH-immunostained axons. However, both types of fibers were closely intermingled as they depart laterally in the form of several distinct fascicles that invade the various basal ganglia components. Interestingly, both SERT+ and TH+ fibers reached their target structures by ascending along major output pathways of the basal ganglia, principally the ansa lenticularis ventrally and the lenticular fasciculus dorsally.

In the present study, two distinct types of axons were noted in the human basal ganglia: thick and beaded fibers as well as thin and varicose axons. This observation is in accordance with previous immunohistochemical studies conducted in different mammalian species including rats (Kosofsky & Molliver, 1987), cats (Mulligan & Tork, 1988) and monkeys (Takeuchi & Sano, 1983; Hornung *et al.*, 1990; Lavoie & Parent, 1990). Using anterograde tracer, Kosofsky and Molliver (1987) have shown that each of the two types of 5-HT axons that innervate the cerebral cortex of the rat has a distinct origin in the midbrain raphe nuclei. The MRN neurons emit large varicose axons whereas the DRN neurons give rise to thin and varicose fibers (Kosofsky & Molliver,

1987). However, because the 5-HT fibers arising from the two raphe nuclei closely intermingle as they ascend towards the human basal ganglia, it was not possible to determine the specific origin of these two types of fibers in the present immunohistochemical study.

Electron microscopic examination of 5-HT axon varicosities in the striatum (Soghomonian *et al.*, 1989; Descarries *et al.*, 1992), the substantia nigra (Moukhles *et al.*, 1997) and the subthalamic nucleus (Parent *et al.*, 2010) has revealed that the 5-HT axon varicosities are rather small and apposed almost exclusively upon dendritic spines or shafts. A small proportion of them display asymmetrical membrane differentiation but the majority of these terminals do not form synaptic contacts (reviewed in Descarries *et al.*, 2010b). The largely asynaptic character of these axon varicosities has been viewed as morphological evidence for the existence of diffuse transmission by such neuronal systems, in addition to their synaptic mode of transmission (reviewed in Descarries & Mechawar, 2008). This has also led to the suggestion that a low ambient level of transmitter might permanently exist in the extracellular space, the fluctuations of which could regulate a variety of physiological processes mediated by 5-HT (Descarries *et al.*, 1997). Hence, more than the proximity of presynaptic 5-HT axon varicosities, it is the expression of various types of 5-HT receptors by target neurons that determine the excitatory or inhibitory influence of 5-HT on local neuronal networks.

A previous studies in the rat showed that the majority of the 5-HT ascending fibers arising from the DRN and MRN formed a widely distributed projection termed *transtegmental system*(Parent *et al.*, 1981). This system characteristically converges as small fascicles through the central tegmentum of the caudal midbrain prior to forming more compact bundles in the ventral tegmental area of the rostral midbrain. A smaller ascending 5-HT system originating from the rostral pole of the DRN was also detected and termed *periventricular system*(Parent *et al.*, 1981). The system follows the trajectory of the dorsal longitudinal fasciculus (of Schütz) and, after emitting distinct fiber

contingents to inferior and superior colliculi and periventricular gray, it arches abruptly ventral-ward, to merge with the fibers of the transtegmental system at caudal hypothalamic level. In macaque monkeys, two ascending 5-HT bundles were also visualized at caudal hypothalamic levels: the medial forebrain bundle and the so-called dorsal raphe cortical tract (Azmitia & Gannon, 1986). The dorsal raphe cortical tract, which was described as ascending to the cerebral cortex through the internal capsule, was reported to contain a much larger number of 5-HT axons than the medial forebrain bundle in macaque monkeys, whereas the inverse situation appears to prevail in rats (Azmitia & Gannon, 1986). However, in previous immunohistochemical study in squirrel monkeys with antibodies directed against 5-HT, no evidence could be found for the existence of the dorsal raphe cortical tract (Lavoie & Parent, 1990). Likewise, SERT+ fibers bundles that might correspond to either the dorsal raphe cortical tract or the periventricuar system could not be found in the human brainstem. Virtually all immunostained axons originating from the raphe nuclei of the upper brainstem in human display an organizational feature that strikingly resembles the transtegmental system described previously in rodents. Although a few isolated and short 5-HT fibers occurred in the periventricular gray matter of the upper brainstem in human, they did not form a distinct bundle equivalent to the periventricular systems in rodents.

2.6.3. Patterns and densities of serotonin innervation in distinct components of human basal ganglia

The substantia nigra

The present study has shown that the substantia nigra is the basal ganglia components that received the heaviest 5-HT innervation in human. This finding agrees with previous biochemical studies which have identified the substantia nigra as one of the brain structures most markedly enriched in 5-HT and its major metabolite 5-hydoxyindolacetic acid (5-HIAA) in rats (Palkovits *et al.*, 1974; Saavedra, 1977), monkeys (Shannak & Hornykiewicz, 1980) and human

(Lloyd *et al.*, 1974; Jellinger *et al.*, 1978; Mackay *et al.*, 1978; Walsh *et al.*, 1982; Hornykiewicz, 1998). These biochemical data were confirmed by the results of various immunohistochemical mapping studies in rats (Steinbusch, 1981; Mori *et al.*, 1987; Parent *et al.*, 2010), cats (Mori *et al.*, 1987) and monkeys (Pasik *et al.*, 1984a; Azmitia & Gannon, 1986; Lavoie & Parent, 1990; Parent *et al.*, 2010).

Axonal transport studies in the rat revealed that the raphe-nigral projection arises mainly from the DRN and arborize more profusely in the pars reticulata than in the pars compacta of the substantia nigra (Azmitia & Segal, 1978). Furthermore, injections of retrograde tracers in rats showed that the raphe-nigral projection is largely composed of collaterals of the raphe-striatal pathway (Van Der Kooy & Hattori, 1980). Evidence for the chemical heterogeneity of the DRN has also been obtained in rats (Descarries *et al.*, 1986), monkeys (Charara & Parent, 1998) and human (Baker *et al.*, 1991b), but little is known on the anatomical organization of the DRN projections to human basal ganglia.

Our current knowledge on the 5-HT innervation of human substantia nigra is largely inferred from immunohistochemical data obtained in monkeys. In squirrel and macaque monkeys, 5-HT axon varicosities are heterogeneously distributed in the pars reticulata of the substantia nigra (Mori *et al.*, 1987; Lavoie & Parent, 1990). They abound in the lateral part (also known as the pars lateralis of the substantia nigra) of the pars reticulata and formed clusters of dense terminal fields distributed between the cell columns of the pars compacta more medially. Some 5-HT axon varicosities are also scattered within the pars compacta itself and immunoreactive fibers ascend along the cell columns of the pars compacta that plunge deeply into the pars reticulata (Lavoie & Parent, 1990).

The present immunohistochemical study has provided the first detailed picture of the 5-HT innervation of the human substantia nigra, which appears

significantly different from what has been documented for nonhuman primates. Very few 5-HT fibers are visible in the human substantia nigra *per se*, but the structure harbors a multitude of very fine and rather uniformly distributed immunoreactive axon varicosities. The size of these isolated axon varicosities lies at the limit of the power of resolution of the optic light microscope so that, when examined at low power, the SERT immunostaining at nigral level appears as a rather diffuse immunoprecipitate that covers both the pars reticulata and compacta of the subsantia nigra. No specific clusters of 5-HT axon varicosities could be detected in any of the two main portions of the structure, but many varicosities could be visualized in close apposition to pigmented (presumably DA) cell bodies of the pars compacta of the substantia nigra. These findings suggest that, through both synaptic and diffuse transmission at the nigral level, 5-HT can alter the activity of pars compacta DA neurons projecting to the striatum and pars reticulata GABAergic neurons projecting to the thalamus and brainstem. The action of 5-HT at nigral level is likely to be mediated by receptors of the 5-HT_1 subtype, which predominates in this basal ganglia component (Di Matteo *et al.*, 2008).

The subthalamic nucleus

The STN has long been known to contain significant amounts of 5-HT and 5-HIAA, as shown by pioneering biochemical studies undertaken in rats (Palkovits *et al.*, 1974), monkeys (Cross & Joseph, 1981) and humans (Lloyd *et al.*, 1974; Walsh *et al.*, 1982). In agreement with these findings, we found the human STN to receive a 5-HT innervation whose density is about half that of the substantia nigra. This innervation arises from thick and beaded fibers that reach the nucleus principally through its dorsal aspects and distributed themselves within the structure according to a mediolateral decreasing gradient. The nucleus also contains numerous, homogeneously distributed 5-HT axon varicosities, some of which in close contact with non-immunoreactive cell bodies. Previous immunohistochemical studies have pointed to inter-species variations in the pattern of the 5-HT innervation of STN (Mori *et al.*,

1985a; Lavoie & Parent, 1990; Parent *et al.*, 2010). Numerous 5-HT immunoreactive fibers were detected in STN of rodents (Steinbusch, 1981; Parent *et al.*, 2010), as well as in that of cats and monkeys (Mori *et al.*, 1985a; Lavoie & Parent, 1990; Parent *et al.*, 2010). These fibers were more abundant and more heterogeneously distributed in monkeys than in non-primate species. Furthermore, thin and markedly varicose 5-HT fibers predominate in the STN of rats and cats, whereas thin varicose fibers are closely intertwined with straight, unbranched, thick fibers in the same structure in monkeys. These comparative studies have revealed significant differences between primate and non-primate species in regards to the pattern of 5-HT innervation of STN, but the functional significance of such species variations is unknown. In human, our SERT immunohistochemical data indicate that the 5-HT innervation of STN shares overall more similarities with that of monkeys than with that of non-primates.

The STN exerts a potent glutamate-mediated excitatory influence upon the pallidum and the subtantia nigra and, as such, it is considered as one of the driving forces of the basal ganglia (Parent & Hazrati, 1995b; Xiang *et al.*, 2005). Furthermore, this nucleus is currently the major target for deep brain stimulation designed to alleviate the motor symptoms of Parkinson's disease (Benabid *et al.*, 2009). The literature reviewed above indicates that, besides excitatory inputs from the cerebral cortex and inhibitory inputs from the pallidum, the activity of STN neurons is modulated by 5-HT afferents from the DRN of the brainstem. Yet, despite many pharmacological and electrophysiological studies, the exact role that 5-HT plays at STN level remains uncertain. Local application of 5-HT was shown to increase the firing rate of STN neurons (Xiang *et al.*, 2005), but occasionally neurons displayed a biphasic responses consisting of excitation followed by inhibition, while still others were frankly inhibited (Stanford *et al.*, 2005). Furthermore, 5-HT is reported to inhibit the glutamate-mediated excitatory action of cortical inputs as well as the GABA-mediated inhibitory effects of pallidal inputs upon STN neurons by acting at presynaptic level (Shen & Johnson, 2008). The

presynaptic action of 5-HT is apparently mediated through receptors of the 5-HT_{1B} subtype (Shen & Johnson, 2008), whereas the postsynaptic effects noted above would be exerted through 5-HT_4 and 5-HT_{2C} receptor subtypes (Stanford *et al.*, 2005; Xiang *et al.*, 2005). Hence, the facts that 5-HT can act at both pre- and postsynaptic levels and that its action is mediated by a multitude of functionally distinct 5-HT receptors (5-HT_1 to 5-HT_7) explain, at least in part, the multifaceted role that this neurotransmitter exerts upon neurons of STN.

The importance of the 5-HT innervation of STN in the control of motor behavior has been underlined in a recent pharmacological study undertaken in an animal model of Parkinson's disease in which the nigrostriatal DA pathway was lesioned by injection of the neurotoxin 6-OHDA (Marin *et al.*, 2009). When these animals are treated with L-DOPA to replenish their DA striatal store, they exhibit involuntary abnormal movements that resemble L-DOPA-induced dyskinesia (LID), which are a common side effect of L-DOPA therapy in human parkinsonian patients (Carta *et al.*, 2007b). Interestingly, the intra-STN administration of sarizotan, a compound with full 5-HT_{1A} agonist properties, was found to significantly attenuate LID in this animal model of Parkinson's disease (Marin *et al.*, 2009). Although the direct mechanisms of sarizotan on STN neuronal activity remain to be established, this finding indicates that the pharmacological manipulation of the 5-HT neural transmission at the STN level might be a fruitful avenue for the development of novel therapeutic approaches for the treatment of abnormal movements.

The pallidal complex

The human pallidum receives a dense 5-HT projection in the form of numerous thick or thin varicose 5-HT fibers that ramify more profusely in the internal than in the external pallidal segment. Yet, the pallidum harbors relatively few isolated axon varicosities by comparison to other basal ganglia nuclei. These immunohistochemical findings are congruent with the presence of high concentrations of 5-HT and 5-HIAA in the pallidal complex of rats (Palkovits *et*

al., 1974; Saavedra, 1977), monkeys (Shannak & Hornykiewicz, 1980) and human, where the levels of the neurotransmitter and its metabolite are significantly higher in the internal than in the external segment of the pallidum (Walsh *et al.*, 1982). The pallidum is also enriched in 5-HT_1 and poor in 5-HT_2 receptors in rats (Pazos & Palacios, 1985), monkeys (Stuart *et al.*, 1986) and human (Pazos *et al.*, 1987b). In human, the density of 5-HT_1 receptors, which are mainly of the 5-HT_{1C} subtype, appears to be higher in the internal than in the external segment of the pallidum (Pazos *et al.*, 1987b; Di Matteo *et al.*, 2008).

Immunohistochemical studies with antibodies against 5-HT have underlined major differences between primates and non-primates species in regard to the 5-HT innervation of the pallidal complex. While the entopeduncular nucleus (homologue of the primate internal pallidum) and the globus pallidus (homologue of the primate external pallidum) receive a homogeneous innervation in rats and cats (Mori *et al.*, 1985b), the external pallidum is less densely innervated than the internal pallidum and most 5-HT fibers arborize in a typical band-like pattern in both pallidal segments in monkeys (Mori *et al.*, 1985b; Lavoie & Parent, 1990). The latter pattern of arborization is characteristic of most pallidal afferents, which terminate principally on the dendritic shafts and crests of pallidal neurons (Pasik *et al.*, 1984b). This band-like arrangement is conditioned by the large and dicoidal dendritic arborization of pallidal neurons that lie parallel to medullary laminae and perpendicular to the incoming axons to which they present their greatest discoidal surface (Parent & Hazrati, 1995b). Surprisingly, the human pallidum did not display such a band-like pattern in the SERT-immunostained material analyzed in the present study. Whether this represents a genuine species difference between human and nonhuman primates or simply reflects methodological variations due to tissue fixation (perfusion versus immersion) or immunohistochemical procedures (SERT versus 5-HT immunostaining) remains to be elucidated.

In vitro electrophysiological study indicates that, as it is the case for STN, 5-HT

mediates its effect via both pre- and postsynaptic mechanisms at pallidal level (Rav-Acha *et al.*, 2008). Presynaptically, 5-HT attenuates GABA release, probably through activation of 5-HT_{1B} receptors, whereas postsynaptically, 5-HT activates a hyperpolarizing cation channel, probably via 5-HT_{1A} receptors. Furthermore, 5-HT appears to decrease the fast synaptic depression characteristic of the striatal afferent input (Rav-Acha *et al.*, 2008). Altogether, these findings suggest that decreased 5-HT concentrations may lead to a depression of pallidal activity and hence contributes to the emergence of abnormal synchronous oscillations observed in various basal ganglia components under pathological conditions, such as those encountered in Parkinson's disease. Quantitative studies of the 5-HT innervation in parallel with determination of 5-HT receptor levels in the internal pallidum of normal individuals compared with patients who suffered from Parkinson's disease or Huntington's chorea are obviously needed to better understand how 5-HT modulates basal ganglia output structures in both health and diseases.

The striatum

Biochemically, 5-HT and 5-HIAA concentrations are reportedly lower in the striatum than in other basal ganglia components in rats (Palkovits *et al.*, 1974; Saavedra, 1977), monkeys (Shannak & Hornykiewicz, 1980) and humans (Walsh *et al.*, 1982), and yet the human striatum receives a massive 5-HT innervation, as revealed in the present study. This innervation is about half as dense as that of the substantia nigra, but its most striking feature is a marked heterogeneity in the distribution of 5-HT axon varicosities, which makes it unique among basal ganglia components.

At rostral striatal level, the 5-HT axon terminals were distributed according to a slight dorsoventral decreasing gradient, whereas the inverse occurs at caudal level. This finding is at variance with immunohistochemical data gathered in rats, cats and monkeys, where 5-HT axon terminals were found to be more abundant in the ventral than in dorsal striatum (see Lavoie & Parent, 1990).

Furthermore, 5-HT axon terminals were reportedly more abundant in the rostral than in the caudal portion of the striatum in squirrel monkeys (Lavoie & Parent, 1990), whereas the inverse was found in macaque monkeys (Mori *et al.*, 1985b). In the present study, we did not note significant variations in the density of 5-HT axon terminals along the caudorostral axis of the human striatum, but a recent biochemical study in human postmortem material have reported a slight caudorostral decreasing gradient in 5-HT concentrations (Kish *et al.*, 2008).

The 5-HT heterogeneity was particularly obvious in the head of the caudate nucleus, whose ventral border displays dense patches of 5-HT axon terminals. Similar zones of 5-HT hyperinnervation were noted in various species, including monkeys (Mori *et al.*, 1985b; Lavoie & Parent, 1990). These densely innervated patches should not be confounded with zones of poor 5-HT immunoreactivity surrounded by larger and more densely innervated areas reported previously in striatum of squirrel monkeys (Lavoie & Parent, 1990). The latter zones were in register with TH-poor and ENK-rich areas of similar size and hence correspond to the striatal compartment termed striosomes (see Graybiel & Ragsdale, 1983). In the present study, no 5-HT-poor zones that might correlate with the ENK-rich striosomes could be detected in the caudate nucleus, putamen and ventral striatum, indicating that the distribution of 5-HT fibers and axon terminals in the human striatum do not obey the striosomes and matrix compartmentalization.

As it is the case for other basal ganglia components, electrophysiological and pharmacological studies have reported excitatory, inhibitory or even excitatory followed by inhibitory postsynaptic responses following electrical stimulation of the dorsal raphe nucleus or local application of 5-HT in the striatum (see Lavoie & Parent, 1990). The multiple 5-HT receptor types expressed by various neuronal elements at pre- and postsynaptic levels might explain the multifarious effects of 5-HT at the striatum level (see Di Matteo *et al.*, 2008). The existence of both junctional and non-junctional relationships between 5-HT

terminals and their target sites may also account for some of the variation noted above (Soghomonian *et al.*, 1989). For instance, direct depolarizing monosynaptic responses to dorsal raphe nucleus stimulation could results from an axospinous action of 5-HT, whereas inhibitory or modulatory effects might be mediated through non-synaptic, axo-axonic appositions (Lavoie & Parent, 1990). Such axo-axonic interactions likely play a crucial role in the functional organization of the striatum by allowing 5-HT to modulate presynaptically the glutamatergic afferents from the cerebral cortex and thalamus, as well as the DA projection from the substantia nigra pars compacta.

Recent evidences gathered form clinical work and basic research have emphasized the importance of the complex functional interaction that exists between 5-HT and DA systems in the overall basal ganglia functioning (see Di Matteo *et al.*, 2008). The present immunohistochemical investigation of the human basal ganglia has revealed that the 5-HT axons arborize as densely and as widely as the DA axons at striatal level. Furthermore, the numerous 5-HT axon terminals noted in close apposition to human nigral DA cells indicate that 5-HT neurons of the midbrain raphe nuclei can exert their influence at both ends of the nigrostriatal DA projection, probably through collaterals of the same axons (Van Der Kooy & Hattori, 1980). An interesting feature of the 5-HT/DA interactions at the striatal level is the capability of 5-HT terminals to convert exogenous L-DOPA to DA through L-aromatic amino acid decarboxylase (AADC), and store and release DA through the vesicular monoamine transporter-2 (VMAT-2) in an activity dependent manner (see Carta *et al.*, 2007b). Hence, in certain conditions, such as in parkinsonian patients undergoing L-DOPA therapy, the striatal 5-HT terminals can contribute to improve motor disabilities by acting as a local source of DA. However, because they lack the DA transporter (DAT), the striatal 5-HT terminals can not properly control the release of DA. This non-physiological release of DA by 5-HT terminals might lead to excessive stimulation of DA receptors and provoke dyskinesia, a major and common side effect of L-DOPA therapy in parkinsonian patients (Carta *et al.*, 2007b). Altogether, these findings indicate

that 5-HT and DA systems act in concert to ensure the proper functioning of the basal ganglia and an adequate control of motor behavior.

Concluding remarks

The present study has provided the first morphological account of the 5-HT innervation of human basal ganglia. Neurons of the dorsal and median raphe nucleus were found to emit axons that traverse the brainstem via the transtegmental system, ascend towards the forebrain within the medial forebrain bundle and reach their various target sites by coursing along the major output pathways of the basal ganglia. These 5-HT axons arborize in virtually all basal ganglia components with the substantia nigra receiving the densest innervation and the striatum the most heterogeneously distributed one. Although the striatum – the major input structure of the basal ganglia – appears to be a common termination site for many of the 5-HT ascending axons, our results reveal that the widely distributed 5-HT neuronal system can also act directly upon neurons located within the two major output structures of the basal ganglia, namely the internal pallidum and the substantia nigra pars reticulata. This system appears also to have a direct access to neurons at the origin of the DA nigrostriatal pathway, a finding that underlines the importance of the 5-HT/DA interactions in the physiopathology of basal ganglia.

2.7. Acknowledgements

This work was supported by grant 386396 of the Natural Sciences and Engineering Research Council of Canada to Martin Parent. The authors express their sincere gratitude to Dr. Peter V. Gould for the neuropathological analysis of the brains, Dr. Claudio Cuello for having provided the enkephalin antibody, Mrs. Doris Côté and Marie-France Champigny for expert technical assistance and Dr. André Parent for his significant contribution to this manuscript.

2.8. Figures

TABLE 2.1. – Subject characteristics

Specimen	Age (years)	Sex	Postmortem delay (h)	Cause of death	Plane of section
1	60	M	10	Myocardial infarction	Coronal
2	80	F	12	Pulmonary failure	Coronal
3	65	M	10	Myocardial infarction	Sagittal
4	75	M	12	Abdominal aorta rupture	Sagittal
5	54	M	11	Myocardial infarction	Coronal
6	20	M	10	Polytraumatism	Coronal
7	24	M	15	Polytraumatism	Coronal
8	21	M	15	Polytraumatism	Coronal
9	25	M	9	Abdominal aorta rupture	Coronal

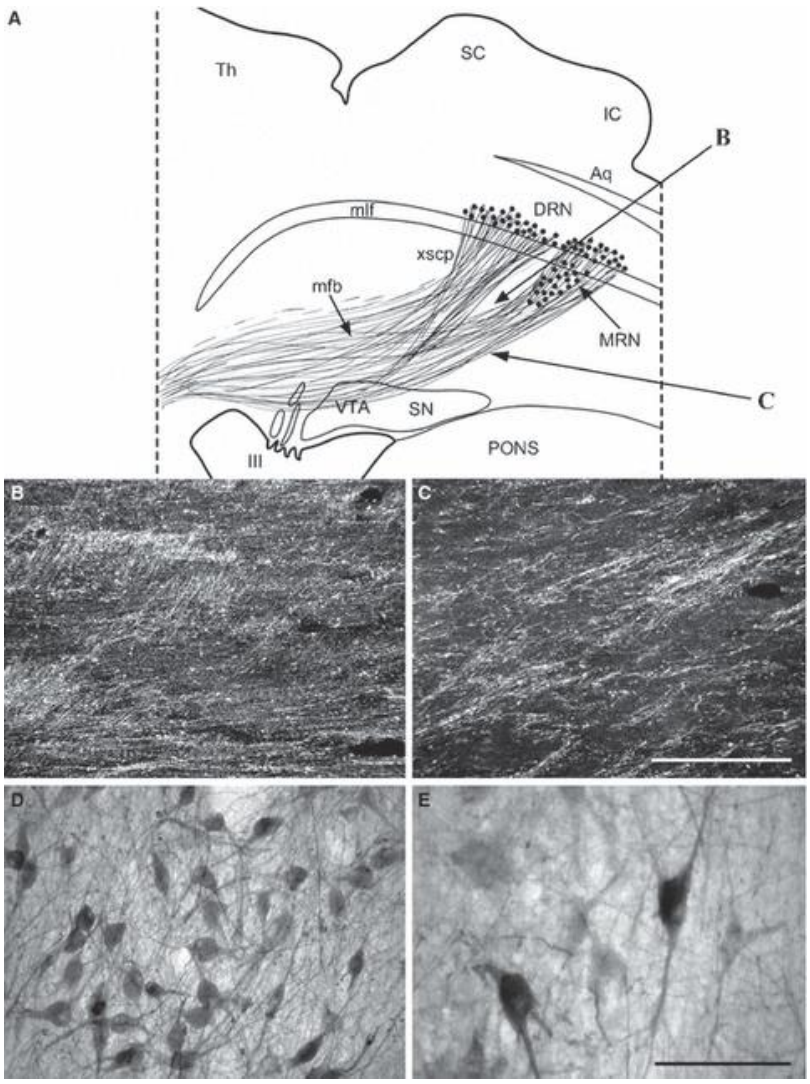

FIGURE 2.1. - (A) Distribution of the ascending 5-HT axons (thin and sinuous lines) originating from neurons (small dots) of median (MRN) and dorsal (DRN) raphe nuclei depicted on a drawing of a sagittal section taken through the human brainstem. This global picture of the ascending 5-HT system was obtained by superimposing the examined sections immunostained for SERT or TPH. (B,C) Dark-field photomicrographs of ascending axons immunostained for SERT (for exact location see arrows in A). (D, E) Neurons of the dorsal (D) and median (E) raphe nuclei displaying TPH immunostaining. Scale bar = 400 μm (C; also valid for B and D) and 100 μm (E). Abbreviations: DRN, dorsal raphe nucleus; MRN, median raphe nucleus; SERT, serotonin transporter; TPH, tryptophane hydroxylase; 5-HT, 5-hydroxytryptamine (serotonin).

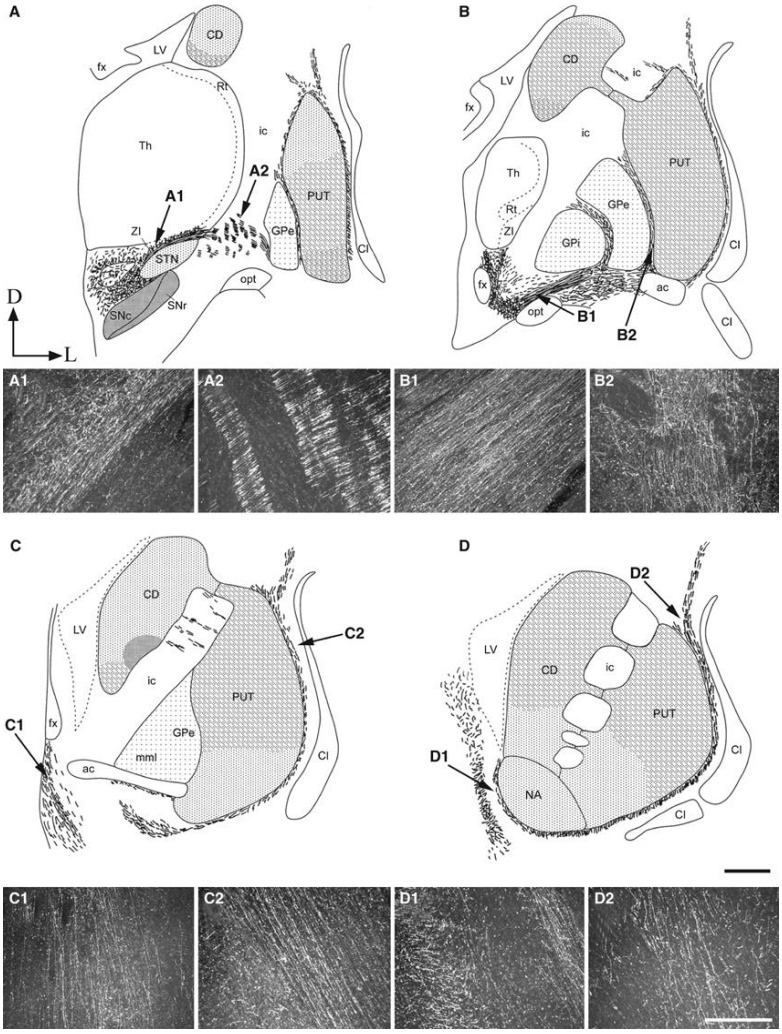

FIGURE 2.2. - (A–D) Schematic drawings depicting the 5-HT innervation of human basal ganglia at four different caudorostral levels, as revealed by SERT immunostaining. The sinuous lines in each diagram represent 5-HT axons closely surrounding the various basal ganglia components. Stippled areas of different intensities are used to represent the variations in the density of the two major types of SERT-immunoreactive axons as well as the multitude of isolated SERT+ axon varicosities encountered within each basal ganglia component. The density of SERT innervation in the thalamus and the claustrum was not analysed. (A^1–D^2) Each drawing is complemented by two dark-field photomicrographs that illustrate the morphological aspect of SERT+ axons. Arrows indicate the exact location where photomicrographs were taken. Scale bars = 5 mm (D; also valid for A–C) and 400 μm (D^2; also valid for A^1–D^1). Abbreviations: SERT, serotonin transporter; 5-HT, 5-hydroxytryptamine (serotonin).

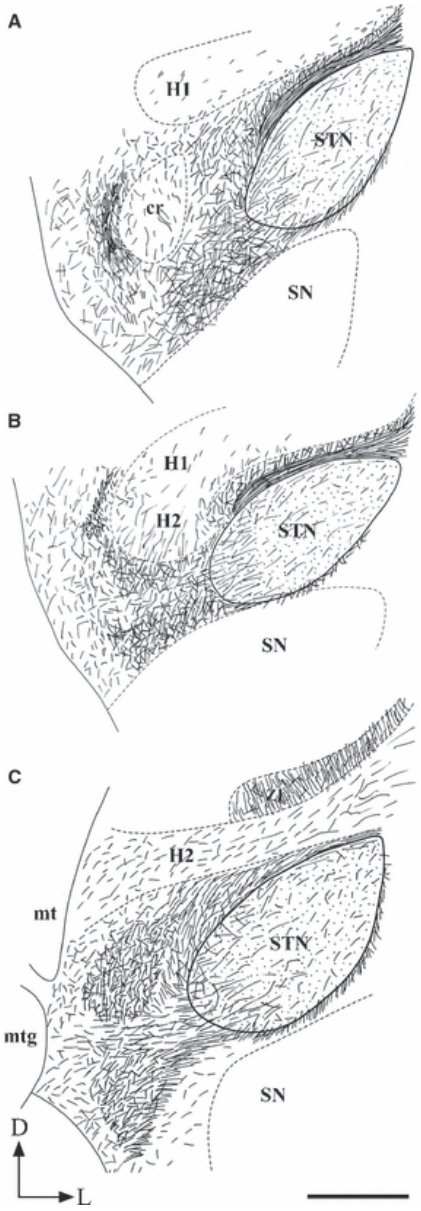

FIGURE 2.3. - Schematic drawings showing the 5-HT innervation of the human subthalamic nucleus (STN) and immediate surroundings, as visualized with SERT immunohistochemistry. The drawings represent sections taken through the posterior (A), middle (B) and anterior (C) thirds of STN. Scale bar = 2 mm (C; also valid for A and B). Abbreviations: SERT, serotonin transporter; STN, subthalamic nucleus; 5-HT, 5-hydroxytryptamine (serotonin).

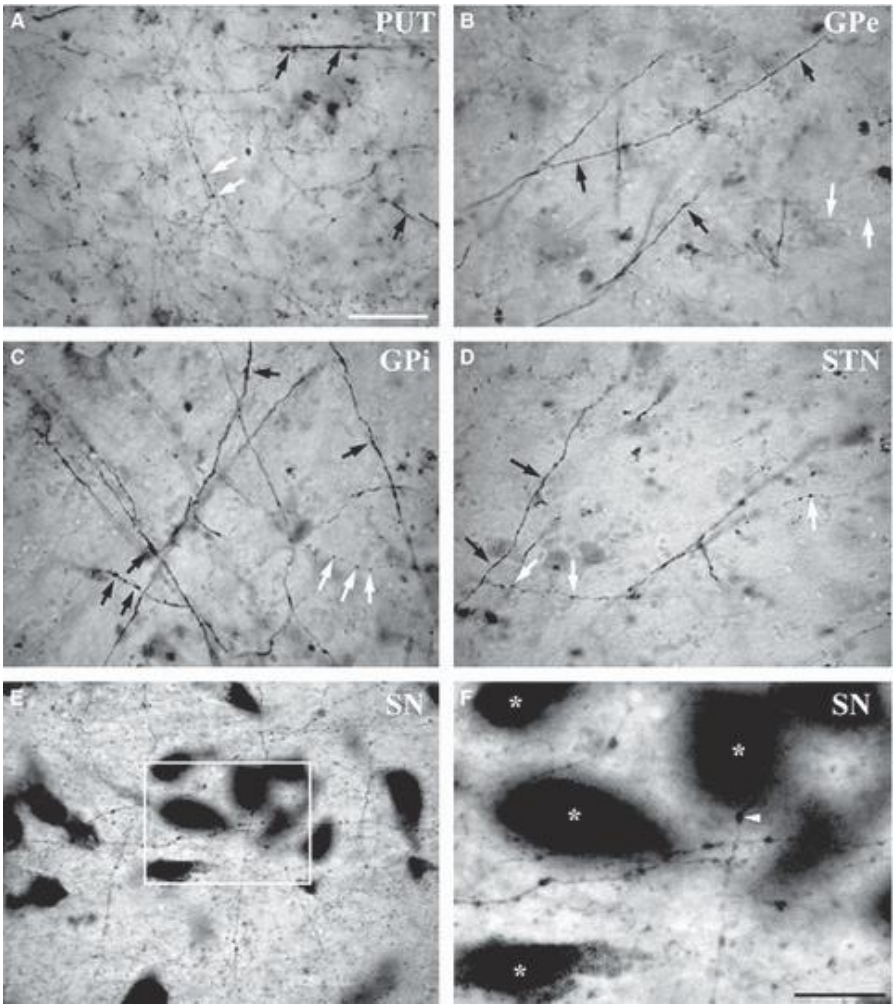

FIGURE 2.4. - Light-field photomicrographs illustrating various morphological features of the 5-HT (SERT+) axons in: (A) the putamen (PUT), (B) the external segment of the pallidum (GPe), (C) the internal segment of the pallidum (GPi), (D) the subthalamic nucleus (STN), and (E, F) the substantia nigra (SN). The photomicrograph in (F) is a higher magnification of the field outlined by the rectangle in (E). In A–D, the white arrows point to axon varicosities present on fibers of small diameter, whereas the black arrows indicate axon varicosities on fibers of larger diameter. The asterisks in (F) indicate neurons of the substantia nigra pars compacta that are markedly enriched in neuromelanin pigment. The white arrowhead in the same figure points to one of the numerous SERT+ axon varicosities closely apposed to the soma of a pars compacta neuron. Scale bars = 50 μm (A; also valid for B–E) and 25 μm (F). Abbreviations: GPe, external segment of the pallidum; GPi, internal segment of the pallidum; PUT, putamen; SERT, serotonin transporter; 5-HT, 5-hydroxytryptamine (serotonin).

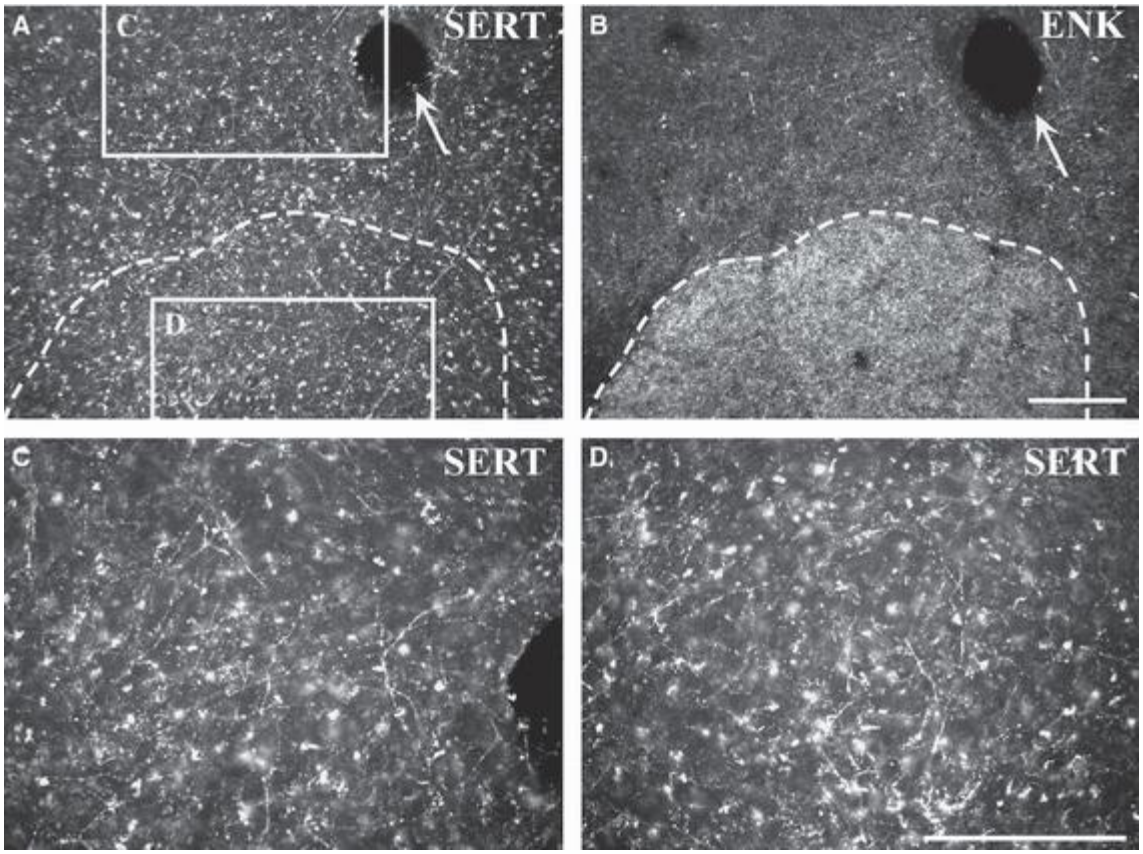

FIGURE 2.5. - Dark-field photomicrographs illustrating the 5-HT innervation of the striosomal compartment of the human striatum. The axons were immunostained for SERT (A, C, D), whereas the striosomes (B) were revealed on adjacent sections by enkephalin immunostaining. The blood vessel indicated by the arrow in A and B was used as a landmark, whereas the stippled lines in the same figures delimit the boundaries of a striosome. The SERT+ axons located outside and inside this striosome are shown at a higher magnification in C and D, respectively (see rectangles in A for exact locations). Scale bars = 200 μm (B; also valid for A) and 200 μm (D; also valid for C). Abbreviations: SERT, serotonin transporter; 5-HT, 5-hydroxytryptamine (serotonin).

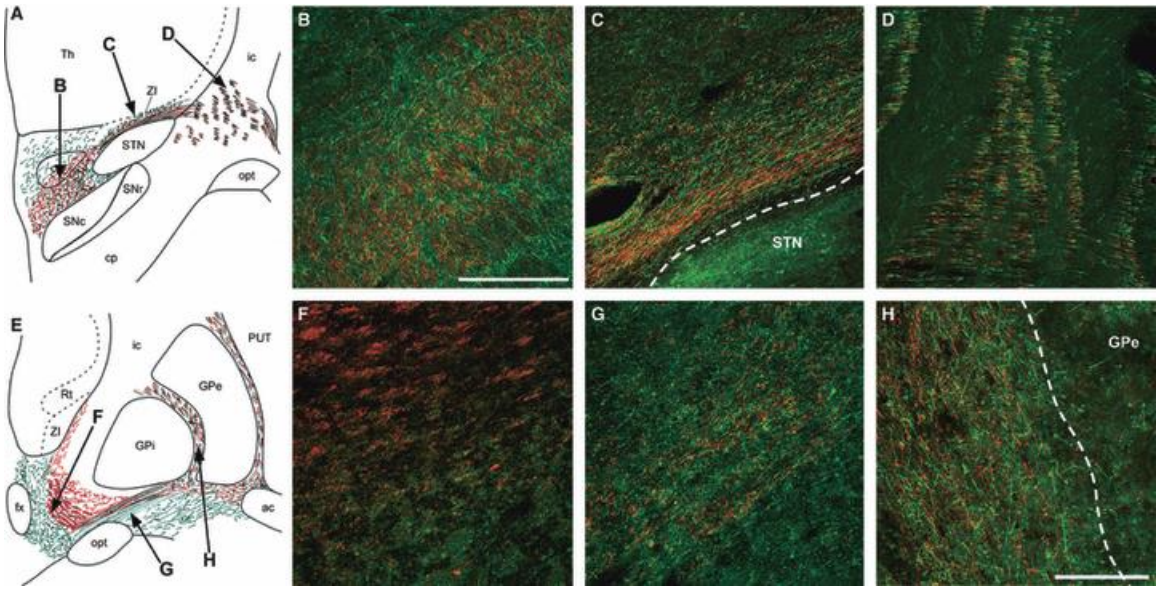

FIGURE 2.6. - Color confocal photomicrographs comparing on single sections the co-distribution of SERT- (green) and TH- (red) immunostained axons at the caudal (A–D) and medial (E–H) levels of the human basal ganglia (corresponding respectively to the first and second levels illustrated in Fig 2). The arrows in A and E indicate where various photomicrographs were taken. Caudally, the two types of fibers ascend within the medial forebrain bundle, where SERT+ fibers are more diffusely distributed than TH+ fibers (B), course along the dorsal aspect of the subthalamic nucleus (STN, C) and traverse the internal capsule (ic, D) en route to the pallidum. More rostrally, SERT+ positive fibers stand ventromedially to TH+ fibers within the medial forebrain bundle (F), are more abundant and more diffusely distributed than TH+ fibers at the basis of the pallidal complex (G), whereas both types of fibers occur in about equal number in the internal medullary lamina (H), which separates the external pallidum (GPe) from the internal pallidum (GPi). The stippled lines in C and H indicate the dorsal border of STN and the lateral border of the internal medullary lamina, respectively. Scale bars = 500 μm (B; also valid for C, D, F and G) and 200 μm (H). Abbreviations: GPe, external segment of the pallidum; GPi, internal segment of the pallidum; SERT, serotonin transporter; STN, subthalamic nucleus; TH, tyrosine hydroxylase.

CHAPITRE 3 :

DISRIBUTION OF VGLUT3 IN HIGHLY COLLATERALIZED AXONS FROM THE DORSAL RAPHE NUCLEUS AS REVEALED BY SINGE-NEURON RECONSTRUCTIONS

CHAPITRE 3 – *DISTRIBUTION OF VGLUT3 IN HIGHLY COLLATERALIZED AXONS FROM THE RAT DORSAL RAPHE NUCLEUS AS REVEALED BY SINGLE-NEURON RECONSTRUCTIONS*

Dave Gagnon et Martin Parent

Centre de recherche CERVO
2601, Ch. de la Canardière, Québec, Québec
Canada G1J 2G3

PLoS One (2014) 9 : e87709

3.1. Résumé

Cette étude fournit la toute première description morphologique et neurochimique détaillée, au niveau unitaire, des neurones du noyau raphé dorsal chez le rat, incluant la distribution de la protéine VGLUT3 à l'intérieur de ces axones. Des injections stéréotaxiques sous guidage électrophysiologique ont permis de marquer les neurones du noyau raphé dorsal avec un traceur antérograde. Le domaine somatodendritique et axonal des neurones marqués a été reconstruit entièrement et individuellement à partir de sections sériées et en utilisant un système d'analyse d'image informatisé. Sous anesthésie, les neurones du noyau raphé dorsal montrent une activité électrophysiologique spontanée hautement rythmique (1.72 ± 0.50 Hz). Ils possèdent un corps cellulaire de taille moyenne (9.8 ± 1.7 µm) avec 2-4 dendrites primaires orientées principalement dans l'axe antéropostérieur. Les axones ascendants du noyau raphé dorsal sont hautement collatéralisés (longueur d'axone totale pouvant atteindre 18.7 cm), ce qui leur permet d'interagir à la fois avec plusieurs structures du télencéphale telles que le striatum, le cortex préfrontal et l'amygdale. Les caractéristiques morphologiques ainsi que le contenu en VGLUT3 varient significativement en fonction des structures cibles des neurones reconstruits. L'analyse en microscopie confocale de la distribution de VGLUT3 dans des axones individuellement marqués a démontré que les varicosités axonales qui expriment VGLUT3 sont plus volumineuses (0.74 ± 0.03 µm) que celles qui ne présente pas cette protéine (0.55 ± 0.03 µm). De plus, le pourcentage de varicosités axonales qui contiennent le VGLUT3 est légèrement plus élevé dans le striatum (93%) que dans le cortex moteur (75%), suggérant un mécanisme complexe d'aiguillage de la protéine VGLUT3 dans les axones hautement collatéralisés des neurones du noyau raphé dorsal. Nos résultats fournissent la première preuve directe que les projections ascendantes en provenance du noyau raphé dorsal sont composées d'axones fortement collatéralisés, dont la capacité à co-libérer la sérotonine et le glutamate varie d'une structure cible à l'autre.

3.2. Abstract

This study aimed at providing the first detailed morphological description, at the single-cell level, of the rat dorsal raphe nucleus neurons, including the distribution of the VGLUT3 protein within their axons. Electrophysiological guidance procedures were used to label dorsal raphe nucleus neurons with biotinylated dextran amine. The somatodendritic and axonal arborization domains of labeled neurons were reconstructed entirely from serial sagittal sections using a computerized image analysis system. Under anaesthesia, dorsal raphe nucleus neurons display highly regular (1.72 ± 0.50 Hz) spontaneous firing patterns. They have a medium size cell body (9.8 ± 1.7 µm) with 2-4 primary dendrites mainly oriented anteroposteriorly. The ascending axons of dorsal raphe nucleus are all highly collateralized and widely distributed (total axonal length up to 18.7 cm), so that they can contact, in various combinations, forebrain structures as diverse as the striatum, the prefrontal cortex and the amygdala. Their morphological features and VGLUT3 content vary significantly according to their target sites. For example, high-resolution confocal analysis of the distribution of VGLUT3 within individually labeled-axons reveals that serotonin axon varicosities displaying VGLUT3 are larger (0.74 ± 0.03 µm) than those devoid of this protein (0.55 ± 0.03 µm). Furthermore, the percentage of axon varicosities that contain VGLUT3 is higher in the striatum (93%) than in the motor cortex (75%), suggesting that a complex trafficking mechanism of the VGLUT3 protein is at play within highly collateralized axons of the dorsal raphe nucleus neurons. Our results provide the first direct evidence that the dorsal raphe nucleus ascending projections are composed of widely distributed neuronal systems, whose capacity to co-release serotonin and glutamate varies from one forebrain locus to the other.

3.3. Introduction

Neurons of the raphe nuclei are involved in multitudinous functions, such as the regulation of sleep-waking cycle, the modulation of pain signals and the pathogenesis of mood disorders. This multifaceted role of raphe neurons is possible because they form a widely distributed neuronal system that reaches virtually all major brain structures, as indicated by previous immunolabeling studies (Steinbusch, 1981). Originally divided into nine entities (Dahlstroem & Fuxe, 1964b), the raphe nuclei are actually considered to form a small caudal and a large rostral group having distinct efferent projections (Tork, 1990; Hornung, 2003; Monti & Jantos, 2008). The caudal group comprises medullary raphe nuclei, which project to the spinal cord whereas the rostral group, scattered along the pons and midbrain, contains the dorsal (DRN, B6 and B7) and median (B8) raphe nuclei, which supply about 85% of the serotonin (5-hydroxytryptamine, 5-HT) forebrain innervation (Hornung, 2003).

Retrograde double-labeling experiments have suggested that many raphe neurons are endowed with a markedly collateralized axon (Van Der Kooy & Hattori, 1980; Kohler *et al.*, 1982; Kohler & Steinbusch, 1982; Sarter & Markowitsch, 1984; Imai *et al.*, 1986; Li *et al.*, 2001a; Waselus *et al.*, 2011). Bulk injections of anterograde tracers have also revealed that the dorsal raphe efferent projections are widely distributed (Azmitia & Segal, 1978; Vertes, 1991a; Morin & Meyer-Bernstein, 1999b; Vertes *et al.*, 1999b). This notion was further extended by antidromic invasion experiments (Condes-Lara *et al.*, 1989). More recently, single-cell recording and labeling were conducted in the rat DRN, but without providing entire axon reconstructions (Li *et al.*, 2001b; Kocsis *et al.*, 2006). Similar approach was also used to gather morphological data on 5-HT neurons of the rat medulla (Gao & Mason, 1997).

It has previously been reported that vesicular glutamate transporter 3 (VGLUT3), which is responsible for glutamate vesicular packaging, is expressed in the DRN (Fremeau *et al.*, 2002; Gras *et al.*, 2002; Hioki *et al.*, 2010; Kiyasova *et al.*, 2011; Gaspar & Lillesaar, 2012) and VGLUT3 protein has been

visualized in many 5-HT axon varicosities in specific target sites (Gras *et al.*, 2002; Hioki *et al.*, 2004; Mintz & Scott, 2006; Shutoh *et al.*, 2008; Commons, 2009; Amilhon *et al.*, 2010). This observation, in addition to electrophysiological (Johnson, 1994) and optogenetic studies (Varga *et al.*, 2009) indicate that a proportion of DRN neurons might be able to release glutamate as well as 5-HT in their different target sites. This might play a significant role in neuroadaptative plasticity that take place during development and neurological diseases.

In view of the involvement of DRN neurons in various basic brain functions and brain disease, we thought it worthwhile to investigate, at the single cell level, the trajectory and arborization of their ascending axonal projections as well as the distribution of the VGLUT3 protein within their axons. In order to do so, we combined immunofluorescence with a procedure that allows the injection of very small subsets of electrophysiologically identified neurons and the tracing of single anterogradely-labeled axons arising from the DRN in rats. This research has yielded novel findings that should be taken into account if one hopes to reach a more complete understanding of the anatomical and functional organization of the DRN efferent projections.

3.4. Material and methods

3.4.1. Animals

A total of 15 adult male Sprague-Dawley rats with body weight ranging from 300-450 g were used in the present study. Animal work was performed in accordance to the *Canadian Guide for the Care and Use of Laboratory Animals,* and the Université Laval Institutional Animal Care Committee approved all surgical and animal care procedures (certification #2013-113).

3.4.2. Stereotaxic injections

The animals were first anaesthetized with a mixture of ketamine (80 mg/kg) and xylazine (10 mg/kg) before their heads were placed in a stereotaxic apparatus. Two microiontophoretic injections of biotin dextran amine (BDA; Molecular probes, Eugene, Or) were made in the DRN of each rat, with the help of the stereotaxic atlas of Paxinos and Watson (1986). Microiontophoretic labeling was carried out with glass micropipettes (tip diameter 2-3 µm) filled with a solution of potassium acetate (0.5 M) plus 2% BDA 10,000 MW (Invitrogen). These electrodes had impedance ranging between 6-12 MΩ and were also used to monitor the extracellular activity of the neuronal populations encountered during the penetration of the micropipette, including the typical spontaneous rhythmic activity of DRN neurons. These recordings were obtained from 1-3 neurons at each injection site. When the target was reached, the pipette was connected to a high compliance iontophoresis device (NeuroData) and the tracer was injected by passing positive current pulse of 250 nA (1s on/ 1s off) for 25 minutes.

3.4.3. Tissue processing for axonal reconstructions

After a survival period of 7 days, rats were perfused transcardially with 300 mL of ice-cold sodium phosphate-buffered saline (PBS; 50 mM; pH 7.4), followed by 900 mL of 4% paraformaldehyde (PFA) in 0.1 M sodium phosphate buffer

(PB; pH 7.4) and 300 mL of sucrose 10% in PB 0.1 M. After a post-fixation of 24h in a solution composed of one third PFA 4% and two thirds sucrose 30% diluted in PB, brains were cut along the sagittal plane in 60 µm serial sections using a freezing microtome. Sections were processed for the visualization of BDA according to the avidine-biotine-peroxidase method (ABC, Vector Labs) using nickel intensified 3-3' diaminobenzidene tetrachloride (NiDAB) as the chromagen. In brief, the sections were incubated overnight at 4°C in a solution containing ABC diluted 1:60 in 0.1 M PBS, pH 7.4, plus 1% normal rabbit serum and 0.1% triton X-100. They were then rinsed twice in PBS and once in Tris buffer. The bound peroxidase was revealed by incubating the sections in a solution containing 0.05% DAB, 0.3% nickel-ammonium sulfate, and 0.003% hydrogen peroxide in 0.05M Tris buffer, pH 7.6, for 7-10 minutes at room temperature. The reaction was stopped by two washes in Tris buffer followed by two rinses in PBS. To help identifying structures that harbored labeled axons, sections were counterstained for cytochrome oxidase, according to the histochemical protocol of Wong-Riley (Wong-Riley, 1979). The counterstaining was performed before BDA revelation, and nickel-intensified DAB (dark blue reaction) and unintensified DAB (diffuse brown precipitate) were used to reveal BDA and cytochrome oxidase, respectively. Sections were mounted on gelatin-coated slides, dehydrated in graded alcohols, cleared in toluene, and coverslipped with Permount. Labeled axons were reconstructed in three dimensions by using a light microscope equipped with a motorized stage and an image analysis software (Neurolucida, MicroBrightField, Colchester, VT). Entire and individual axonal reconstructions were obtained from serial sagittal sections, each containing at least one axonal segment. By going from one section to another, we were able to follow and reconstruct individually the injected neurons. The terminal fields of labeled neurons were mapped at lower magnifications to determine their topographic localization.

3.4.4. Immunofluorescence

Some brain sections were also processed for triple immunofluorescence to characterize the distribution of VGLUT3, VMAT2, SERT and 5-HT in BDA-injected neurons. Briefly, the 60 µm-thick sagittal sections were incubated at room temperature in a blocking solution of PBS 0.1 M containing 2% normal serum and 0.1% Triton X-100 for 30 min and then, in the same blocking solution to which primary antiserum against either 5-HT/VGLUT3, SERT/VGLUT3, 5-HT/SERT or VMAT2/VGLUT3 was added (overnight at 4°C). Then, sections were incubated with corresponding secondary antibodies and with streptavidin Texas Red to reveal the BDA in injected neurons for 2h at room temperature (see Table 1 for details on antibodies, concentrations and specificity). The VMAT2/VGLUT3/BDA immunostaining was performed on adjacent sections labeled for 5-HT/VGLUT3/BDA in order to assess the 5-HT nature of the BDA-injected axon that could be traced from one section to the other.

3.4.5. Confocal image analysis

Slides were coverslipped with fluorescence mounting medium (DAKO, Ontario, Canada) and the distribution of immunolabeled proteins within the BDA-filled neurons was analyzed by using a confocal microscope (LSM 700, Zeiss) and an image-analysis software (Imaris, Bitplane). After confocal imaging, sections were reincubated in ABC and NiDAB (as above) to visualize and reconstruct, under a bright field microscope, BDA-injected neurons.

3.5. Results

3.5.1. General labeling features and somatodendritic arborization

The injection procedure used in the present study produces small injection sites involving 15-20 DRN neurons per site. Most injection loci display a dense core of BDA precipitate surrounded by several neurons labeled in a Golgi-like manner (Fig. 1A). The somatodendritic domain (Fig. 1B) and axonal arborization field (Fig. 1D) are entirely labeled. The DRN neurons have a medium sized cell body (9.8 ± 1.7 µm;N = 41) emitting 2-4 long and poorly ramified primary dendrites that are characteristically thick and sparsely spined. Dendrogram analysis reveals that the somatodendritic domain of DRN takes the form of an ellipse (about 700 x 500 x 300 µm) preferentially oriented along the anteroposterior axis (Fig. 1C). Such dendritic field often covers the entire anteroposterior axis of the DRN. Dendrites of DRN neurons occasionally extend beyond the boundaries of the DRN (Fig. 1E). Intensely labeled axons emerge from either the core of the injection sites or from individually labeled neurons located peripherally. In the latter case, the axons stems from either the cell body or a primary dendrite (Fig. 1B). Extracellular recordings of BDA-injected neurons in the DRN indicate a highly rhythmic and regular firing pattern with an average frequency of 1.72 ± 0.50 Hz (Fig. 1C).

3.5.2. Axonal trajectory

General features

The axon of 32 DRN neurons were individually reconstructed in three-dimensions by using a computer image analysis system. Despite a great diversity of axonal branching patterns was noted, many DRN axons follow similar initial trajectories. Most of the reconstructed axons (27/32) pass through the so-called *transtegmental system*, that has been described in details elsewhere (Parent *et al.*, 1981). These axons leave the DRN without

providing any local collaterals and arch rostroventrally to traverse the central portion of the midbrain tegmentum and reach the decussation of the superior cerebellar peduncle. Only 4 reconstructed axons were seen to travel through the so-called *paraventricular system*(Parent *et al.*, 1981) by coursing along the dorsal longitudinal fasciculus, en route to the superior and inferior colliculi. These axons then arch ventrally beneath the posterior commissure to reach the lateral hypothalamic area. Interestingly, one DRN neuron had an axon that bifurcate within the confines of the nucleus; one of its branch travels within the transtegmental pathway, while the other courses along the periventricular pathway (Fig. 1E). As they run anteriorly, most labeled axons ascend within the lateral hypothalamic area, along the medial forebrain bundle, except those that innervate caudal structures such as the subthalamic nucleus and the substantia nigra. Labeled axons that course within the lateral hypothalamic area sweep laterally to innervate various components of the forebrain. Along their caudorostral trajectory in the lateral hypothalamic area, axons from the DRN are mostly beaded, but as they reach their target site, their morphological features vary from one locus to the other. In some forebrain structures, axon collaterals are endowed with varicosities "en passant" whereas in others, axons collaterals branch frequently, providing a dense terminal field. It is noteworthy that most DRN neurons provide two types of axonal projections: thin and varicose, and thick and beaded fibers. However, the vast majority of axonal segments are thin and uniform and endowed with fusiform axon varicosities. No contralateral or local axonal projections were observed. Based on the marked variability of axonal branching patterns noted in the different target sites, the population of DRN appears as highly diversified. Representative examples of reconstructed neurons will now be presented according to their major target areas: the striatum, the diencephalon and midbrain tegmentum, the amygdala and septal area and the cerebral cortex. Detailed information on all 32 reconstructed axons is given as supplementary information (Table S1).

Striatum

Reconstructed neurons that project to the striatum were located rather medially and caudally in the DRN (Fig. 2F and Fig. S2). A striking example of such neuron is illustrated in figure 2A. As for the majority of reconstructed neurons, the main axon exits rostroventrally, enters the medial forebrain bundle and travels through the lateral hypothalamic area. In this area, three main sets of axon collaterals are emitted; they sweep dorsally and remain unbranched until they reach the striatum. There, they break into several short terminal collaterals that spread throughout a large portion of the dorsolateral striatum, considered as the sensorimotor territory. The axon of this particular neuron has a total length of about 11 cm and displays 2,131 axon varicosities in the striatum. Interestingly, the main axonal branch pierces the claustrum to arborize densely in a restricted area of the prefrontal cortex, where it provides only 311 axon varicosities. Two axonal branches bifurcate ventrally to innervate the olfactory tubercle. Another DRN neuron that innervates the striatum (Fig. 2B), emits an axon that passes through the substantia nigra pars compacta, with axon varicosities "en passant", and courses within the lateral hypothalamic area and the magnocellular pre-optic nucleus. The axon exhibits few varicosities in the ventral pallidum and runs dorsally in the corpus callosum where it emits a major collateral that arborize profusely within a wide area of the sensorimotor territory of the striatum. The main axonal branch enters the motor cortex and divides into thinner collaterals that innervate all cortical layers. The neuron shown in figure 2C has an axon emitting a collateral in the lateral hypothalamic area that runs dorsally towards the bed nucleus of the stria terminalis to arborize profusely in the nucleus accumbens. The main axonal branch ends its course in the nucleus accumbens, where it displays a wide and dense terminal arborization. Few beaded axon collaterals are also observed in the lateral hypothalamic area.

Diencephalon and midbrain tegmentum

The axonal arborization of a typical DRN neuron innervating the thalamus is shown in figure 2D. The cell body of this neuron lies centrally in the caudal portion of the DRN (Fig. 2F). The axon runs within the median raphe nucleus before traveling through the paraventricular system where it divides into two main branches, one that sweeps ventrally to innervate the ventral tegmental area, the supramammillary nucleus, the mammillary body and the lateral hypothalamic area, and the other that courses rostrally and dorsally to arborize in the paracentral, parafascicular and lateral habenular nucleus of the thalamus. The main axonal branch terminates within the nucleus accumbens. The neuron depicted in figure 2E emits an axon that arches rostroventrally to travel within the median raphe nucleus and arborize in both the substantia nigra pars compacta and the subthalamic nucleus, two important components of the basal ganglia.

Amygdala

Reconstructed neurons that arborize profusely in the amygdala were principally located in the dorsal and caudal portions of the DRN (Fig. 2F and Fig. S2). One of these neurons is depicted in figure 3A. Its axon runs through the supramammillary nucleus and the lateral hypothalamic area, where it gives off a major collateral that ascends dorsally, enters the bed nucleus of the stria terminalis and invades the stria terminalis itself. After a typical loop along the lateral border of the thalamus, this axon collateral sweep laterally to provide a terminal arborization to the central and basolateral nuclei of the amygdala. The main axonal branch terminates in the nucleus accumbens, considered as the limbic territory of the striatum. Another neuron that aims to the amygdala is depicted in figure 3B; its axon innervates profusely the central and basolateral amygdaloid nuclei, as well as the bed nucleus of the stria terminalis and the ventral pallidum.

Prefrontal cortex

Neurons that innervate the prefrontal cortex have their cell bodies widely distributed in the DRN (Fig. 2F and Fig. S2), and two neurons of this type are depicted in figure 3 (Fig. 3C, D). Their axon typically runs through the transtegmental system. They ascend through the ventral tegmental area and the lateral hypothalamic area to enter the lateral septum (Fig. 3C) or the nucleus accumbens (Fig. 3D), where they provide a small number of axon varicosities. The axon of both neurons reaches the prefrontal cortex where they arborize within all six cortical layers, providing respectively 3,063 and 239 axon varicosities. The axon illustrated in figure 3C also yields a collateral that enters the subiculum and arborizes profusely in CA1, but also in CA2, CA3 and dentate gyrus.

3.5.3. Distribution of VGLUT3, VMAT2, 5-HT and SERT within the BDA-filled axons

The 5-HT nature of individually traced axonal segments from the DRN was examined only in the set of experiments designed to investigate the axonal distribution of VGLUT3 at the single-cell level with confocal microscopy. From 156 BDA-labeled cell bodies mainly located in the central portion of the DRN, 117 (75%) were found to display immunostaining for 5-HT. All BDA/5-HT labeled neurons were immunoreactive for VGLUT3 (Fig. 4). All BDA-filled axonal segments and axon varicosities that were observed and traced in the striatum and the prefrontal cortex were immunoreactive for SERT and 5-HT (Fig. S1). Among those varicosities, the vast majority was immunoreactive for VGLUT3. Overall, from 259 axon varicosities located in the motor cortex that were examined in details with the confocal microscope and that belong to 29 distinct axonal segments of BDA-injected neurons (Figs. 5, 6), 75% (193/259) were immunoreactive for VGLUT3, but this percentage reaches 93% (70/75) in the dorsal striatum after the reconstruction of 10 axonal segments. Although the proportion varies depending on the target site, some VGLUT3+ and VGLUT3- axon varicosities were observed along the same BDA-filled axonal

segment. 13/29 axonal segments observed in motor cortex and 6/10 in dorsal striatum contained axon varicosities that were all VGLUT3+ whereas no axonal segment were completely devoid of VGLUT3+ boutons. Axon varicosities that contain VGLUT3 were larger than those devoid of this marker (0.74 ± 0.03 µm vs. 0.55 ± 0.03 µm, $P< 0.001$). While all BDA-filled axon varicosities and intervaricose axonal segments were immunoreactive for 5-HT, the VGLUT3 protein was restricted to some axon varicosities and absent from intervaricose segments. The vesicular monoamine transporter type 2 (VMAT2) was mostly restricted to axon varicosities but could be seen occasionally in intervaricose segments of BDA-labeled axons. In contrast to the VGLUT3 protein, all BDA-filled axon varicosities that were examined in the prefrontal cortex and the striatum were immunoreactive for the VMAT2 (Fig. 7).

3.6. Discussion

This study has unveiled novel aspects of the organization of DRN ascending projection in the adult rat. By providing detailed reconstructions of single axonal arborization, our work has provided a firm ground for the highly collateralized nature of the DRN axonal projections. Our confocal immunofluorescence analysis has also provided the first demonstration of the precise distribution of VGLUT3, VMAT2, 5-HT and SERT in singly-labeled DRN neurons. Our data indicate that a subset of 5-HT axon varicosities are devoid of the VGLUT3 protein and that this proportion varies depending on target sites. This observation supports the existence of a complex trafficking mechanism of the different types of synaptic vesicles within the highly collateralized axons of the DRN neurons. The present study has also revealed that, based on the diversity of the pattern of their axonal projections, neurons of the DRN form a highly heterogeneous population.

3.6.1. Organization of the somatodendritic domain as an indication of integration capacity

The morphological analysis of the dendritic arborization of DRN neurons have revealed an ellipsoidal shape, measuring approximately 700 µm x 500 µm x 300 µm, with the longest axis being largely parallel to anteroposterior axis of the nucleus. Such elongated unit may cover the whole rostrocaudal extent of the DRN indicating that a single neuron is able to receive and integrate most of the DRN afferent projections. This columnar arrangement of DRN neurons is in accordance with previously published descriptions (Park *et al.*, 1982; Li *et al.*, 2001b; Allers & Sharp, 2003), including the seminal paper of Cajal (Cajal, 1909, 1911).

3.6.2. A highly collateralized axon as the morphological substratum of functional diversity

In accordance to previous study involving bulk injections of anterograde (Azmitia & Segal, 1978; Vertes, 1991a; Morin & Meyer-Bernstein, 1999b; Vertes *et al.*, 1999b) and retrograde tracers (Van Der Kooy & Hattori, 1980; Kohler *et al.*, 1982; Kohler & Steinbusch, 1982; Imai *et al.*, 1986), our data provide direct evidence for the fact that DRN neurons are endowed with a highly collateralized axon that might represent the morphological substratum of the diverse functions played by the 5-HT system. By sending a copy of its efferent message to several target sites, DRN neurons are able to modulate and to possibly synchronize the activity of several functionally diverse brain areas.

Many reconstructed neurons innervate the prefrontal cortex, which is reportedly linked reciprocally to the DRN (Sesack *et al.*, 1989a; Jankowski & Sesack, 2004). Single DRN neurons were observed to innervate both the prefrontal cortex and the hippocampus. It has already been shown that some DRN neurons fire in a time-locked manner to the hippocampus theta rhythm (Kocsis & Vertes, 1992; Kocsis *et al.*, 2006). Our results indicate that the prefrontal cortex activity, which is correlated with hippocampal theta rhythm during spatial working memory task (Hyman *et al.*, 2005; Jones & Wilson, 2005), can potentially be modulated by single DRN neuron that innervates both structures.

Some reconstructed DRN neurons, as exemplified in figure 2B, innervate both the substantia nigra and the striatum, a pattern of axonal arborization that allows a single DRN neuron to exert a dual influence upon nigrostriatal dopaminergic neurons. A single DRN neuron can thus act locally at the somatodendritic domain of nigrostriatal dopaminergic neurons, as well as distally by modulating pre-synaptically the dopaminergic axon terminals at the striatal level. The same logic can be applied to the control mesolimbic dopaminergic projection neurons, with single DRN neuron innervating locally

the ventral tegmental area and distally the nucleus accumbens (Fig. 2D). Although the neurochemical content of entirely reconstructed DRN neurons was not assessed in the present study, we hypothesize that such a modulation of dopamine by DRN neurons could be mediated through the activation of the 5-HT_{2C} receptors, which occurs at striatal axon terminal levels as well as on the cell bodies of nigral and ventral tegmental dopaminergic neurons (Alex *et al.*, 2005).

3.6.3. A broad axon terminal domain to influence wide neuronal populations

Our single cell labeling procedure has revealed that DRN neurons target many areas involved in a brain functions that range from the control of motor behaviour to that of limbic functions. Two types of neurons could be identified based on target sites of their axonal arborization: a) those that ramify principally within structures that typically belong to the limbic system, and b) others that branch mostly within brain nuclei associated with motor system. Both types of neurons possess a highly collateralized and widely distributed axon, which is ideally suited for the ubiquitous modulatory role that 5-HT neurons are known to exert at the forebrain level. Our data reveal that the axonal arborization of DRN neurons varies significantly according to their target sites. For example, single-labeled neurons that aim at the prefrontal cortex display a profuse axonal arborization that encompasses all six cortical layers and covers a wide area of cortical tissue. Likewise, striatal afferent axons branch extensively within a large portion of the structure. In contrast, axons that provide terminal branches within the lateral hypothalamic area are very poorly arborized. These findings indicate that the type of axonal branching pattern is not an intrinsic property of DRN neurons, but instead appears to be dependent on the molecular cues that are contained in each terminal site during development (Schmidt & Rathjen, 2010).

Bulk injections of anterograde tracers combined with immunohistochemistry has revealed the existence of two morphologically distinct types of 5-HT axons in the rat cerebral cortex (Kosofsky & Molliver, 1987). Axonal projections from the median raphe nucleus were reportedly enriched with large and spherical axon varicosities, while displaying significant variations in axonal diameter, whereas DRN projections displayed smaller axon diameter with smaller pleomorphic axon varicosities. Our own detailed neuronal reconstructions reveal that single labeled DRN neurons can display both of these types of axons in the cerebral cortex. However, in accordance with Kosofsky and Molliver's descriptions, the vast majority of DRN axonal segments disclosed on our material are of small and uniform diameter and endowed with fusiform axon varicosities.

As they emerge the DRN, axons bear a significant number of varicosities that appear to establish contact "en passant". Such a phenomenon also occurred in white matter tracks such as the corpus callosum or the median lemniscus. Electron microscopic studies have shown that, in many brain areas, a significant proportion of 5-HT axon varicosities are devoid of synaptic contacts. Such is the case in the rat cerebral cortex (Seguela *et al.*, 1989) and subthalamic nucleus (Parent *et al.*, 2010), where approximately half of 5-HT axon varicosities were asynaptic (Descarries *et al.*, 2010b). This feature has been viewed as morphological evidence for the existence of diffuse transmission by 5-HT systems, in addition to their synaptic mode of transmission (Descarries & Mechawar, 2008). It has also led to the suggestion that a low, ambient level of 5-HT might permanently exist in the extracellular space, the fluctuations of which could regulate a variety of physiological processes mediated by 5-HT and its receptors widely distributed on neuronal, glial and vascular elements. The partially synaptic character of 5-HT system combined to highly collateralized axons providing many axon varicosities "en passant" support the modulatory nature of 5-HT. Convincing electrophysiological evidence for a regulatory role of ambient 5-HT has already been obtained in the rat substantia nigra (Bunin & Wightman, 1998).

3.6.4. Number of axon varicosities as an indication of input strength

While reconstructing DRN neuron individually, we paid a particular attention to the number of axon varicosities emitted in the different terminal fields, as it provides an indication of the input strength of single DRN neurons in the various forebrain nuclei. It also allows to approximate the amount of neurotransmitter released by single DRN neuron since the number of axon varicosities has been shown to be correlated with extracellular neurotransmitter concentrations (Palkovits *et al.*, 1974). Neurons that innervate the prefrontal cortex display a high degree of variability in terms of the number of axon varicosities, which ranges from 85 to 3,063. It has been proposed that a given neuron is limited in its total length, as well as in the number of axonal branch and varicosities that it can emit (Parent & Parent, 2006b). This hypothesis can be illustrated by comparing the axonal arborization of the neuron shown in figure 3C, that provides 3,063 varicosities in the PFC and only 774 in the hippocampus, to the one illustrated in figure 2A that provides only 311 boutons in the PFC, but 2,131 in the striatum. Again, single-neuron reconstructions in the DRN suggest that a given neuron is limited in the number of projections that it can provide. A high degree of axon collateralization might allow exquisitely precise interactions between various brain structures but the maintenance of this morphological feature implies high-energy consumption, which might represent a limiting factor in the extent of axonal aborization that a given neuron can provide (Parent & Parent, 2006b).

3.6.5. VGLUT3 content of 5-HT axon varicosities as a factor that favors neuroplasticity

It has recently been shown that some 5-HT cell bodies located in the DRN express *VGLUT3*(Fremeau *et al.*, 2002; Gras *et al.*, 2002; Schafer *et al.*, 2002;

Takamori *et al.*, 2002; Kiyasova *et al.*, 2011; Gaspar & Lillesaar, 2012) and that only a subset of axon varicosities are immunoreactive for the protein, as indicated by the present immunofluorescence analysis of reconstructed neurons and by previous immunohistochemical studies (Hioki *et al.*, 2004; Somogyi *et al.*, 2004; Shutoh *et al.*, 2008; Commons, 2009; Amilhon *et al.*, 2010). Evidence of co-release of glutamate and 5-HT by DRN neurons has been gathered using electrophysiology (Johnson, 1994) and optogenetic (Varga *et al.*, 2009). Other *in vitro* experiments have indicated that VGLUT3 positively modulates 5-HT transmission (Amilhon *et al.*, 2010), probably through a mechanism termed vesicular-filling synergy in which glutamate co-entry in synaptic vesicles promotes storage of 5-HT by increasing the pH gradient that drives VMAT2 (Gras *et al.*, 2008; Hnasko *et al.*, 2010). Our triple immunofluorescence confocal investigation clearly shows that all axon varicosities from BDA-injected neurons of the DRN contain VMAT2, SERT and 5-HT. This finding is at odd with a previous report that indicates very sparse colocalization of SERT and 5-HT immunolabeling in mice (Amilhon *et al.*, 2010). Whether this discrepancy reflects a methodological variant or a genuine interspecies difference remains to be determined.

In agreement with previous reports (Hioki *et al.*, 2004; Somogyi *et al.*, 2004; Shutoh *et al.*, 2008; Commons, 2009; Amilhon *et al.*, 2010), our results indicate that some 5-HT axon varicosities are devoid of VGLUT3. Furthermore, we detected the presence of both VGLUT3+ and VGLUT3- axons varicosities in all target sites investigated, and these two types of varicosities often occurred along the same 5-HT axonal segment. However, we found that the proportion of axon varicosities that contain VGLUT3 is target-site dependent, a finding that supports the hypothesis of a trafficking mechanism of the VGLUT3 protein within the highly collateralized axons of the DRN neurons. We hypothesise that VGLUT3 proteins are located on the same synaptic vesicles than the VMAT2, as it appears to be the case for vesicular acetylcholine transporter (VAChT) and VGLUT3 in cholinergic axon varicosities of the striatum (Gras *et al.*, 2008) and for VGLUT2 and VMAT2 in dopaminergic striatal terminals (Hnasko *et al.*,

2010). However, our data clearly indicate the existence of a pool of 5-HT synaptic vesicles that contain VMAT2 without VGLUT3, since many VMAT2+/VGLUT3- axon varicosities were observed.

The putative capability of a given DRN neuron to release 5-HT and glutamate together or 5-HT alone is highly relevant for plasticity and neuroadaptative mechanisms that are crucial during development, aging and pathological process. As mentioned above, electron microscopic study has revealed that the synaptic incidence of 5-HT axon varicosities varies depending on target sites but is rather low compared to the glutamatergic system that appears to be entirely synaptic (Bérubé-Carrière *et al.*, 2009), and this has been viewed as the morphological substrate for volume transmission of 5-HT. Moreover, because the existence of junctional complexes implied some structural stability, the converse was suggestive of some mobility of the releasing sites. This has already been considered as a determinant of the remarkable capacities of 5-HT neurons for regeneration in contrast to more hardwired systems (Descarries *et al.*, 1975; Beaudet & Descarries, 1978). It is tempting to speculate that axon varicosities that are devoid of VGLUT3 would show less synaptic contact than those that contain both transmitters. Along this line, it has been reported that dopaminergic axon varicosities that contain VGLUT2 are more synaptic than those that do not (Descarries *et al.*, 2008; Bérubé-Carrière *et al.*, 2009). It is also noteworthy that 5-HT axon varicosities that contain the VGLUT3 were larger, in congruence with the previously reported data that larger 5-HT axon varicosities establish more synapses (Smiley & Goldman-Rakic, 1996). The hypothesis of higher synaptic incidence for 5-HT varicosities that contain the VGLUT3 remains to be tested at the ultrastructural level.

3.7. Acknowledgments

The authors are grateful to Dr. André Parent for critical reading of the manuscript and to André St-Pierre for helpful technical support. DG was the

recipient of a PhD fellowship from the “Centre Thématique de Recherche en Neurosciences”.

3.8. Figures

TABLE 3.1. – *List of antibodies*

Antibody	Company	Catalog #	Dilution	Characterization	Reference
Primary antibodies					
Goat α SERT	Santa Cruz	SC-1458	1: 500	Incubation of antibody with blocking peptide abolished labeling	[64]
Rabbit α 5-HT	Sigma	S5545	1: 500	Incubation of antibody with 5-HT solution abolished labeling	[65]
GP α VGLUT3	Millipore	AB5421	1: 1000	Same labeling as with other antibody. Incubation with blocking peptide abolished labeling	[66]
Rabbit α VMAT2	Synaptic System	138 302	1: 1000	Single strong band at 55 kDa on Western blots of brainstem preparation	[67]
Secondary antibodies					
Alexa 647 donkey α guinea pig	Jackson	706-605-148	1: 200		
Alexa 568 donkey α goat	Invitrogen	A11057	1: 200		
Alexa 488 goat α rabbit	Invitrogen	A11008	1: 200		
Streptavidin Texas Red	Molecular Probes	S-6370	1: 200		
Streptavidin 488	Molecular Probes	S-11223	1: 200		

doi:10.1371/journal.pone.0087709.t001

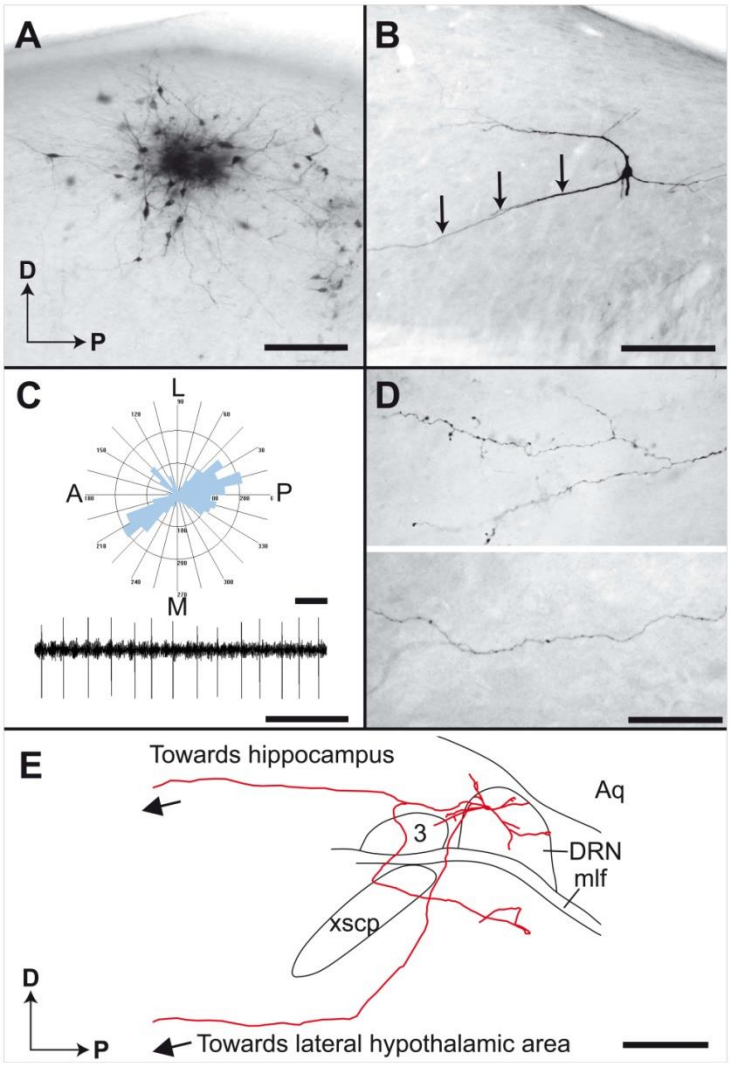

FIGURE 3.1.–*Neurons of the rat DRN filled with BDA.*(**A**) Example of an injection site placed in the DRN with a dense core of BDA precipitate and 15 to 20 distinctly labeled neurons. (**B**) Higher magnification of a Golgi-like labeled neuron with 4 primary dendrites. The axon is emitted by a primary dendrite, as indicated by arrows. (**C**) Typical dendrogram of reconstructed neurons showing preferential anteroposterior orientation of the dendrites and patterns of neuronal activity that characterize DRN, as recorded during a single brain penetration with a glass injection micropipette. (**D**) Examples of labeled axons observed in the ventral pallidum (upper panel) and the prefrontal cortex (lower panel). (**E**) Sagittal view of the somatodendritic domain and initial axonal trajectory of a DRN neuron. 3, oculomotor nucleus; A, anterior; Aq, aqueduct; D, dorsal; DRN, dorsal raphe nucleus; L, lateral; M, medial; mlf, medial longitudinal fasciculus; P, posterior; xscp, superior cerebellar peduncle decussation. Scale bars = 150 µm (A), 50 µm (B and D), 200 µm and 2 s (C), 1 mm (E).

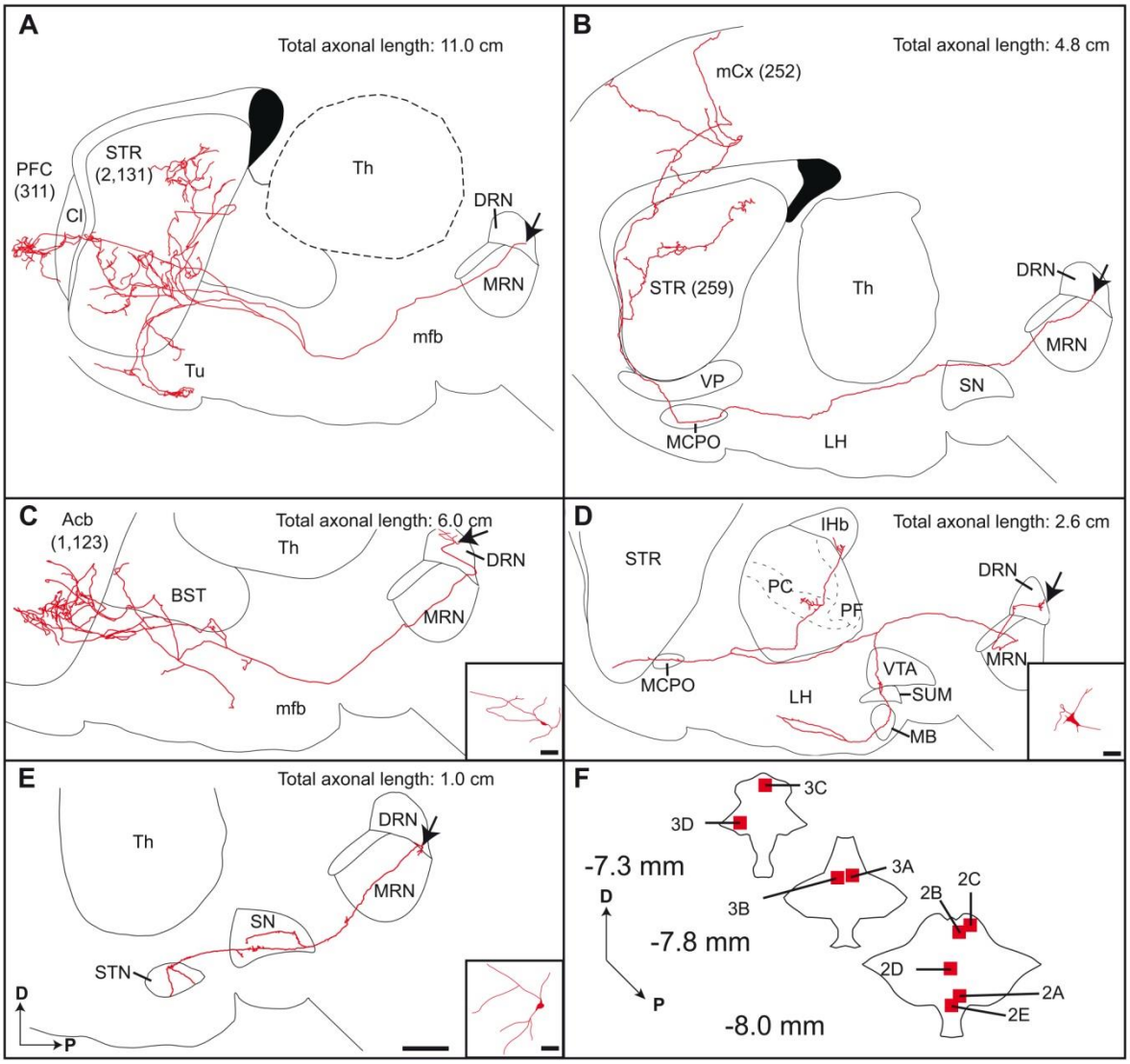

FIGURE 3.2.– *Axonal arborisation of DRN neurons, as viewed on sagittal plane.*The number of axon varicosities observed in each target site is indicated in parenthesis. Arrows indicate the location of cell bodies. (**A–E**) Composite reconstructions were obtained by superposing all serial sections that contained labeled profiles onto a single two-dimension frame. This way of doing inevitably leads to some image distortion because of the tortuous three-dimension course of the axon and also because the structures in which the axon courses and arborizes are not necessarily at the same plane than the one chosen for the illustration. Hence, the limits of the various structures should be taken as mere indications. This word of caution also applies to figure 3. Inserts in C–E provide reconstructions of somatodendritic domains. (**F**) Schematic representation of 3 rostrocaudal transverse sections through the DRN showing the exact location of parent cell bodies. The numbers refer to panels in which

entire axonal arborizations are shown. Acb, accumbens nucleus; BST, bed nucleus of the stria terminalis; Cl, claustrum; D, dorsal; DRN, dorsal raphe nucleus; LH, lateral hypothalamic area; lHb, lateral habenula; MB, mammillary body; MCPO, magnocellular preoptic nucleus; mCx, motor cortex; mfb, medial forebrain bundle; MRN, median raphe nucleus; P, posterior; PC, paracentral thalamic nucleus; PF, parafascicular thalamic nucleus; PFC, prefrontal cortex; SN, substantia nigra; STN, subthalamic nucleus; STR, striatum; SUM, supramammillary nucleus; Th, thalamus; Tu, olfactory tubercle; VP, ventral pallidum; VTA, ventral tegmental area. Scale bar = 1 mm (E, also valid for A–D) and 10 μm (inserts C–E).

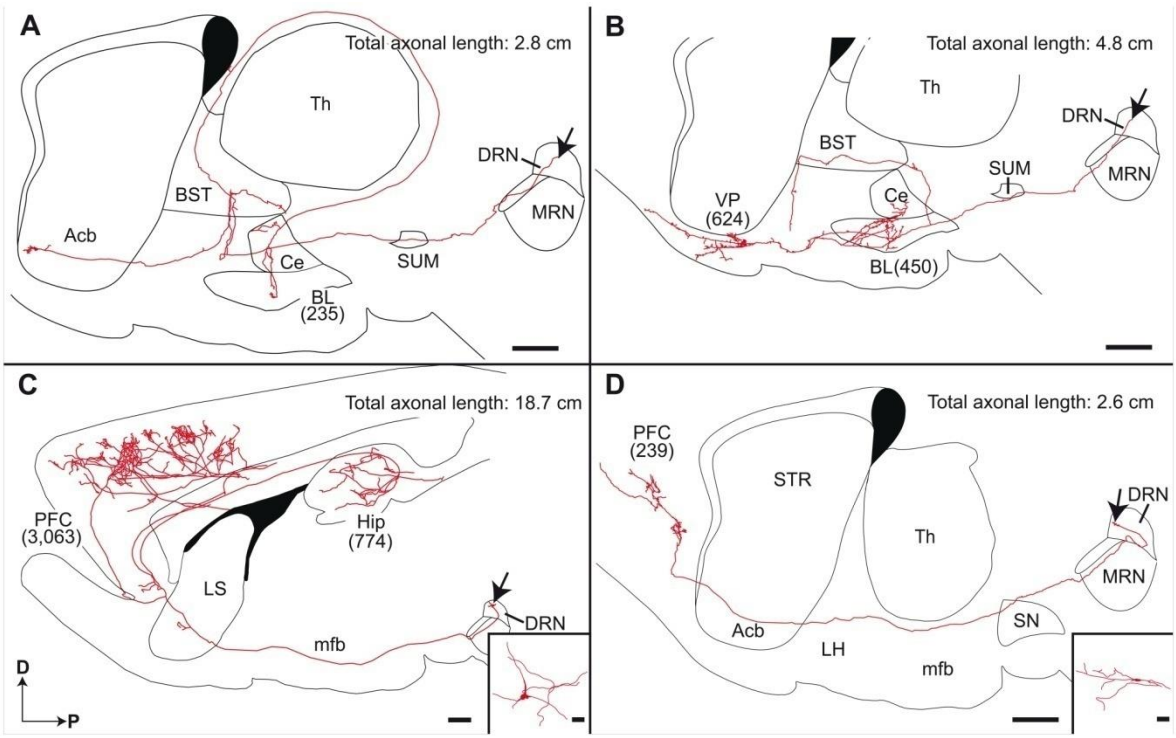

FIGURE 3.3. - *Sagittal view of entire reconstructed axonal arborization of DRN neurons.* The number of axon varicosities observed in each target site is indicated in parenthesis. Arrows indicate the location of the parent cell bodies. Inserts in C and D provide recontructions of somatodendritic domains. Acb, accumbens nucleus; BL, basolateral amygdaloid nucleus; BST, bed nucleus of the stria terminalis; Ce, central amygdaloid nucleus; D, dorsal; DRN, dorsal raphe nucleus; Hip, hippocampus; LH, lateral hypothalamic area; LS, lateral septum; mfb, medial forebrain bundle; MRN, median raphe nucleus; P, posterior; PFC, prefrontal cortex; SN, substantia nigra; SUM, supramammillary nucleus; Th, thalamus; VP, ventral pallidum. Scale bars = 1 mm (A–D) and 10 µm (inserts C, D).

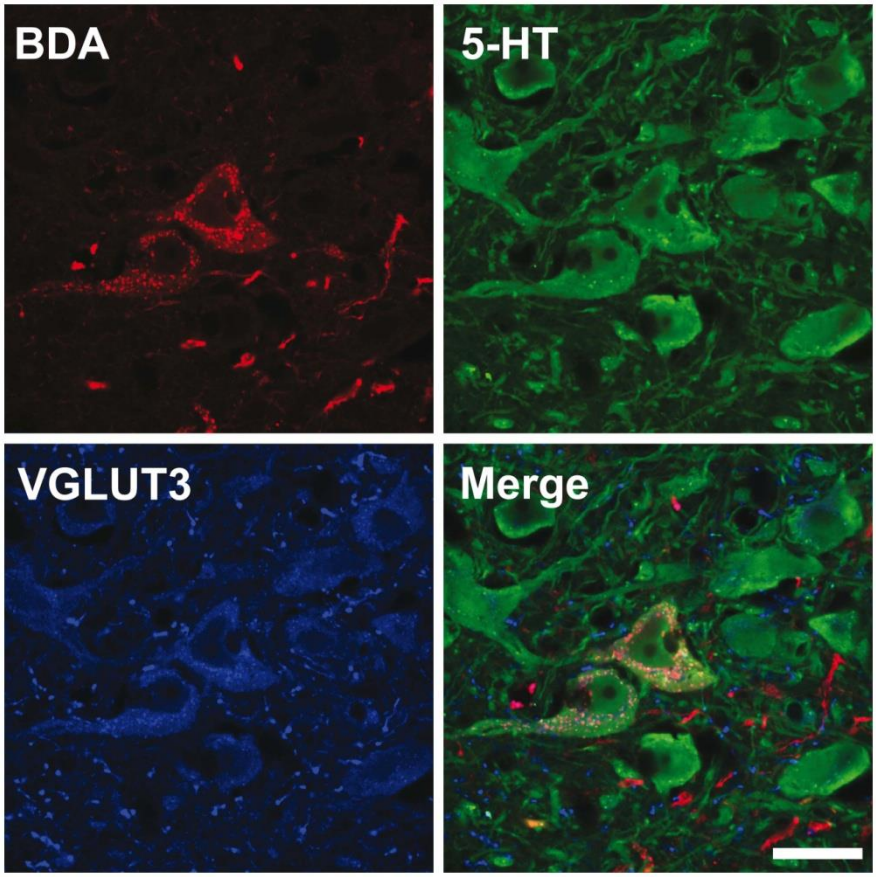

FIGURE 3.4. - *Confocal image of two BDA-injected neurons (red) immunoreactive for 5-HT (green) and VGLUT3 (blue).*
Scale bar = 10 µm.

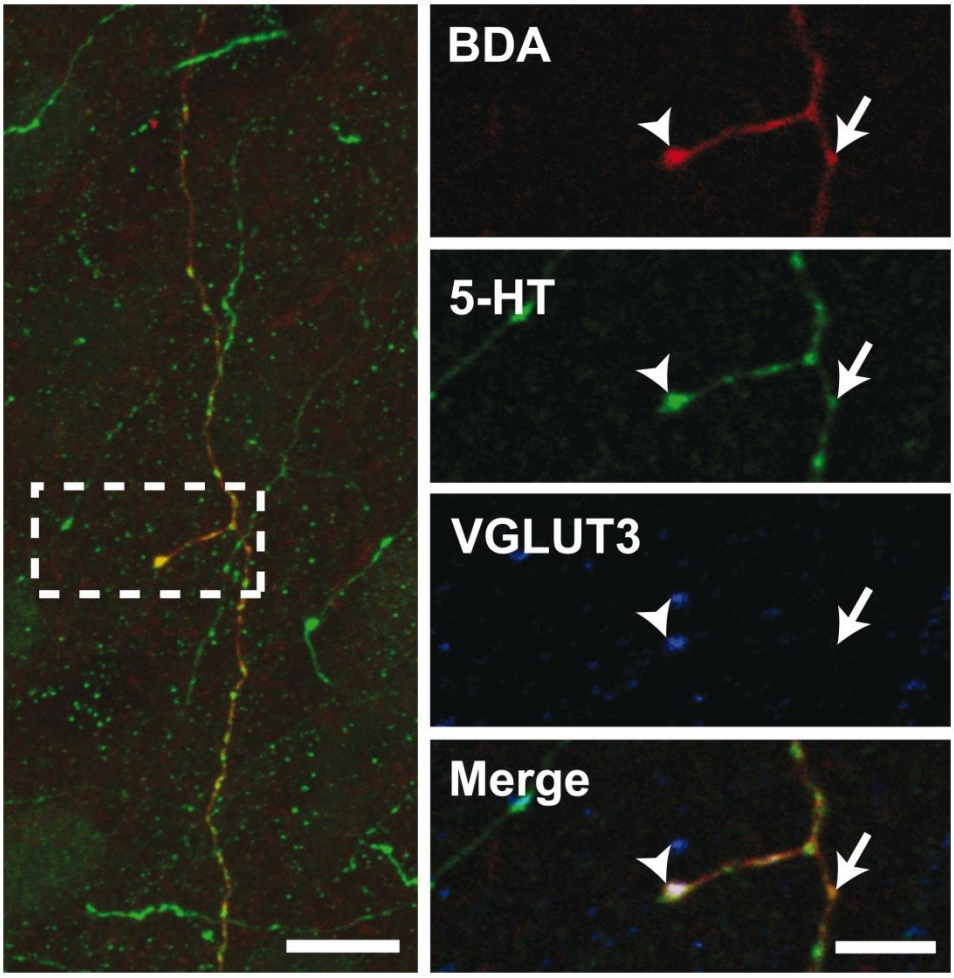

FIGURE 3.5. - *Confocal image of an axonal segment in the rat motor cortex emitted by a DRN neuron injected with BDA.* Immunoreactivity for BDA, 5-HT and VGLUT3 are shown in red, green and blue, respectively. Arrowheads show an axon varicosity containing 5-HT and VGLUT3 whereas arrows point to a 5-HT axon terminal devoid of VGLUT3. The left panel is from a 20 µm-thick Z-stack whereas the right panels are single plane images. Scale bars = 10 µm (left) and 5 µm (right).

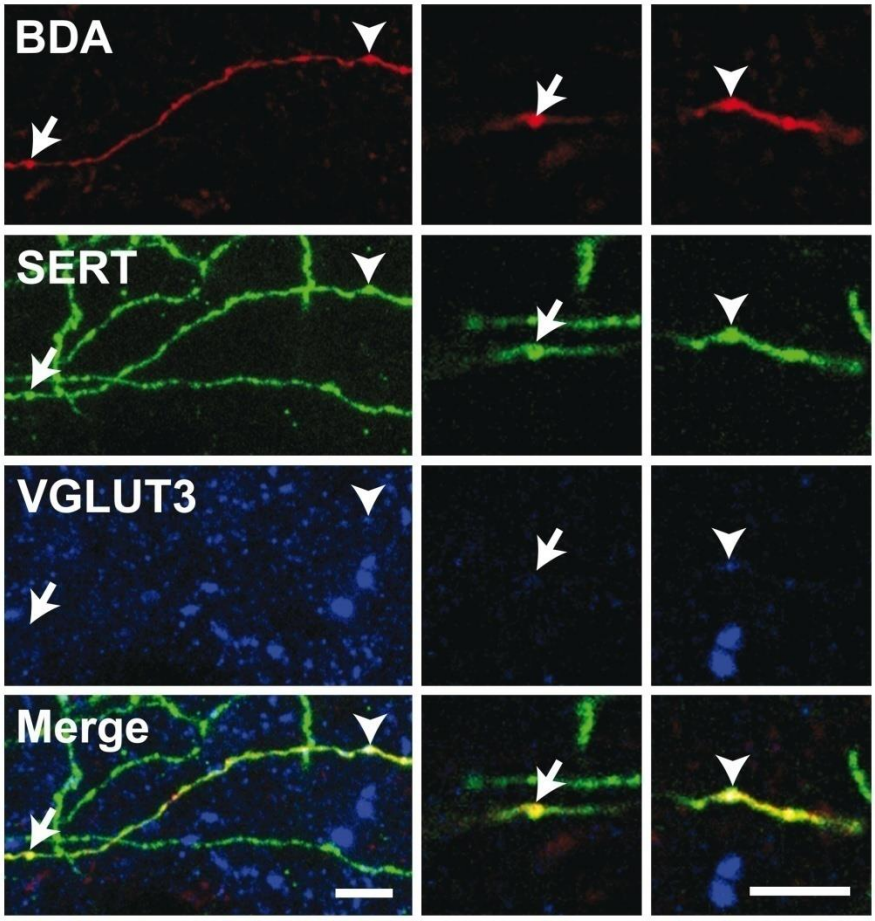

FIGURE 3.6. - *Confocal images of a BDA-filled axonal segment observed in the motor cortex.* Immunoreactivity for BDA, SERT and VGLUT3 are shown in red, green and blue, respectively. Arrows indicate an axon varicosity from the BDA-labeled axon that is devoid of VGLUT3 whereas arrowheads point to an axon terminal immunoreactive for SERT and VGLUT3. Left panels are from a 12 µm-thick Z-stack whereas right panels are images from single planes. Scale bars = 5 µm.

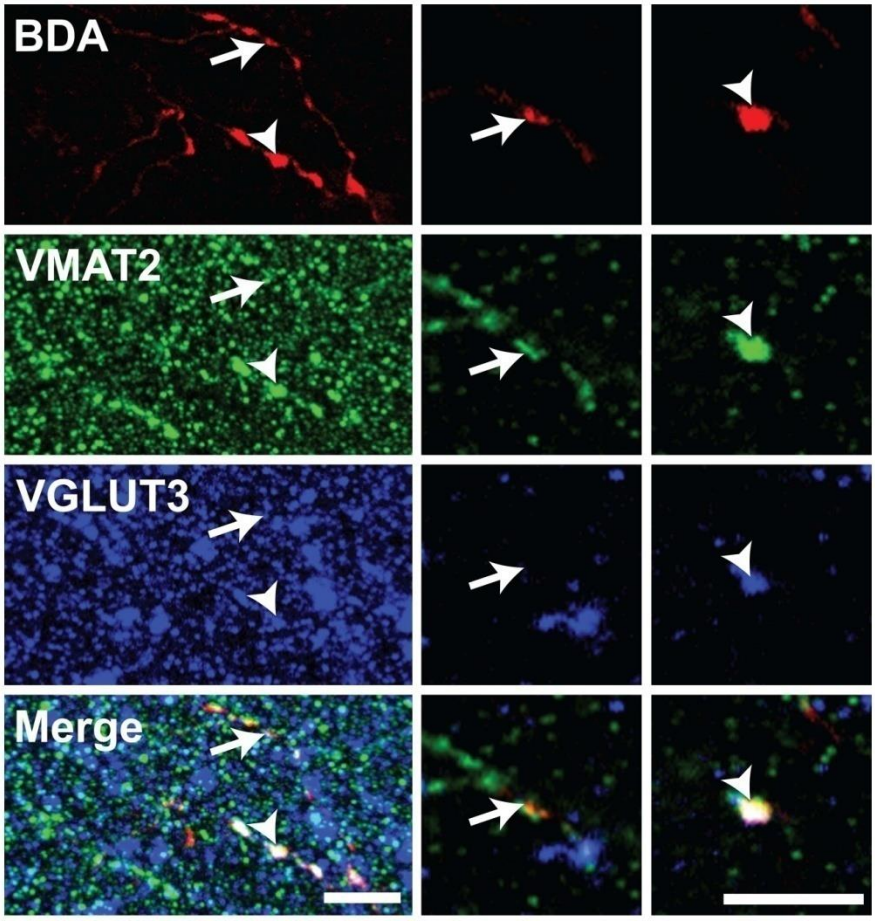

FIGURE 3.7. - *Confocal image of an axonal segment coursing in the motor cortex emitted by a DRN neuron injected with BDA.* Immunoreactivity for BDA, VMAT2 and VGLUT3 are shown in red, green and blue, respectively. Arrows point to a BDA-labeled axon varicosity immunoreactive for VMAT2 but devoid of VGLUT3 whereas arrowheads indicate a bouton that contains VMAT2 and VGLUT3. Left panels are from a 30 μm-thick Z-stack whereas right panels are images from single planes. Scale bars = 5 μm.

CHAPITRE 4 :

SEROTONIN HYPERINNERVATION OF THE STRIATUM WITH HIGH SYNAPTIC INCIDENCE IN PARKINSONIAN MONKEYS

CHAPITRE 4 – *SEROTONIN HYPERINNERVATION OF THE STRIATUM WITH HIGH SYNAPTIC INCIDENCE IN PARKINSONIAN MONKEYS*

Dave Gagnon, Laurent Grégoire, Thérèse Di Paolo et Martin Parent

Centre de recherche CERVO
2601, Ch. de la Canardière, Québec, Québec
Canada G1J 2G3

Brain Structure and Function (2016) 221 : 3675-3691

4.1. Résumé

L'utilisation chronique de L-DOPA afin d'atténuer les symptômes moteurs de la maladie de Parkinson produit souvent des effets secondaires comme des dyskinésies. La libération non régulée de dopamine par les axones sérotoninergiques suivant l'administration de L-DOPA est un déterminant présynaptique majeur de ces mouvements involontaires anormaux. Cette étude avait pour objectif de caractériser la réorganisation des afférences striatales sérotoninergiques suivant une dénervation dopaminergique chez un modèle simien de la maladie de Parkinson. Notre échantillon comprend huit singes macaques : quatre qui ont été rendu parkinsoniens après l'administration de MPTP et quatre contrôles. L'état de l'innervation sérotoninergique et dopaminergique a été évaluée par immunohistochimie avec des anticorps dirigés contre le transporteur de la sérotonine (SERT) et la tyrosine hydroxylase. Une étude stéréologique détaillée a révélé une augmentation significative du nombre de varicosités sérotoninergiques dans le striatum de singes intoxiqués au MPTP. Cette augmentation est particulièrement prononcée dans le territoire sensorimoteur du striatum, là où la dénervation dopaminergique est la plus sévère. L'étude en microscopie électronique indique que, contrairement au noyau accumbens où l'innervation dopaminergique est préservée, les varicosités axonales SERT+ observées dans le territoire sensorimoteur du putamen forment deux fois plus de contacts synaptiques chez le singe intoxiqué au MPTP que chez les contrôles. Ces découvertes démontrent la nature hautement plastique des afférences striatales sérotoninergiques, une caractéristique qui est particulièrement évidente en absence de dopamine striatale. Même si le nombre de neurones sérotoninergique du noyau raphé dorsal reste constant, tel que démontré dans cette étude, les projections axonales ascendantes subissent des changements adaptatifs et synaptiques importants qui pourraient jouer un rôle significatif dans la libération non régulée et ectopique de dopamine par les axones sérotoninergiques après un traitement antiparkinsonien à la L-DOPA.

4.2. Abstract

The chronic use of L-DOPA for alleviating the motor symptoms of Parkinson's disease often produces adverse effects such as dyskinesia. Unregulated release of dopamine by serotonin axons following L-DOPA administration is a major presynaptic determinant of these abnormal involuntary movements. The present study was designed to characterize the reorganization of serotonin striatal afferents following dopaminergic denervation in a primate model of Parkinson's disease. Our sample comprised eight cynomolgus monkeys: four that were rendered parkinsonian following MPTP administration and four controls. The state of striatal serotonin and dopamine innervation was evaluated by means of immunohistochemistry with antibodies against serotonin transporter (SERT) and tyrosine hydroxylase. A detailed stereological investigation revealed a significant increase in the number of serotonin axon varicosities in the striatum of MPTP-intoxicated monkeys. This increase is particularly pronounced in the sensorimotor territory of the striatum, where the dopamine denervation is the most severe. Electron microscopic examinations indicate that, in contrast to the nucleus accumbens where the dopamine innervation is preserved, the SERT+ axon varicosities observed in the sensorimotor territory of the putamen establish twice as many synaptic contacts in MPTP-injected monkeys than in controls. These findings demonstrate the highly plastic nature of the serotonin striatal afferent projections, a feature that becomes particularly obvious in the absence of striatal dopamine. Although the number of dorsal raphe serotonin neurons remains constant in parkinsonian monkeys, as shown in the present study, their ascending axonal projections undergo marked proliferative and synaptic adaptive changes that might play a significant role in the potential unregulated and ectopic release of dopamine by serotonin axons after L-DOPA treatment of Parkinson's disease.

4.3. List of abbreviations

4 :	trochlear nucleus
5-HT :	serotonin, 5-hydroxytryptamine
AADC :	aromatic L-amino acid decarboxylase
ac:	anterior commissure
Acb:	nucleus accumbens
Aq :	cerebral aqueduct
Cd :	caudate nucleus
DA :	dopamine
DAB :	3,3'diaminobenzidine tetrahydrochloride
DAT :	dopamine transporter
db :	dendritic branch
DRN :	dorsal raphe nucleus
ic :	internal capsule
L-DOPA :	L-3,4-dihydroxy-phenylalanine
LIDs :	L-Dopa-induced dyskinesia
MPTP :	1-methyl-4-phenyl-1,2,3,6-tetrahydropyridine
MRN :	median raphe nucleus
PB :	sodium phosphate buffer
PBS :	sodium phosphate-buffered saline
PAG :	periaqueducal gray
PET :	positron emission tomography
PFA :	paraformaldehyde
Put :	putamen
RT :	room temperature
SC :	superior colliculus
SERT :	serotonin transporter
SNc :	substantia nigra pars compacta
TBS :	tris-saline buffer
TH :	tyrosine hydroxylase
TpH :	tryptophan hydroxylase
VMAT2 :	vesicular monoamine transporter 2
xscp:	decussation of superior cerebellar peduncle

4.4. Introduction

Parkinson's disease is characterized by the progressive degeneration of nigrostriatal dopaminergic (DA) neurons of the substantia nigra pars compacta (SNc), which leads to typical motor impairments, including bradykinesia, rigidity, tremor and postural instability. These motor symptoms can be alleviated by the administration of the DA precursor L-3,4-dihydroxy-phenylalanine (L-DOPA), but the chronic use of this DA precursor is often accompanied by severe side effects. Within 10 years of L-DOPA treatment, 75% of parkinsonian patients experience motor complications, including L-DOPA-induced dyskinesia (LIDs), that can be more debilitating that the disease itself (Yahr, 1972; Obeso *et al.*, 2000b; Rajput *et al.*, 2002a; Hely *et al.*, 2005b).

The physiopathology of the nigrostriatal DA system in Parkinson's disease has received wide attention, but the other chemospecific neurotransmitter systems also known to be involved in the disease have been significantly neglected (Scatton *et al.*, 1983; Agid, 1991; Miyawaki *et al.*, 1997). This is particularly the case of the massive striatal serotonin (5-hydroxytryptamine, 5-HT) input, which originates mainly from the midbrain dorsal raphe nucleus (DRN) (Hornung, 2003). By virtue of its highly plastic nature (reviewed in Michelsen *et al.*, 2008), the 5-HT striatal afferents are believed to be involved in the expression of LIDs (Lopez *et al.*, 2001), the 5-HT axons being able to release DA, but in a non-physiological manner, following L-DOPA administration (reviewed in Carta *et al.*, 2008a; Carta & Tronci, 2014).

Neuronal losses (Mann & Yates, 1983a; Jellinger, 1989; Halliday *et al.*, 1990; Paulus & Jellinger, 1991) in some of the raphe nuclei of autopsied Parkinson's disease brains along with depletion of various biochemical 5-HT markers (Bernheimer *et al.*, 1961; Scatton *et al.*, 1983; Cash *et al.*, 1985; Raisman *et al.*, 1986; Birkmayer & Birkmayer, 1987; Chinaglia *et al.*, 1993; Calon *et al.*, 2003; Kerenyi *et al.*, 2003; Kim *et al.*, 2003; Guttman *et al.*, 2007; Kish *et al.*, 2008) have called attention to the possible involvement of the 5-HT system in

various non-motor symptoms of Parkinson's disease. Although these findings point to impairment of 5-HT striatal innervation in the late stages of idiopathic Parkinson's disease, some striatal 5-HT hyperinnervation has been reported following lesion of the nigrostriatal DA system in adult animal models of Parkinson's disease (Gaspar *et al.*, 1993a; Guerra *et al.*, 1997; Rozas *et al.*, 1998; Yamazoe *et al.*, 2001; Balcioglu *et al.*, 2003; Maeda *et al.*, 2005b). Our own human post-mortem investigation has shown that the 5-HT striatal innervation is preserved and even slightly increased in parkinsonian brains (Bédard *et al.*, 2011), and recent neuroimaging studies indicate that the 5-HT system is preserved in many Parkinson's disease patients, a feature that may be predictive of LIDs severity (Politis *et al.*, 2014).

In the light of the conflicting nature of the results regarding the state of the 5-HT striatal innervation in Parkinson's disease, it was thought of interest to acquire detailed quantitative data on the status of the striatal 5-HT innervation in a non-human primate model of Parkinson's disease. Based on the hypothesis that the alteration of the 5-HT striatal afferent projections plays a significant role in the expressions of LIDs, we designed experiments to provide a detailed description of the reorganization of 5-HT striatal innervation that occurs as a consequence of the degeneration of DA striatal afferent projections, at the light and electron microscopic levels.

4.5. Material and methods

4.5.1. Animals

This study was carried out on eight naïve ovariectomized female cynomolgus monkeys (*Macaca fascicularis,* Primus Bioressources)of 4 years old, weighing between 2.8 and 3.9 kg (see Online resource 1 for individual weight). Animals were housed under a 12 h light-dark cycle with water and food ad libitum and all experimental procedures were approved by the *Comité de Protection des Animaux de l'Université Laval*, in accordance with the Canadian Council on

Animal Care's Guide to the Care and Use of Experimental Animals (Ed2). Maximum efforts were made to minimize the number of animals used.

4.5.2. Parkinsonian syndrome induction

Four months after ovariectomy, four monkeys received *1-methyl-4-phenyl-1,2,3,6-tetrahydropyridine* (MPTP, Sigma-Aldrich Canada Ltd., Oakville, Canada) continuously, during 14 days, via a subcutaneous osmotic mini-pump filled with 14 mg of MPTP. Subsequent intramuscular MPTP injections were given as needed, until stabilization of bilateralparkinsonian symptoms (see Online resource 1 for total MPTP administered to each monkey). Behavioural response to MPTP intoxication was assessed by using a faithful motor scale that takes into account posture, mobility, climbing, gait, grooming, voicing, social interaction and tremor (see Hadj Tahar *et al.*, 2004 for details). Animals were scored twice, one week before transcardiac perfusion, from 2 h video recordings during which behaviours were scored every 15 min. The four MPTP monkeys scored between 6.8 and 9.6/16.0 (see Online resource 1 for individual scores), representing moderate to severe parkinsonian syndromes. At the time of perfusion, all MPTP monkeys were stabilized and did not show any sign of behavioural recovery.

4.5.3. Immunohistochemistry

TH and Nissl staining of the SNc

Five months after MPTP administration, animals were deeply anesthetized with a mixture of ketamine (20 mg/kg, i.m.) and xylazine (4 mg/kg, i.m.) and maintained under isoflurane (3%) anaesthesia. They were perfused transcardially with 300 mL of ice-cold sodium phosphate-buffered saline (PBS, 0.1 M; pH 7.4), followed by 1 L of cold 4% paraformaldehyde (PFA) to which 0.1% glutaraldehyde was added and by 1.5 L of PFA 4%. Brains were rapidly dissected out, post-fixed by immersion in 4% PFA for 24 h at 4°C and cut with a vibratome (model VT1200 S; Leica, Germany) into 50 µm-thick transverse sections collected in PBS.

To assess the extent of the DA lesion induced by MPTP administration, five transverse sections per brain were randomly selected throughout the SNc, from anterior commissure -5 mm to -10 mm (Bowden & Martin, 2000b), at a fixed interval of 900 µm. The sections were immunostained for tyrosine hydroxylase (TH), the catalytic enzyme of DA synthesis, with a monoclonal antibody (product no. 22941; Immunostar, Hudson, USA) raised in mouse. Briefly, free-floating sections were sequentially incubated at room temperature (RT) in: (i) a blocking solution of PBS, containing 2% normal horse serum and 1% Triton X-100 (1 h); (ii) the same solution containing a 1/1000 dilution of mouse monoclonal antibody against TH (overnight); and (iii) a 1/1000 dilution of biotinylated horse anti-mouse antibody (catalog no. BA-2000; Vector Laboratories, Burlingame, CA, USA) diluted in the same solution (2 h). After rinses in PBS, sections were incubated for 1 h at RT in avidin-biotin-peroxidase complex (Vector Laboratories) diluted 1/100 in the blocking solution. They were then rinsed and the bound peroxidase revealed by incubating the sections for 3 min at RT in a 0.025% solution of 3,3'diaminobenzidine tetrahydrochloride (DAB; catalog no. D5637; Sigma-Aldrich) in TBS, to which 0.005% of H_2O_2 was added. The reaction was stopped and the sections mounted on gelatin-coated slides and air-dried, dehydrated in 70% ethanol for 10 min, rehydrated in distilled water for 5 min and stained with cresyl violet for 20 min. Sections were then dehydrated in graded alcohol series, cleared in toluene and coverslipped with Permount.

TH and DAT immunostaining of the striatum

The striatal DA denervation was assessed using an infrared imaging system (Odyssey CLx; LI-COR Biosciences, Lincoln, NE, USA) from three transverse sections per brain that were taken through the striatum at 3 mm, 0 mm and -3 mm relative to the anterior commissure (Bowden & Martin, 2000b). Sections were immunostained for TH and dopamine transporter (DAT), using secondary antibodies coupled to infrared fluorescent dyes. The primary antibody against

TH was the same as above (1/1000, product no. 22941; Immunostar). The monoclonal antibody against DAT (1/500, product no. MAB369, EMD Millipore Corporation, Billerica, USA) was raised in rat. Goat anti-mouse 680 (1/1000, catalogue no. 926-68070, LI-COR Biosciences) and goat anti-rat 800 (1/1000, catalogue no. 926-32219, LI-COR Biosciences) were used as secondary antibodies. The infrared imaging system was used to scan the immunostained sections, and optical density measurements were taken from functional territories of the striatum that were delineated based on the work reviewed by Parent and Hazrati (1995), at the three anteroposterior levels selected. The resolution of the scanner was set at 21 μm and the gain at 1. Two solid-state diode lasers (685 nm and 785 nm) were used to excite secondary antibodies coupled to infrared fluorescent dyes.

TpH immunostaining of the DRN

For each monkey brain, eight transverse sections were selected through the DRN at a fixed interval of 600 µm. The free floating sections were labeled by using the same immunoperoxidase methodological approach described above, but by using a primary antibody against tryptophan hydroxylase (TpH), the rate limiting enzyme in 5-HT synthesis. The polyclonal antibody against TpH (catalog no. AB1541; EMD Millipore Corporation) was raised in sheep by using a recombinant rabbit TpH as an immonugen. The primary antibody was diluted 1/250 and a biotinylated rabbit anti-sheep (1/200, catalogue no. BA-6000; Vector Laboratories) was used as the secondary antibody.

SERT immunolabeling of the striatum

To provide a detailed and quantitative description of the 5-HT axon distribution in normal and DA-denervated striatum at the light microscopic level, 21 transverse sections were selected across the entire striatum (from 6 to -6 mm, relative to the anterior commissure), with a fixed interval of 600 µm, and immunostained using the immunoperoxidase method described above with an antibody against the 5-HT transporter (SERT, 1/1000, catalog no. SC-1458;

Santa Cruz Biotechnology, Dallas, TX, USA). A biotinylated rabbit anti-goat antibody (1/1000, catalog no. BA-5000; Vector Laboratories) was used as secondary antibody.

For electron microscopy, sections of the eight monkeys were immunostained for SERT as above, but in the absence of Triton X-100, which was replaced by 0.5% gelatin in all solutions. The primary and secondary antibodies were used at a concentration of 1/500. Sections were osmicated, dehydrated in ethanol and propylene oxide, and flat-embedded in Durcupan (catalog no. 44611-14; Fluka, Buchs, Switzerland) to be processed and examined as described below.

4.5.4. Material analysis

Quantitative assessment of TH immunoreactive cell bodies in the SNc

Transverse TH-immunostained sections of the SNc were used to estimate the number of TH-immunolabeled (+) cell bodies in the right SNc with an unbiased stereological approach (see Fig. 1). In brief, a light microscope equipped with a digital camera, a motorized stage and a *Z*-axis indicator was controlled by a computer running StereoInvestigator software (v. 7.00.3; MicroBrightField, Colchester, VT, USA). First, we used a stereotaxic atlas (Bowden & Martin, 2000b) to draw the contour of the SNc of the right mesencephalon at a low magnification on each transverse section. The sampling process for estimations of the total number of TH+ cell bodies began by a randomly translated grid formed by 800 x 800 µm squares. At each intersection of the grid that fell into the sector, a counting frame measuring 250 μm × 250 μm was drawn and examined with a 20x (0.70 N.A.) objective. Nuclei of immunolabeled cells that fell inside the counting frame and did not contact the exclusion lines were counted whenever they came into focus within a 6 µm-thick optical disector centered in the section. The thickness of the mounted tissue was measured for each counting frame, yielding mean values between 7 µm and 10 µm. An

average of 91 ± 12 TH+ cell bodies were counted in each SNc of MPTP monkey and 341 ± 38 in control animals, yielding coefficients of error (Gunderson, *m* = 1 and 2nd Schmitz-Hof) between 0.05 and 0.12.

Quantitative assessment of TH immunoreactivity of the striatum

The DA denervation of the striatum was assessed by using the infrared imaging system and three transverse sections per brain taken at the pre-commissural, commissural and post-commissural levels. These sections were immunostained for TH and DAT, as described above, and optical density measurements were taken from entire delineated functional territories of the striatum, as previously described (Parent & Hazrati, 1995b). Sections from the pre-commissural striatum were divided in 5 sectors: associative caudate nucleus, sensorimotor caudate nucleus, associative putamen, sensorimotor putamen and nucleus accumbens, whereas commissural and post-commissural striatum were both divided into 4 sectors: associative caudate nucleus, sensorimotor caudate nucleus, associative putamen and sensorimotor putamen (see Fig. 2 for details).

Quantitative assessment of TpH immunoreactive cell body density in the DRN

A similar unbiased stereological approach was used to estimate the total number of TpH+ cell bodies in the DRN from eight equally-spaced transverse sections immunostained for TpH. The grid was formed by 650 µm x 500 µm rectangles and applied over the entire DRN that could be easily delineated at low magnification with the help of a stereotaxic atlas (Bowden & Martin, 2000b). At each intersection of the grid that fell into the sector, a counting frame measuring 250 μm × 250 μm was drawn and examined with a 40× (NA = 0.85) objective. Nuclei of immunostained neurons that came into focus within a 20 µm-thick optical disector were counted. The thickness of the

mounted tissue was measured for each counting frame and range between 25 µm and 43 µm. An average of 448 ± 85 TpH+ cells were counted in each monkey brain leading to coefficients of error (Gunderson, *m* = 1 and 2nd Schmitz-Hof) ranging between 0.05 and 0.07. The density of TpH+ cell bodies was obtained by using the total number of TpH+ cells calculated by the optical disector and the volume of the DRN estimated by the Cavalieri's method.

Quantitative assessment of the density of SERT immunoreactive axon terminals

Twenty-one SERT-immunostained sections of the striatum taken from each monkey were used to estimate the total number of SERT+ axon terminals in the striatum. A precise description of the regional distribution of SERT+ axon varicosities throughout the striatum was achieved by dividing it into 13 distinct sectors. The anteroposterior axis was first divided into three parts: sections 1 to 7 belonging to the pre-commissural striatum, sections 8-14 to the commissural striatum and sections 15-21 to the post-commissural striatum. The pre-commissural striatum was further subdivided in 5 sectors: associative caudate nucleus, sensorimotor caudate nucleus, associative putamen, sensorimotor putamen and nucleus accumbens, whereas commissural and post-commissural striatum were divided into 4 sectors each: associative caudate nucleus, sensorimotor caudate nucleus, associative putamen, sensorimotor putamen (see Fig. 2 for details). This procedure allowed to delineate a total of 13 striatal sectors based on the functional striatal territories, as previously described (Parent & Hazrati, 1995b).

The sampling process leading to estimations of the total number of SERT+ axon varicosities in each of the striatal sectors began by randomly translating grids formed by 1,700 µm × 1,200 µm rectangles (for large striatal sectors) and by 650 µm × 600 µm (for small striatal sectors). At each intersection of the grid that fell into the sector, a counting frame measuring 30 µm × 30 µm

was drawn and examined with a 100× (NA = 1.30) oil-immersion objective. In the light microscope, SERT+ varicosities appear as round or ovoid axonal dilations, > 0.25 μm in transverse diameter. Varicosities that fell inside the counting frame and did not contact the exclusion lines were counted whenever they came into focus within a 10 μm-thick optical disector centered in the section. The thickness of the mounted tissue was measured for each counting frame and ranged between 15 µm and 26 µm. An average of 786 $\pm$ 156 SERT+ axon varicosities were counted in each striatal sector leading to coefficients of error (Gunderson, *m* = 1 and 2nd Schmitz-Hof) ranging between 0.03 and 0.08. For each striatal sector, the density of SERT innervation was expressed in million (10^6) axon varicosities per mm^3 of tissue, using the total number calculated by the optical disector and the volume of the sector estimated by the Cavalieri's method.

Quantitative assessment of the length of SERT immunoreactive axons in the striatum

The total length of SERT+ axons in each delineated striatal sectors was estimated using the "spaceballs" stereological probe (Mouton *et al.*, 2002). The same grid and contours that were outlined for the estimation of the number of SERT+ axon varicosities were used. At each intersection of the grid that fell into the striatal sector, a 10 μm diameter hemisphere was drawn. While focussing through the section, intersection points between SERT+ axons and the hemisphere were counted, providing an unbiased estimate of the total axonal length within each striatal sector. By dividing the number of SERT+ axon varicosities estimated using the optical disector probe by the length of SERT+ axons estimated by the space ball stereological probe, we were able to provide the number of SERT+ axon varicosities per 10 µm of axon.

Ultrastructural analysis of SERT immunoreactive axon varicosities

In each of the eight monkeys, quadrangular pieces of the dorsolateral putamen and the nucleus accumbens were cut from the flat-embedded SERT-immunostained sections taken at the level of the anterior commissure for the dorsolateral putamen, and at 3 mm from the anterior commissure for the nucleus accumbens. After being glued on the tip of resin blocks, they were cut ultrathin (~80 nm) with an ultramicrotome (model EM UC7, Leica). Ultrathin sections were collected on bare 150-mesh copper grids, stained with lead citrate and examined by using a transmission electron microscope (Tecnai 12; Philips Electronic, Amsterdam, Netherlands), at 100 kV, and an integrated digital camera (MegaView II; Olympus, Müster, Germany). Profiles of varicosities were readily identified as such by their diameter, > 0.25 µm, and their content in aggregated synaptic vesicles, often associated with one or more mitochondria. The SERT+ varicosities were sampled randomly, at a working magnification of 11 500×, by taking a picture of every such profile encountered, until 50 or more showing a full contour and distinct content were available for analysis in each animal. For sake of comparison, unlabeled profiles of axon varicosities were randomly selected from the same micrographs.

The randomly selected unlabeled varicosities and the SERT+ varicosities were analyzed, using the public domain ***IMAGE J***processing software from NIH (v.1.45), for the long and short axis and cross-sectional area. They were then categorized as containing or not a mitochondrion, and as showing or not a synaptic junctional complex, i.e. a localized straightening of apposed plasma membranes associated with a slight widening of the intercellular space and a thickening of the pre- and/or postsynaptic membrane. All synaptic junctions were also characterized as symmetrical or asymmetrical, the synaptic target identified, and the length of junctional complexes measured. The synaptic incidence observed in single section was then extrapolated to the whole volume of varicosities by means of the formula of Beaudet and Sotelo (Beaudet

& Sotelo, 1981), using the long axis as diameter, according to Umbriaco *et al*(Umbriaco *et al.*, 1994).

4.5.5. Statistical analysis

All statistical differences between control and MPTP-intoxicated monkeys were assessed using Mann-Whitney U tests. Variations in the density of SERT+ axon varicosities along the anteroposterior axis of the striatum in control monkeys were assessed using a Kruskall-Wallis one-way analysis of variance. Differences were considered statistically significant at $P< 0.05$. Statistical analysis was done using GraphPad Prism software (v. 6.01; GraphPad Software, San Diego, CA, USA). Mean and standard error of the mean are used throughout the text as central tendency and dispersion measure, respectively.

4.6. Results

4.6.1. Intoxication with MPTP caused a severe DA denervation of the sensorimotor striatum

Stereological estimations of the number of TH+ neurons located in the SNc were performed to assess the extent of the lesion caused by MPTP administration. A 77% decrease of TH+ neurons was observed in SNc after MPTP administration (21,053 ± 2,387 TH+ neurons in MPTP monkeys compared to 91,097 ± 7,009 in controls, $P = 0.0286$, Fig. 1). Neurons of the ventral tegmental area were relatively spared. Optical density measurements with the infrared imaging system in delineated striatal sectors of MPTP monkeys revealed a significant decrease of TH and DAT immunoreactivity in the sensorimotor and associative functional striatal territories, whereas no significant changes were observed in the limbic striatal territory (Fig. 2). Overall, an 82% decrease of TH immunoreactivity was observed in the sensorimotor territory of the putamen and a 90% decrease in the sensorimotor territory of the caudate nucleus. Similarly, significant decreases of TH

immunoreactivity were detected throughout the three anteroposterior levels in the associative territory of the putamen and caudate nucleus (70% and 85%). The MPTP-induced decrease of TH immunoreactivity was more severe in the sensorimotor territory than the associative territory in both putamen and caudate nucleus. The slight decrease (15%) of TH immunoreactivity observed in the limbic striatal territory (nucleus accumbens) of MPTP monkeys did not reach statistical significance (P = 0.4857). The examination of DAT-immunostained sections yielded similar results: significant decreases in immunoreactivity of the sensorimotor area of caudate nucleus and putamen (89% and 82%) and the associative territory of caudate nucleus and putamen (86% and 70%). In contrast, monkeys of the two groups did not differ statistically in regard to the DAT immunostaining of nucleus accumbens (Online resource 2).

4.6.2. Neuronal density of TpH immunoreactive neurons was unchanged in the DRN of MPTP monkeys

Stereological examinations of TpH-immunolabeled sections revealed that the whole DRN in normal cynomolgus monkeys comprised 58,144 ± 10,655 TpH+ neurons packed in a volume of 10.7 ± 1.2 mm^3, leading to a mean density of 5,355 ± 742 TpH+ neurons/mm^3 of tissue. Typically, these TpH+ neurons displayed a medium-sized cell body (22.4 ± 0.4 µm; N = 50) emitting 2-4 long and poorly ramified primary dendrites that were characteristically thick and sparsely spined (Fig. 3). Our stereological estimations of the density of TpH+ neuronal cell bodies in the DRN of MPTP monkeys (4,833 ± 354 TpH+ neurons/mm^3 of tissue) revealed no significant differences compared to controls (P = 0.9999, Fig. 3). Furthermore, MPTP administration did not alter the morphology of the somatodendritic domains of TpH+ neurons in the DRN.

4.6.3. The density of striatal SERT immunoreactive axon varicosities was higher in MPTP monkeys

A dense network of fine and highly varicose SERT+ axons uniformly covered the entire striatum of control monkeys (Fig. 4A, C),without sign of a patch-matrix organizational pattern, but with a few thick and beaded immunoreactive axons scattered throughout the structure. Our unbiased estimations of the density of SERT+ axon varicosities in control monkeys indicate a significant anteroposterior-increasing gradient in the associative striatal regions. The associative region of the putamen at the pre-commissural level contained ($0.53 \pm 0.06 \times 10^6$ SERT+ axon varicosities/mm^3 compared to 1.06 ± 0.10 for the same region, at the post-commissural level ($P = 0.0098$, Fig. 5B). The associative region of the caudate nucleus at the pre-commissural level contained $0.43 \pm 0.05 \times 10^6$ SERT+ axon varicosities/mm^3 of tissue compared to 0.61 ± 0.01 for the same region, at the post-commissural level ($P = 0.0243$, Fig. 5B). No such gradients were observed in the sensorimotor striatum (Fig. 5A). This observation reflects the heterogeneous innervation of the primate striatum by SERT+ axons in normal conditions.

In MPTP-intoxicated monkeys, highly immunoreactive and fairly restricted zones composed of dense networks of markedly varicose SERT+ axons occured in the sensorimotor and associative functional territories of caudate nucleus and putamen (Fig. 4B). The absence of such intense SERT+ zones in different extrastriatal forebrain areas that receive SERT+ axons confirmed their striatal specificity. Examinations at high magnification indicated no differences between MPTP and control monkeys in regard to the size and shape of SERT+ axons, at the light microscopic level.

Our stereological investigation revealed that, compared to controls, the density of SERT+ axon varicosities was significantly higher in the sensorimotor putamen of MPTP monkeys, at the post-commissural level ($0.62 \pm 0.05 \times 10^6$ SERT+ varicosities/mm^3 in MPTP vs. 0.41 ± 0.01 in controls, $P = 0.0286$) and

in the sensorimotor territory of the caudate nucleus, at the commissural level (0.71 ± 0.05 x 10^6 SERT+ varicosities/mm^3 in MPTP vs. 0.39 ± 0.05 in controls monkeys, *P* = 0.0286). In regard to the associative territory of the caudate nucleus, the density of SERT+ axon varicosities was significantly higher only at the commissural level (0.75 ± 0.07 x 10^6 SERT+ varicosities/mm^3 in MPTP vs. 0.52 ± 0.04 in controls, *P* = 0.0286). Differences in the density of SERT+ axon varicosities between MPTP-intoxicated and control monkeys did not reach statistical significance in the associative territory of the putamen and no significant differences were observed in the limbic striatal territory (Fig. 5B).

4.6.4. SERT immunoreactive axons were longer in MPTP monkeys but the number of varicosities per given axonal length was unchanged

All striatal regions of MPTP monkeys displayed higher density of SERT+ axons per mm^3 of tissue, when compared to controls. These higher values reached statistical significance at pre-commissural levels for both the associative putamen (4.75 ± 0.25 m of SERT+ axons/mm^3 of tissue in MPTP monkeys vs. 3.75 ± 0.19 in controls, *P* = 0.0286) and the associative caudate nucleus (4.66 ± 0.37 vs. 2.68 ± 0.25 m of axons/mm^3, *P* = 0.0286). Dividing the number of SERT+ axon varicosities by the estimated axonal length allowed us to approximate the number of SERT+ varicosities per 10 μm of axon. Our results indicated no significant differences between MPTP-intoxicated monkeys and control animals in the number of SERT+ axon varicosities per 10 μm of axon in the three functional striatal territories, suggesting that the increase of the density of SERT+ axon varicosities reported above is caused by the sprouting of varicose SERT+ axons rather than by the appearance of newly formed axon varicosities on non growing SERT+ axon (Online resource 3).

4.6.5. SERT immunoreactive axon varicosities in the striatum of control monkeys displayed a low synaptic incidence

The SERT+ axon varicosities in the dorsolateral putamen and the nucleus accumbens of normal cynomolgus monkey shared some ultrastructural features with SERT+ terminals present in other parts of the brain (reviewed in Descarries *et al.*, 2010b). They derived from unmyelinated axons, were generally ovoid, contained aggregated small and clear vesicles and frequently harboured one or more mitochondria. Their axoplasm was filled with a DAB immunoprecipitate of variable density, which typically lined the plasma membrane and the outer surface of organelles (Fig. 6). In contrast to the nucleus accumbens, the SERT+ axon varicosities present in the dorsolateral putamen were significantly smaller than unlabeled varicosities selected at random from the surrounding neuropil (0.26 ± 0.01 μm^2 vs. 0.33 ± 0.03 μm^2, P = 0.0286, Table 1). Furthermore, the mean diameter of SERT+ profiles in the putamen was smaller than in nucleus accumbens (0.55 ± 0.01 µm vs. 0.71 ± 0.03 µm, P = 0.0286).

In both the nucleus accumbens and the dorsolateral area of the putamen, the proportion of axon varicosities that displayed a synaptic contact was lower for SERT+ profiles than for unlabeled counterparts. In the dorsolateral putamen, the synaptic incidence measured in single-thin sections amounted to 6 ± 1% for SERT+ profiles compared to 35 ± 4% for unlabeled profiles (P = 0.0286). In the nucleus accumbens, 9 ± 1% of the SERT+ profiles examined displayed a synaptic contact compared to 25 ± 2% for unlabeled profiles (P = 0.0286), as measured from single-thin sections. When extrapolated to the whole volume of varicosities with the stereological formula of Beaudet and Sotelo (1981), the synaptic incidence for SERT+ varicosities amounted to 18 ± 4% in the putamen and 23 ± 5% in the nucleus accumbens. The same extrapolation performed on the randomly selected unlabeled profiles yielded considerably higher values of synaptic incidence (82 ± 12% in the putamen and 68 ± 13% in the nucleus accumbens). Virtually all synaptic contacts established by the

SERT+ axon varicosities were asymmetrical and found on dendritic spines of striatal neurons. Only one symmetric synaptic contact was observed on a dendritic shaft.

4.6.6. SERT immunoreactive axon varicosities established more synaptic contacts in the DA-denervated striatal area

Electron microscopic examination of the sensorimotor territory of the putamen and the limbic striatal territory of MPTP monkeys indicated no significant changes in size, shape or vesicular content of SERT+ axon varicosities when compared to those observed in control animals. Strikingly, the sensorimotor putamen of MPTP-intoxicated animals was characterized by significant higher synaptic incidence (44 ± 2%) than the same region incontrol animals (18 ± 4%, $P = 0.0286$). In contrast, the limbic striatal territory (nucleus accumbens) displayed no significant difference in synaptic incidence between MPTP monkeys (16 ± 5%) and controls (23 ± 5% $P = 0.2000$), suggesting that the increase of the synaptic incidence observed in the striatum after MPTP intoxication was restricted to the DA-denervated area of the striatum. As in controls, synaptic contacts in MPTP monkeys occured essentially on dendritic spines of striatal neurons, where they displayed an asymmetric specialisation (Table 1). One asymmetric synapse was nevertheless detected on a striatal cell body, while another occurred on an unlabeled axon in the striatum of MPTP monkeys.

4.7. Discussion

The present study has provided detailed quantitative and ultrastructural evidences for major neuroadaptive changes of the striatal 5-HT axonal projection in adult cynomolgus monkeys rendered parkinsonian by MPTP administration. The regional distribution of the striatal 5-HT and DA

innervations in MPTP monkeys compared to controls demonstrates an intimate relationship between DA denervation and 5-HT hyperinnervation, as revealed by one of the most faithful animal model of Parkinson's disease currently available. For the first time, electron microscopic examination provides insights into the rearrangement of the striatal microcircuitry that occurs in Parkinson's disease, with 5-HT axon varicosities as a major actor. Taken together, our data indicate a significant 5-HT hyperinnervation of the striatum that coincides with the marked DA depletion. The striatal 5-HT hyperinnervation is particularly evident in the sensorimotor striatal area, which suffers from the most severe DA denervation. The presence of multiple synaptic vesicles and the significantly higher synaptic incidence of 5-HT axon varicosities noted after MPTP administration indicate that sprouting of 5-HT axons may favor the release of 5-HT, but may also potentiate the release of DA and the expression of dyskinesia, when L-DOPA is administered. Through their ability to convert exogenous L-DOPA into DA by means of aromatic L-amino acid decarboxylase (AADC) (Arai *et al.*, 1994), and to store and release DA in an activity dependent manner via vesicular monoamine transporter 2 (VMAT2) (Ng *et al.*, 1970a; Ng *et al.*, 1971; Hollister *et al.*, 1979b; Arai *et al.*, 1994; Arai *et al.*, 1995b; Tanaka *et al.*, 1999b; Maeda *et al.*, 2005b), the 5-HT neurons are indeed able to transform exogenous L-DOPA into DA. Consequently, DA can be released from 5-HT axons in a non-physiological manner, leading to abnormal receptor stimulation and dyskinesia (reviewed in Carta *et al.*, 2008b).

4.7.1. Topographical distribution of 5-HT axon varicosities in the striatum of normal cynomolgus monkeys

The regional distribution of the 5-HT axon varicosities in the striatum of normal cynomolgus monkeys indicates an heterogeneous distribution of this innervation, as previously reported for Japanese monkeys (*Macaca fuscata*) (Mori *et al.*, 1985b), squirrel monkeys (*Saimiri sciureus*) (Lavoie & Parent, 1990) and human (reviewed in Parent *et al.*, 2011; Wallman *et al.*, 2011). Similarly to what is reported here in macaque monkey, the ventral part of the

human putamen and caudate nucleus receive a denser 5-HT innervation at the post-commissural level, when compared to the pre-commissural level (Wallman *et al.*, 2011). Similar observations were made in the caudate nucleus of *Macaca fuscata*, where the number of varicose fibers increased gradually along the anteroposterior axis (Mori *et al.*, 1985b). In squirrel monkeys, the 5-HT axons are reportedly distributed according to an anteroposterior-decreasing gradient (Lavoie & Parent, 1990), a finding that is at variance with the results reported here in macaques. This discrepancy may be explained either by interspecies differences between New World and Old World monkeys or methodological variations.

4.7.2. Density of 5-HT axon varicosities in the striatum of MPTP-intoxicated cynomolgus monkey

The 5-HT neurons are known for their high plastic capacity (Michelsen *et al.*, 2008), as exemplified by their regrowth following lesions or grafts of 5-HT neurons in rodents (Berger *et al.*, 1985; Zhou *et al.*, 1991; Descarries *et al.*, 1992). We believe that the highly malleable feature of 5-HT neurons underlies the remarkable rearrangement of the 5-HT innervation that occurred in DA-denervated striatal area of adult monkeys. In MPTP monkeys, a 53% and 57% increase of 5-HT axon varicosity densities were noted in the sensorimotor areas of the putamen and caudate nucleus, where the DA denervation was the most severe. In parallel with increases in the number of 5-HT axon varicosities, we found increases in the length of axonal branches in the same striatal territories, indicating that the increase in the 5-HT innervation of the sensorimotor striatal territory results mainly from the sprouting of varicose axons and not from the appearance of novel varicosities on non-growing axons. The absence of significant loss of 5-HT cell bodies in the DRN in MPTP monkeys, as noted here in accordance with previous findings obtained in MPTP-intoxicated mice (Gupta *et al.*, 1984) and monkeys(Langston *et al.*, 1984; Gaspar *et al.*, 1993a), further supports the notion of a rearrangement of existing 5-HT neurons and the sprouting of their varicose axons in the

striatum. Since the increase of 5-HT innervation was restricted to DA-denervated striatal areas and MPTP intoxication did not change the number and somatodendritic morphology of DRN 5-HT neurons, it may be concluded that the sprouting of 5-HT axons is a consequence of the DA striatal deafferentation induced by MPTP administration rather than a direct effect of MPTP on 5-HT neurons.

The increases in 5-HT striatal innervation reported here are congruent with previous studies demonstrating a striatal 5-HT hyperinnervation in different animal models of Parkinson's disease, including the 6-OHDA-lesioned rat (Zhou *et al.*, 1991; Guerra *et al.*, 1997; Maeda *et al.*, 2003), the MPTP mouse (Rozas *et al.*, 1998), the MPTP monkey (Gaspar *et al.*, 1993a; Zeng *et al.*, 2010) and the pituitary homeobox 3 (Pitx3)-deficient mouse (Smits *et al.*, 2008). Our data are also in accordance with examination of autopsied Parkinson's disease brains indicating a slight but significant increase of SERT immunoreactivity in the striatum, when compared to healthy controls (Bédard *et al.*, 2011). The present study is the first one to provide a detailed quantitative and ultrastructural account of the DA denervation-induced 5-HT striatal hyperinnervation, with emphasis on the regional aspects of the phenomenon.

Post-mortem examinations of the raphe nuclei inparkinsonian patients have provided some evidence for degeneration of 5-HT neurons in late stages of the disease, but Lewy bodies appear to be mainly confined to neurons of the caudal raphe nuclei (reviewed in Braak *et al.*, 2003b) that project their axons towards the spinal cord and the cerebellum (reviewed in Azmitia & Gannon, 1986; Hornung, 2003). Regarding neurons of the rostral raphe nuclei, some Lewy bodies were reported in the DRN (Halliday *et al.*, 1990), but cell loss appears to be restricted to the median raphe nucleus, (Mann & Yates, 1983a; Halliday *et al.*, 1990; Gai *et al.*, 1991; Cheshire *et al.*, 2015). However, at least one post-mortem study of Parkinson's disease brains has reported widespread brainstem neuronal degeneration, including cell losses in the DRN and the locus coeruleus (Paulus & Jellinger, 1991). It is tempting to speculate

that the DRN-striatal projections may be less vulnerable than ascending projections arising from the median raphe nucleus to the progressive neurodegenerative processes at play in Parkinson's disease, which are obviously different from the direct MPTP intoxication. A search for possible loss or gain of 5-HT innervation in various extrastriatal forebrain areas would greatly help our understanding of the involvement of the raphe nuclei in this pathological condition.

Moderate decreases of 5-HT concentration and its metabolites (Bernheimer *et al.*, 1961; Calon *et al.*, 2003; Kish *et al.*, 2008)and of SERT binding sites (Cash *et al.*, 1985; Raisman *et al.*, 1986; Chinaglia *et al.*, 1993; Kish *et al.*, 2008) were observed in the striatum of Parkinson's disease brains, a finding that was interpreted as evidence of a modest loss of 5-HT innervation, possibly related to the depressive state or other non-motor symptoms of Parkinson's disease. The conversion of L-DOPA into DA in 5-HT terminals is believed to cause a local displacement of endogenous 5-HT (Rozas *et al.*, 1998), a phenomenon that might explain, at least in part, the decrease in 5-HT concentrations noted in the biochemical studies of Parkinson's disease brains. Likewise, studies in rats and mice have shown that L-DOPA administration is accompanied by a decrease in 5-HT content (Everett & Borcherding, 1970; Carta *et al.*, 2007b; Navailles *et al.*, 2010; 2011).

In a study reporting a reduction of 5-HT markers in Parkinson's disease brains, Kish and co-workers noted the remarkable variability in the state of 5-HT markers in advanced parkinsonian population, some patients displaying normal levels of such tracers (Kish *et al.*, 2008). Neuroimaging studies with ^{11}C-DASB, a marker of SERT availability, indicate a progressive and non-linear loss of 5-HT terminals in parkinsonian patients and a relative preservation of 5-HT function in both the caudal and rostral groups of raphe nuclei, until advanced clinical phases (Albin *et al.*, 2008; Politis *et al.*, 2010a). These studies also indicate that the 5-HT innervation of the thalamus, hypothalamus and anterior cingulate cortex are affected early in the disease compared to the 5-HT

projection to the putamen, which is altered later (Politis *et al.*, 2010a). Another study with early Parkinson's disease patients indicates no reduction of SERT either in the caudate nucleus or the putamen, when compared to healthy controls (Strecker *et al.*, 2011). Therefore, it is believed that the presence of 5-HT axon varicosities in the striatum may be an important pre-synaptic determinent of LIDs, as indicated by a recent imaging investigation showing that Parkinson's disease patients with LIDs have striatal 5-HT axons terminals relatively well preserved throughout the disease (Politis *et al.*, 2014).

Data gathered in MPTP-lesioned monkeys also point to significant variability in striatal 5-HT innervation, with reports of increased (Schneider, 1990; Huot *et al.*, 2012b), unaltered (Pifl *et al.*, 1991) or decreased (Perez-Otano *et al.*, 1991; Russ *et al.*, 1991; Riahi *et al.*, 2011) 5-HT striatal levels. Interestingly, augmented levels of 5-HT in DA-depleted striatum of chronically exposed MPTP monkeys were noted in the putamen and caudate nucleus, but not in the nucleus accumbens (Schneider, 1990). These data are in accordance with our own findings, which show a sprouting of 5-HT axons in the sensorimotor territory of the putamen and caudate nucleus, but not in the limbic striatal territory.

Taken together, data reported in the present study and those gathered previously in human indicate that the sprouting of 5-HT fibers in DA-denervated striatal areas may represent an initial compensatory mechanism designed to cope with the severe DA denervation. Indeed, neuroimaging and behavioural studies of MPTP monkeys show that an increase in striatal 5-HT level is positively correlated with motor recovery from MPTP (Boulet *et al.*, 2008; Beaudoin-Gobert *et al.*, 2015). The existence of such a compensatory mechanism is supported by the present report of higher 5-HT striatal innervation preferentially in the DA-denervated striatal territories and by negative correlations between DAT and SERT binding in the striatum of Parkinson's disease patients (Strecker *et al.*, 2011) and Parkinson's disease autopsied brains (Fahn *et al.*, 1971; Kish *et al.*, 2008).

4.7.3. Ultrastructural features of striatal 5-HT axon varicosities in normal cynomolgus monkeys

Our ultrastructural analysis of non-human primate striatal tissue under normal condition reveals that the vast majority of 5-HT axon terminals are devoid of synaptic contact. Synaptic incidences, as extrapolated to the whole volume of varicosity, amount for 18% in the sensorimotor striatal territory and 23% in the limbic striatal territory. Such synaptic incidences for 5-HT axon terminals are significantly lower than those obtained for randomly selected unlabeled profiles. Low synaptic incidence of striatal 5-HT axon varicosities has been previously reported in early electron microscopic studies made in cat (Calas *et al.*, 1976), rat (Arluison & de la Manche, 1980), and monkey (Pasik *et al.*, 1982; Pasik & Pasik, 1982). The lack of synaptic specialization on many 5-HT terminals of the striatum was later confirmed in a detailed investigation in rats, where a significant number of 5-HT varicosities were either partially examined from single thin sections or entirely examined from serial sections (Soghomonian *et al.*, 1989). Whether extrapolated stereologically from single sections or directly observed in serial sections, the proportion of junctional 5-HT varicosities was found to be very small. Such a low synaptic incidence was viewed as the morphological evidence for the existence of a diffuse mode of transmission by 5-HT axons (reviewed in Descarries & Mechawar, 2008). The results of the present study clearly support the idea that 5-HT is released in the primate striatum through both synaptic and diffuse transmission. The diffuse mode of transmission has led to the suggestion that an ambient level of 5-HT might permanently exist in the extracellular space, the fluctuation of which could regulate, through the activation of 5-HT presynaptic receptors (Riad *et al.*, 2000; Bubser *et al.*, 2001), the release of glutamate by the corticostriatal axons (Mathur *et al.*, 2011; Tassone *et al.*, 2011), known to be altered in Parkinson's disease and LIDs (reviewed in Calabresi *et al.*, 2015).

The present study has provided the first detailed account of 5-HT ultrastructural features of the 5-HT innervation in the nucleus accumbens of

non-human primates. Our data indicate that the SERT+ axon varicosity profiles observed in the limbic striatal territory are larger than those in the dorsal striatum and display a low synaptic incidence. The latter finding is at odds with the results of previous investigations conducted in rats, in which synaptic membrane specializations were observed on approximately half of the 5-HT profiles examined from single thin sections of nucleus accumbens (Van Bockstaele & Pickel, 1993; Van Bockstaele *et al.*, 1996). It is, however, in agreement with the low synaptic incidences of 5-HT axon terminals noted in other components of primate basal ganglia, such as the internal and external pallidum (Eid *et al.*, 2013) and the subthalamic nucleus (Descarries *et al.*, 2010b). Whether the differences between rodents and primates reported above represent genuine species variations or simply reflect some methodological variations remains to be determined.

4.7.4. Ultrastructural features of striatal 5-HT axon varicosities in MPTP-intoxicated cynomolgus monkey

The 5-HT axon varicosities in the sensorimotor territory of the putamen of MPTP-intoxicated monkeys are all endowed with synaptic vesicles and their size and shape do not differ from those observed in control animals, indicating that they are fully functional. Our data indicate a 144% increase in the proportion of 5-HT axon varicosities that are engaged in synaptic relationship with striatal neurons of the sensorimotorputamen of MPTP monkeys. We believe that such high synaptic incidence in MPTP-intoxicated animals represents an immature feature (Crissman *et al.*, 1993) in line with axonal sprouting of 5-HT axons that occurs in the DA-depleted area of the striatum. The fact that no significant increases of synaptic incidence of 5-HT axon varicosities between MPTP and control monkeys were detected in the nucleus accumbens, a striatal region where the DA innervation is well preserved and for which no significant increase in the density of 5-HT axons or axon varicosities were observed, indicate that the change in synaptic incidence is specific to the DA-denervated area of the striatum.

The sprouting of 5-HT axons along with new synaptic axon varicosities in the sensorimotor striatal area is morphological evidence for altered striatal microcircuitry in the DA-denervated striatum. Such a change may lead to an increase in the probability of release of 5-HT, but also of DA when L-DOPA is administered. In order to better understand the functional consequences of newly formed 5-HT synaptic contacts, the neurochemical nature of the post-synaptic targets has to be identified. The fact that most of the 5-HT synapses occurred on dendritic spines in MPTP monkeys indicates that the newly formed 5-HT axon varicosities are well positioned to directly influence the activity of medium spiny projection neurons of the striatum and, therefore, to affect the overall functioning of the basal ganglia through a modulation of the striatofugal pathway.

We have previously reported a significant increase in synaptic incidence of 5-HT axon varicosities in the striatum of 6-OHDA-lesioned rats that were treated with L-DOPA (Rylander *et al.*, 2010). These results led to the suggestion that L-DOPA administration can, by itself, make 5-HT striatal axons sprout, in a dose-dependent manner, along with an increase in synaptic incidence. The present study in monkeys provides the first evidence that the DA denervation of the striatum, without L-DOPA treatment, is sufficient to induce 5-HT sprouting and increase in synaptic incidence.

4.7.5. Conclusion

The data presented here reveal that, in MPTP-intoxicated monkeys, the 5-HT ascending axonal projections undergo marked proliferative and synaptic adaptive changes that might play a significant role in the expression of Parkinson's disease motor symptoms and LIDs. These changes have to be taken into account to better understand the pathophysiology of Parkinson's disease and the adverse effects often induce by its most common pharmacological treatment.

4.8. Figures

TABLE 4.1. - Morphometric and junctional features of SERT-Immunostained and unlabeled axon varicosity profiles in MPTP and control cynomolgus monkeys

	Putamen				Nucleus accumbens			
	Control		MPTP		Control		MPTP	
	SERT	*Unlabeled*	*SERT*	*Unlabeled*	*SERT*	*Unlabeled*	*SERT*	*Unlabeled*
Number examined	231	275	248	245	200	200	208	208
Dimensions								
Short axis (µm)	$0.40 \pm 0.01^{\#}$	$0.45 \pm 0.02^{\#}$	0.38 ± 0.02	0.43 ± 0.01	0.56 ± 0.04	0.61 ± 0.02	0.46 ± 0.03	0.52 ± 0.03
Long axis (µm)	$0.69 \pm 0.01^{\#}$	$0.75 \pm 0.03^{\#}$	0.67 ± 0.05	0.70 ± 0.03	0.87 ± 0.03	0.88 ± 0.02	0.79 ± 0.04	0.81 ± 0.03
Aspect ratio	0.62 ± 0.01	$0.64 \pm 0.01^{\#}$	0.63 ± 0.02	0.64 ± 0.01	0.67 ± 0.03	0.70 ± 0.01	0.62 ± 0.01	0.67 ± 0.02
Diameter (µm)	$0.55 \pm 0.01^{\#}$	0.60 ± 0.03	0.53 ± 0.04	0.56 ± 0.02	0.71 ± 0.03	0.67 ± 0.06	0.63 ± 0.03	0.59 ± 0.07
Area (μm^2)	$0.26 \pm 0.01^{+\#}$	$0.33 \pm 0.03^{\#}$	0.24 ± 0.03	0.29 ± 0.02	0.47 ± 0.04	0.50 ± 0.03	0.34 ± 0.04	0.39 ± 0.03
% With mitochondria	$72 \pm 3^{+}$	33 ± 4	$73 \pm 2^{+}$	32 ± 3	$77 \pm 2^{+}$	32 ± 5	$72 \pm 5^{+}$	33 ± 1
Synaptic incidence (%)								
Single section	$6 \pm 1^{+}$	35 ± 4	$15 \pm 1^{+\#}$	$41 \pm 4^{\#}$	$9 \pm 1^{+}$	25 ± 2	$4 \pm 1^{+}$	27 ± 3
Whole volume	$18 \pm 4^{+}$	82 ± 12	$44 \pm 2^{+\#}$	109 ± 11	$23 \pm 5^{+}$	68 ± 13	$16 \pm 5^{+}$	84 ± 9
Length of synaptic junction (µm)	$0.22 \pm 0.03^{+\#}$	0.37 ± 0.03	$0.22 \pm 0.01^{+}$	$0.28 \pm 0.01^{*}$	0.43 ± 0.05	0.33 ± 0.04	$0.22 \pm 0.01^{*}$	0.29 ± 0.02

*Means ± SEM from four monkeys. * $P < 0.05$ for MPTP versus control. + $P < 0.05$ for SERT versus unlabeled. # $P < 0.05$ for putamen versus nucleus accumbens*

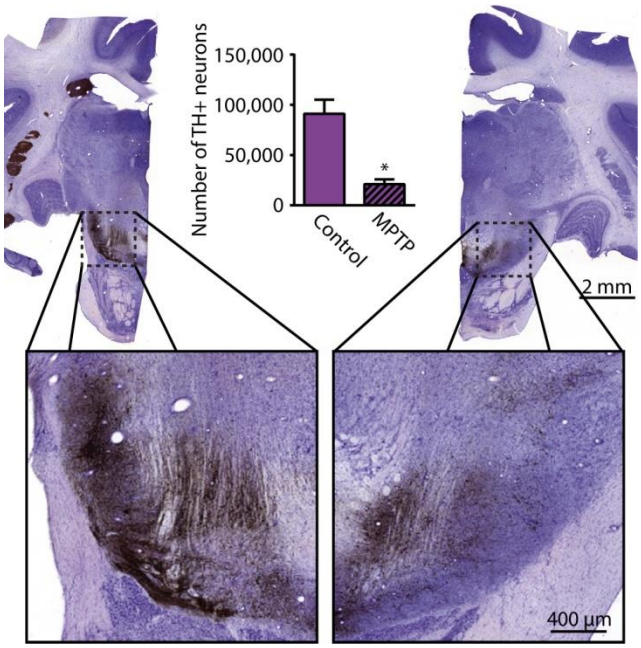

FIGURE 4.1. - Total number of tyrosine hydroxylase (TH) immunoreactive (+) neurons in the substantia nigra pars compacta (SNc) of control and MPTP-intoxicated monkeys. Transverse sections taken through the SNc and stained for TH (*brown*) and Nissl (*purple*) in control (*left*) and MPTP (*right*) monkeys. Inserts provide higher magnification of the SNc and histogram shows the total estimated number of TH+ neurons in the SNc of control and MPTP-intoxicated monkeys. Our stereological analysis reveals a 77 % decrease in the number of TH+ neurons in MPTP-intoxicated monkeys, when compared to controls. *$P < 0.05$ using Mann–Whitney test

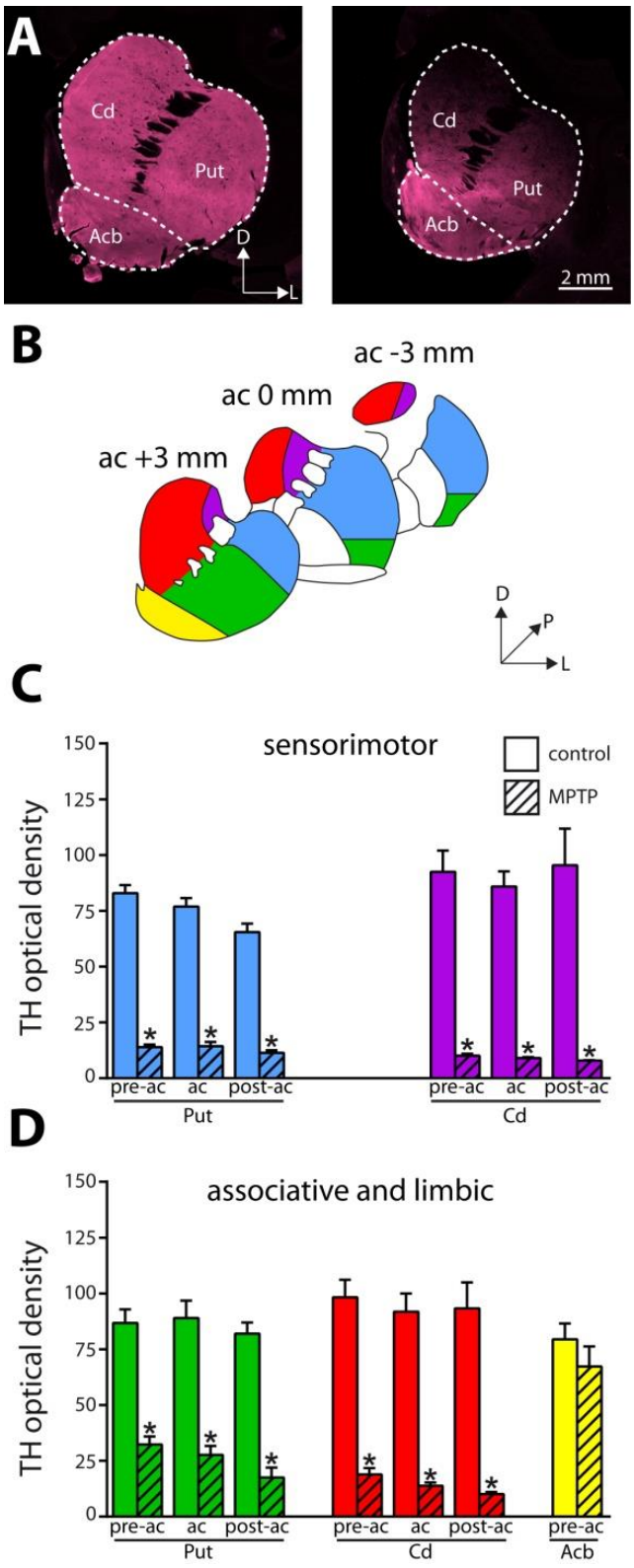

FIGURE 4.2. - Immunoreactivity for tyrosine hydroxylase (TH) in the striatum of control and MPTP-intoxicated monkeys. **a** Transverse sections of control

(*left*) and MPTP (*right*) monkeys taken from the pre-commissural striatum and immunostained for TH using near infrared secondary antibodies. **b** Schematic representations of the striatal functional territories from transverse sections taken at the pre-commissural (pre-ac), commissural (ac) and post-commissural (post-ac) levels. The sensorimotor territories of the caudate nucleus (Cd) and the putamen (Put) are shown in *purple* and *blue*, whereas the associative territories of the Cd and Put are illustrated *red* and *green*, respectively. The limbic striatal territory corresponding to the nucleus accumbens (Acb) is shown in *yellow*. **c**, **d**Histograms showing the optical density of TH immunoreactivity in the sensorimotor (**c**), the associative and the limbic (**d**) striatal territories, at the three anteroposterior levels examined indicating lower TH immunoreactivity throughout the striatum of MPTP-intoxicated monkeys, except for the limbic territory. *$P < 0.05$ using Mann–Whitney *U* test

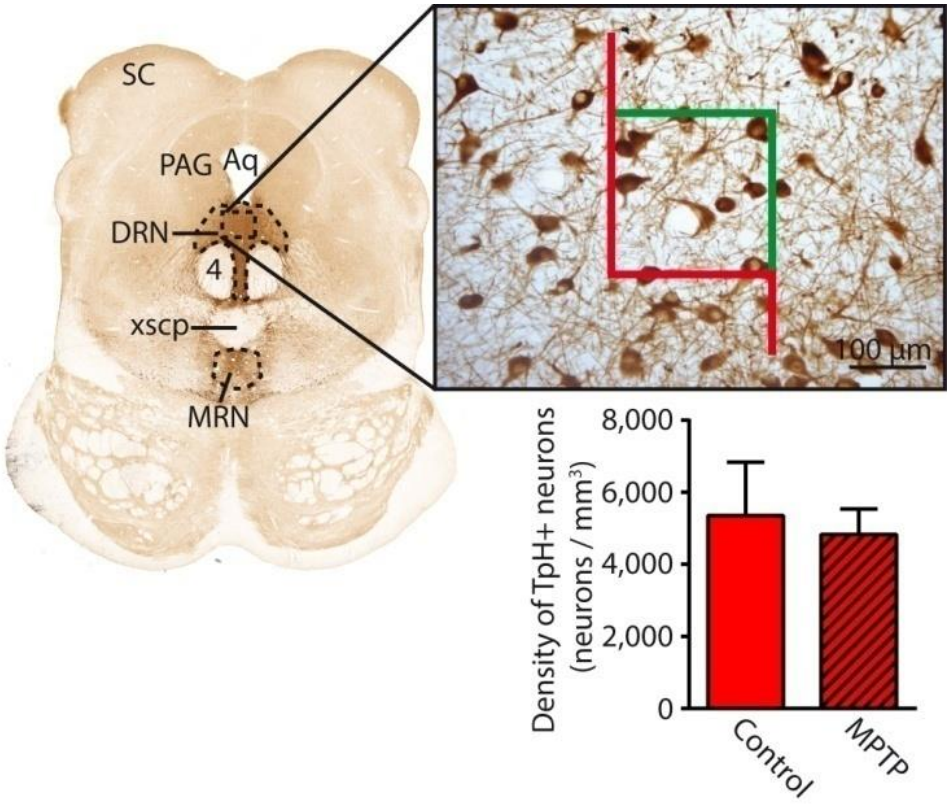

FIGURE 4.3. - Tryptophan hydroxylase (TpH)+ neurons in the dorsal raphe nucleus (DRN) of control and MPTP-intoxicated monkeys. Transverse section through the DRN and immunostained for TpH, using DAB as the chromogen. The insert provides a higher magnification of TpH+ cell bodies in the dorsal raphe nucleus (DRN) as well as an example of a counting frame used for stereology. The histogram shows the density of TpH+ neurons in the DRN of control and MPTP-intoxicated monkeys. No significant changes were observed between control and MPTP monkeys. *4* trochlear nucleus, *Aq*cerebral aqueduct, *MRN* median raphe nucleus, *PAG* periaqueductal gray, *SC* superior colliculus, *xscp* decussation of superior cerebellar peduncle

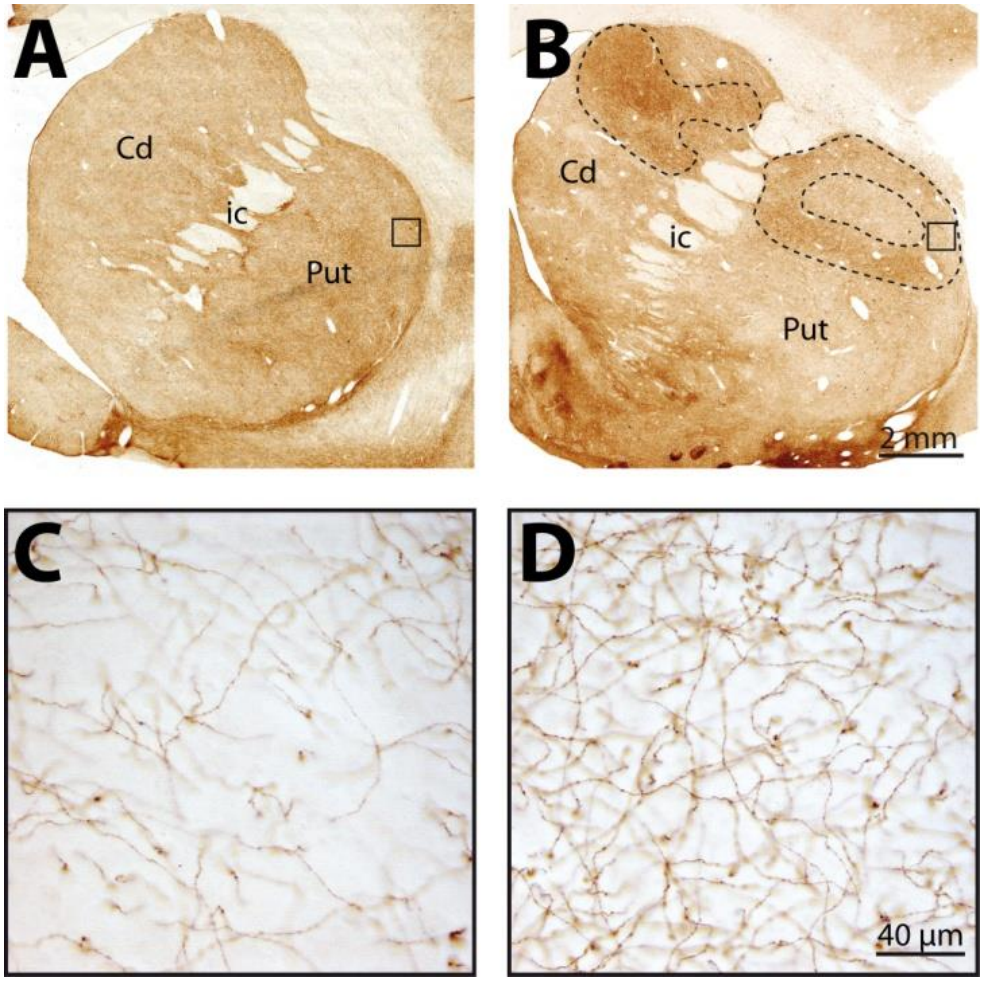

FIGURE 4.4. - Immunolabeling for SERT in the striatum of control and MPTP-intoxicated monkeys. **a**, **b** Transverse sections taken through the pre-commissural striatum and immunostained for SERT, in control (**a**) and MPTP (**b**) monkeys. *Dashed lines* in **b** indicate dense SERT immunoreactive zones mainly located in the dorsolateral sector of the striatum in MPTP monkeys. *Squares* delineate the regions that are shown at higher magnification in **c** and **d**. **c**, **d** Higher magnification of SERT+ varicose axons observed in the dorsolateral putamen (Put) of control (**c**) and MPTP (**d**) monkeys. *ic* internal capsule, *Put* Putamen, *Cd* Caudate nucleus

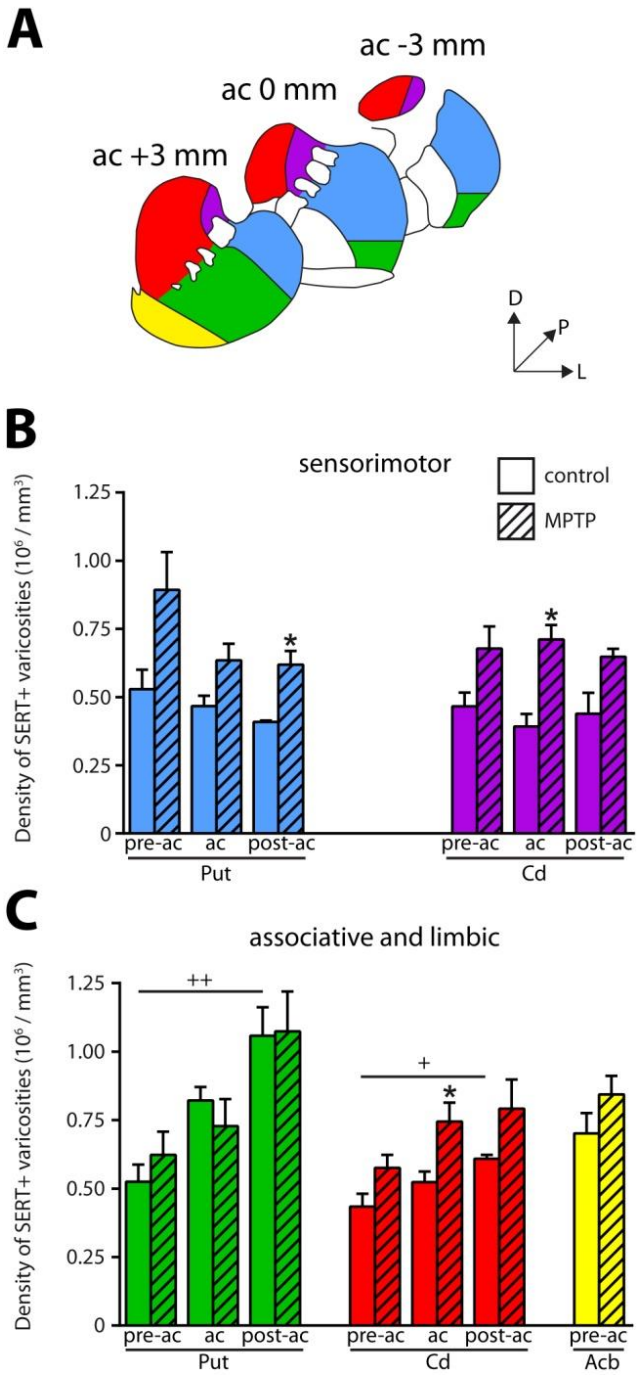

FIGURE 4.5. - Density of SERT immunoreactive axon varicosities in different functional territories of the striatum of control and MPTP-intoxicated monkeys. **a** Schematic representations of the striatal functional territories, at three anteroposterior levels, each identified with its own *color* (see Fig. 2 legend for further details). **b**, **c** Histograms showing the density of SERT+ axon varicosities in the sensorimotor (**b**), the associative and the limbic

(**d**) striatal territories, at the three anteroposterior levels examined. *$P < 0.05$ between MPTP and controls, by Mann–Whitney *U* test; $^{+}P < 0.05$, $^{++}P < 0.01$ between pre and post-commissural levels of controls monkeys, by Kruskal–Wallis one-way analysis of variance

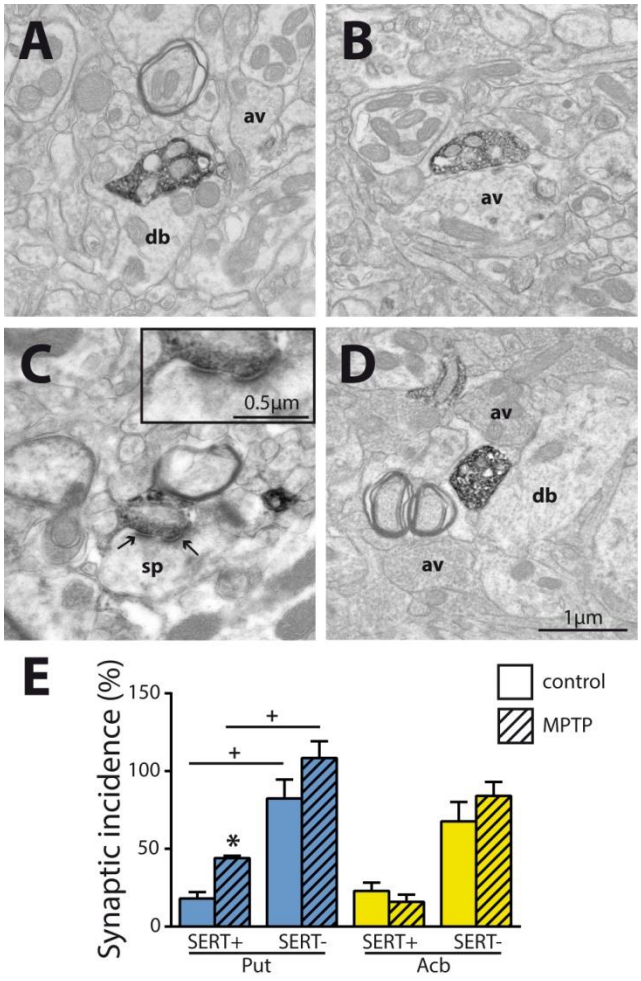

FIGURE 4.6. - Electron microscopic visualization of SERT immunoreactive (+) axon varicosities in the dorsolateral putamen of control (**a**, **b**) and MPTP-intoxicated (**c**, **d**) monkeys. The SERT+ axon varicosities look similar in size, shape and vesicular content between controls and MPTP monkeys (see Table 1). The SERT+ axon varicosities observed in MPTP monkeys establish significantly more synaptic contacts than those in control animals. The SERT+ axon varicosity shown in **c** establishes a perforated asymmetrical synaptic contact (between *arrows*) on a dendritic spine (sp). The *inset* provides higher magnification. **e** Histogram showing the extrapolated synaptic incidence of SERT+ and SERT− axon varicosities observed in the putamen (Put, *blue*) and the nucleus accumbens (Acb, *yellow*) of control and MPTP-intoxicated monkeys. *av* axon varicosity, *db* dendritic branch, *sp* dendritic spine

CHAPITRE 5 :

SPROUTING OF SEROTONIN AND DOPAMINE AXONS IN THE PALLIDUM OF PARKINSONIAN MONKEY

CHAPITRE 5 – EVIDENCE FOR SPROUTING OF DOPAMINE AND SEROTONIN AXONS IN THE PALLIDUM OF PARKINSONIAN MONKEYS

Dave Gagnon, Lara Eid, Dymka Coudé, Carl Whissel, Thérèse Di Paolo et Martin Parent

Centre de recherche CERVO
2601, Ch. de la Canardière, Québec, Québec
Canada G1J 2G3

Frontiers in neuroanatmy (in press)

5.1. Résumé

Cet article renferme des données inédites concernant les changements neuroadaptatifs que subissent les axones sérotoninergiques (5-HT) et dopaminergiques (DA) qui innervent le segment interne (GPi) et externe (GPe) du pallidum dans un modèle simien de la maladie de Parkinson. L'intoxication au MPTP de singe macaque (*Macaca fascicularis*) induit une augmentation de près du double de la densité de varicosités axonales 5-HT dans le pallidum. Cette augmentation semble particulièrement prononcée dans les territoires pallidaux associatifs et limbiques. Tel qu'attendu, l'administration de MPTP conduit à une dénervation DA significative du striatum. De façon surprenante, ce type d'innervation est approximativement 8 fois plus intense dans le territoire sensorimoteur du GPi chez les singes MPTP, comparativement aux contrôles. En somme, nos données démontrent un bourgeonnement significatif des afférences pallidales 5-HT, possiblement en accord avec l'expression précoce de symptômes non-moteurs de la maladie de Parkinson, ainsi qu'une hyperinnervation DA, potentiellement impliquée dans la normalisation des patrons de décharges des neurones du pallidum interne, associée à une expression tardive des symptômes moteurs.

5.2. Abstract

This light and electron microscopic immunohistochemical quantitative study aimed at determining the state of the dopamine (DA) and serotonin (5-HT) innervations of the internal (GPi) and external (GPe) segments of the pallidum in cynomolgus monkeys (Macaca fascicularis) rendered parkinsonian by systemic injections of 1-methyl-4-phenyl-1,2,3,6-tetrahydropyridine (MPTP). In contrast to the prominent DA denervation of striatum, the GPi in MPTP monkeys was found to be markedly enriched in DA (TH+) axon varicosities. The posterior sensorimotor region of this major output structure of the basal ganglia was about 8 times more intensely innervated in MPTP monkeys (0.71 ± 0.08 x 106 TH+ axon varicosities/mm3) than in controls (0.09 ± 0.01 × 106). MPTP intoxication also induced a two-fold increase in the density of 5-HT (SERT+) axon varicosities in both GPe and GPi. This augmentation was particularly pronounced anteriorly in the so-called associative and limbic pallidal territories. The total length of the labeled pallidal axons was also significantly increased in MPTP monkeys compared to controls, but the number of DA and 5-HT axon varicosities per axon length unit remained the same in the two groups, indicating that the DA and 5-HT pallidal hyperinnervations seen in MPTP monkeys result from axon sprouting rather than from the appearance of newly formed axon varicosities on non-growing axons. At the ultrastructural level, pallidal TH+ and SERT+ axons were morphologically similar in MPTP and controls, and their synaptic incidence was very low suggesting a volumic mode of transmission. Altogether, our data reveal a significant sprouting of DA and 5-HT pallidal afferents in parkinsonian monkeys, the functional significance of which remains to be determined. We suggest that the marked DA hyperinnervation of the GPi represents a neuroadaptive change designed to normalize pallidal firing patterns associated with the delayed appearance of motor symptoms, whereas the 5-HT hyperinnervation might be involved in the early expression of non-motor symptoms in Parkinson's disease.

5.3. Abbreviations

5-HT	Serotonin
a	Axon
A	Anterior
av	Axon varicosity
CB	Calbindin
cp	Cerebral peduncle
db	Dendritic branch
DA	Dopamine
DAB	3,3'diaminobenzidine tetrahydrochloride
DAT	Dopamine transporter
DBH	Dopamine beta-hydroxylase
GDNF	glial-cell-line-derived neurotrophic factor
GPe	External segment of the globus pallidus
GPi	Internal segment of the globus pallidus
H2	Lenticular fasciculus
ic	Internal capsule
L-DOPA	L-3,4-dihydroxy-phenylalanine
MPTP	1-methyl-4-phenyl-1,2,3,6-tetrahydropyridine
P	Posterior
PBS	Sodium phosphate-buffered saline
PET	Positron emission tomography
PFA	Paraformaldehyde
RT	Room temperature
SERT	Serotonin transporter
SN	Substantia nigra
SNc	Substantia nigra pars compacta
STN	Subthalamic nucleus
TBS	Tris-buffered saline
TH	Tyrosine hydroxylase
TpH	Tryptophan hydroxylase
VTA	Ventral tegmental area

5.4. Introduction

The main neuropathological hallmark of Parkinson's disease (PD) is a progressive degeneration of dopamine (DA) neurons located in the substantia nigra pars compacta (SNc) leading to a massive loss of DA input to the striatum. The decrease of striatal DA content is believed to be central in the expression of bradykinesia, resting tremor and rigidity that characterize PD. On the other hand, there is a growing interest in the fate of 5-hydroxytryptamine (serotonin or 5-HT) neurons in PD, mainly because of evidence that 5-HT striatal afferents are the main presynaptic determinant in the expression of L-3,4-dihydroxy-phenylalanine (L-Dopa)-induced dyskinesia (Carta *et al.*, 2007a), a motor disability characterized by abnormal involuntary movements that affect more than 75% of PD patients after only 15 years of dopatherapy (Yahr, 1972; Obeso *et al.*, 2000a; Rajput *et al.*, 2002b; Hely *et al.*, 2005a).

In addition to the striatum, the primate pallidum also receives significant DA and 5-HT inputs (Eid *et al.*, 2013; Eid & Parent, 2015b). However, by comparison to our knowledge of striatal DA and 5-HT involvement in the pathogenesis of PD, the possible contribution of such extrastriatal DA and 5-HT innervations is still unknown. Therefore, in the hope to shed a new light on the role of pallidal DA and 5-HT innervations in PD pathogenesis, we designed a study to determine the state of DA and 5-HT axonal projections to the internal (GPi) and external (GPe) segments of the pallidum in cynomolgus monkeys rendered parkinsonian after MPTP intoxication.

5.5. Material and methods

5.5.1. Animals and behavioural assessment

Eight female cynomolgus monkeys (*Macaca fascicularis,* Primus Bio-Ressources inc.) of 4 years old, weighing between 2.8 and 3.9 kg were used. All monkeys were naïve and did not receive any other compounds unrelated to our study. For ethical and financial reasons, these monkeys were used in a previously published post-mortem analysis of the 5-HT striatal innervation (Gagnon *et al.*, 2016), allowing direct comparisons with the present work dealing with pallidal innervation. Ovariectomy was performed on these animals to model the hormonal status of menopause women. This is particularly relevant to the fact that most parkinsonian women are menopause and that estrogens are known to be neuroprotective (Bourque *et al.*, 2015). Animals were housed under a 12 h light-dark cycle with water and food *ad libitum*. All experimental procedures were approved by the *Comité de Protection des Animaux de l'Université Laval*, in accordance with the Canadian Council on Animal Care's Guide to the Care and Use of Experimental Animals (Ed2). Maximum efforts were made to minimize the number of animals used. Four monkeys received MPTP (Sigma-Aldrich Canada Ltd., Oakville, Canada) via a subcutaneous osmotic mini-pump for 14 days. Behavioural response to MPTP intoxication was assessed by using a faithful motor scale that takes into account posture, mobility, climbing, gait, grooming, voicing, social interaction and tremor (see Hadj Tahar *et al.*, 2004 for details). Individual doses of MPTP as well as motor disability scores obtained for each monkey are given in Table 1.

5.5.2. Tissue preparation and immunohistochemistry

Five months after MPTP administration, animals were perfused transcardially as described in Eid and Parent (2017). Brains were then rapidly dissected out, post-fixed by immersion in 4% PFA for 24 h at 4°C and cut with a vibratome (model VT1200 S; Leica, Germany) into 50 µm-thick transverse sections collected in PBS.

The method used to assess the DA lesion induced by MPTP in these monkeys as been described elsewhere (Gagnon *et al.*, 2016). Briefly, using standard immunoperoxidase method, equidistant transverse sections selected throughout the SNc and the striatum were immunostained for tyrosine hydroxylase (TH), the catalytic enzyme of DA synthesis, and/or the DA transporter (DAT), using 3,3'-diaminobenzidine tetrahydrochloride (DAB; catalog no. D5637; Sigma-Aldrich) as the chromagen. Sections taken through the SNc were immunostained for TH and counterstained with cresyl violet whereas striatal sections were stained for DAT and TH (see Table S1 for antibodies). Unbiased stereological counting of TH+ neurons was performed on SNc sections whereas striatal DA denervation was assessed using an infrared imaging system (Odyssey CLx; LI-COR Biosciences, Lincoln, NE, USA) and optical density measurements taken from delineated functional territories of the striatum (see Gagnon *et al.*, 2016 for details).

The calbindin (CB) expression by TH immunoreactive neurons was assessed using a confocal imaging system (Zeiss, LSM 700; Oberkochen, Germany) and one double immunostained transverse section per brain taken through the SNc at -9 mm relative to the anterior commissure (Bowden & Martin, 2000a) (see Table S1 for antibodies).

The number of tryptophan hydroxylase (TpH)-immunostained neurons of the dorsal raphe nucleus has been assessed in each monkey using the immunoperoxidase methodological approach and unbiased stereology with a primary antibody against TpH, the rate-limiting enzyme in 5-HT synthesis, as described previously (Gagnon *et al.*, 2016).

To assess the state of the DA innervation of the pallidum, a quantitative stereological analysis at the light microscope level was performed on 4 transverse sections taken through the pallidum (from -6 to 0 mm, relative to the anterior commissure, with a fixed interval of 1800 µm) and immunostained for TH. In order to rule out the noradrenergic nature of TH+ axons observed in

the pallidum, sections taken through the posterior GPi were doubly stained for TH and dopamine beta-hydroxylase (DBH), the enzyme that catalyze the hydroxylation of DA into noradrenaline, in both experimental groups. The absence of doubly labeled neuronal element in the pallidum was confirmed using confocal microscopy (see Fig. S1).

For electron microscopy, sections of the eight monkeys taken at -3 mm relative to the anterior commissure were also immunostained for TH, but in the absence of Triton X-100, which was replaced by 0.5% gelatin in all solutions. Sections were osmicated, dehydrated in ethanol and propylene oxide, and flat-embedded in Durcupan (catalog no. 44611-14; Fluka, Buchs, Switzerland) to be processed and examined as described below.

To provide a detailed and stereological quantitative description of the 5-HT axon distribution through the pallidum at the light microscope level, 10 transverse sections were selected across the entire pallidum (from -6 to 0 mm, relative to the anterior commissure), with a fixed interval of 600 µm. These sections were immunostained according to the immunoperoxidase method with an antibody against the 5-HT transporter (SERT, see Table S1). Other sections were also taken through the pallidum of all monkeys, at -3 mm relative to the anterior commissure, immunostained for SERT, but prepared for electron microscopy as described above.

5.5.3. Stereology

Immunostained sections intended for stereology were examined under a light microscope equipped with a digital camera, a motorized stage and a Z-axis indicator controlled by a computer running StereoInvestigator software (v. 7.00.3; MicroBrightField, Colchester, VT, USA). The precise regional distribution of immunoreactive axons and axon terminals (varicosities) throughout the GPe and GPi was determined by dividing each pallidal segment into eight sectors, according to the method described in Eid *et al.* (2013).

Numbers of TH-positive (+) and SERT+ axon varicosities were estimated using the optical fractionator probe (West *et al.*, 1991) available in the StereoInvestigator software. Briefly, at each intersection of a grid formed by squares of 200 x 200 µm (TH+) and 600 x 600 µm (SERT+), a counting frame measuring 35 x 35 µm was drawn and examined with the 100x oil-immersion objective (NA 1.3, HCX PL Fluotar). Axon varicosities that fell inside of the counting frame and did not contact the exclusion lines were counted whenever they came into focus within the 10 µm-thick disector. An average of 210 ± 17 (TH+) and 391 ± 23 (SERT+) varicosities were counted in each sector, yielding coefficients of error (Gundersen, m = 1 and 2nd Schmitz-Hof) between 0.03 and 0.22. Densities of TH+ and SERT+ varicosities were obtained using the total number of varicosities estimated by the optical disector and the volume of each sector estimated by Cavalieri's method.

The density of TH+ and SERT+ axons was assessed using the *spaceball* stereological probe (Mouton *et al.*, 2002) that generates hemispheres on which a marker is placed when an immunolabeled axon intersects. For this experiment, 10 µm diameter hemispheres were randomly placed in the middle of the section at intersections of 200 x 200 µm grid for TH and 600 x 600 µm grid for SERT. A 100x oil-immersion objective was used for sampling. An average of 770 ± 39 (TH+) and 226 ± 13 (SERT+) markers were placed in each sector, yielding coefficients of error (Gundersen, m = 1 and 2nd Schmitz-Hof) between 0.05 and 0.46. Densities of TH+ and SERT+ axons were obtained using the total length of axons estimated by the spaceball and the volume of each sector estimated by Cavalieri's method. Thick TH+ or SERT+ axons could easily be distinguished from thin and varicose axons by their smooth aspect and their diameter larger than 1 µm.

5.5.4. Ultrastructural analysis of SERT+ and TH+ axon varicosities

Quadrangular pieces were cut in the GPe and GPi of each monkey from flat-embedded SERT or TH-immunostained sections. After being glued on the tip of a resin block, they were cut at 80 nm with an ultramicrotome (model EM UC7, Leica). Ultrathin sections were collected on bare 150-mesh copper grids, stained with lead citrate and examined by using a transmission electron microscope (Tecnai 12; Philips Electronic, 100 kV) and an integrated digital camera (XR-41, Advanced Microscopy Techniques). Axon varicosities were randomly sampled at a working magnification of 11,500x by taking a picture every time such profile was encountered until 45 or more pictures were available for analysis in each pallidal segment, for each monkey. From the same photomicrographs, unlabeled axon varicosities were randomly selected for comparison. Morphometric features of labeled and unlabeled axon varicosities were analyzed using the ImageJ software (v 1.50b, NIH, USA) running a custom-made java application (Dave Gagnon: https://github.com/Fishwithatie/TEM_AnalysisWorkFlow). The synaptic incidence obtained from single-ultrathin sections was then extrapolated to the whole volume of varicosities by means of the formula of (Beaudet & Sotelo, 1981), using the long axis as diameter, according to (Umbriaco *et al.*, 1994).

5.5.5. Statistical analysis

Because the data gathered from our 2 experimental groups, each composed of 4 animals, were not normally distributed, all statistical differences were assessed using a non-parametric statistical test, namely the Mann-Whitney U test. Non-linear regressions were performed to analyse correlations between the density of axon varicosities and PD motor disability scores. Pearson correlation coefficient (R) was used to determine the correlation strength. Differences were considered statistically significant at $P < 0.05$. Statistical analysis was done using GraphPad Prism software (v. 6.01; GraphPad

Software, San Diego, CA, USA). Mean and standard error of the mean are used throughout the text as central tendency and dispersion measure, respectively.

5.6. Results

5.6.1. MPTP intoxication induces a significant DA lesion and motor impairments

Compared to controls, the number of TH+ neurons in the SNc of MPTP monkeys is decreased by 70.5 - 82.5% (Fig. 1) (see also Gagnon *et al.*, 2016), leading to a 84.0 - 89.4% decline of TH and to a 82.4 - 90.0% diminution of DAT immunoreactivity in the sensorimotor functional territory of the striatum (Table 1). No significant changes were observed in the limbic striatal territory. Virtually all of the few TH+ neurons that remain in the SNc of MPTP monkeys are CB+ and they occur predominantly in the dorsal tier of the structure (Fig. 2). The is no significant variation between controls and MPTP monkeys in regard to number of tryptophane hydroxylase-positive (TpH+) neurons in the dorsal raphe nucleus, with 5355 ± 742 TpH+ neurons/mm^3 of tissue in controls compared to 4833 ± 354 in MPTP monkeys. Motor response to MPTP intoxication indicates scores ranging between 6.78/16 and 9.64/16, corresponding to moderate to severe PD states (see Table 1 for individual values).

5.6.2. TH+ innervation of the pallidum in normal condition

At the light microscope level, the TH innervation of the pallidum appears to be composed of two types of TH+ axons: (a) small (0.52 ± 0.04 µm in diameter), highly varicose and tortuous, and (b) thick (1.63 ± 0.06 µm in diameter) and smooth (Fig. 3). The thin and varicose axons represent 32% of all TH+ axons in the GPe and 37% in the GPi. The remaining thick and smooth axons travel

mainly in bundles through a rather straight direction across both pallidal segments, en route to the putamen.

The DA innervation is similar in the two pallidal segments, with 0.14 ± 0.01 × 10^6 TH+ varicosities/mm^3 in GPe and 0.18 ± 0.06 × 10^6 in GPi (Fig. 4). A noticeable mediolateral-decreasing gradient of DA innervation is present in the GPe, with 0.19 ± 0.02 × 10^6 TH+ axon varicosities/mm^3 in the medial region compared to 0.09 ± 0.01 × 10^6 in the lateral region (P = 0.0286). In contrast, the TH+ varicosities appear homogeneously distributed in the GPi. Estimates of the number of TH+ varicosities per 10 µm of axon were obtained by dividing the number of TH+ axon varicosities by the total length of the small calibre TH+ axons, and these values are similar in the GPe (1.90 ± 0.28 varicosities/10 µm of TH+ axons) and the GPi (1.79 ± 0.34, P = 0.8286).

5.6.3. TH+ innervation of the pallidum in parkinsonian monkeys

The estimated volumes of the GPe and the GPi do not differ significantly between MPTP monkeys (53.24 ± 2.67 mm^3 for GPe and 33.60 ± 2.80 mm^3 for GPi) and controls (49.59 ± 3.76 mm^3 for GPe and 37.15 ± 2.41 mm^3 for GPi). In contrast to the striatum, which is markedly depleted of TH immunoreactivity in MPTP monkeys, the DA innervation of the pallidum is increased in all of its sectors. Such augmentation in the density of TH+ axon varicosities is particularly obvious in the posterior region of the GPi, with 0.71 ± 0.08 × 10^6 TH+ axon varicosities/mm^3 of tissue in MPTP monkeys compared to only 0.09 ± 0.01 × 10^6 in controls (P = 0.0286, Fig. 4).

The higher density of TH+ axon varicosities observed in the GPi after MPTP lesion is also reflected by the increase of the total length of the thin and varicose TH+ axons (4.8 ± 0.6 m of thin TH+ axons/mm^3 of tissue in MPTP monkeys compared to only 1.3 ± 0.4 in controls, P = 0.0286). Again, this difference is more pronounced in the posterior region of the GPi with 6.0 ± 0.8

m of thin TH+ axons/mm^3 in MPTP monkeys compared to only 0.43 ± 0.04 in controls (P = 0.0286). In accordance with a higher density of TH+ axon varicosities and TH+ thin axons, the number of varicosities/10 µm of small-caliber TH+ axons does not change significantly after MPTP administration in both pallidal segments, suggesting that the increase of the density of TH+ axon varicosities is caused by the sprouting of varicose TH+ axons rather than by the appearance of newly formed axon varicosities on non-growing axon. In contrast to the density of the thin and varicose axons that increases significantly in the GPi of MPTP monkeys, the density of the thick and smooth TH+ axons appears similar. Interestingly, the two MPTP-intoxicated monkeys with the lowest motor disability scores (6.78 and 7.20) show the largest increase in density of TH+ axons and axon varicosities in the GPi. This observation suggests a possible negative correlation between motor disability score and DA GPi hyperinnervation that would become statistically significant with a larger sample (R = -0.8660, P = 0.1922, Fig. S2).

In contrast to the GPi, the density of the thick and smooth TH+ axons in the GPe, which are probably heading to the striatum, is significantly reduced after MPTP intoxication reaching 0.75 ± 0.02 m of TH+ axons/mm^3 of tissue in MPTP monkeys compared to 1.8 ± 0.1 in controls (P = 0.0286), whereas the density of the thin and varicose TH+ axons appears unaltered following MPTP administration. The TH+ axons present in the pallidum do not display DBH immunoreactivity, a finding that dismisses their possible noradrenergic nature (Fig. S1).

5.6.4. Ultrastructural features of TH+ axon varicosities

When examined at the ultrastructural level, the two types of TH+ fibers detected in the GPi of normal monkeys (thin and varicose versus large and smooth) stand out as small unmyelinated axons and large myelinated axons, respectively (Fig. 3G, H). In the GPi of MPTP monkeys, only thin unmyelinated TH+ axons are observed. No significant difference regarding the size and

shape of TH+ axon varicosities can be found between MPTP and control monkeys. When extrapolated to the whole volume of varicosities by means of the stereological formula of Beaudet and Sotelo (1981), similar synaptic incidences are also noted for TH+ axon varicosities observed in the two experimental groups (7 ± 3% in the GPi of MPTP monkeys compared to 13 ± 7% in control animals, when extrapolated to the whole volume of axon varicosities). In comparison, the synaptic incidence of unlabeled, randomly selected axon varicosity profiles in the GPi of control animals was 28 ± 3% (Table 2). All synaptic contacts made by TH+ axon varicosities occur on dendritic profiles.

5.6.5. 5-HT innervation of the pallidum in normal condition

The 5-HT innervation of the pallidum is mainly composed of thin (0.5 ± 0.1 µm) and varicose SERT+ axons that display a tortuous course without any preferential orientation (Fig. 5). Using a stereological approach, we estimate that, in control animals, this type of axons represents 92% of SERT+ axons in the GPe and 93% in the GPi. The remaining axons are thick (1.1 ± 0.1 µm), do not show varicosity and do not travel in bundle or show any preferential orientation.

Overall, the density of SERT+ axon varicosities appears similar between the GPe (0.32 ± 0.05 $\times$ 10^6 SERT+ axon varicosities/mm^3 of tissue) and the GPi (0.43 ± 0.05 $\times$ 10^6, Fig. 6). Both pallidal segments display an anteroposterior-decreasing gradient of 5-HT innervation that becomes significant only in the GPi with 0.53 ± 0.05 $\times$ 10^6 SERT+ axon varicosities/mm^3 of tissue in its anterior part compared to 0.28 ± 0.06 $\times$ 10^6 in its posterior region (P = 0.0286). This gradient is also reflected by unbiased estimations of the density of SERT+ axons indicating that, in contrast to the thick SERT+ axons that are homogeneously distributed through both pallidal segments, the thin and varicose SERT+ axons are more abundant in the anterior part of the GPi (7.7 ± 1.1 m of axons/mm^3 of tissue) than in posterior region (3.1 ± 0.5, P =

0.0286). By dividing the estimated number of SERT+ axon varicosities by the total length of small calibre SERT+ axons, we can approximate the number of SERT+ varicosities per 10 µm of axon. These values are similar in the GPe (0.84 ± 0.08 SERT+ axon varicosities/10 µm of axon) and the GPi (0.84 ± 0.11), as well as across different pallidal regions. It is noteworthy that SERT+ pallidal afferents display a lower number of varicosities/10 µm of axon than the TH+ pallidal projections.

In the GPe of control animals, the density of SERT+ axon varicosity is significantly higher than that of TH+ (0.32 ± 0.03 × 10^6 SERT+ axon varicosities/mm^3 vs. 0.14 ± 0.01 × 10^6 TH+ axon varicosities/mm^3, P = 0.0286). This difference becomes particularly significant in the anterior part of the GPe, which harbors 0.37 ± 0.05 × 10^6 SERT+ varicosities/mm^3 compared to 0.15 ± 0.02 × 10^6 TH+ varicosities/mm^3 (P = 0.0286). In the GPi, only the posterior region shows higher density for SERT+ axon varicosities with 0.28 ± 0.06 × 10^6/mm^3 vs. 0.09 ± 0.01 × 10^6 axon varicosities/mm^3 for TH+ axon varicosities (P = 0.0286).

5.6.6. 5-HT innervation of the pallidum in parkinsonian monkeys

In MPTP-intoxicated monkeys, the density of SERT+ axon varicosities is increased by 91% in the GPe to reach 0.61 ± 0.05 × 10^6 SERT+ varicosities/mm^3 (P = 0.0286) and by 74% the GPi to reach 0.75 ± 0.07 × 10^6 SERT+ varicosities/mm^3 (P = 0.0286). This augmentation is more significant in the anterior sectors of the GPe with 0.72 ± 0.06 × 10^6 SERT+ varicosities/mm^3, representing a two-fold increase compared to control animals (0.37 ± 0.05 × 10^6). In the GPi, the increased density of SERT+ axon varicosities is statistically significant only in anterior sectors with 0.94 ± 0.06 × 10^6 SERT+ varicosities/mm^3 compared to 0.53 ± 0.05 × 10^6 in control animals (P = 0.0286).

The higher density of SERT+ axon varicosities in the pallidum of MPTP monkeys is also reflected by a significant increase of the density of the thin and varicose SERT+ axons in the GPe (6.2 ± 0.2 m of SERT+ axons/mm^3 of tissue in MPTP monkeys compared to 4.2 ± 0.6 in controls, $P = 0.0286$). Such a gain does not reach statistical significance in the GPi (7.7 ± 0.5 in MPTP animals compared to 5.4 ± 0.8 in controls). In the GPe, increase in the density of the thin and varicose SERT+ axons is significant in the anterior sectors (7.9 ± 0.4 m of SERT+ axons/mm^3 of tissue in MPTP monkeys compared to 5.3 ± 0.7 in controls, $P = 0.0286$) and in the medial sectors (7.6 ± 0.3 m of SERT+ axons/mm^3 of tissue in MPTP monkeys compared to 4.7 ± 0.7 in control animals, $P = 0.0286$, Fig. 6). In accordance with a higher density of SERT+ axon varicosities and SERT+ thin axons, no significant differences between MPTP and control monkeys are observed when considering the number of SERT+ varicosities/10 µm of axon in the GPe nor the GPi. Also, there is no significant change in regard to the density of the thick SERT+ axons in the GPe and the GPi, and no statistically significant correlation could be made between the increased SERT+ pallidal innervation reported above for the density of axon varicosities in MPTP monkeys and their PD motor disability scores.

5.6.7. Ultrastructural features of SERT+ axon varicosities

At the electron microscope level, SERT+ axon varicosities were seen to derive exclusively from unmyelinated axons and the ones present in the GPe and GPi of MPTP monkeys were similar in size and shape to those in controls (Fig. 5G-J, Table 3). These axon varicosities are usually ovoid, contain aggregated and small vesicles and often display one or more mitochondria. Statistical analysis of morphometric measurements, such as diameter and cross-sectional area, reveals that SERT+ axon varicosities in both GPe and GPi are similar in MPTP and control animals, and are also similar to randomly selected, unlabeled axon varicosity profiles.

Interestingly, in both pallidal segments of control and MPTP monkeys, very few SERT+ axon varicosities display a synaptic contact when compared to unlabeled profiles (P = 0.0248). The synaptic incidence of the SERT+ axon varicosities is estimated at 31 ± 10% in the GPe and 23 ± 2% in GPi compared to 80 ± 22% and 77 ± 6% for unlabeled axon varicosities (Table 3). The synaptic incidence of the SERT+ axon varicosity profiles is similar to the one reported above for the TH+ profiles and, like TH+ axon varicosities, significantly lower than unlabeled counterparts. These values indicate that approximately 70% of SERT+ axon varicosities present in both pallidal segments are devoid of any synaptic specialization. Interestingly, there is no significant difference between MPTP and control monkeys regarding the synaptic incidence of SERT+ axon varicosities present in the GPe and GPi (21 ± 7% vs. 31 ± 10% in the GPe and 16 ± 3% vs. 23 ± 2% in the GPi). In both pallidal segments of control and MPTP monkeys, synapses formed by SERT+ axon varicosities occur exclusively on pallidal dendrites and are of the symmetrical or asymmetrical types.

5.7. Discussion

This study provides the first detailed quantitative and ultrastructural analysis of neuroadaptive changes displayed by the DA and 5-HT pallidal afferents in a non-human primate model of PD. Our stereological estimations show a significant DA hyperinnervation of the GPi in MPTP monkeys that contrasts strikingly with the massive degeneration of the nigrostriatal pathway. We also report a significant increase of the 5-HT pallidal innervation in MPTP monkeys compared to controls, particularly in the anterior pallidal sectors, where the associative and limbic functional territories reside. The DA hyperinnervation is overall more pronounced than that of 5-HT and occurs mainly within the posterior regions of the GPi, where the sensorimotor territory is located. We argue that these significant neuroadaptive changes of the DA and 5-HT pallidal

innervations play a significant role in delayed expression of motor symptoms and early expression of non-motor symptoms of PD, respectively.

5.7.1. The morphological characteristics of dopamine and serotonin pallidal afférents

The density of the DA pallidal innervation in cynomolgus monkeys was found to be similar in the GPe and GPi. Both pallidal segments harbour numerous thin and varicose axons together with a smaller number of thick and smooth axons, as is also the case in the globus pallidus of rats (Rodrigo *et al.*, 1998; Fuchs & Hauber, 2004; Debeir *et al.*, 2005), squirrel monkeys (Eid & Parent, 2015b), African green monkeys (Jan *et al.*, 2000a) and human (Prensa *et al.*, 2000). When examined under the electron microscope, the thick and smooth axons were found to be heavily myelinated, whereas the thin and varicose axons were devoid of myelin sheath. The course and morphological aspect of these two types of fibers indicate that the thick and smooth ones are fibers of passage en route to the striatum, whereas the thin and varicose axons are the ones that arborize locally within the pallidum. The synaptic incidence displayed by the thin and varicose fibers was found to be very low in comparison to that of unlabeled axon varicosities present in the same microenvironment.

The density of axons and axon varicosities of the 5-HT type is also similar in the two pallidal segments. Although the 5-HT pallidal input in primates is known to be overall more prominent than the DA input (Eid *et al.*, 2013; Eid & Parent, 2015b; 2016), a detailed comparison of the GPe and GPi of the cynomolgus monkey reveal that the two types of innervations display a similar proportion in each pallidal segment. Our electron microscopic findings indicate that, as it is the case for the DA input, the 5-HT influence upon pallidal neurons is largely mediated through an asynaptic mode of transmission.

5.7.2. The DA pallidal innervation is significantly increased in parkinsonian monkeys

The present study provides the first quantitative demonstration that the MPTP-induced lesion of the DA nigrostriatal pathway induces a significant DA hyperinnervation in the GPi, particularly in its posterior regions where the sensorimotor territory is located.

Previous works on this issue has led to conflicting results. Some studies indicate that the DA pallidal innervation in MPTP monkeys is preserved (Parent *et al.*, 1990; Schneider & Dacko, 1991; Parent & Lavoie, 1993; Mounayar *et al.*, 2007a; Dopeso-Reyes *et al.*, 2014; Ballanger *et al.*, 2016), whereas others suggest that this type of innervation is decreased (Pifl *et al.*, 1991; 1992; Jan *et al.*, 2000a). In human, positron emitting tomography (PET) study of the brain of PD patients indicate that the DA pallidal innervation is either preserved (Lewis *et al.*, 2012) or increased (Whone *et al.*, 2003a; Moore *et al.*, 2008; Pavese *et al.*, 2012). The latter findings are at variance with the biochemical decrease in DA concentrations detected in post-mortem samples of the pallidum of PD patients (Hornykiewicz, 1966; Bernheimer *et al.*, 1973b; Ploska *et al.*, 1982; Jan *et al.*, 2000a; Rajput *et al.*, 2008). However, the information yielded by such post-mortem investigations is limited to only one precise moment in the disease progression, often its end-stage, and does not provide clues as to how the various neuronal systems rearrange themselves during the earlier phases of the pathology. Interestingly, PET studies indicate that the increase of the DA pallidal innervation occurs in the early stage of disease (Whone *et al.*, 2003a; Moore *et al.*, 2008; Pavese *et al.*, 2011) and that the loss of DA pallidal innervation in latter periods may represent a pivotal step in disease progression. We therefore presume that the DA sprouting in the GPi detected in the present study occurs rapidly after MPTP intoxication. We see such a sprouting as a mechanism designed to compensate the MPTP-induced degeneration of the DA nigrostriatal pathway that could play a significant role in delaying the expression of motor symptoms. Under certain conditions, such

a compensatory mechanism might lead to a partial recovery of motor functions, until the surviving DA neurons are no longer able to maintain a functional level of DA in the pallidum.

The low synaptic incidence of DA as well as 5-HT axon varicosities has been viewed as the morphological evidence of diffuse (volumic) transmission. The 8-fold increase of DA innervation that occurred in the sensorimotor region of the GPi in MPTP monkeys, as reported here, indicates that, in this particular pathological condition, the diffuse mode of transmission might indeed contribute to the maintenance of a functional DA ambient level in the pallidum. Such neuroadaptive changes of the nigropallidal projection can be seen as part of a compensatory mechanism designed to delay the onset of PD motor symptoms. Such a view is indeed supported by a trend towards a negative correlation (R = -0.87) between the severity of motor symptoms and the level of sprouting of pallidal DA axons observed in our 4 MPTP monkeys. Also congruent with this hypothesis is the fact that injections of glial-cell-line-derived neurotrophic factor (GDNF) in the caudate nucleus and the SNc of MPTP monkeys lead to significant increase in pallidal DA levels, along with a certain degree of motor recovery (Gash *et al.*, 1996b). Furthermore, intra-pallidal (GPe) injections of DA antagonists were shown to worsen PD symptoms in monkeys that have recovered from MPTP-intoxication (Neumane *et al.*, 2012). Altogether, these data indicate that DA hyperinnervation of the pallidum may lead to a delayed onset of PD motor symptoms that would explain why motor deficits do not appear before a 70 - 90% decrease of striatal DA content occurs in PD patients (Bernheimer *et al.*, 1973b; Riederer & Wuketich, 1976) as well as in MPTP-intoxicated monkeys (German *et al.*, 1988; Bezard *et al.*, 2001b; Meissner *et al.*, 2003).

The robust increase of the GPi DA innervation is in striking contrast with the 80% loss of DA neurons that we noted in the SNc of MPTP monkeys. This finding indicates that the remaining DA midbrain neurons undergo an important morphological reorganization, including a significant sprouting of

their axon projecting to the pallidum. These surviving neurons were found to abound principally in the dorsal tier of SNc and to express CB, in agreement with previous post-mortem studies undertaken in other MPTP monkeys (Parent *et al.*, 1990; Lavoie & Parent, 1991a; Parent & Lavoie, 1993; Dopeso-Reyes *et al.*, 2014) or in PD human brains (Yamada *et al.*, 1990; German *et al.*, 1992a; Hurley *et al.*, 2013). Altogether, these findings have led to the hypothesis that CB could exert a neuroprotective effect upon the DA SNc neurons at the origin of the nigropallidal DA projection. Indeed, the fact that the severe reduction of the striatal DA innervation is paralleled by a marked hypertrophy of the DA pallidal innervation in MPTP monkeys favours the idea of a distinct origin and a lesser susceptibility to neurotoxic insults of the nigropallidal DA projection. In support of a specific origin of the nigropallidal projection are the results of a previous single-axon study of SNc and retrorubral field projection neurons in African green monkeys, which reveal that such axons innervate either the pallidum or the striatum, but not both structures (Jan *et al.*, 2000a). Beside the presence of CB, the difference in length and degree of axonal arborisation may also explain why the nigrostriatal pathway is more prone to degenerate than the nigropallidal projection. As we have argued elsewhere (Parent & Parent, 2006a), the maintenance of the morphological and functional integrity of the nigrostriatal DA pathway, which comprises long, highly collateralized and widely distributed axons, is extremely demanding in terms of metabolic energy and this renders such axons highly vulnerable to the neurodegenerative processes at play in PD (see also Bolam & Pissadaki, 2012a). Such an energetic burden would not be as great for the nigropallidal projection, which is composed of shorter, thinner and less profusely arborized axons than those of the nigrostriatal pathway. In line with such a view, the thick and myelinated DA pallidal axons, which are most likely nigrostriatal fibers en route to the striatum, were found to be specifically targeted in our MPTP monkeys, whereas the thin and varicose DA pallidal axons are those that proliferate in the same animals.

The functional impact of the increase of DA innervation of GPi in PD condition is currently unknown, but this neuroadaptive change could represent a compensatory mechanism designed to lower the GPi neuronal activity that is abnormally augmented in PD animal models (see above). Indeed, DA could exert a presynaptic inhibitory effect on GPi neurons through the activation of the D_1 excitatory receptor located on striatal GABAergic inhibitory afferents to the pallidum, facilitating GABA release in the GPi (Kliem *et al.*, 2007a; Kliem *et al.*, 2010a). The D_2 inhibitory DA receptor, which is also expressed presynaptically in the GPi, could allow DA to inhibit GPi neurons by reducing the release of glutamate by pallidal afferents originating from the subthalamic nucleus (Hadipour-Niktarash *et al.*, 2012a).

5.7.3. The 5-HT pallidal innervation is significantly increased in parkinsonian monkeys

The present stereological analysis reveals a 91% increase of the density of 5-HT axon varicosities in the GPe compared to a 74% augmentation in the GPi of MPTP monkeys. The fate of the 5-HT pallidal innervation in MPTP monkeys has been the subject of only a few studies, some reporting a preservation (Zeng *et al.*, 2010) and others a decrease of this type of innervation (Rylander *et al.*, 2010). Such a discrepancy might reflect variations in the animal survival time, which did not allow the documentation of compensatory mechanisms that are likely to be more prominent early in the evolution of PD symptoms (our monkeys were perfused 5 months after MPTP intoxication) than in later phases of the disease. Studies of the state of the striatal 5-HT innervation in animal models of PD have yielded much more consistent results, with a sprouting of the 5-HT striatal axons reported in 6-OHDA rats (Zhou *et al.*, 1991; Guerra *et al.*, 1997; Maeda *et al.*, 2003; Maeda *et al.*, 2005a), 6-OHDA mice (Bez *et al.*, 2016), MPTP mice (Rozas *et al.*, 1998), as well as MPTP monkeys (Gaspar *et al.*, 1993b; Zeng *et al.*, 2010; Gagnon *et al.*, 2016).

Stereological analyses of the dorsal raphe nucleus in our MPTP monkeys reveal that the density and morphological features of 5-HT cell bodies are not affected (Gagnon *et al.*, 2016), a finding that supports the idea of a rearrangement of the surviving 5-HT neurons and the sprouting of their varicose axons in the pallidum. Such a sprouting of 5-HT axons, as observed in the GPe, the GPi (current study) and the striatum (Gagnon *et al.*, 2016), suggests that these axons originate from 5-HT neurons endowed with a highly collateralized axon that undergo a significant morphological rearrangement in PD condition. Congruent with such a view, our previous single-axon tracing experiments in rats have shown that most neurons of the dorsal raphe nucleus that send their axon to the pallidum also project to the striatum through a widely distributed set of collaterals (Gagnon & Parent, 2014). Moreover, the fact that the 5-HT axon varicosities observed in the putamen and the pallidum share similar morphological features, including their size, also favours the hypothesis that they arise from the same neuronal population located in the dorsal raphe nucleus.

The 5-HT axons are known to be able to metabolize L-Dopa administered to PD patients into DA, thanks to their content in aromatic L-amino acid decarboxylase (Arai *et al.*, 1994). They can also store and release DA via the vesicular monoamine transporter 2 (Ng *et al.*, 1970b; Ng *et al.*, 1971; Hollister *et al.*, 1979a; Arai *et al.*, 1994; Arai *et al.*, 1995a; Tanaka *et al.*, 1999a; Maeda *et al.*, 2005a). However, being devoid of the D_2 autoreceptor and DAT, 5-HT axons release DA in a non-physiological manner. This phenomenon occurring in the DA-denervated striatum has been viewed as the main presynaptic determinant of L-Dopa-induced dyskinesia (reviewed in Carta *et al.*, 2008a; Carta & Tronci, 2014). The significant DA hyperinnervation of the GPi in MPTP monkeys, as reported here, led us to believe that the role played by 5-HT axons in the uncontrolled release of DA following L-Dopa administration at pallidal level is not as significant as what might occur in the striatum where a severe DA denervation is observed.

The fact that the highest increase of pallidal 5-HT innervation in MPTP monkeys occurs in the limbic and associative functional territories of this basal ganglia component reinforces the notion of the involvement of 5-HT in the expression of non-motor symptoms of PD, such as depression, apathy and anxiety that precede, sometimes by several years, the expression of motor symptoms (Schapira *et al.*, 2017). We hypothesize that the increase of the 5-HT pallidal tone most likely influences other pallidal inputs, including the GABAergic afferent projections arising from the striatum that are known to express the presynaptic inhibitory receptor 5-HT_{1B} (Bonaventure *et al.*, 1998b; Castro *et al.*, 1998; Riad *et al.*, 2000; Sari, 2004a; Mostany *et al.*, 2005b). This adaptation would therefore significantly contribute to the disinhibition of the GPi, whose neuronal activity is increased in PD (Miller & DeLong, 1987; Filion & Tremblay, 1991; Wichmann *et al.*, 1999). Congruent with such a view is the finding that 5-HT_{1B} receptor agonists increase the firing rate of both GPi and GPe neurons in monkeys (Kita *et al.*, 2007).

Despite a significant augmentation of the pallidal 5-HT innervation, levels of 5-HT receptors, including 5-HT_{1A} (Riahi *et al.*, 2012), 5-HT_{1B} (Riahi *et al.*, 2013) and 5-HT_{2A} (Riahi *et al.*, 2011), are not significantly altered in MPTP monkeys, suggesting that the effect on pallidal neural activity is mainly mediated through an increase in the local 5-HT concentration rather than a rise of the expression of 5-HT receptor by pallidal neurons or their afferent projections. The low synaptic incidence of the 5-HT innervation of the primate pallidum might be the ideal morphological substratum for such an elevation of 5-HT local pallidal concentration in MPTP monkeys. We estimate that approximately 70% of 5-HT axon varicosities observed in the GPe and the GPi are in fact devoid of any synaptic contact (see also Eid *et al.*, 2013). This finding can be viewed as the morphological evidence of the existence of a diffuse mode of 5-HT transmission (reviewed in Descarries *et al.*, 2010a), allowing the maintenance of a local concentration of 5-HT susceptible to play a significant role in the functional organization of the pallidum under normal and pathological conditions.

5.8. Conclusion

We report significant neuroadaptive changes of the DA and 5-HT pallidal afferent projections in PD monkeys. On the one hand, we hypothesize that the sprouting of DA axons in the sensorimotor territory of the GPi is an early compensatory mechanism designed to restore normal GPi activity and involved in the delayed appearance of motor symptoms. On the other hand, we suggest that the sprouting of 5-HT axons in the associative and limbic pallidal territories is involved in the appearance of non-motor symptoms of PD that precede, often by several years, the expression of motor symptoms.

5.9. Acknowledgments

This study was supported by a research grant from the Canadian Institutes of Health Research (CIHR 376952) to MP, who also benefited from of a Junior II career award from the Fonds de Recherche du Québec - Santé (FRQ-S). DG, LE and DC were recipients of PhD fellowships from FRQ-S. The authors are grateful to Marie-Josée Wallman, Caroline Côté and Annabelle Braun for technical assistance and to André Parent for critical reading of the manuscript. The authors have no conflict of interest to declare.

5.10. Figures

Table 5.1 Specific information on control and MPTP-intoxicated monkeys

Group	*Animal ID*	*Sex*	*Weight (kg)*	*Total MPTP (mg)*	*Motor disability score*	*Decrease of TH+ SNc neurons (%)*	*Decrease of TH striatal immunoreactivity* (%)*	*Decrease of DAT striatal immunoreactivity* (%)*
Control	S-2310	Female	3.9	NA	NA	NA	NA	NA
	S-2311	Female	3.0	NA	NA	NA	NA	NA
	S-2312	Female	3.5	NA	NA	NA	NA	NA
	S-2313	Female	3.8	NA	NA	NA	NA	NA
MPTP	S-2268	Female	3.2	6.00	8.23 / 16	82.5	87.9	87.2
	S-2269	Female	3.1	14.25	9.64 / 16	79.5	89.4	90.0
	S-2270	Female	2.8	11.50	6.78 / 16	70.5	84.0	83.4
	S-2273	Female	3.3	8.75	7.20 / 16	75.1	85.2	82.4

*Values are from the sensorimotor striatal territory (see Gagnon *et al.*, 2016 for more details)

Table 5.2 Specific information on antibodies used

Staining	Primary antibody	Product #	Dilution	Secondary antibody	Product #	Dilution
TH staining of SNc neurons	Mouse α TH	**22941;** Immunostar, Hudson, USA	1 / 1000	Biotinylated Horse α mouse	**BA-2000;** Vector Laboratories, Burlingame, CA, USA	1 / 1000
TH and CB double staining of SNc neurons	Rabbit α TH	**AB151;** Chemicon International Inc., Temecula, USA	1 / 1000	Donkey α rabbit 488	**711-545-152;** Jackson ImmunoResearch Inc., West Grove, USA	1 / 1000
	Mouse α CB	**C-9848;** Sigma-Aldrich, Oakville, Canada	1 / 1000	Donkey α mouse Cy5	**715-175-150;** Jackson ImmunoResearch Inc., West Grove, USA	1 / 1000
TH and DAT double staining of striatal axons	Mouse α TH	**22941;** Immunostar, Hudson, USA	1 / 1000	Goat α mouse 680	**926-68070;** LI-COR Biosciences, Lincoln, NE, USA	1 / 1000
	Rat α DAT	**MAB369;** EMD Millipore Corporation, Billerica, USA	1 / 500	Goat α rat 800	**926-32219;** LI-COR Biosciences, Lincoln, NE, USA	1 / 1000
TpH staining of dorsal raphe neurons	Sheep α TpH	**AB1541;** EMD Millipore Corporation, Billerica, USA	1 / 250	Biotinylated rabbit α sheep	**BA-6000;** Vector Laboratories, Burlingame, CA, USA	1 / 200
SERT staining of GPe and GPi axons	Goat α SERT	**SC-1458;** Santa Cruz Biotechnology, Dallas, TX, USA	1 / 1000	Biotinylated rabbit α goat	**BA-5000;** Vector Laboratories, Burlingame, CA, USA	1 / 1000
TH staining of GPe and GPi axons	Mouse α TH	**22941;** Immunostar, Hudson, USA	1 / 1000	Biotinylated horse α mouse	**BA-2000;** Vector Laboratories, Burlingame, CA, USA	1 / 200

Table 3 Morphometric characteristics of SERT+ axon varicosities in the GPe and GPi of control and MPTP monkeys

	GPe				GPi			
	Control (n=4)		*MPTP (n=4)*		*Control (n=4)*		*MPTP (n=4)*	
	SERT	Unlabeled	*SERT*	Unlabeled	*SERT*	Unlabeled	*SERT*	Unlabeled
Number examined	213	185	212	195	216	198	238	214
Dimensions								
Short axis (µm)	0.55 ± 0.05	0.49 ± 0.01	0.48 ± 0.03	0.50 ± 0.03	0.49 ± 0.03	0.50 ± 0.03	0.46 ± 0.03	0.48 ± 0.01
Long axis (µm)	0.94 ± 0.13	0.75 ± 0.04	0.77 ± 0.06	0.75 ± 0.04	0.79 ± 0.05	0.75 ± 0.02	0.77 ± 0.03	0.76 ± 0.02
Diameter (µm)	0.74 ± 0.09	0.62 ± 0.02	0.62 ± 0.04	0.63 ± 0.03	0.64 ± 0.04	0.62 ± 0.02	0.61 ± 0.03	0.62 ± 0.01
Aspect ratio	1.75 ± 0.11	1.58 ± 0.05	1.64 ± 0.03	1.54 ± 0.05	1.64 ± 0.03	1.58 ± 0.05	1.72 ± 0.04	1.62 ± 0.02
Area (μm^2)	0.51 ± 0.09	0.35 ± 0.03	0.38 ± 0.06	0.36 ± 0.03	0.39 ± 0.05	0.36 ± 0.02	0.35 ± 0.04	0.35 ± 0.03
% with mitochondria	72 ± 3*	59 ± 4	62 ± 5	52 ± 2	79 ± 3*	55 ± 3	68 ± 5	60 ± 4
Synaptic incidence (%)								
Single section	7 ± 2*	24 ± 5	7 ± 2*	20 ± 1	7 ± 1*	23 ± 1	5 ± 1*	17 ± 3
Whole volume	31 ± 10	80 ± 22	21 ± 7*	69 ± 9	23 ± 2*	77 ± 6	16 ± 3*	64 ± 9
Length of synaptic junction (µm)	0.26 ± 0.05	0.25 ± 0.02	0.29 ± 0.06	0.22 ± 0.02	0.25 ± 0.03	0.22 ± 0.01	0.27 ± 0.03	0.20 ± 0.01
Junctions								
Symmetrical	48 ± 5*	83 ± 3	35 ± 22	87 ± 3	63 ± 14	96 ± 4	60 ± 16	92 ± 5
Asymmetrical	52 ± 5	17 ± 3	65 ± 22	13 ± 3	38 ± 14	4 ± 4	40 ± 16	8 ± 5

Data are presented as means ± SEM. The unlabeled profiles were selected at random from the same micrographs displaying SERT+ profiles. * : $P = 0.0248$ for SERT+ vs. unlabeled.

Table 4 Morphometric characteristics of TH+ axon varicosities in the GPi of control and MPTP monkeys

	GPi			
	Control (n=4)		*MPTP (n=4)*	
	TH	Unlabeled	*TH*	Unlabeled
Number examined	269	267	285	286
Dimensions				
Short axis (µm)	0.60 ± 0.04*	0.43 ± 0.01	0.47 ± 0.03	0.45 ± 0.02
Long axis (µm)	1.23 ± 0.11*+	0.73 ± 0.03	0.89 ± 0.07	0.75 ± 0.03
Diameter (µm)	0.92 ± 0.08*+	0.58 ± 0.02	0.68 ± 0.05	0.60 ± 0.03
Aspect ratio	0.56 ± 0.02+	0.62 ± 0.01	0.58 ± 0.01*	0.62 ± 0.01
Area (μm^2)	0.72 ± 0.11*+	0.27 ± 0.02	0.37 ± 0.05	0.29 ± 0.02
% with mitochondria	65 ± 4*	40 ± 5	77 ± 18	45 ± 5
Synaptic incidence (%)				
Single section	3 ± 1*	10 ± 1	2 ± 1	4 ± 2
Whole volume	13 ± 7	28 ± 3	7 ± 3	8 ± 4
Length of synaptic junction (µm)	0.19 ± 0.06	0.26 ± 0.02	0.31 ± 0.11	0.34 ± 0.14
Junctions				
Symmetrical	0 ± 0+	35 ± 22	67 ± 33	57 ± 30
Asymmetrical	100 ± 0+	65 ± 22	33 ± 33	43 ± 30

Data are presented as means ± SEM. The unlabeled profiles were selected at random from the same micrographs displaying TH+ profiles. * : $P = 0.0248$ for TH+ vs. unlabeled, + : $P = 0.0248$ for SERT + vs. TH+.

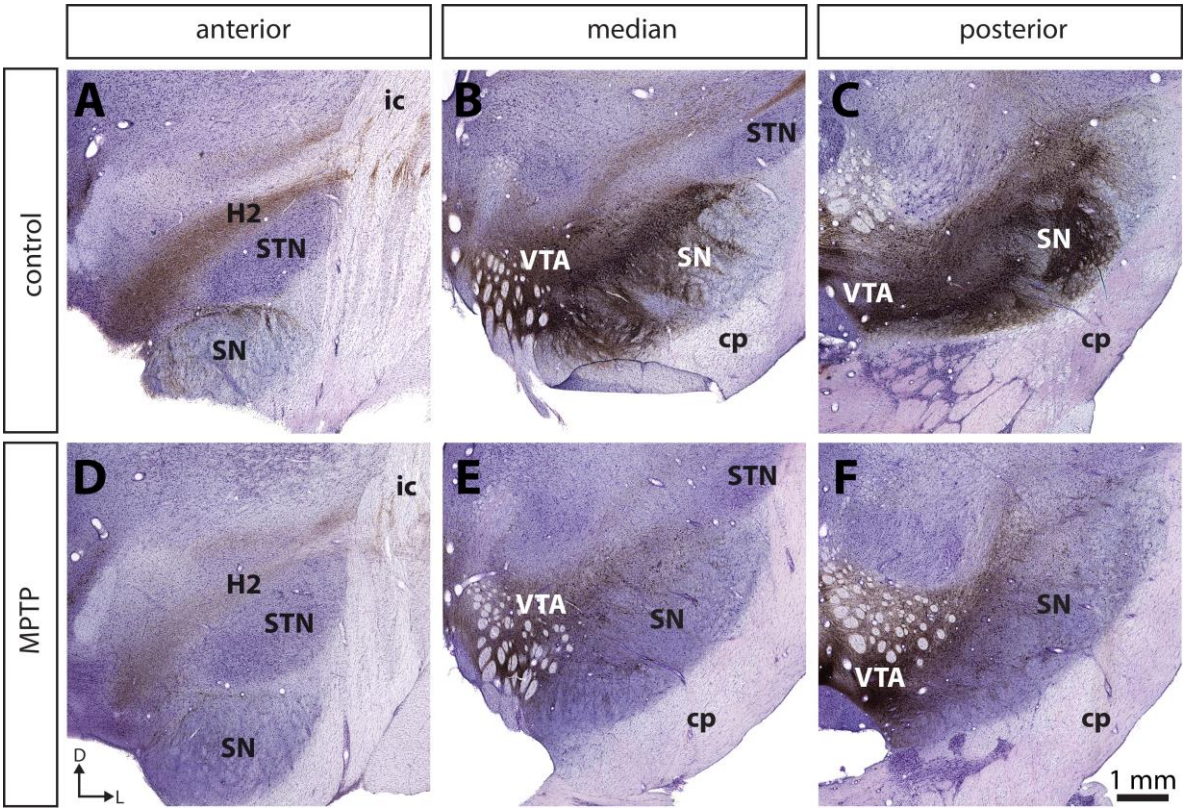

Figure 5.1. The number of tyrosine hydroxylase (TH) immunoreactive (+) neurons in the substantia nigra pars compacta (SNc) is significantly decreased in MPTP-intoxicated monkeys (D-F) compared to controls (A-C). Transverse sections through the whole anteroposterior axis of the SNc and stained for tyrosine hydroxylase (TH, brown) and cresyl violet (purple) in control (A-C) and MPTP monkeys (D-F). Our stereological analysis reveals a 77 % decrease in the number of TH+ neurons in the SNc of MPTP-intoxicated monkeys, compared to controls.

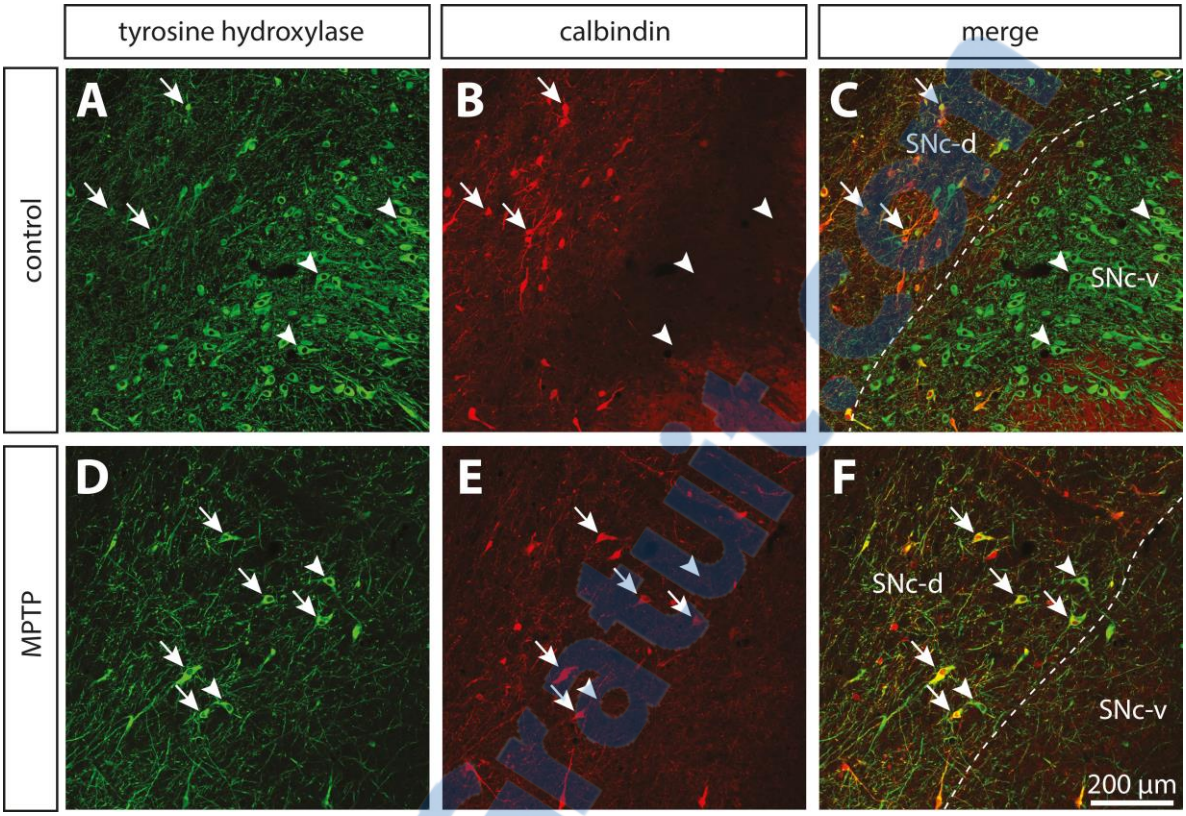

Figure 5.2. The DA neurons that are spared in the SNc of MPTP-intoxicated monkeys are mainly located in the dorsal tier (SNc-d) and display calbindin (CB) immunoreactivity. Confocal images of transverse section through the SNc and immunostained for tyrosine hydroxylase (TH, green, A, D) and CB (red, B, E) in control (A-C) and MPTP monkeys (D-F). Arrowheads point to neurons that express only TH, whereas arrows indicate SNc neurons that are immunoreactive for TH and CB.

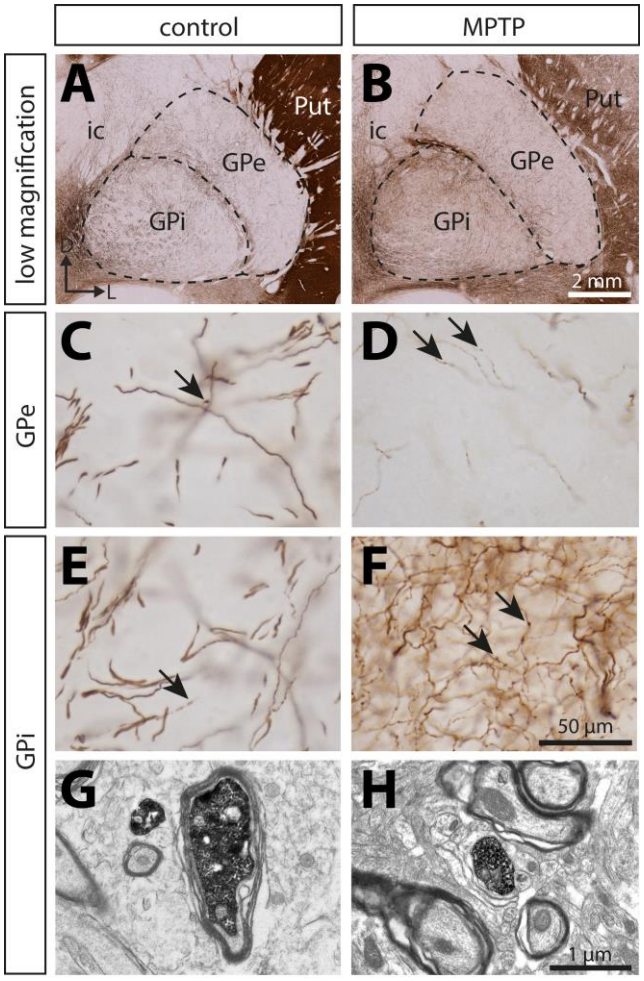

Figure 5.3. In contrast to the significant dopamine denervation of the putamen (Put), the immunoreactivity for tyrosine hydroxylase (TH) is significantly increased in the GPi of MPTP monkeys. Transverse sections through the GPe and GPi and immunostained for TH in controls (A, C, E, G) and MPTP monkeys (B, D, F, H). Higher magnifications of TH+ axons observed in the GPe (C, D) and the GPi (E, F) are also provided. Arrows indicate examples of TH+ axon varicosities. Electron micrographs of TH+ axon profiles are also shown (G, H). In contrast to MPTP-intoxicated monkeys, large and myelinated TH+ axons are often observed in control animals (G). They likely correspond to the thick and non-varicose axons observed at the light microscope level, en route to the striatum.

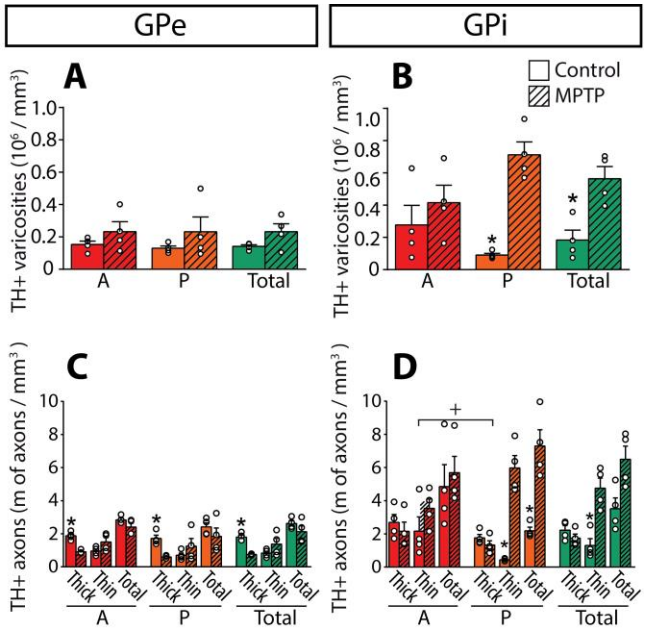

Figure 5.4. In MPTP monkeys, the axonal length of the thin and varicose TH+ axons increases significantly in the GPi whereas the length of the thick and non-varicose axons decreases in the GPe. Histograms showing the density of axon varicosities (A, B) as well as the axonal length (C, D) of the thin and the thick TH+ axons observed in the GPe (A, C) and GPi (B, D). Dots represent individual values obtained for each monkey. * $P < 0.05$ for MPTP vs. control monkeys, + $P < 0.05$ for anterior (A) vs. posterior (P) pallidal sectors.

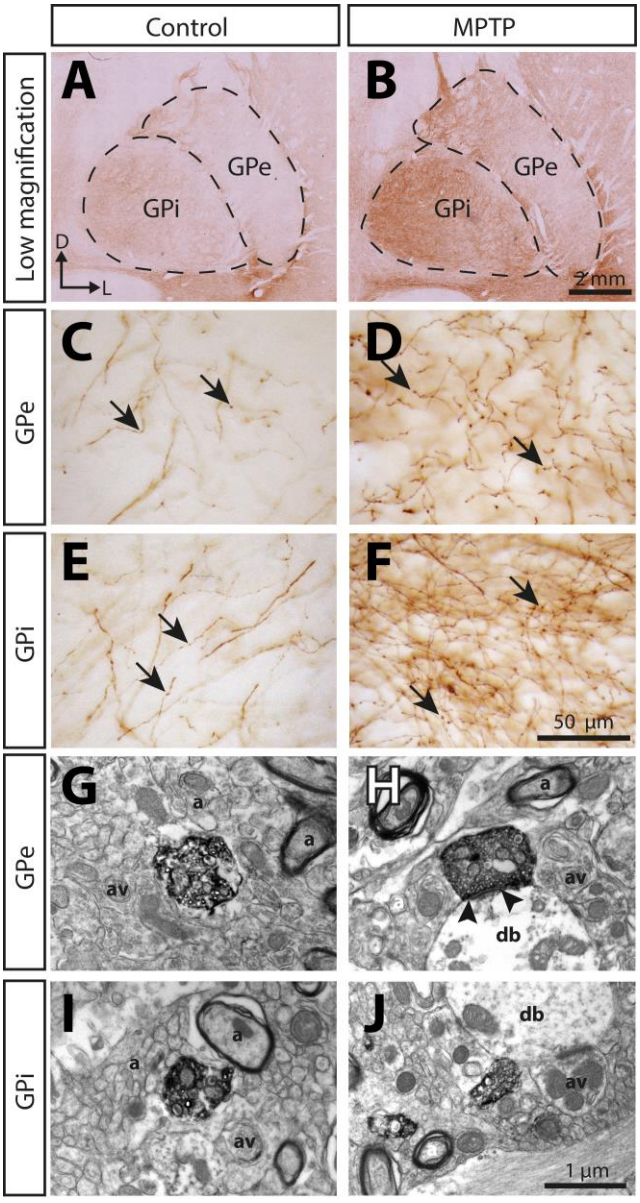

Figure 5.5. The immunoreactivity for the serotonin membrane transporter (SERT) is significantly increased in the pallidum of MPTP-intoxicated monkeys. Transverse sections through the GPe and the GPi and immunostained for SERT in control (A, C, E, G, I) and MPTP monkeys (B, D, F, H, J). Higher magnifications of SERT+ axons observed in the GPe (C, D) and the GPi (E, F) are also provided. Arrows indicate examples of SERT+ axon varicosities. Electron micrographs of SERT+ axon varicosity profiles are also shown (G-J). SERT+ axon varicosities are often observed apposed to small myelinated or unmyelinated axons (a) and axon varicosities (av). The SERT+ axon varicosity

profile depicted in H establishes an asymmetric synaptic contact (between arrows) with a pallidal dendritic branch (db) whereas the three others (G, I, J) are devoid of synaptic membrane specialization.

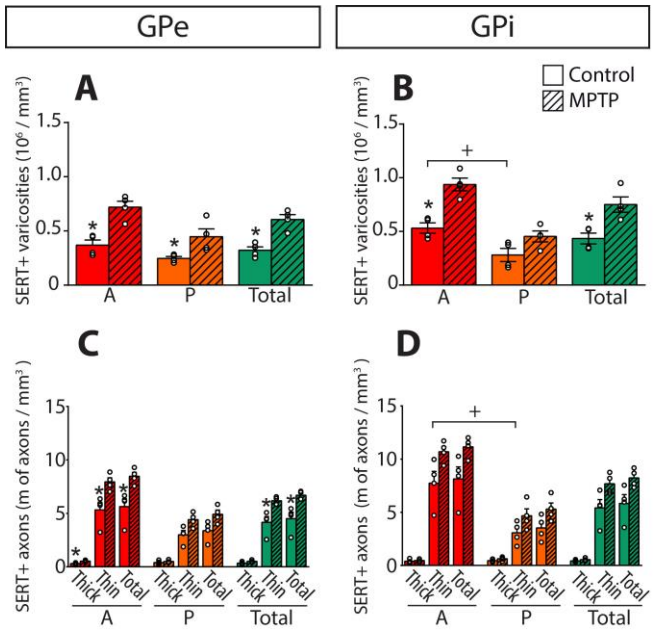

Figure 5.6. In MPTP monkeys, the densities of SERT+ axon varicosities and SERT+ axons are significantly increased in the GPe and GPi, particularly in their anterior sectors. Histograms showing the density of SERT+ axon varicosities (A, B) as well as the axonal length (C, D) of the thick and thin SERT+ axons observed in the GPe (A, C) and the GPi (B, D). Dots represent individual values obtained for each monkey. * $P < 0.05$ for MPTP vs. control monkeys, + $P < 0.05$ for anterior vs. posterior pallidal sectors.

CHAPITRE 6 :

STRIATAL NEURONS EXPRESSING D_1 AND D_2 RECEPTORS ARE MORPHOGICALLY DISTINCT AND DIFFERENTLY AFFECTED BY DOPAMINE DENERVATION IN MICE

CHAPITRE 6 – *STRIATAL NEURONS EXPRESSING D_1 AND D_2 RECEPTORS ARE MORPHOGICALLY DISTINCT AND DIFFERENTLY AFFECTED BY DOPAMINE DENERVATION IN MICE*

Dave Gagnon, Sarah Petryszyn, Maria Gabriela Sanchez, Cyril Bories, Jean-Martin Beaulieu, Yves De Koninck, André Parent et Martin Parent

Centre de recherche CERVO
2601, Ch. de la Canardière, Québec, Québec
Canada G1J 2G3

Scientific Reports (2017) 7

6.1. Résumé

La dégénérescence des neurones nigrostriés dopaminergiques dans la maladie de Parkinson conduit à une réduction du nombre d'épines dendritiques sur les neurones de projections du striatum (NPS) qui expriment le récepteur D_1 ou D_2. Les conséquences sur les NPS exprimant les deux types de récepteurs (NPS D_1/D_2) sont actuellement inconnues. Nous avons caractérisé les changements induits par une dénervation dopaminergique sur la densité, la distribution régionale et les caractéristiques morphologiques et neurochimiques des NPS D_1/D_2, en comparant des souris doubles transgéniques BAC (Drd_1a-tdTomato/Drd_2-EGFP) lésées à la 6-OHDA à des souris SHAM. En condition normale, les NPS D_1/D_2 sont uniformément distribués à travers le striatum (1.9% des NPS). En revanche, ils sont distribués de manière hétérogène et sont plus nombreux dans le striatum ventral (14.6% dans la coquille et 7.3% dans le cœur). Comparativement au NPS D_1 et D_2, les NPS D_1/D_2 sont dotés d'un plus petit corps cellulaire et d'une arborisation dendritique moins importante présentant moins d'épines dendritiques. La densité d'épines dendritiques des NPS D_1/D_2, mais aussi des NPS D_1 et NPS D_2, est significativement réduite chez les souris lésées à la 6-OHDA, comparativement aux contrôles. Contrairement aux NPS D_1 et NPS D_2, l'arborisation dendritique des NPS D_1/D_2 semble inaltérée chez la souris lésée à la 6-OHDA. Nos résultats indiquent que les NPS D_1/D_2 dans le striatum de souris forment une population neuronale distincte qui est affectée différemment par une déafférentation dopaminergique qui caractérise la maladie de Parkinson.

6.2. Abstract

The loss of nigrostriatal dopamine neurons in Parkinson's disease induces a reduction in the number of dendritic spines on medium spiny neurons (MSNs) of the striatum expressing D_1 or D_2 dopamine receptor. Consequences on MSNs expressing both receptors (D_1/D_2 MSNs) are currently unknown. We looked for changes induced by dopamine denervation in the density, regional distribution and morphological features of D_1/D_2 MSNs, by comparing 6-OHDA-lesioned double BAC transgenic mice (Drd_1a-tdTomato/Drd_2-EGFP) to sham-lesioned animals. D_1/D_2 MSNs are uniformly distributed throughout the dorsal striatum (1.9% of MSNs). In contrast, they are heterogeneously distributed and more numerous in the ventral striatum (14.6% in the shell and 7.3% in the core). Compared to D_1 and D_2 MSNs, D_1/D_2 MSNs are endowed with a smaller cell body and a less profusely arborized dendritic tree with less dendritic spines. The dendritic spine density of D_1/D_2 MSNs, but also of D_1 and D_2 MSNs, is significantly reduced in 6-OHDA-lesioned mice. In contrast to D_1 and D_2 MSNs, the extent of dendritic arborization of D_1/D2 MSNs appears unaltered in 6-OHDA-lesioned mice. Our data indicate that D_1/D_2 MSNs in the mouse striatum form a distinct neuronal population that is affected differently by dopamine deafferentation that characterizes Parkinson's disease.

6.3. Introduction

The striatum is the main input structure as well as the largest integrative component of the basal ganglia. It receives a multitude of neurochemical inputs that are largely processed by striatal projection neurons. At the somatodendritic level, these cells form a rather morphologically homogeneous population, each element being endowed with a medium-sized cell body and typical spiny dendrites. These so-called medium spiny neurons (MSNs) all use γ-aminobutyric acid (GABA) as a neurotransmitter and represent approximately 90-95% of the striatal neuronal population in rodents (Graveland & DiFiglia, 1985). Despite their morphological similarities, MSNs can be divided into two subpopulations based on their neurochemical content and axonal projection sites. Roughly half of the MSNs express dopamine (DA) receptor of the D_1 type and contain the neuropeptides substance P (SP) and dynorphin (DYN). They innervate mainly the substantia nigra *pars reticulata* and the entopeduncular nucleus (rodent homologue of primate internal pallidum) and form the so-called "direct pathway." The other half of the MSNs expresses DA receptor of the D_2 type and contains the neuropeptide enkephalin (ENK). Their axon arborizes principally in the pallidum (rodent homologue of primate external pallidum) and forms the first segment of the so-called "indirect pathway" (Gerfen *et al.*, 1990; Albin *et al.*, 1995; Le Moine & Bloch, 1995; Wichmann & DeLong, 1998). However, it is worth noting that single-axon tracing experiments in rodents (Wu *et al.*, 2000) and primates (Levesque & Parent, 2005) indicate that most striatofugal axons arborize into the three main striatal targets. To this regards, it has recently been shown that both D_1 and D_2 MSNs located in the nucleus accumbens (Acb) can either inhibit or disinhibit thalamic activity depending on their projection pattern and not on their genetic characteristics (Kupchik *et al.*, 2015).

The D_1 and D_2 receptors are reportedly co-expressed in a certain proportion of MSNs, but the size of such D_1/D_2 subpopulation is still a matter of controversy. Earlier studies undertaken with *in situ* hybridization methods, immunohistochemistry or reverse transcription polymerase chain reaction have

reported high percentages of striatal neurons expressing both DA receptors (Meador-Woodruff *et al.*, 1991; Weiner *et al.*, 1991; Lester *et al.*, 1993; Le Moine & Bloch, 1995; Yung *et al.*, 1995; Shetreat *et al.*, 1996; Surmeier *et al.*, 1996; Surmeier *et al.*, 1998; Aizman *et al.*, 2000; Aubert *et al.*, 2000), but a much smaller number of D_1/D_2 MSNs was detected in transgenic mice expressing fluorescent reporters for D_1 or D_2(Bertran-Gonzalez *et al.*, 2008; Shuen *et al.*, 2008; Gangarossa *et al.*, 2013b; Thibault *et al.*, 2013).

When co-expressed by MSNs, the D_1 and the D_2 receptors are reportedly able to form heteromers, the activation of which can lead to a distinct intracellular signalling pathway (Lee *et al.*, 2004; Perreault *et al.*, 2010; Perreault *et al.*, 2012; Perreault *et al.*, 2016; Rico *et al.*, 2016). The independent activation of the D_1 or the D_2 DA receptor is known to differentially regulate cyclic-AMP activity, respectively leading to the activation (D_1 coupled to G_s) or inhibition (D_2 coupled to G_i) of MSNs (Beaulieu & Gainetdinov, 2011; Beaulieu *et al.*, 2015). In contrast, the activation of D_1/D_2 heteromers would result in a distinct phospholipase C-mediated calcium signalling through activation of G_q protein (Lee *et al.*, 2004; Perreault *et al.*, 2010; Perreault *et al.*, 2012; Perreault *et al.*, 2016). However, while co-expression of D_1 and D_2 receptors is well accepted, the existence of D_1/D_2 heteromers *in vivo* remains controversial (Biezonski *et al.*, 2015; Frederick *et al.*, 2015).

The fate of MSNs expressing D_1 or D_2 DA receptor in the context of DA striatal deafferentation that characterizes Parkinson's disease (PD) has already been studied. In a mouse model of PD, lesion of the striatal DA input was shown to induce spine pruning, principally on the D_2 MSNs (Day *et al.*, 2006; Shen *et al.*, 2007) and less markedly on the D_1 MSNs (Day *et al.*, 2006; Shen *et al.*, 2007; Fieblinger *et al.*, 2014; Suarez *et al.*, 2014; Toy *et al.*, 2014). Such spine pruning appears to be a highly plastic phenomenon since the reduction of spine density observed on the D_2 MSNs, but not that on D_1 MSNs, could be restored by long-term administration of L-DOPA (Fieblinger *et al.*, 2014; Suarez *et al.*, 2014). Reduction in the number of dendritic spine of striatal MSNs has also

been reported in non-human primate model of PD (Villalba *et al.*, 2009b) and in PD patients (McNeill *et al.*, 1988; Stephens *et al.*, 2005; Zaja-Milatovic *et al.*, 2005). Surprisingly, the fate of MSNs expressing both the D_1 and the D_2 DA receptors (the D_1/D_2 MSNs) has never been investigated in PD condition. Therefore, we have designed a study to provide the first detailed description of changes induced by DA denervation in the density, regional distribution and fine morphological characteristics of dendritic processes of D_1/D_2 MSNs that populate the dorsal striatum and the Acb, the main component of the ventral striatum, of mice. Using stereological approaches and single-neuronal injections performed on striatal sections from sham and 6-hydroxydopamine (6-OHDA)-lesioned double BAC transgenic mice (*Drd1a*-tdTomato/*Drd2*-EGFP), we show that the D_1/D_2 MSNs are affected differently than the D_1 and D_2 MSNs by striatal DA deafferentation that characterizes PD.

6.4. Results

6.4.1. Unilateral 6-OHDA injections cause severe TH+ cell loss in the SNc and VTA, significant DA depletion in the striatum and in the Acb and spontaneous ipsilateral rotations

Immunolabeling of the striatum and the substantia nigra *pars compacta* (SNc) for the DA transporter (DAT) and tyrosine hydroxylase (TH) indicate a severe DA lesion caused by 6-OHDA unilateral injections performed in the medial forebrain bundle (Fig. 1). Counts of TH+ cell bodies in the midbrain show a more severe DA cell loss in the SNc compared to the VTA (80.7 ± 7.5% decrease in SNc vs. 48.9 ± 9.2% decrease in VTA, compared to control side, Fig. 1A, B). LI-COR® slide scanner measurements indicate an average of 81.3% decrease of TH and 87.5% of DAT immunoreactivity in the dorsal striatum when compared to control side as well as a 80.1% reduction of TH and a 79.3% decrease of DAT immunoreactivity in the Acb, when compared to control side (Fig. 1C, D). Behavioral assessments show a significant preference for spontaneous rotations ipsilateral to the lesioned side in mice that were unilaterally injected with 6-OHDA (57.1 ± 6.4 spontaneous ipsilateral rotations / 10 min vs. 1.1 ± 0. 8 contralateral rotations, $P< 0.0001$, Fig. 1E).

6.4.2. The D_1/D_2 MSNs contain dynorphin but not enkephalin

Examination of ENK and DYN-immunostained sections from colchicine-treated mice reveals that, as expected, D_1 MSNs are immunoreactive for DYN but not for ENK. In contrast, D_2 MSNs contain ENK but are devoid of DYN. In regard to D_1/D_2 MSNs, they are immunopositive for DYN but immunonegative for ENK (Fig. 2).

6.4.3. D_1/D_2 MSNs are homogeneously distributed throughout the dorsal striatum but heterogeneously scattered in the nucleus accumbens

The regional distribution of D_1, D_2 and D_1/D_2 MSNs in the dorsal striatum of sham mice was estimated stereologically. The overall densities of D_1 and D_2 MSNs are 108 ± 5 and 95 ± 4 x 10^3 cells / mm^3, representing respectively 52.2 ± 1.1% and 45.9 ± 1.1% of the total MSNs population of the striatum. In contrast, the D_1/D_2 MSNs have a much lower density with only 3.8 ± 0.3 x 10^3 cells / mm^3 ($P< 0.0001$), representing 1.9 ± 0.2% of the striatal MSNs. Although not statistically significant ($P = 0.2341$), the density of the D_1/D_2 MSNs in the ventromedial sector of the striatum was lower in the post-commissural striatum (1.8 ± 0.4 x 10^3 cells / mm^3) than in the pre-commissural striatum (4.3 ± 0.3 x 10^3 cells / mm^3). Statistical evaluations (ANOVA) of neuronal densities in different striatal regions reveal no statistical differences (Fig. 3), supporting the homogeneous regional distribution of the D_1, D_2 and D_1/D_2 MSNs throughout the dorsal striatum. Occasionally, some D_1/D_2 MSNs can be seen to form small clusters of 2-3 cells at different striatal levels. Assessment of the distribution of D_1/D_2 MSNs in striosomes and matrix striatal compartments, as delineated on immunostained sections for μ-opioid receptor, reveals no significant difference, neither at the pre-commissural level ($P = 0.4857$), nor at the post-commissural level ($P = 0.8286$, Fig. S1). Our quantitative analyses reveal that the D_1/D_2 MSNs are more heterogeneously distributed in the Acb than in the dorsal striatum. As shown in figure 4D, a dense region located in the medial part of the shell of the Acb was almost entirely composed of the D_1/D_2 type of MSNs. A closer examination of the lateral striatal stripe indicates no significant difference regarding the density of the D_1/D_2 MSNs compared to other regions of the lateral area of the shell of the Acb. The density of the D_1/D_2 MSNs is overall significantly higher in the Acb compared to the striatum. This difference becomes statistically significant in the shell compartment of the Acb with 45.0 ± 10.9 x 10^3 cells / mm^3 compared

to 3.8 ± 0.3 x 10^3 cells / mm^3 in the dorsal striatum (P = 0.0098, Fig. 3C). Our stereological estimations indicate that the D_1/D_2 MSNs represent 14.6 ± 3.0% of the MSN population in the shell and 7.3 ± 2.2% in the core compartment of the Acb, percentages that are significantly higher than what was noted in the dorsal striatum (1.9 ± 0.2%, P = 0.0098). Interestingly, the density of the D_1 MSNs is also higher in the shell of the Acb when compared to the dorsal striatum (180.0 ± 13.6 vs. 108.2 ± 5.4 x 10^3 cells / mm^3, P = 0.0244, Fig. 3A) whereas no difference is noted regarding the density of the D_2 MSNs between the dorsal striatum and the Acb. A higher density of the D_1 and the D_1/D_2 MSNs in the Acb is congruent with an overall higher density of all MSNs in the shell (298.6 ± 15.0) and the core (267.9 ± 24.5 cells / mm^3) compartments of the Acb compared to the dorsal striatum (123.5 ± 5.4 x 10^3 cells / mm^3).

6.4.4. The striatal D_1/D_2 MSNs display a smaller cell body and a shorter dendritic arborization than the two other types of MSNs

In sham animals, the cell body of dorsal striatum D_1/D_2 MSNs injected with Lucifer yellow are smaller than those of the D_1 and the D_2 MSNs: the mean diameter of the D_1/D_2 MSN perikarya is 12.5 $\pm$ 0.4 μm compared to 14.3 $\pm$ 0.4 μm for the D_1 (P = 0.0094) and to 15.0 $\pm$ 0.5 μm for the D_2 MSNs (P = 0.0009). The reconstruction of somatodendritic domains of Lucifer yellow-filled MSNs reveals that the total dendritic length of D_1/D_2 MSNs is also smaller than that of the D_1 and the D_2 MSNs. The mean total dendritic length for the D_1/D_2 MSNs is 0.75 ± 0.06 mm compared to 1.48 ± 0.13 mm for D_1 (P< 0.0001) and 1.08 ± 0.08 mm for D_2 MSNs (P = 0.0296, Fig. 5A). We also noted that the dendritic arborization of the D_1 MSNs is significantly longer than that of the D_2 MSNs (P = 0.0089). The dendritic arborization of the D_1/D_2 MSNs is significantly less profuse than that of the D_1 and D_2 MSNs, as indicated by a smaller number of dendritic branching points (9.5 ± 0.8 branching points) compared to the D_1 (16.6 ± 1.5 branching points, P = 0.0015) and the D_2 MSNs (15.0 ± 1.4 branching points, P = 0.0087, Fig. 5B).

6.4.5. D_1/D_2 MSN dendrites harbor fewer spines than the two other types of MSNs

By dividing the number of spines by the total dendritic length for each reconstructed neuron in sham animals, we were able to evaluate the overall spine density for each of the three types of striatal MSNs. Our data reveal that the D_1/D_2 MSNs have a 37% lower spine density (4.0 ± 0.2 spines / 10 μm) than the D_1 (6.4 $\pm$ 0.3 spines / 10 μm, $P< 0.0001$) and the D_2 (6.6 $\pm$ 0.2 spines / 10 μm, $P< 0.0001$) MSNs (Fig. 5C). A Sholl analysis performed on all reconstructed neurons indicates that this lower spine density is maintained throughout the entire dendritic extent of the D_1/D_2 MSNs, the difference being statistically significant on a distance ranging between 45 and 105 μm from their parent cell bodies (Fig. 5D).

6.4.6. The density of D_1/D_2 MSNs is unaltered in 6-OHDA-lesioned mice

In 6-OHDA mice, the density of the D_1/D_2 MSNs in the dorsal striatum was 3.8 ± 0.3 x 10^3 cells / mm^3, accounting for 2.1 ± 0.2% of total MSN population. In comparison, the density of the D_1 and the D_2 MSNs was 108.2 ± 5.4 x 10^3 cells / mm^3 and 94.9 ± 4.1 x 10^3 cells / mm^3, representing 53.5 ± 1.0% and 44.4 ± 1.1% of the total MSN population, respectively (Fig. 3). There is no statistically significant difference between sham and 6-OHDA-lesioned animals in regard to these figures. Likewise, assessment of MSN densities in the Acb does not reveal any significant differences between the sham and 6-OHDA-lesioned animals (Fig. 3). The density of the D_1/D_2 MSNs obtained in the shell compartment of the Acb of 6-OHDA-lesioned mice was 29.7 ± 6.0 x 10^3 cells / mm^3 whereas the neuronal density of D_1 and D_2 MSNs in the same experimental group were 193.1± 8.7 and 104.7 ± 5.7 x 10^3 cells / mm^3, respectively. Values obtained in the core compartment of the Acb of 6-OHDA-

lesioned mice reach 11.9 ± 1.4, 168.4 ± 13.8 and 102.9 ± 13.6 x 10^3 cells / mm^3 for the D_1/D_2, D_1 and D_2MSNs, respectively (Fig. 3).

6.4.7. The extent of D_1/D_2 MSN dendritic arborization is unaffected by 6-OHDA lesion, in contrast to that of D_1 and D_2 MSNs

Statistical comparison between sham and 6-OHDA-lesioned mice in regard to the extent of somatodendritic domain belonging to the D_1, D_2 and D_1/D_2 MSNs in the dorsal striatum indicates that the total dendritic length of the D_1 MSNs was reduced in the DA-depleted striatum by 60% (0.60 ± 0.04 vs. 1.48 ± 0.13 mm, *P*< 0.0001, Fig. 6A) and by 28% for the D_2 MSNs (0.78 ± 0.09 vs. 1.08 ± 0.08 mm, *P* = 0.0191, Fig. 6B). Surprisingly, no significant differences between sham and 6-OHDA-lesioned mice were observed regarding the total dendritic length of the D_1/D_2 MSNs (0.61 ± 0.05 vs. 0.75 ± 0.07 mm, *P* = 0.6356, Fig. 6C). Accordingly, in 6-OHDA-lesioned mice, a lower number of dendritic branching points were observed for the D_1 MSNs (8.7 ± 0.7 vs. 16.6 ± 1.5 branching points, *P*< 0.0001) and the D_2 MSNs (10.7 ± 0.9 vs. 15.0 ± 1.4 branching points, *P* = 0.0120) but not for the D_1/D_2 MSNs with 9.5 ± 0.8 branching points in both experimental groups (*P*> 0.9999).

6.4.8. The spine density on D_1/D_2 MSN dendrites is reduced in 6-OHDA-lesioned mice

Lesion of the striatal DA afferent projections leads to a significant decrease of spine density on dendrites belonging to the three types of MSNs. The overall spine density was 4.0 ± 0.4 spines / 10 μm in 6-OHDA compared to 6.4 ± 0.3 in sham (*P*< 0.0001) for the D_1 MSNs; 5.1 $\pm$ 0.3 spines / 10 μm compared to 6.6 $\pm$ 0.2 (*P* = 0.0018) for the D_2 MSNs and 3.0 $\pm$ 0.1 spines / 10 μm compared to 4.0 $\pm$ 0.2 (*P* = 0.0427) for the D_1/D_2 MSNs. These reductions accounted for a 37.5% loss on the D_1, 22.7% on the D_2 and 25.0% on the

D_1/D_2 MSNs. The Sholl analysis indicates that such lower spine density is maintained throughout the entire dendritic arborization of the three types of MSNs (Fig. 7).

6.5. Discussion

The present study provides the first detailed description of the morphological characteristics, density and regional distribution of D_1/D_2 MSNs of the dorsal striatum and Acb in normal mice, as well as the first characterization of changes induced in this striatal subpopulation by striatal DA denervation. Our data gathered in normal animals reveal that the D_1/D_2 MSNs are morphologically distinct from the D_1 and D_2 MSNs: they have a smaller cell body, a less profusely arborized dendritic tree with branches that bear fewer spines than those of the D_1 and D_2 MSNs. They are uniformly scattered throughout the striatum, where they represent approximately 2%of the total number of MSNs, but heterogeneously distributed and more abundant in the Acb, where their proportion ranged from 7 to 15% of all MSNs. In 6-OHDA-lesioned mice, the density and regional distribution of all 3 types of MSNs is essentially unaltered. In contrast to the D_1 and the D_2 MSNs, the D_1/D_2neurons do not show any significant reduction in the length of their dendritic arborization after intoxication with 6-OHDA. However, a reduction in dendritic spine density was noted in all three types of MSNs following DA depletion, but this pruning phenomenon was more prominent in the D_1 than in the D_2 or D_1/D_2 MSNs. The significance of these results will now be discussed in the light of relevant literature.

It is now well established that co-expression of D_1 and D_2 receptors occurs in some striatal MSNs, but there is still some controversy regarding the relative importance of such a unique neuronal population. In the literature, the percentage of striatal MSNs that coexpress D_1 and D_2 ranges from low (Gerfen *et al.*, 1990; Lester *et al.*, 1993; Aubert *et al.*, 2000; Deng *et al.*, 2006; Perreault *et al.*, 2010), moderate (Meador-Woodruff *et al.*, 1991; Ariano *et al.*, 1992; Surmeier *et al.*, 1996) to nearly 100% (Aizman *et al.*, 2000). Such substantial differences may be explained, on one hand, by the various methods and species used and, on the other hand, by the specificity of the antibodies or the *in situ* hybridization probes employed to detect $D_1$and D_2receptors. In the present study, depending on striatal sectors that were examined, we estimate

that the D_1/D_2 MSNs account for 0.8-2.4% of the total number of striatal MSNs, a proportion that agrees with figures reported in other studies conducted in BAC transgenic mice (Bertran-Gonzalez *et al.*, 2008; Thibault *et al.*, 2013; Escande *et al.*, 2016).

Despite that they represent only 2% of the total MSNs population of the adult mice dorsal striatum, the D_1/D_2 MSNs might play an important role in striatal functioning, as it is the case of striatal interneurons, which account only for 2-3% of striatal neurons in rodents (Rymar *et al.*, 2004; Tepper & Bolam, 2004). Their presence throughout the dorsal striatum suggest that the D_1/D_2 MSNs are involved in the sensorimotor and associative functions of the striatum, which are integrated mainly within the caudolateral and the rostromedial sector of the structure, respectively (Parent & Hazrati, 1995b). However, the prevalence of the D_1/D_2 MSNs in the Acb indicates that these neurons are even more actively implied in the limbic aspect of striatal functioning. Indeed, we found the density of D_1/D_2 MSNs in the Acb to be significantly higher than in the dorsal striatum, a finding that is congruent with data from previous studies conducted in transgenic mice (Bertran-Gonzalez *et al.*, 2008; Hasbi *et al.*, 2009; Perreault *et al.*, 2010; Gangarossa *et al.*, 2013a; Gangarossa *et al.*, 2013b) and by a higher number of D_1/D_2 heteromer in the rat and monkey Acb (Perreault *et al.*, 2016; Rico *et al.*, 2016). The shell compartment of the Acb was significantly more enriched in D_1/D_2 MSNs than the core compartment, supporting the notion that latter is more similar to the dorsal striatum than the former, which has been described as a transition zone between the striatum and the extended amydgdala (Harlan *et al.*, 2003). The fact that the D_1/D_2 MSNs form the vast majority of MSNs in the medial area of the shell compartment, as noted here, is interesting since this medial region of the Acb shell is known to be involved in feeding behaviors (Kelley & Swanson, 1997; Stratford & Kelley, 1997; Basso & Kelley, 1999; Lopes *et al.*, 2007) as well as in the response to noxious stimuli (Lopes *et al.*, 2007). Whether or not the D_1/D_2 MSNs present in the Acb play a role in the antidepressant and anxiolytic

effects observed after disruption of the D_1-D_2 complex (Shen *et al.*, 2015) remains to be investigated.

Besides their difference in the expression of DA receptors, the two major types of striatal MSNs express different neuropeptides in both rodents and primates (Gerfen *et al.*, 1990; Surmeier *et al.*, 1996; Steiner & Gerfen, 1998), the D_1 MSNs containing SP and DYN while the D_2 MSNs are enriched with ENK (Bertran-Gonzalez *et al.*, 2008). As for the D_1/D_2 MSNs, a previous report has suggested that they express both ENK and DYN in the rat (Perreault *et al.*, 2010), whereas the present findings clearly show that they display immunoreactivity only for DYN. Such a discrepancy might reflect a species difference, but most likely results from a variation in the methodological approach. We used highly specific transgenic fluorescent reporters to identify the D_1, D_2 and D_1/D_2 striatal MSNs, whereas (Perreault *et al.*, 2010) employed antibodies against the D_1 and D_2 receptors, which are known to be also highly expressed in the striatal neuropil, a situation that might have hampered the proper identification of the various peptide expressing MSNs. Our data indicate that, in regard to neuropeptide content, the striatal D_1/D_2 neurons in mice have more in common with the D_1 than with the D_2 MSNs.

This first detailed report on the morphological organization of D_1/D_2 MSNs reveals that these neurons have a smaller cell body and a shorter dendritic tree than their D_1 or D_2 counterparts. Our data also underline the less profuse dendritic aborization of the D_2 compared to the D_1 MSNs, a morphological feature that might explain, at least in part, why the D_2 MSNs are more excitable than D_1 MSNs (Gertler *et al.*, 2008). Based on the morphology of their somatodendritic domains, it is tempting to speculate that the excitability and input resistance of the D_1/D_2 MSNs would be higher than the D_1 or even the D_2 MSNs, but such a view needs to be confirmed by detailed investigations of electrophysiological properties of the D_1/D_2 MSNs.

In addition to a smaller dendritic tree, the D_1/D_2 MSNs also contain less dendritic spines than D_1 and D_2 MSNs. The head of dendritic spines is the preferential synaptic contact site of glutamatergic corticostriatal projections arising from the cerebral cortex and the intralaminar thalamic nuclei (Moss & Bolam, 2008). With their less profuse dendritic arborization, the D_1/D_2 MSNs might receive significantly less glutamatergic input and thus be less vulnerable to excitotoxicity involved in different neuropathological conditions such as Huntington's disease. More importantly in the context of the present study is the spatial distribution of DA terminals in contact with different parts of the MSNs. Those terminals that contact the cell body and proximal dendritic shafts might produce a relatively non-specific effect mediated by the volumic release of DA (Descarries & Mechawar, 2000). In contrast, as suggested Freund and colleagues (Freund *et al.*, 1984), the major DA input that occurs on the necks of dendritic spines is likely to be much more selective since it could prevent the excitatory glutamatergic input to the same spines from reaching the dendritic shaft. One of the main functions of striatal DA release might be to alter the pattern of firing of striatal output neurons by regulating their input (Freund *et al.*, 1984).

Lesions with 6-OHDA in rats were shown to increase the expression of D_2 and decrease that of D_1 by MSNs (Gerfen, 2000). Here we report that the density and regional distribution of D_1/D_2 MSNs in mice striatum are unaltered by 6-OHDA lesions, suggesting that DA denervation does not alter the D_1 expression by D_2 MSNs or the D_2 expression by D_1 MSNs. However, it should be noted that the BAC transgenic reporter system used here does not fully allow to rule out the possibility that DA lesion may induce more subtle variations of DA receptor gene expression or receptor trafficking and degradation that could have remained undetected. The D_1/D_2 MSNs do not display any reduction of their dendritic tree following 6-OHDA lesions, in contrast to D_1 and D_2 MSNs, but the D_1/D_2 MSNs show a lower dendritic spine density in the DA-denervated striatum, as it is also the case for D_1 and D_2 MSNs. Reduction of the dendritic length of D_1 and D_2 MSNs following DA lesion is supported by observations

gathered in mice (Fieblinger *et al.*, 2014; Toy *et al.*, 2014), monkeys (Villalba *et al.*, 2009b) and PD patients (McNeill *et al.*, 1988; Stephens *et al.*, 2005; Zaja-Milatovic *et al.*, 2005). However, some studies in rats (Zhang *et al.*, 2013) and mice (Suarez *et al.*, 2014) failed to demonstrate such a phenomenon. The time between DA lesion and animal sacrifice might explain such a discrepancy. The interval between 6-OHDA injection and animal perfusion in the latter two studies ranged from 4 to 5 weeks, whereas the delay was much longer (8 weeks) in the present study. In face of such differences, it is tempting to speculate that the reduction in dendritic length occurs after the spine loss has occurred, that is in the late stages of the disease.

We documented spine loss for the three types of striatal MSNs, in accordance with data obtained for D_1 and the D_2 MSNs in mice (Fieblinger *et al.*, 2014; Suarez *et al.*, 2014; Fieblinger & Cenci, 2015), rats (Ingham *et al.*, 1993; Zhang *et al.*, 2013; Nishijima *et al.*, 2014), monkeys (Villalba *et al.*, 2009b) and PD patients (Stephens *et al.*, 2005; Zaja-Milatovic *et al.*, 2005). Interestingly, other studies have suggested that such spine loss may be restricted to the D_2 MSNs in mice (Day *et al.*, 2006; Shen *et al.*, 2007) . As mentioned above, DA axons are ideally positioned on the dendritic spine neck to influence the effect of corticostriatal and thalamostriatal glutamatergic input (Moss & Bolam, 2008). It has been hypothesized that the loss of DA afferents may destabilize the morphological integrity of the spine, potentially leading to spine pruning, a phenomenon that might be the result of maladaptive calcium influx through the L-type calcium channels located on MSNs (Day *et al.*, 2006). Moreover, evidence has recently been gathered regarding the implication of acetylcholine, the level of which is known to be increased in PD (Barbeau, 1962; Aosaki *et al.*, 2010), in spine pruning of the D_2 MSNs through the modulation of Kir2 channels, leading to an increase of dendritic excitability driven by the activation of M1 muscarinic receptor (Shen *et al.*, 2007).
The exact function of the D_1/D_2 MSNs of the striatum remains elusive. Colocalization of the D_1 and D_2 DA receptors has been reported in axons

located in various basal ganglia components (Perreault *et al.*, 2010). Whether this observation indicates a distinct striatofugal pathway remains unclear (Perreault *et al.*, 2011). However, the existence of such unique striatofugal projections would imply a complementary functional role of the D_1/D_2 MSNs, working in concert with the D_1 and the D_2 MSNs for harmonious basal ganglia functioning. Single-axon tracing studies in rodents (Kawaguchi *et al.*, 1990; Wu *et al.*, 2000) and monkeys (Parent *et al.*, 1995; Levesque & Parent, 2005) have emphasized the highly collateralized nature of the striatofugal projections, challenging the concept of a simple dual (direct/indirect) striatofugal system. Whether the D_1/D_2 MSNs contribute to these highly collateralized striatofugal projections is currently unknown and single-axon tracing of D_1/D_2 MSNs is obviously needed to better appreciate their functional role in the basal ganglia functioning.

6.6. Material and methods

6.6.1. Animals

This study was carried out on 25 double BAC transgenic mice (*Drd1a*-tdTomato/*Drd2*-EGFP) of 2 month old weighing between 20-30 g. Equal numbers of male and female were used. These D_1/D_2 mice were generated by breeding B6SJLF1-D_1tdTomato BAC transgenic mice (Shuen *et al.*, 2008) with C57Bl6J-D_2-EGFP BAC animals (Gong *et al.*, 2003). They allow direct identification of the D_1, D_2 and D_1/D_2 MSNs (Fig. 8). In order to minimize over expression artifacts, all mice where heterozygous for each individual BAC transgene. Animals were housed under a 12 h light-dark cycle with water and food ad libitum. All procedures were approved by the *Comité de Protection des Animaux de l'Université Laval,* in accordance with the Canadian Council on Animal Care's Guide to the Care and Use of Experimental Animals (Ed2) and with the ARRIVE guidelines. Maximum efforts were made to minimize the number of animals used.

6.6.2. Stereotaxic injections

6-OHDA unilateral injection and behavioral assessment

Nineteen *Drd1a*-tdTomato/*Drd2*-EGFP transgenic mice received an intracerebral injection of 6-OHDA (catalog no. H4381; Sigma-Aldrich, Saint-Louis, MO, USA) in the right medial forebrain bundle (mfb). Approximately 30 minutes before 6-OHDA administration, mice received intraperitoneal injection of desipramine (25 mg/kg) diluted in saline (0.9%) at a concentration of 2 mg/mL. Mice were then anaesthetized using 2% isoflurane and their head were fixed in a stereotaxic apparatus. A hole was drilled and the following stereotaxic coordinates were aimed: anteroposterior (bregma) = -1.2 mm; mediolateral = 1.1 mm; dorsoventral = -5.0 mm, corresponding to the mfb, according to the mouse brain atlas of (Franklin & Paxinos, 1997). A glass micropipette of 35 µm diameter at the tip containing a freshly prepared 6-

OHDA solution was introduced in the mfb. The 6-OHDA was then pressure-injected and the micropipette was left in place for 2 min both prior and following the injection. The 6-OHDA was diluted in ascorbic acid (catalog no. A5960; Sigma-Aldrich) at a concentration of 6 µg/µL. A total volume of 0.25 µL of 6-OHDA, corresponding to a dose of 1.5 µg of the neurotoxin, was injected into the right mfb. The sham-lesioned group was composed of 4 mice that only received injections of the vehicle (0.02% ascorbic acid). After surgery, the skin was sutured and mice were allowed to recover.

Thirty days after surgery, mice from the two experimental groups were introduced in a large glass cylinder and spontaneous motor behavior was recorded during 10 min. Spontaneous rotations were counted by a blinded experimenter. Complete ipsilateral and contralateral rotations to the 6-OHDA-lesioned side were counted and used as behavioral indication of the severity of the DA lesion.

Fifty-six days after the 6-OHDA lesion, animals were deeply anesthetized with a mixture of ketamine (100 mg/kg) and xylazine (10 mg/kg). They were transcardially perfused with an initial wash of 40 mL of ice-cold sodium phosphate-buffered saline (PBS, 0.1M; pH 7.4), followed by 150 mL of paraformaldehyde (PFA, 4% diluted in phosphate buffer). Brains were dissected out, post-fixed for 24 h in a 4% PFA solution and cut with a vibratome (model VT1200; Leica, Germany) into 50 µm-thick coronal sections, which were serially collected in sodium phosphate-buffered saline (PBS, 0.1M, pH 7.4). The pre and post-commissural parts of the striatum were cut at 50 µm and used for immunohistochemistry and stereology whereas the commissural part was cut at 250 µm for intracellular injections.

Bilateral colchicine injections

Two other double BAC transgenic mice received bilateral injections of colchicine (catalog no. C9754; Sigma-Aldrich) in the striatum, a drug that block axonal transport, allowing optimal immunostaining of neuropeptides contained in

MSNs cell bodies. For intra-cerebral injections of colchicine, the following stereotaxic coordinates were used: anteroposterior (bregma): 0.14 mm; mediolateral: 2.00 mm; dorsoventral: 3.20 mm, corresponding to the dorsal part of the striatum at the commissural level, according to the mouse brain atlas of (Franklin & Paxinos, 1997). One µL of colchicine diluted at 23 mg/mL in saline was pressure-injected in each side of the brain. One week after injections, colchicine-injected mice were transcardially perfused, as described above. Their whole brains were dissected out and cut with a vibratome into 50 µm-thick transverse sections.

6.6.3. Immunohistochemistry

TH and DAT immunohistochemistry

To assess the extent of the DA lesion induced by 6-OHDA injections, one 50 µm-thick section was selected from the pre-commissural striatum (0.14 mm from bregma) and from the SNc (-3.52 mm from bregma), in each mouse. These sections were immunostained for TH, the catalytic enzyme of DA synthesis, by using a polyclonal antibody (catalog no. AB152; Millipore Corporation, Billerica, USA) raised in rabbit. Briefly, the free-floating sections were sequentially incubated in (i) a blocking solution of PBS containing 2% normal goat serum and 0.01% Triton X-100 (1 h, RT); (ii) the same solution containing a 1/1000 dilution of rabbit polyclonal antibody against TH (overnight, 4 °C); and (iii) a 1/500 solution of biotinylated goat anti-rabbit (catalog no. BA-1000; Vector Laboratories, Burlingame, CA, USA) diluted in the same blocking solution (2 h at room temperature (RT)). After rinses in PBS, sections were incubated for 1 h at RT in an avidin-biotin-peroxydase complex solution (Vector Laboratories) diluted 1/100 in the blocking solution. Sections were then rinsed and the bound peroxidase revealed by incubating the sections for 3 min at RT in a 0.025% solution of 3,3'diaminobenzidine tetrahydrochloride (DAB; catalog no. D5637; Sigma-Aldrich) diluted in Tris-buffered saline (TBS; 50 mM; pH 7.4), to which 0.005% of H_2O_2 was added. The reaction was stopped and the sections mounted on gelatin-coated slide

and air-dried. Sections were then dehydrated in graded alcohol, cleared in toluene and coverslipped with Permount (catalog no. SP15-500; Fisher Scientific). The TH-immunostained sections taken through the midbrain were used to assess the number of DA cell bodies in the SNc and VTA, as delineated based on the mouse brain atlas of Franklin et Paxinos(Franklin & Paxinos, 1997). On these sections, all TH+ cell bodies were counted and results expressed as percentage of control side.

In each mouse, the DA lesion was also assessed using an infrared imaging system (Odyssey CLx; LI-COR Biosciences, Lincoln, NE, USA) from a 50 µm-thick section taken at the pre-commissural level of the striatum (1.34 mm from bregma). Sections were immunostained for TH and DAT, using secondary antibodies coupled to infrared fluorescent dyes. The primary antibody against TH was the same as above (1/1000, overnight at 4°C). The monoclonal antibody against DAT (1/1000, overnight at 4°C, catalog no. MAB369; EMD Millipore Corporation, Billerica, USA) was raised in rat. Donkey anti-rabbit 680 (1/1000, 2h at RT, catalog no. 926-68073; LI-COR Biosciences) and goat anti-rat 800 (1/1000, 2h at RT, catalog no. 926-32219; LI-COR Biosciences) were used as secondary antibodies. Two solid-state diode lasers (685 nm and 785 nm) were used to excite secondary antibodies coupled to infrared fluorescent dyes. Intensity values of TH and DAT immunoreactivity were taken from six 0.16 mm^2 squares randomly placed over the striatum and from one 0.16 mm^2 square placed over the Acb.

Calbindin immunohistochemistry

In order to precisely delineate the core and the shell regions of the Acb, transverse sections adjacent to those used for stereology were immunostained for calbindin (CB). Briefly, the immunoperoxidase protocol described above was used but with a monoclonal primary antibody against CB (1/500, overnight at 4°C, catalog no. C-9848, Sigma-Aldrich) and a biotinylated horse anti-

mouse secondary antibody (1/200, 2h at RT, catalog no. BA-2000; Vector Laboratories).

μ-opioid receptor immunohistochemistry

In order to delineate the striosomes and matrix striatal compartments, 2 transverse sections were taken at the pre-commissural and post-commissural striatal levels and immunostained for μ-opioid receptor (MOR). These sections were used to assess differences in the density of D_1/D_2 MSNs between the 2 striatal compartments. Briefly, sections were incubated with a primary antibody against MOR (1/200, overnight at 4°C, catalog no. AB5509; Chemicon, Darmstadt, Germany) followed by incubation into a donkey anti-guinea pig secondary antibody coupled to Cy5 (1/200, 2h at RT, catalog no. 706-175-148; Jackson ImmunoResearch, West Grove, PA, USA).

Enkephalin and dynorphin immunohistochemistry

Neuropeptide content of the D_1, D_2 and D_1/D_2 MSNs was assessed on singly labeled sections for ENK or DYN, taken from the 2 colchicine-injected mice. Briefly, sections were incubated with either a mouse anti-ENK (1/50, NOC1; Medicorp, Montreal, QC, Canada) or a rabbit anti-DYN (1/200, catalog no. SP1215; Acris, San Diego, CA, USA) antibody overnight at 4°C. Sections were then incubated with either a horse anti-mouse (1/200, catalog no. BA-2000; Vector Laboratories) biotinylated secondary antibodies for 2 h at RT, followed by streptavidin-Cy5 (1/200, catalog no. SA1011; Invitrogen, Carlsbad, CA, USA) for 1 h at RT in the case of ENK, or directly with a goat anti-rabbit-Cy5 (1/200, catalog no. 111-175-003; Jackson ImmunoResearch) for 2 h at RT in the case of DYN. Images were acquired using a confocal microscope (Zeiss, LSM 700; Oberkochen, Germany).

6.6.4. Quantitative assessment of D_1, D_2 and D_1/D_2 MSNs in the striatum

Four sham and 4 6-OHDA-lesioned mice were used for stereological estimation of the number of D_1, D_2 and D_1/D_2 MSNs. In each mouse, 6 sections were selected from the pre-commissural striatum. Three adjacent sections were selected at 0.26 mm from bregma and 3 others at 1.10 mm. Three more sections were taken at -0.94 mm from bregma. These sections were used to estimate the number of D_1, D_2 and D_1/D_2 MSNs in the pre-commissural (0.26 mm from bregma) and post-commissural striatum (-0.94 mm from bregma), as well as in the Acb (1.10 mm from bregma), with an unbiased stereological method using a confocal microscope equipped with a digital camera and a motorized stage controlled by a computer running the StereoInvestigator software (v. 7.00.3; MicroBrightField, Colchester, VT, USA). First, on each section, striatal contour was traced and 4 striatal sectors were delineated corresponding to a dorsolateral, dorsomedial, ventrolateral and ventromedial sectors (Fig. 4). The Acb was divided into its core and shell compartments based on CB-immunostained adjacent sections.

On each section, the striatum was entirely scanned through multiple Z-stacks using a 40x objective (NA 1.4, oil immersion, Plan-Apochromat, Zeiss) and the 488 and 568 diode lasers at 2% of power. Optical resolution of the Z-stacks was 512 x 512 pixel (pixel size = 0.10 μm^2), with Z-steps of 3 µm corresponding to the optical slice determined by the pinhole. The thickness of Z-stacks was fixed at 30 µm and the gain setting for each channel was kept constant during the entire acquisition process.

The process leading to the estimation of the total number of D_1 and D_2 MSNs began by randomly translating a grid formed by 235 x 580 µm rectangles on the previously acquired confocal images of the striatum and the Acb. At each intersection of the grid that fell into the sector, a counting frame measuring 157 x 157 µm was drawn and examined. Cell bodies containing tdTomato (D_1)

or GFP (D_2) that fell inside the counting frame and did not contact the exclusion lines were counted whenever they came into focus within a 12 µm-thick optical disector placed at 9 µm from the top of the section. An average number of 2939 ± 186 D_1 and 2477 ± 160 D_2 neurons were counted in the striatum and 1187 ± 98 D_1 and 642 ± 64 D_2 cell bodies in the Acb of each mouse, yielding coefficient of error (Gundersen, m=1) ranging between 0.05 and 0.18.

Because less numerous, the number of striatal cells containing both tdTomato (D_1) and GFP (D_2), here called the D_1/D_2 MSNs, was estimated with stereological parameters different from those employed to estimate the number of D_1 and D_2 MSNs. Selected transverse sections of the striatum were entirely examined with an optical disector of the same size of the one described above. An average of 599 ± 106 D_1/D_2 cells were counted in the striatum compared to 993 ± 191 D_1/D_2 neurons in the Acb of each mouse, yielding coefficient of error (Gundersen, m=1) ranging between 0.08 and 0.27. The density of D_1, D_2 and D_1/D_2 MSNs was obtained by dividing the number of striatal cells estimated by the optical disector by the volume of striatal sectors sampled, as estimated by the Cavalieri's method (Gundersen & Jensen, 1987).

In the 4 sham-lesioned animals, the 2 transverse sections taken at the pre-commissural (0.26 mm from bregma) and post-commissural (-0.94 mm from bregma) striatal levels that were immunostained for MOR were used to estimate the number of D_1/D_2 MSNs in the striosomes and matrix compartments. Again, all striatal D_1/D_2 MSNs were counted from previously acquired confocal images and the striosomes and matrix compartments were delineated by using MOR immunoreactivity.

6.6.5. Single-cell injections of identified MSNs

Fine morphological changes of MSN dendritic arborization that might be induced by DA denervation were characterized by single-neuronal injections of

Lucifer yellow applied to PFA-fixed brain sections from the *Drd1a*-tdTomato/*Drd2*-EGFP transgenic mice, using a method previously described (Buhl & Lubke, 1989; Dumitriu *et al.*, 2011). Sharp heat-pulled glass micropipettes filled with a 4% solution of Lucifer yellow (catalog no. L453; Life Technologies, Carlsbad, CA, USA) and containing a silver electrode connected to a computer-controlled microelectrode amplifier (Multiclamp 700A, Axon Instruments) were inserted into 250 µm-thick brain section kept in ice-cold PBS (0.1M), under an epifluorescence microscope (model no. E600FM, Nikon, Tokyo). After the insertion of the micropipette into the soma of visually identified MSNs located in the dorsal striatum, a negative direct current of 5 nA was administered for 20 minutes during which MSNs were filled with the negatively charged Lucifer yellow tracer. A 488 nm filter was used to visualize GFP contained in D_2 MSNs whereas a 568 nm filter was used to detect the presence of tdTomato into D_1 MSNs. Each neurons being injected was carefully inspected with both filters in order to determine content in GFP and/or tdTomato with a 40X water immersion objective (NA 0.80). All injected MSNs were located in the dorsal striatal region, at the commissural level, and restricted to 0.02-0.26 mm in the anteroposterior axis relative to the bregma, 1-3 mm in the mediolateral axis and 2-3 mm in the dorsoventral axis, according to the stereotaxic mouse brain atlas (Franklin & Paxinos, 1997).

The 250 µm-tick sections containing injected striatal neurons were mounted on glass slides and coverslipped with a fluorescence mounting medium (S3023; Dako, Mississauga, Ontario, Canada). Z-stack of Lucifer yellow-filled neurons were obtained from the confocal microscope using a 405 nm diode laser and a 63x oil immersion objective (NA 1.4, Plan-Apochromat, Zeiss). The pixel size was 0.001 μm^2 whereas the optical slicing was 0.3 μm. A tiling process was used when dendritic arborization extend beyond the field of view.

6.6.6. Morphological analysis of injected MSNs

Analyses of dendritic arborization and spine density were performed using the freely available *NeuronStudio* software (CNIC, Mount Sinai School of Medecine, New York, NY, USA). The entire somatodendritic domains of injected neurons were carefully reconstructed using maximum intensity projection in *NeuronStudio* software, as previously described (Bories *et al.*, 2013). By using a combination of automatic spine detection from *NeuronStudio* software followed by a careful examination of individual spine, we were able to provide faithful three-dimensional reconstructions of somatodendritic domains of injected MSNs. From these reconstructions, Sholl analyses were performed on individual MSNs of the D_1, D_2 and D_1/D_2 types. Measurements of the size of the cell body were conducted by using the *ImageJ* software (Version 1.48). In this software, maximum intensity projections of Z-stacks were generated and diameters of cell bodies were measured. Dendritic arborization analyses and size measurements were performed on 19 D_1, 27 D_2, 20 D_1/D_2 Lucifer-yellow-injected MSNs from 4 sham-lesioned animals and on 18 D_1, 17 D_2 and 22 D_1/D_2 MSNs from 19 6-OHDA-lesioned mice.

6.6.7. Statistical analysis

Statistical differences of neuronal densities between different striatal and Acb regions were assessed using Kruskal-Wallis non-parametric statistical test. Differences between sham and 6-OHDA-lesioned mice regarding neuronal densities and spontaneous rotations were assessed with Mann-Whitney non-parametric test. Variations in immunoreactivity for TH and DAT between sham and 6-OHDA-lesioned mice were detected using the Mann-Whitney statistical test. A Sholl analysis with 15 µm increments was used to determine the spine density and statistical differences for dendritic morphology (number of branching points, spine density and dendritic length) and for cell body diameters between the two experimental groups and the three types of MSNs were assessed with the two-way analysis of variance (ANOVA) followed by a Bonferroni multiple comparison test. All statistical tests were performed using

GraphPad Prism software (v. 6.01; GraphPad Software, San Diego, CA, USA). Mean and standard error of the mean are used throughout the text as central tendency and dispersion measure, respectively.

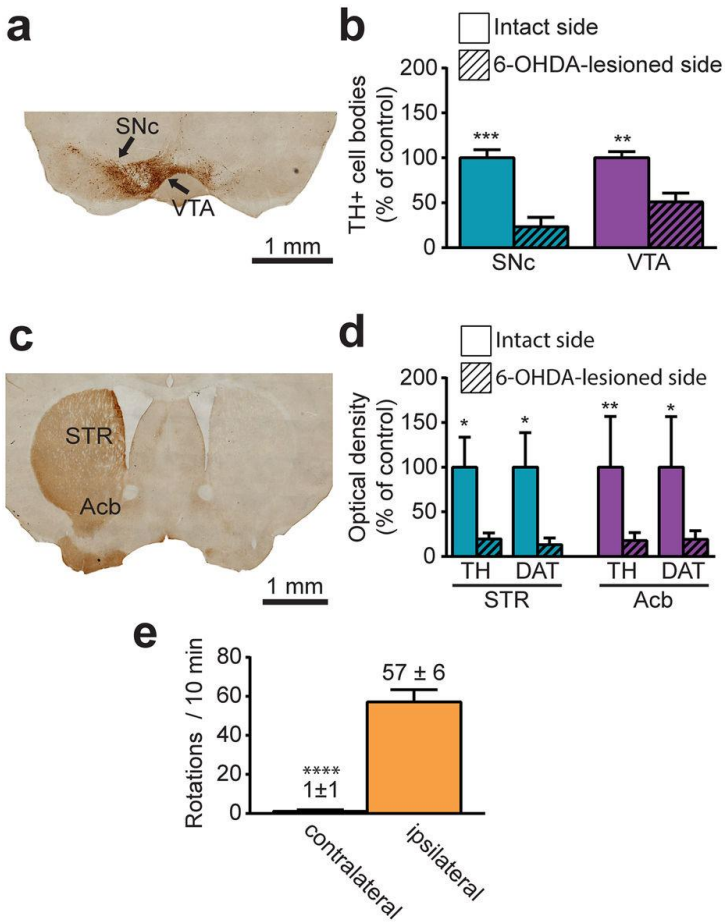

FIGURE 6.1. - (**a)** Transverse section taken through the substantia nigra *pars compacta* (SNc) and the ventral tegmental area (VTA) that was immunostained for tyrosine hydroxylase (TH) to assess the dopaminergic lesion induced by stereotaxic injection of 6-OHDA in the right medial forebrain bundle. (**b**) Histogram showing the percentage of TH + cell loss in the SNc and the VTA, as expressed in percentage of intact side. (**c**) Transverse section taken through the striatum (STR) and immunostained for TH. (**d**) Histogram showing immunoreactivity of the STR and the nucleus accumbens (Acb) for the tyrosine hydroxylase (TH) and the dopamine transporter (DAT) in the 6-OHDA-lesioned side, as expressed in percentage of intact side. (**e**) Behavioural response induced by 6-OHDA lesion, as shown in number of contralateral and ipsilateral spontaneous rotations observed in 10 minutes. $*P < 0.05$, $**P < 0.01$, $***P < 0.001$ for intact side vs. 6-OHDA-lesioned side, $****P < 0.0001$ for ipsilateral vs. contralateral rotations, by Mann-Whitney test.

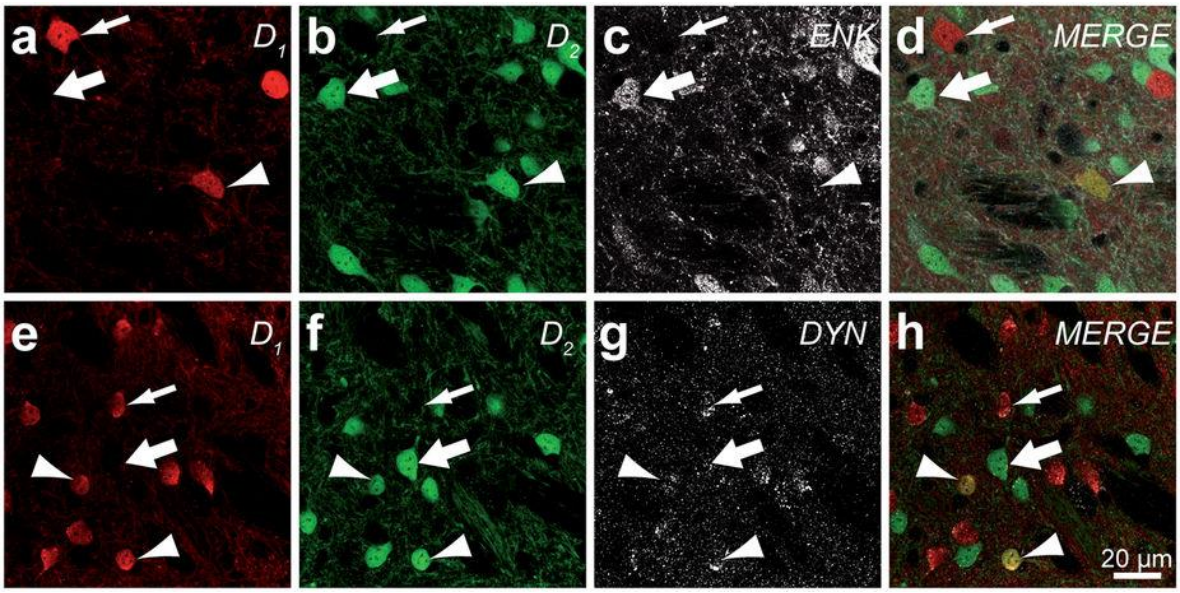

FIGURE 6.2. - Transverse sections taken from the dorsolateral striatum of a D_1/D_2 transgenic mouse that were immunostained for enkephalin (ENK, **a–d**) or dynorphin (DYN, **e–h**). Thin arrows indicate D_1 MSNs, thick arrows point to D_2 MSNs and arrowheads to D_1/D_2 MSNs. The D_1/D_2 MSNs are immunoreactive for dynorphin but not for enkephalin in the D_1/D_2transgenic mouse.

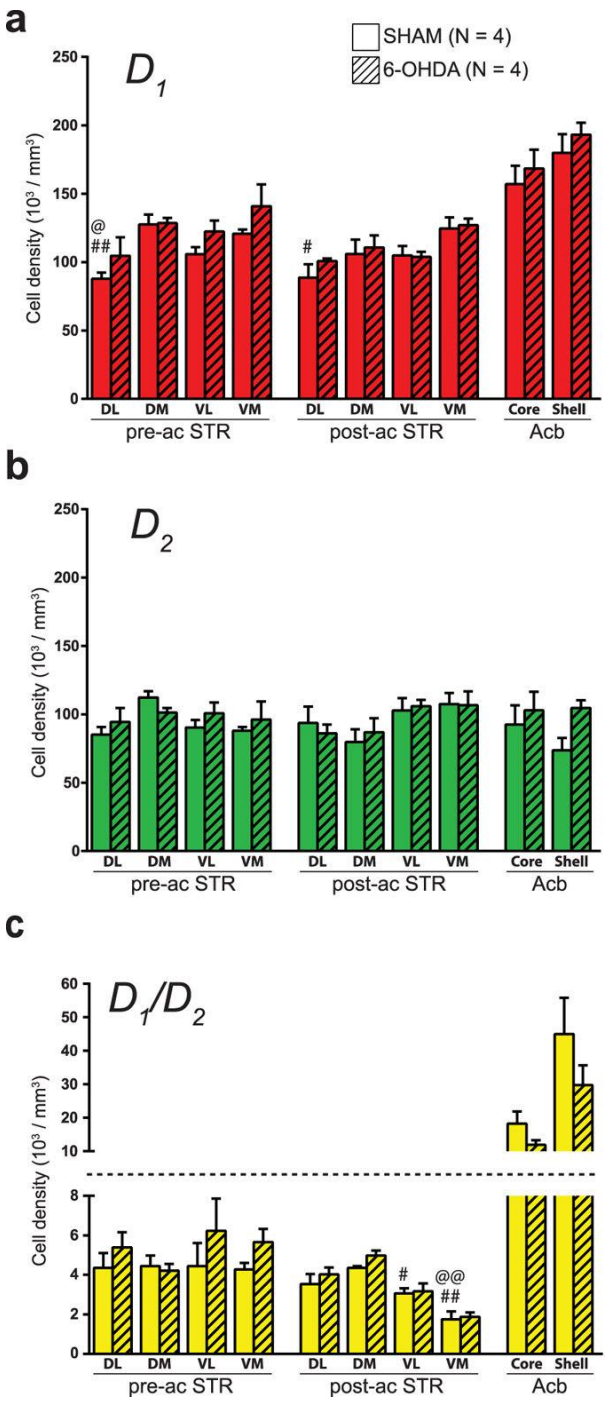

FIGURE 6.3. - Histograms showing the density of D_1 (**a**), D_2 (**b**) and D_1/D_2 (**c**) MSNs in different regions of the striatum (STR) and the nucleus accumbens (Acb) of sham and 6-OHDA-lesioned mice. $^{\#}P < 0.05$, $^{\#\#}P < 0.01$ vs. the shell compartment of the Acb and $^{@}P < 0.05$, $^{@@}P < 0.01$ vs. the core compartment of the Acb, by Kruskal-Wallis test.

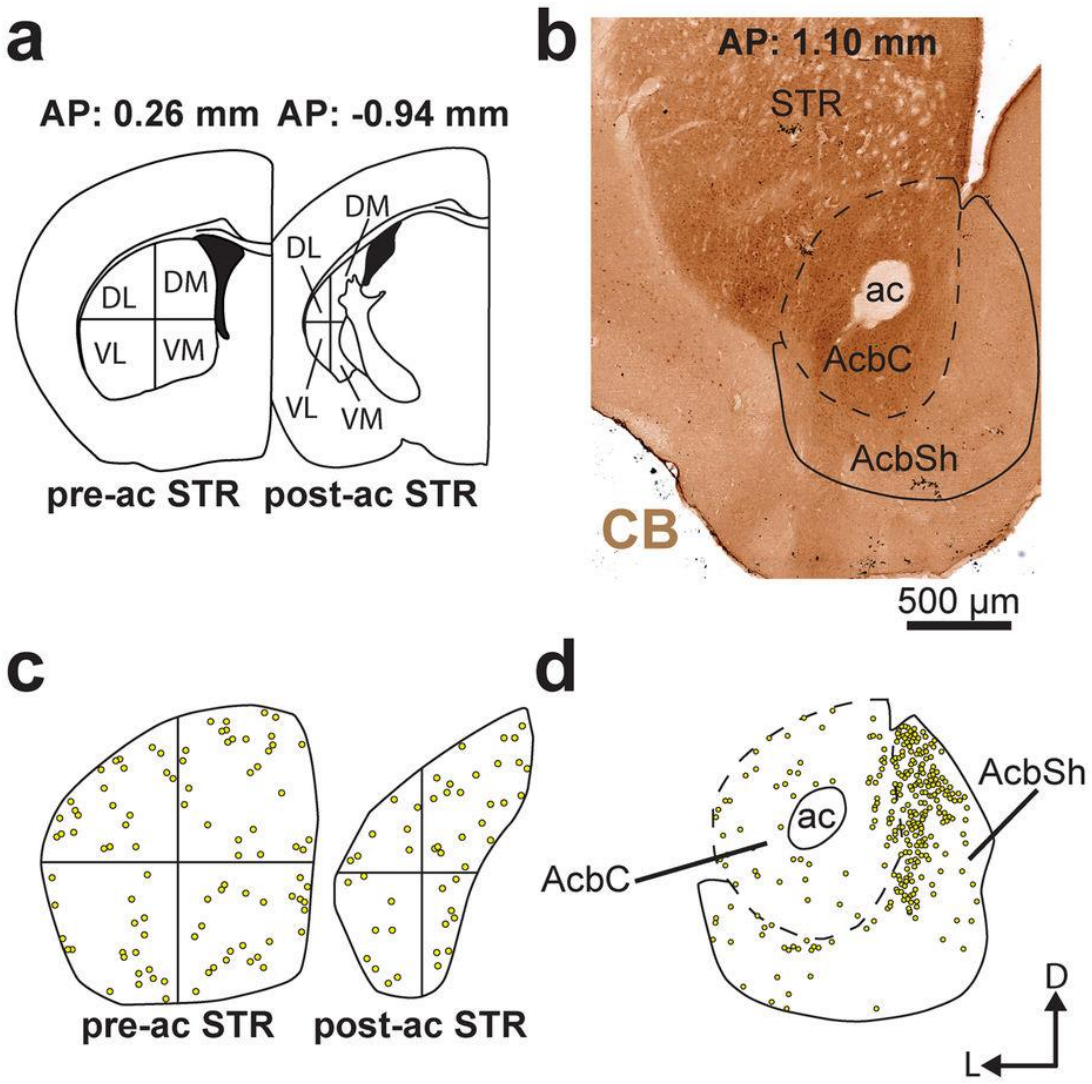

FIGURE 6.4. - (a,b) Schematic representations of transverse sections taken at 0.26, −0.94 and 1.10 mm from bregma on which sectors that were sampled to provide unbiased stereological estimation of the number of D_1, D_2 and D_1/D_2 MSNs in the striatum (STR, **a**) and the nucleus accumbens (Acb, (**b**) are delineated. (**c,d)** Schematic representations of the distribution of D_1/D_2 MSNs at the pre and post-commissural level of the STR (**c**) as well as in the core (AcbC) and the shell (AcbSh) of the nucleus accumbens. The transverse section shown in (**b**) was immunostained for calbindin and used to delineate the AcbC from the AcbSh.

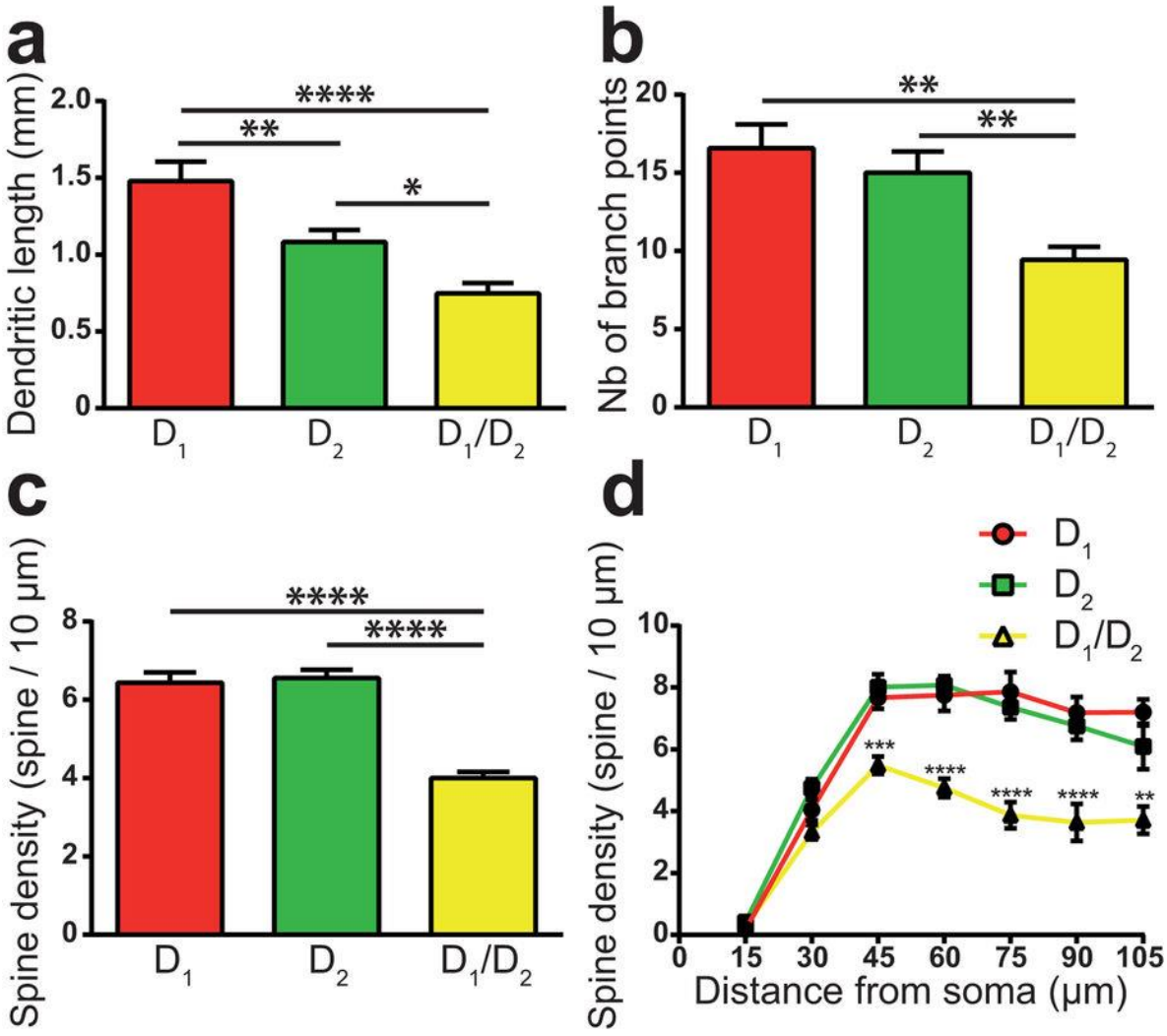

FIGURE 6.5. - **(a–c)** Histograms showing the total dendritic length (**a**), the number of dendritic branch points (**b**) and the overall spine density (**c**) of the D_1 (red), the D_2 (green) and the D_1/D_2 (yellow) striatal MSNs in sham-lesioned mice. (**d)** Sholl analysis of spine density of the 3 types of MSNs, as measured in sham-lesioned mice. $*P < 0.05$, $**P < 0.01$, $***P < 0.001$, $****P < 0.0001$ for D_1 vs. D_2 vs. D_1/D_2 by One-way (**a–c**) or Two-way (**d**) ANOVA, followed by Bonferroni's multiple comparison test.

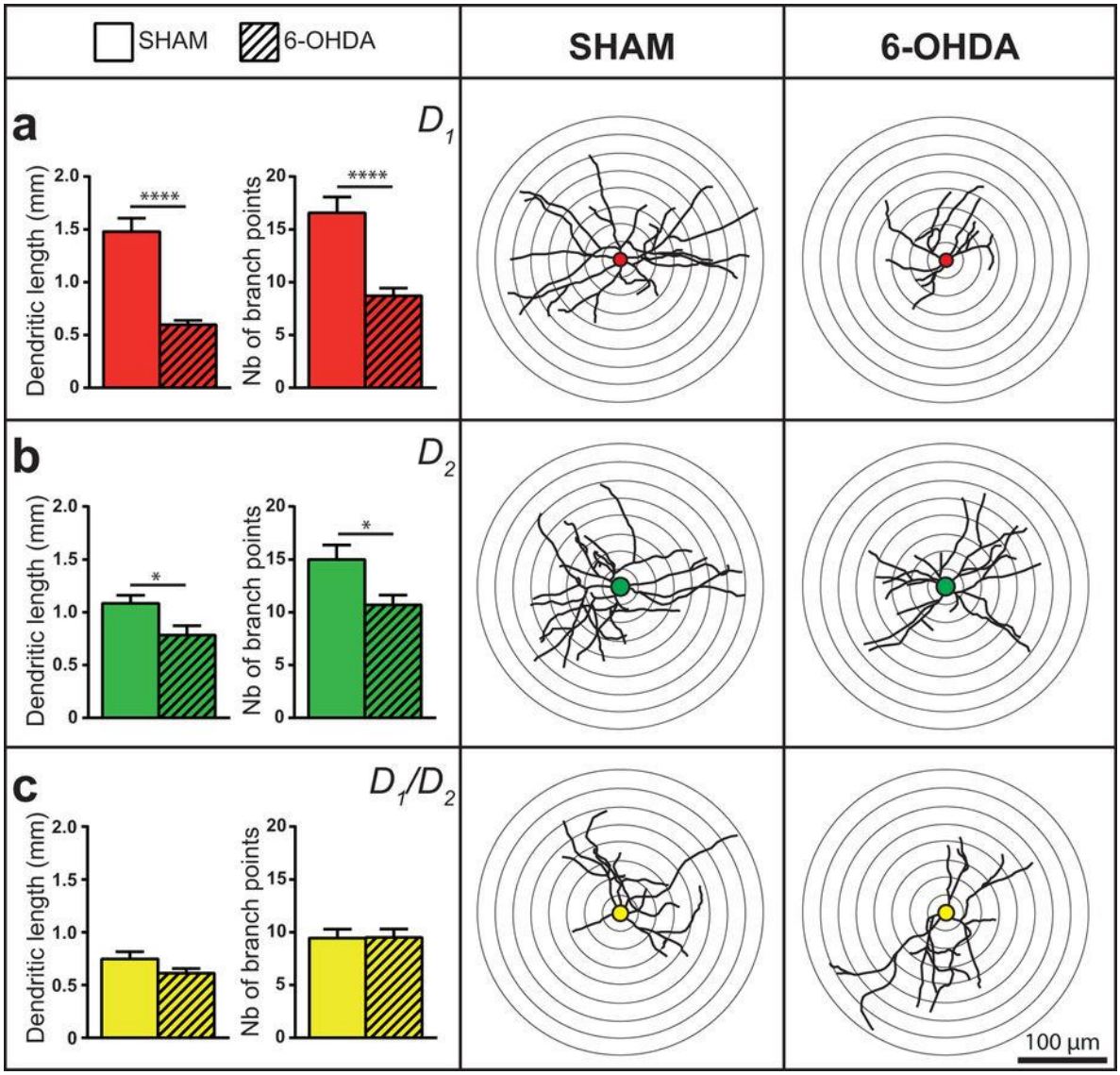

FIGURE 6.6. - Histograms showing the total dendritic length and the number of dendritic branch points in sham (plain columns) and 6-OHDA (hatched columns) lesioned mice. The center and right columns provide schematic representations of D_1 (red), D_2(green) and D_1/D_2 (yellow) MSNs dendritic arborization in sham (center column) and 6-OHDA (right column) lesioned mice. $*P < 0.05$, $****P < 0.0001$ for sham vs. 6-OHDA-lesioned mice, by Student's T-test.

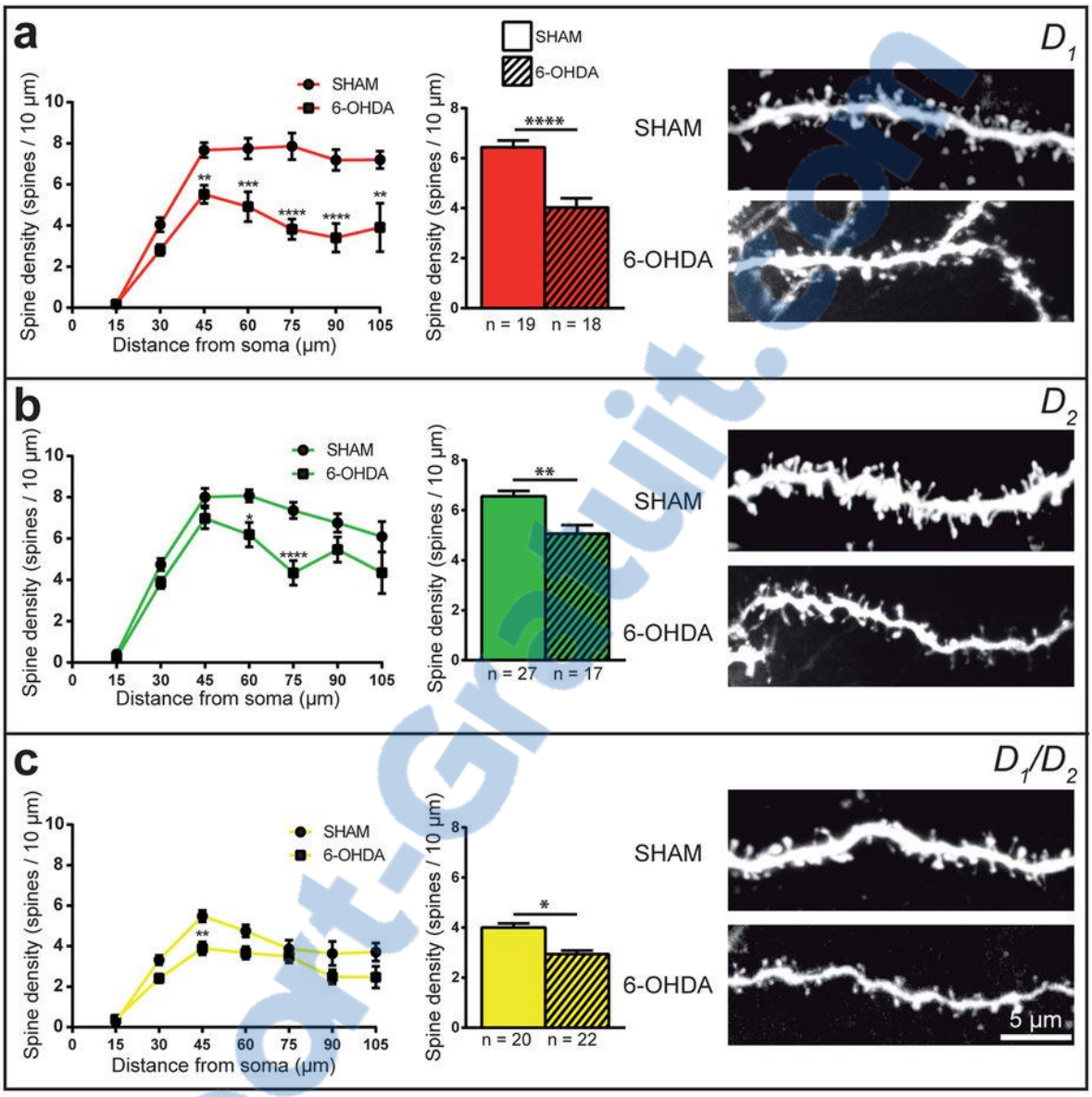

FIGURE 6.7. - Sholl analysis of spine density (left column) and histograms showing the overall spine density (center column) of the D_1 ((**a**), red), D_2 ((**b**), green) and D_1/D_2 ((**c**), yellow) striatal MSNs in sham (circles and plain columns) and 6-OHDA (square and hatched columns) lesioned mice. The right column provides representative examples of dendritic segments belonging to the D_1, D_2 or D_1/D_2 MSNs that were filled with Lucifer yellow in sham and 6-OHDA-lesioned mice. $*P < 0.05$, $**P < 0.01$, $***P < 0.001$, $****P < 0.0001$ for sham vs. 6-OHDA by a Student's T-test (histograms) or Two-way ANOVA followed by Bonferroni's multiple comparison test (Sholl analysis).

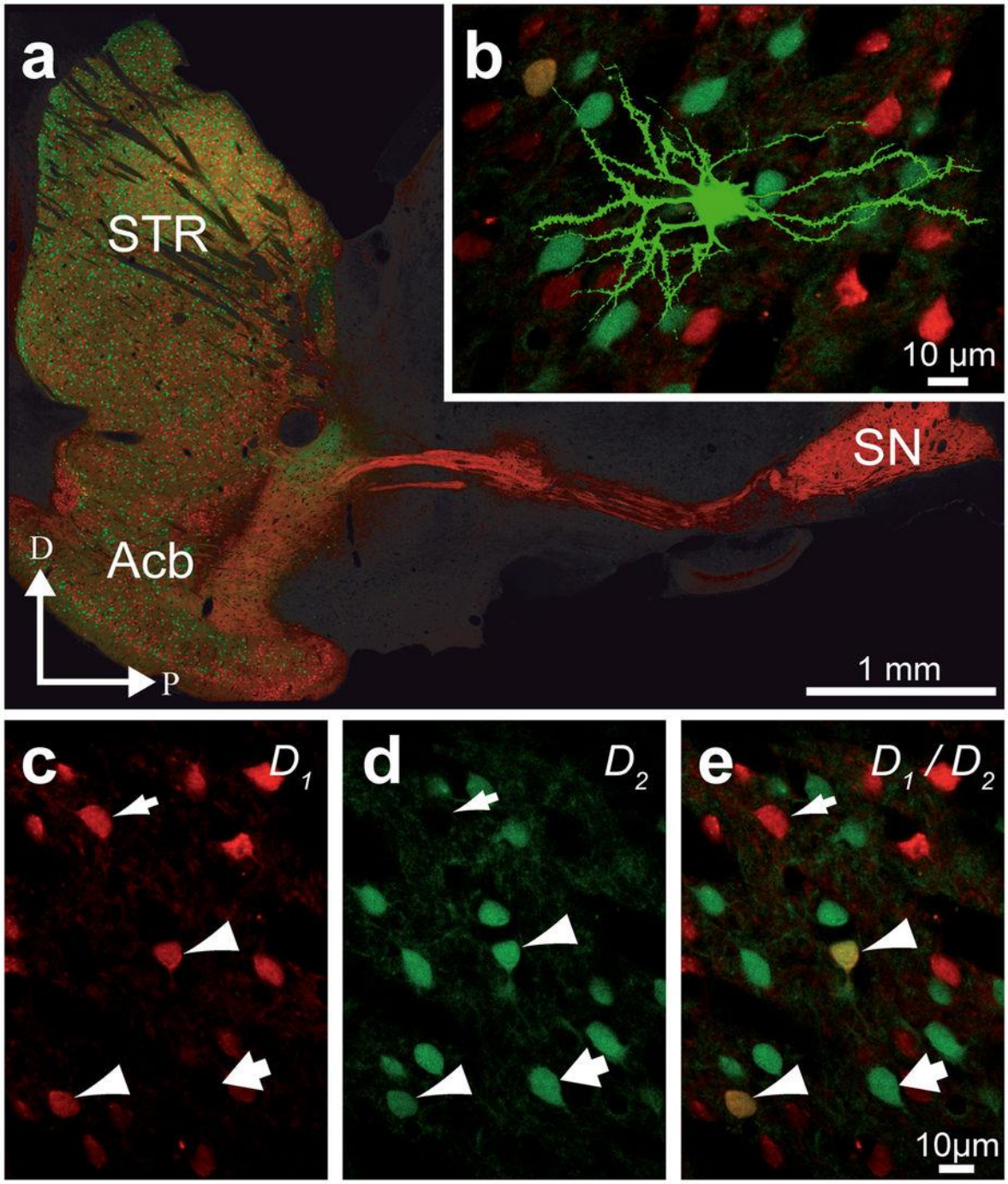

FIGURE 6.8. - Confocal images from the Drd1a-tdTomato/Drd2-EGFP double BAC transgenic mice (D_1/D_2) in which the expression of a red fluorescent protein (tdTomato) is under control of the D_1 promoter and the expression of a green fluorescent protein (EGFP) is under control of the D_2 promoter. (**a**) Confocal image of a sagittal section from a D_1/D_2 transgenic mouse taken through the striatum (STR) and the substantia nigra (SN). (**b)** Example of a

Lucifer yellow-injected MSN located in the dorsal STR. (**c–e)** High magnification of striatal MSNs that contain the D_1 (red, thin arrows), the D_2 (green, thick arrows) or both D_1/D_2 (yellow, arrowheads) dopamine receptors.

CHAPITRE 7 :

CONCLUSIONS GÉNÉRALES

CHAPITRE 7 – CONCLUSIONS GÉNÉRALES

Les descriptions anatomiques de l'innervation 5-HT obtenues chez le rat, le singe et l'humain qui sont présentées dans cette thèse ont permis d'admirer le système 5-HT dans toute sa complexité. En condition normale, il a été possible d'observer des différences d'innervation 5-HT entre des composantes des ganglions de la base ainsi qu'entre différentes espèces de mammifères. L'utilisation de modèles animaux de la maladie de Parkinson nous a permis d'observer les changements compensatoires que subit la microcircuiterie dans les ganglions de la base.

7.1 L'innervation sérotoninergique en conditions normales

Dans l'article qui constitue mon premier chapitre, nous avons pu fournir la première description anatomique complète de l'innervation 5-HT des ganglions de la base chez l'humain. Les neurones du NRD et du NRM ont montré des axones qui traversent le tronc cérébral en passant par le système transtegmentaire pour ensuite progresser vers le faisceau prosencéphalique médian pour rejoindre les principaux noyaux des ganglions de la base. Les axones 5-HT s'arborisent dans toutes les composantes des ganglions de la base avec la substance noire recevant l'innervation la plus dense et le striatum la plus hétérogène. Même si le striatum semble être la cible terminale pour beaucoup d'axones 5-HT ascendants, nos résultats indiquent que le système neuronal 5-HT hautement distribué est capable d'influencer directement l'activité des neurones des 2 principales structures de sortie des ganglions de la base, c'est-à-dire le GPi et la SNr. Ce système semble aussi avoir un accès direct aux neurones DA responsables de l'innervation nigrostriée, une découverte qui met en valeur l'importance de l'interaction 5-HT/DA dans la physiopathologie des ganglions de la base.

L'étude composant mon deuxième chapitre a révélé de nouveaux aspects de l'organisation des projections ascendantes du NRD chez le rat. Cette étude nous a permis pour la toute première fois d'apprécier l'étendue et la nature hautement collatéralisée de l'innervation 5-HT provenant du NRD au niveau neuronal unitaire. Ces injections de traceurs antérogrades nous ont aussi permis de faire la première démonstration de la distribution de VGLUT3 dans un seul axone marqué. Nos données indiquent qu'un sous-groupe d'axone 5-HT est dépourvu de VGLUT3 et que cette proportion varie selon la structure cible. Ces observations supportent l'existence d'un système complexe d'aiguillage de différents types de vésicules synaptiques à l'intérieur des axones hautement collatéralisés des neurones du DRN. Cette étude nous a aussi permis de mettre en lumière que, basés sur la diversité des patrons d'innervation de leurs projections axonales, les neurones du NRD forment une population hautement hétérogène.

7.1.2. La colibération de neurotransmetteurs

Il est difficile de parler du système 5-HT sans parler de la colibération de neurotransmetteurs. Cette facette de l'innervation 5-HT récemment découverte (Fremeau *et al.*, 2002; Gras *et al.*, 2002; Hioki *et al.*, 2010; Kiyasova *et al.*, 2011; Gaspar & Lillesaar, 2012) ouvre la porte à de nombreuses hypothèses. En effet, le rôle de la libération de glutamate par les axones 5-HT est encore nébuleux. La colibération de neurotransmetteurs est loin d'être un phénomène unique, il est donc normal que certaines hypothèses reposent sur les résultats déjà disponibles concernant d'autres systèmes. Tout comme les neurones 5-HT, les interneurones cholinergiques striataux peuvent emmagasiner et libérer le glutamate par l'expression de VGLUT3 (Gras *et al.*, 2002; Nickerson Poulin *et al.*, 2006). La libération de glutamate par les axones cholinergiques permet de faciliter la libération d'ACh suivant un phénomène que l'on appelle « synergie vésiculaire » (Gras *et al.*, 2008; Nelson *et al.*, 2014a). À ce jour, aucune étude n'a permis de confirmer ce genre de phénomène pour les axones

5-HT. La distribution de VGLUT3 dans les axones ACh indique la présence de cette protéine dans pratiquement toutes les varicosités axonales (Gras *et al.*, 2002; Schafer *et al.*, 2002; Boulland *et al.*, 2004).

Nos travaux sur la distribution de VGLUT3 à l'intérieur d'axones 5-HT chez le rat nous ont permis d'observer une distribution hétérogène de cette protéine. En effet, tout dépendant de la région innervée, la proportion de varicosités axonales 5-HT qui expriment VGLUT3 tend à varier, et ce, pour un même axone. Cette caractéristique permet de croire qu'il y a très probablement un système d'aiguillage lors du transport de cette protéine conduisant à une distribution du VGLUT3 hétérogène. Celle-ci permettrait aux varicosités axonales contenant VGLUT3 d'influencer les cibles postsynaptiques grâce à un relâchement synaptique rapide de glutamate, donc de modifier significativement l'action de la 5-HT dans les structures cibles où les axones 5-HT contiennent plus de VGLUT3. Ce signal excitateur rapide permettrait de complémenter l'action neuromodulatrice de la 5-HT qui agit sur une fenêtre de temps plus longue (voir El Mestikawy *et al.*, 2011). De plus, tel que mentionné plus haut, les axones 5-HT utilisent deux modes de libération; synaptique et volumique. La libération volumique est la plus communément rencontrée dans le système 5-HT(voir Descarries & Mechawar, 2008). D'un autre côté, les axones glutamatergiques libèrent leurs neurotransmetteurs presque que totalement de manière synaptique (voir Chua *et al.*, 2010). De plus, les niveaux de glutamate extracellulaires sont hautement régulés par les cellules gliales et d'autres processus de dégradation et de recapture faisant en sorte que la demi-vie de ce neurotransmetteur dans le milieu extracellulaire est limitée (voir Bergles *et al.*, 1999). Ces facettes de la libération de glutamate nous permettent d'émettre l'hypothèse que les varicosités axonales 5-HT contenant le VGLUT3 seraient plus susceptibles de former des synapses. Cette supposition pourrait se montrer particulièrement pertinente dans certains processus pathologiques où, comme chez nos singes parkinsoniens, une augmentation de l'incidence synaptique de l'innervation 5-HT est observée. Ces données suggéraient que ces varicosités axonales 5-HT dans le striatum

exprimeraient VGLUT3 plus fréquemment qu'en condition normale, conduisant à une formation de synapses accrue. Malheureusement, nous n'avons pas pu tester cette hypothèse dans notre cadre expérimental vu l'indisponibilité d'anticorps spécifiques à VGLUT3 chez les primates. Il serait donc pertinent de mener des études approfondies en microscopie électronique chez le rongeur afin de déterminer le rôle de VGLUT3 dans les neurones 5-HT concernant la formation de synapse et des changements apportés par cette protéine dans un processus pathologique telle la maladie de Parkinson.

7.2. Changement de la microcircuiterie des ganglions de la base dans la maladie de Parkinson

Dans le cadre de cette thèse, deux composantes des ganglions de la base ont été particulièrement étudiées : le GP et le striatum. Ces deux structures à l'organisation neuroanatomique et aux fonctions bien différentes jouent un rôle clé dans le contrôle moteur. Les changements plastiques majeurs qu'elles subissent dans la maladie de Parkinson sont à la fois similaires dans leur augmentation et différents dans leur portée ainsi que dans les changements morphologiques fins présents dans les varicosités axonales.

L'étude du striatum présentée au chapitre 4 a fourni la première description quantitative et ultrastructurelle détaillée de changements neuroadaptatifs majeurs que subissent les axones 5-HT striataux chez le singe intoxiqué au MPTP. La distribution régionale de l'innervation 5-HT et DA chez le singe MPTP comparée au contrôle démontre une relation particulière entre la dénervation DA et l'hyperinnervation 5-HT, dans l'un des modèles les plus fidèles de la maladie de Parkinson. Pour la première fois, des observations en microscopie électronique nous ont permis d'observer le rôle majeur que les axones 5-HT jouent dans le réarrangement de la microcircuiterie striatale qui se produit dans la maladie de Parkinson. Nos résultats indiquent qu'une hyperinnervation 5-HT coïncide avec une déplétion DA marquée. Cette hyperinnervation 5-HT est particulièrement évidente dans le territoire sensorimoteur striatal qui subit

la dénervation DA la plus importante. La présence de plusieurs vésicules synaptiques et l'incidence synaptique significativement plus élevée des varicosités axonales 5-HT observées chez le singe MPTP indiquent que le bourgeonnement des axones 5-HT pourrait favoriser la relâche de 5-HT, mais pourraient aussi potentialiser la relâche de DA et l'expression des DILs.

L'étude du GP présenté au chapitre 5 a fourni, quant à elle, la première description quantitative et ultrastructurelle détaillée des changements neuroadaptatifs que subissent les afférences 5-HT et DA pallidales chez un modèle de primate non-humain de la maladie de Parkinson. Nos estimations stéréologiques montrent une augmentation significative de l'innervation 5-HT pallidale chez le singe MPTP comparativement au groupe contrôle, particulièrement dans la partie antérieure du GP, où résident les territoires fonctionnels limbique et associatif. Du côté de l'innervation DA, nous avons observé une hyperinnervation significative du GPi chez le singe MPTP qui contraste fortement avec la dégénération massive de la voie nigrostriée. Cette hyperinnervation DA est en moyenne plus prononcée que l'hyperinnervation 5-HT et semble se produire principalement dans les régions postérieures du GPi, où les territoires sensorimoteurs se trouvent. Nous supposons que ces changements neuroadaptatifs significatifs de l'innervation pallidale 5-HT et DA jouent un rôle important, respectivement, dans l'expression précoce des symptômes non-moteurs et dans l'expression retardée des symptômes moteurs de la maladie de Parkinson.

L'augmentation de l'innervation 5-HT dans le striatum et le GP ne fait aucun doute d'après nos estimations stéréologique. Le bourgeonnement des axones 5-HT dans le GP est beaucoup plus important (GPe : 91%et GPi : 74%) que dans le striatum (36%). Contrairement à ce que l'on avait soupçonné dans le chapitre 4 de la thèse, il semble que le bourgeonnement des axones 5-HT ne soit pas simplement corrélé à la dénervation DA. En effet, la perte d'axone DA est beaucoup moins importante dans le GP par rapport au striatum dans nos modèles. Une conservation de l'innervation DA a aussi été rapportée dans les

deux segments du GP (Parent *et al.*, 1990; Schneider & Dacko, 1991; Parent & Lavoie, 1993; Mounayar *et al.*, 2007b; Dopeso-Reyes *et al.*, 2014). Après une intoxication au MPTP chez le singe, nos résultats démontrent sans aucun doute et pour la première fois que l'innervation DA bourgeonne de façon importante dans le GPi. Cette hyperinnervation DA se traduit principalement par une augmentation de 1289% des axones variqueux et d'une augmentation significative de la densité de varicosités DA dans la partie postérieure du GPi. L'hyperinnervation 5-HT plus importante dans le GP que dans le striatum pourrait s'expliquer par le changement majeur d'activité électrophysiologique que le GP subit lors d'une dénervation DA. En effet, le chamboulement de la régulation de l'activité des NPS emmène une disinhibition des neurones du GPi, une hyperactivité qui mène à une inhibition du mouvement. Des changements neuroadaptatifs importants s'organiseraient chez les axones DA des neurones restants de la SNc ainsi que chez les axones 5-HT.

Ces variations d'activités neuronales pourraient être la cause de la plupart de ces changements plastiques chez les neurones 5-HT qui seraient plutôt des changements compensatoires visant à rétablir une activité neuronale plus normale dans les 2 parties du GP. De plus, à la lumière d'une étude récente, la production de facteur neurotrophique issu du cerveau (BDNF) pourrait aussi influencer les changements plastiques montrés par les axones 5-HT (Tronci *et al.*, 2017). Ces travaux montrent qu'après une lésion DA chez le rat, la surexpression de BDNF mène à un bourgeonnement accru des axones 5-HT dans le GP et le striatum. Il semble même que cette hyperinnervation pourrait être plus importante dans le GP ce qui suggère possiblement que les axones 5-HT innervant cette structure soient plus sensibles aux variations de BDNF. Ces résultats pourraient donc expliquer une partie des différences observées entre le bourgeonnement de l'innervation 5-HT du striatum et du GP.

Du côté de l'innervation DA striatale, aucun phénomène compensatoire n'a pu être observé chez les axones DA restants. La lésion produite par l'administration de MPTP affecte la grande majorité des axones DA (environ

seulement 10% des axones survivent). Effectivement, seulement la partie ventromédiane du putamen située à la bordure de la lame médullaire externe semble conserver une immunoréactivité TH relativement élevée. Il est aussi intéressant de mentionner que les parties dorsales du putamen et du noyau caudé, régions les plus dénervées en DA, étaient celles qui montrent l'augmentation de densité de varicosités 5-HT la plus importante. De plus, la région la moins dénervée en DA, le noyau accumbens, ne montre aucun changement au niveau des axones 5-HT. La dénervation DA est l'un des facteurs les plus importants causant un changement d'activité des NPS, il est possible de supposer que l'activité des NPS dans le noyau accumbens est donc beaucoup moins altérée que dans le striatum dorsal. Ces observations pourraient aussi appuyer que le changement d'activité important des neurones d'une structure puisse induire la plasticité des axones 5-HT.

Cette thèse a aussi traité des changements morphologiques fins tel qu'observés en microscopie électronique. Les varicosités axonales 5-HT dans le striatum montrent une incidence synaptique plus élevée chez les singes intoxiqués au MPTP par rapport aux singes contrôles (44% vs 18%). Un phénomène que l'on ne retrouve pas dans le GP (19% chez le singe MPTP comparé à 27% chez les animaux contrôles). Par contre, les incidences synaptiques obtenues dans le GP sont similaires à celles estimées dans le noyau accumbens une région où aucune dénervation DA significative n'est observée après une intoxication au MPTP chez le singe. En condition normale, la distance moyenne entre les varicosités DA est estimée à 4 µm (Gonon, 1997). Ce chiffre met en perspective le grand vide que laisse la dénervation DA dans le striatum ce qui ferait en sorte d'enclencher une multitude de changements plastique dans la structure. De plus, cette perte d'axone entraine une diminution significative des entrées synaptiques sur les NPS comme le montrent nos résultats et d'autres études (Ingham *et al.*, 1989; Ingham *et al.*, 1998; Day *et al.*, 2006; Villalba *et al.*, 2009b; Fieblinger *et al.*, 2014; Suarez *et al.*, 2014). Les axones DA interagissent principalement avec les NPS formant des synapses axosomatiques, axodendritiques et axoépineuses, (Freund *et al.*,

1984)et ce pour environ 40% des varicosités axonales (Descarries *et al.*, 1996). Les contacts axoépineux forment la majorité des interactions synaptiques des axones DA et interagissent avec le cou et la tête des épines dendritiques (Freund *et al.*, 1984; Groves *et al.*, 1994). Cette interaction semble d'ailleurs cruciale dans le maintien de l'intégrité des épines dendritiques et des synapses corticostriées chez les NPS (Ingham *et al.*, 1989; Ingham *et al.*, 1998; Day *et al.*, 2006; Villalba *et al.*, 2009b; Fieblinger *et al.*, 2014; Suarez *et al.*, 2014). Les axones 5-HT du striatum chercheraient alors à combler le vide laissé par les axones DA en reformant une partie des synapses manquantes. Le nombre de nouvelles varicosités estimées dans le striatum est d'ailleurs augmenté de même que l'incidence synaptique suggérant que le bourgeonnement axonal aurait pour but de combler ce manque de synapses sur les dendrites et les épines des NPS. Dans cette optique, il serait intéressant de savoir si une lésion complète de l'innervation 5-HT striatale pourrait induire une augmentation de l'incidence synaptique chez les axones DA innervant le striatum. Ce genre d'expérience pourrait permettre de savoir si un équilibre existe entre les synapses des varicosités axonales 5-HT et DA. Il serait aussi intéressant d'établir si ce genre de lésion serait capable d'influencer significativement le domaine somatodendritique des NPS de la voie directe et indirecte et d'ainsi établir le rôle de l'innervation 5-HT striatale dans le maintien des épines dendritiques des neurones de projections striataux.

Du côté du GP, tel que mentionné plus haut, il ne semble pas y avoir de changements significatifs de l'incidence synaptique des varicosités 5-HT après une intoxication au MPTP. Le même constat peut être fait au niveau des axones DA (13% vs 7%). Il est quand même intéressant de mentionner que le nombre total de synapses 5-HT et DA se retrouve augmenté dans le GP suite à une lésion DA grâce à l'augmentation du nombre de varicosités axonales. Aucune étude n'est actuellement disponible sur de possibles modifications postsynaptiques que ce genre d'augmentations pourrait induire chez les neurones du GP. Cette augmentation, comme expliquée dans les chapitres 4 et 5, pourrait être en mesure de modifier significativement le domaine

somatodendritique des neurones du GP. Cet aspect des phénomènes neuroadaptatifs subis par le GP serait une piste intéressante à suivre dans des études morphologiques subséquentes afin de mieux comprendre ces mécanismes compensatoires dans le GP après une lésion DA.

La réorganisation de la microcuiterie du striatum peut aussi se présenter dans les NPS. L'étude dont le chapitre 6 fait l'objet nous a permis de faire la première description des caractéristiques morphologiques, de la densité et de la distribution régionale de NPS D_1/D_2 du striatum dorsal et noyau accumbens chez la souris normale, en plus de fournir la première caractérisation des changements induits par la dénervation DA striatal chez cette population neuronale. Nos résultats ont permis de démontrer que les NPS D_1/D_2 forment une population morphologiquement distincte des NPS D_1 et NPS D_2 : ils ont un plus petit corps cellulaire, une arborisation dendritique moins complexe qui montre moins d'épines dendritiques que les NPS D_1 et NPS D_2. Les NPS D_1/D_2 sont uniformément distribués dans le striatum où ils représentent approximativement 2% du nombre total de NPS, mais ils sont distribués de manière hétérogène et plus abondant dans le noyau accumbens, où leur proportion se situe entre 7 à 15% de tous les NPS. Chez la souris lésée à la 6-OHDA, la densité et la distribution des 3 types de NPS restent inchangées. Contrairement aux NPS D_1 et NPS D_2, les NPS D_1/D_2 ne montrent aucune réduction de la longueur totale de leurs dendrites après une intoxication au 6-OHDA. Par contre, une réduction de la densité d'épines dendritiques a été notée chez les 3 types de NPS, mais cette réduction était plus proéminente chez les NPS D_1 que chez les D_2 et D_1/D_2. La fonction exacte des NPS D_1/D_2 reste encore un mystère. Il n'est toujours pas défini si ces neurones composent une voie neuronale distincte des NPS D_1 et NPS D_2. Par contre, si une telle voie existait, cela suggérait un rôle fonctionnel complémentaire des NPS D_1/D_2, travaillant de concert avec les NPS D_1 et NPS D_2 dans le fonctionnement harmonieux des ganglions de la base.

7.3. Conclusion

Les derniers chapitres de cette thèse ont rendu possible la démonstration de l'importance de l'hétérogénéité de l'innervation 5-HT des différentes composantes des ganglions de la base, une caractéristique qui reflète la pluralité des rôles que ce neuromodulateur peut jouer dans le système nerveux central. Il a aussi été possible de mettre en lumière des phénomènes plastiques majeurs que subissent les axones 5-HT dans un modèle de la maladie de Parkinson. Cette capacité à s'adapter montre la polyvalence de ce neurotransmetteur comme neuromodulateur capable de contribuer au maintien d'une activité normale de certaines composantes des ganglions de la base, malgré une insulte neurodégénérative. Cette thèse démontre aussi que d'autres neuromodulateurs comme la DA peuvent voir leur innervation grandement augmentée même lorsqu'ils subissent des processus dégénératifs. De plus, il a été possible de faire la démonstration que ces changements majeurs d'innervations de DA et de 5-HT sont en mesure d'induire des modifications importantes du domaine somatodendritique des neurones ciblés. En effet, les différents sous-types de NPS du striatum sont affectés morphologiquement de manières différentes suite à une dénervation DA importante du striatum. Les approches méthodologiques utilisées dans le cadre de ces projets sont uniques et apportent à la communauté scientifique des descriptions d'une précision et d'une qualité inégalée concernant la plasticité dans les ganglions de la base qui survient dans la maladie de Parkinson.

Les mécanismes compensatoires observés et quantifiés dans le cadre de cette thèse mettent en valeur le caractère neuroadaptatif de la microcircuiterie des ganglions de la base. Il permet de constater que ce regroupement de structure a l'incroyable capacité de se réorganiser afin de faire face à des phénomènes neurodégénératifs majeurs. Cependant, il reste énormément de travail à effectuer afin d'étudier l'ensemble des phénomènes compensatoires prenant place lors d'une dégénérescence des neurones DA de la SNc. Des études stéréologiques et morphologiques plus approfondies du système 5-HT dans les

autres composantes des ganglions de la base seraient sans aucun doute nécessaires en plus de l'étude d'autres systèmes neuronaux neuromodulateurs comme les systèmes cholinergique et noradrénergique. Ces résultats permettraient de mieux comprendre la pathophysiologie de la maladie de Parkinson en plus de mieux comprendre les changements neuroadaptatifs menant, par exemple, à l'apparition des DILs ainsi qu'à l'apparition des symptômes moteurs et non-moteurs associés à cette pathologie.

8. Bibliographie

(2001) Deep-brain stimulation of the subthalamic nucleus or the pars interna of the globus pallidus in Parkinson's disease. *N Engl J Med*, **345**, 956-963.

Absher, J.R., Vogt, B.A., Clark, D.G., Flowers, L.D., Gorman, G.D., Keyes, J.W. & Wood, F.B. (2000) Hypersexuality and hemiballism due to subthalamic infarction. *Cognitive and Behavioral Neurology*, **13**, 220-229.

Afsharpour, S. (1985) Topographical projections of the cerebral cortex to the subthalamic nucleus. *Journal of Comparative Neurology*, **236**, 14-28.

Aghajanian, G. & Wang, R.Y. (1977) Habenular and other midbrain raphe afferents demonstrated by a modified retrograde tracing technique. *Brain research*, **122**, 229-242.

Agid, Y. (1991) Parkinson's disease: pathophysiology. *Lancet*, **337**, 1321-1324.

Åhlander-Lüttgen, M., Madjid, N., Schött, P.A., Sandin, J. & Ögren, S.O. (2003) Analysis of the role of the 5-HT1B receptor in spatial and aversive learning in the rat. *Neuropsychopharmacology : official publication of the American College of Neuropsychopharmacology*, **28**, 1642.

Aizman, O., Brismar, H., Uhlen, P., Zettergren, E., Levey, A.I., Forssberg, H., Greengard, P. & Aperia, A. (2000) Anatomical and physiological evidence for D1 and D2 dopamine receptor colocalization in neostriatal neurons. *Nat Neurosci*, **3**, 226-230.

Albin, R.L., Koeppe, R.A., Bohnen, N.I., Wernette, K., Kilbourn, M.A. & Frey, K.A. (2008) Spared caudal brainstem SERT binding in early Parkinson's disease. *Journal of Cerebral Blood Flow & Metabolism*, **28**, 441-444.

Albin, R.L., Young, A.B. & Penney, J.B. (1989) The functional anatomy of basal ganglia disorders. *Trends in neurosciences*, **12**, 366-375.

Albin, R.L., Young, A.B. & Penney, J.B. (1995) The functional anatomy of disorders of the basal ganglia. *Trends in neurosciences*, **18**, 63-64.

Alex, K.D., Yavanian, G.J., McFarlane, H.G., Pluto, C.P. & Pehek, E.A. (2005) Modulation of dopamine release by striatal 5-HT2C receptors. *Synapse*, **55**, 242-251.

Alexander, G.E. & DeLong, M.R. (1985) Microstimulation of the primate neostriatum. I. Physiological properties of striatal microexcitable zones. *J Neurophysiol*, **53**, 1401-1416.

Alexander, G.E., DeLong, M.R. & Strick, P.L. (1986) Parallel organization of functionally segregated circuits linking basal ganglia and cortex. *Annual review of neuroscience*, **9**, 357-381.

Allers, K.A. & Sharp, T. (2003) Neurochemical and anatomical identification of fast- and slow-firing neurones in the rat dorsal raphe nucleus using juxtacellular labelling methods in vivo. *Neuroscience*, **122**, 193-204.

Amilhon, B., Lepicard, E., Renoir, T., Mongeau, R., Popa, D., Poirel, O., Miot, S., Gras, C., Gardier, A.M., Gallego, J., Hamon, M., Lanfumey, L., Gasnier, B., Giros, B. & El Mestikawy, S. (2010) VGLUT3 (vesicular glutamate transporter type 3) contribution to the regulation of serotonergic transmission and anxiety. *The Journal of neuroscience : the official journal of the Society for Neuroscience*, **30**, 2198-2210.

Antonini, A., Vontobel, P., Psylla, M., Günther, I., Maguire, P.R., Missimer, J. & Leenders, K.L. (1995) Complementary positron emission tomographic studies of the striatal dopaminergic system in Parkinson's disease. *Archives of Neurology*, **52**, 1183-1190.

Aosaki, T., Miura, M., Suzuki, T., Nishimura, K. & Masuda, M. (2010) Acetylcholine-dopamine balance hypothesis in the striatum: an update. *Geriatrics & gerontology international*, **10 Suppl 1**, S148-157.

Arai, R., Karasawa, N., Geffard, M. & Nagatsu, I. (1995a) L-DOPA is converted to dopamine in serotonergic fibers of the striatum of the rat: a double-labeling immunofluorescence study. *Neurosci Lett*, **195**, 195-198.

Arai, R., Karasawa, N., Geffard, M. & Nagatsu, I. (1995b) L-DOPA is converted to dopamine in serotonergic fibers of the striatum of the rat: a double-labeling immunofluorescence study. *Neurosci Lett*, **195**, 195-198.

Arai, R., Karasawa, N., Geffard, M., Nagatsu, T. & Nagatsu, I. (1994) Immunohistochemical evidence that central serotonin neurons produce dopamine from exogenous L-DOPA in the rat, with reference to the involvement of aromatic L-amino acid decarboxylase. *Brain Res*, **667**, 295-299.

Arai, R., Karasawa, N. & Nagatsu, I. (1996) Aromatic L-amino acid decarboxylase is present in serotonergic fibers of the striatum of the rat. A double-labeling immunofluorescence study. *Brain research*, **706**, 177-179.

Ariano, M.A., Stromski, C.J., Smyk-Randall, E.M. & Sibley, D.R. (1992) D2 dopamine receptor localization on striatonigral neurons. *Neuroscience letters*, **144**, 215-220.

Arias, B., Gutierrez, B., Pintor, L., Gasto, C. & Fananas, L. (2001) Variability in the 5-HT2A receptor gene is associated with seasonal pattern in major depression. *Molecular psychiatry*, **6**, 239.

Arluison, M. & de la Manche, I.S. (1980) High-resolution radioautographic study of the serotonin innervation of the rat corpus striatum after intraventricular administration of [3H]5-hydroxytryptamine. *Neuroscience*, **5**, 229-240.

Arluison, M., Dietl, M. & Thibault, J. (1984) Ultrastructural morphology of dopaminergic nerve terminals and synapses in the striatum of the rat using tyrosine hydroxylase immunocytochemistry: a topographical study. *Brain research bulletin*, **13**, 269-285.

Arnsten, A. & Goldman-Rakic, P. (1984) Selective prefrontal cortical projections to the region of the locus coeruleus and raphe nuclei in the rhesus monkey. *Brain research*, **306**, 9-18.

Asai, H., Udaka, F., Hirano, M., Minami, T., Oda, M., Kubori, T., Nishinaka, K., Kameyama, M. & Ueno, S. (2005) Increased gastric motility during 5-HT 4 agonist therapy reduces response fluctuations in Parkinson's disease. *Parkinsonism Relat Disord*, **11**, 499-502.

Aubert, I., Ghorayeb, I., Normand, E. & Bloch, B. (2000) Phenotypical characterization of the neurons expressing the D1 and D2 dopamine receptors in the monkey striatum. *The Journal of comparative neurology*, **418**, 22-32.

Azmitia, E.C. & Gannon, P.J. (1986) The primate serotonergic system: a review of human and animal studies and a report on Macaca fascicularis. *Adv Neurol*, **43**, 407-468.

Azmitia, E.C. & Segal, M. (1978) An autoradiographic analysis of the differential ascending projections of the dorsal and median raphe nuclei in the rat. *The Journal of comparative neurology*, **179**, 641-667.

Baker, K.G., Halliday, G.M., Halasz, P., Hornung, J.P., Geffen, L.B., Cotton, R.G. & Tork, I. (1991a) Cytoarchitecture of serotonin-synthesizing neurons in the pontine tegmentum of the human brain. *Synapse*, **7**, 301-320.

Baker, K.G., Halliday, G.M., Hornung, J.P., Geffen, L.B., Cotton, R.G. & Tork, I. (1991b) Distribution, morphology and number of monoamine-synthesizing and substance P-containing neurons in the human dorsal raphe nucleus. *Neuroscience*, **42**, 757-775.

Balcioglu, A., Zhang, K. & Tarazi, F.I. (2003) Dopamine depletion abolishes apomorphine- and amphetamine-induced increases in extracellular serotonin levels in the striatum of conscious rats: a microdialysis study. *Neuroscience*, **119**, 1045-1053.

Ballanger, B., Beaudoin-Gobert, M., Neumane, S., Epinat, J., Metereau, E., Duperrier, S., Broussolle, E., Thobois, S., Bonnefoi, F., Tourvielle, C., Lavenne, F., Costes, N., Lebars, D., Zimmer, L., Sgambato-Faure, V. & Tremblay, L. (2016) Imaging Dopamine and Serotonin Systems on MPTP Monkeys: A Longitudinal PET Investigation of Compensatory Mechanisms. *J Neurosci*, **36**, 1577-1589.

Ballanger, B., Klinger, H., Eche, J., Lerond, J., Vallet, A.E., Le Bars, D., Tremblay, L., Sgambato-Faure, V., Broussolle, E. & Thobois, S. (2012) Role of serotonergic 1A receptor dysfunction in depression associated with Parkinson's disease. *Movement disorders : official journal of the Movement Disorder Society*, **27**, 84-89.

Ballanger, B., Strafella, A.P., van Eimeren, T., Zurowski, M., Rusjan, P.M., Houle, S. & Fox, S.H. (2010) Serotonin 2A receptors and visual hallucinations in Parkinson disease. *Archives of Neurology*, **67**, 416-421.

Ballard, P.A., Tetrud, J.W. & Langston, J.W. (1985) Permanent human parkinsonism due to 1-methy 1–4-phenyl-1, 2, 3, 6-tetrahydropyridine (MPTP) Seven cases. *Neurology*, **35**, 949-949.

Barbeau, A. (1962) The pathogenesis of Parkinson's disease: a new hypothesis. *Canadian Medical Association journal*, **87**, 802-807.

Barden, H. (1975) The histochemical relationships and the nature of neuromelanin. *Aging*, **1**, 79-117.

Barnes, N.M. & Sharp, T. (1999) A review of central 5-HT receptors and their function. *Neuropharmacology*, **38**, 1083-1152.

Basso, A.M. & Kelley, A.E. (1999) Feeding induced by GABA(A) receptor stimulation within the nucleus accumbens shell: regional mapping and characterization of macronutrient and taste preference. *Behavioral neuroscience*, **113**, 324-336.

Bastide, M.F., Meissner, W.G., Picconi, B., Fasano, S., Fernagut, P.-O., Feyder, M., Francardo, V., Alcacer, C., Ding, Y. & Brambilla, R. (2015) Pathophysiology of L-dopa-induced motor and non-motor complications in Parkinson's disease. *Progress in neurobiology*, **132**, 96-168.

Beaudet, A. & Descarries, L. (1978) The monoamine innervation of rat cerebral cortex: synaptic and nonsynaptic axon terminals. *Neuroscience*, **3**, 851-860.

Beaudet, A. & Sotelo, C. (1981) Synaptic remodeling of serotonin axon terminals in rat agranular cerebellum. *Brain Res*, **206**, 305-329.

Beaudoin-Gobert, M., Epinat, J., Metereau, E., Duperrier, S., Neumane, S., Ballanger, B., Lavenne, F., Liger, F., Tourvielle, C., Bonnefoi, F., Costes, N., Bars, D.L., Broussolle, E., Thobois, S., Tremblay, L. & Sgambato-Faure, V. (2015) Behavioural impact of a double dopaminergic and serotonergic lesion in the non-human primate. *Brain : a journal of neurology*, **138**, 2632-2647.

Beaulieu, J.M., Espinoza, S. & Gainetdinov, R.R. (2015) Dopamine receptors - IUPHAR Review 13. *British journal of pharmacology*, **172**, 1-23.

Beaulieu, J.M. & Gainetdinov, R.R. (2011) The physiology, signaling, and pharmacology of dopamine receptors. *Pharmacological reviews*, **63**, 182-217.

Beckstead, R. (1983a) Long collateral branches of substantia nigra pars reticulata axons to thalamus, superior colliculus and reticular formation in monkey and cat. Multiple retrograde neuronal labeling with fluorescent dyes. *Neuroscience*, **10**, 767-779.

Beckstead, R.M. (1983b) A pallidostriatal projection in the cat and monkey. *Brain research bulletin*, **11**, 629-632.

Beckstead, R.M., Domesick, V.B. & Nauta, W.J. (1993) Efferent connections of the substantia nigra and ventral tegmental area in the rat *Neuroanatomy*. Springer, pp. 449-475.

Bédard, C., Wallman, M.-J., Pourcher, E., Gould, P.V., Parent, A. & Parent, M. (2011) Serotonin and dopamine striatal innervation in Parkinson's disease and Huntington's chorea. *Parkinsonism Relat Disord*, **17**, 593-598.

Benabid, A.L., Chabardes, S., Mitrofanis, J. & Pollak, P. (2009) Deep brain stimulation of the subthalamic nucleus for the treatment of Parkinson's disease. *Lancet Neurol*, **8**, 67-81.

Benabid, A.L., Pollak, P., Louveau, A., Henry, S. & de Rougemont, J. (1987) Combined (thalamotomy and stimulation) stereotactic surgery of the VIM thalamic nucleus for bilateral Parkinson disease. *Appl Neurophysiol*, **50**, 344-346.

Benazzouz, A., Boraud, T., Feger, J., Burbaud, P., Bioulac, B. & Gross, C. (1996) Alleviation of experimental hemiparkinsonism by high-frequency stimulation of the subthalamic nucleus in primates: a comparison with L-Dopa treatment. *Movement disorders : official journal of the Movement Disorder Society*, **11**, 627-632.

Benloucif, S., Keegan, M.J. & Galloway, M.P. (1993) Serotonin-facilitated dopamine release in vivo: pharmacological characterization. *Journal of Pharmacology and Experimental Therapeutics*, **265**, 373-377.

Bennett, B.D. & Wilson, C.J. (2003) TANs, PANs and STANs. In Graybiel, A.M., Delong, M.R., Kitai, S.T. (eds) *The Basal Ganglia VI*. Springer US, Boston, MA, pp. 225-235.

Bennett, J.L. & Aghajanian, G.K. (1974) D-LSD binding to brain homogenates: possible relationship to serotonin receptors. *Life sciences*, **15**, 1935-1944.

Bennouar, K.-E., Uberti, M.A., Melon, C., Bacolod, M.D., Jimenez, H.N., Cajina, M., Kerkerian-Le Goff, L., Doller, D. & Gubellini, P. (2013) Synergy between L-DOPA and a novel positive allosteric modulator of metabotropic glutamate receptor 4: implications for Parkinson's disease treatment and dyskinesia. *Neuropharmacology*, **66**, 158-169.

Berding, G., Brücke, T., Odin, P., Brooks, D., Kolbe, H., Gielow, P., Harke, H., Knoop, B., Dengler, R. & Knapp, W. (2003) [123 I] β-CIT SPECT imaging of dopamine and serotonin transporters in Parkinson's disease and multiple system atrophy. *Nuklearmedizin Archive*, **42**, 31-38.

Berendse, H.W. & Groenewegen, H.J. (1990) Organization of the thalamostriatal projections in the rat, with special emphasis on the ventral striatum. *Journal of Comparative Neurology*, **299**, 187-228.

Berger, T.W., Kaul, S., Stricker, E.M. & Zigmond, M.J. (1985) Hyperinnervation of the striatum by dorsal raphe afferents after dopamine-depleting brain lesions in neonatal rats. *Brain Res*, **336**, 354-358.

Bergles, D.E., Diamond, J.S. & Jahr, C.E. (1999) Clearance of glutamate inside the synapse and beyond. *Current opinion in neurobiology*, **9**, 293-298.

Bergman, H., Wichmann, T. & DeLong, M.R. (1990) Reversal of experimental parkinsonism by lesions of the subthalamic nucleus. *Science*, **249**, 1436-1438.

Bernheimer, H., Birkmayer, W. & Hornykiewicz, O. (1961) Distribution of 5-hydroxytryptamine (serotonin) in the human brain and its behavior in patients with Parkinson's syndrome. *Klinische Wochenschrift*, **39**, 1056-1059.

Bernheimer, H., Birkmayer, W., Hornykiewicz, O., Jellinger, K. & Seitelberger, F. (1973a) Brain dopamine and the syndromes of Parkinson and Huntington Clinical, morphological and neurochemical correlations. *Journal of the neurological sciences*, **20**, 415-455.

Bernheimer, H., Birkmayer, W., Hornykiewicz, O., Jellinger, K. & Seitelberger, F. (1973b) Brain dopamine and the syndromes of Parkinson and Huntington. Clinical, morphological and neurochemical correlations. *J Neurol Sci*, **20**, 415-455.

Bertran-Gonzalez, J., Bosch, C., Maroteaux, M., Matamales, M., Herve, D., Valjent, E. & Girault, J.A. (2008) Opposing patterns of signaling activation in dopamine D1 and D2 receptor-expressing striatal neurons in response to cocaine and haloperidol. *The Journal of neuroscience : the official journal of the Society for Neuroscience*, **28**, 5671-5685.

Bérubé-Carrière, N., Riad, M., Dal Bo, G., Lévesque, D., Trudeau, L.E. & Descarries, L. (2009) The dual dopamine-glutamate phenotype of growing mesencephalic neurons regresses in mature rat brain. *The Journal of comparative neurology*, **517**, 873-891.

Bérubé-Carrière, N., Guay, G., Fortin, G.M., Kullander, K., Olson, L., Wallén-Mackenzie, Å., Trudeau, L.E. & Descarries, L. (2012) Ultrastructural characterization of the mesostriatal dopamine innervation in

mice, including two mouse lines of conditional VGLUT2 knockout in dopamine neurons. *European Journal of Neuroscience*, **35**, 527-538.

Beucke, J., Plotkin, M., Winter, C., Endrass, T., Amthauer, H., Juckel, G. & Kupsch, A. (2011) Midbrain serotonin transporters in de novo and L-DOPA-treated patients with early Parkinson's disease–a [123I]-ADAM SPECT study. *European journal of neurology*, **18**, 750-755.

Bez, F., Francardo, V. & Cenci, M.A. (2016) Dramatic differences in susceptibility to l-DOPA-induced dyskinesia between mice that are aged before or after a nigrostriatal dopamine lesion. *Neurobiol Dis*, **94**, 213-225.

Bezard, E., Brotchie, J.M. & Gross, C.E. (2001a) Pathophysiology of levodopa-induced dyskinesia: potential for new therapies. *Nat Rev Neurosci*, **2**, 577-588.

Bezard, E., Dovero, S., Prunier, C., Ravenscroft, P., Chalon, S., Guilloteau, D., Crossman, A.R., Bioulac, B., Brotchie, J.M. & Gross, C.E. (2001b) Relationship between the appearance of symptoms and the level of nigrostriatal degeneration in a progressive 1-methyl-4-phenyl-1,2,3,6-tetrahydropyridine-lesioned macaque model of Parkinson's disease. *J Neurosci*, **21**, 6853-6861.

Bezard, E., Gross, C.E., Fournier, M.-C., Dovero, S., Bloch, B. & Jaber, M. (1999) Absence of MPTP-induced neuronal death in mice lacking the dopamine transporter. *Experimental neurology*, **155**, 268-273.

Biezonski, D.K., Trifilieff, P., Meszaros, J., Javitch, J.A. & Kellendonk, C. (2015) Evidence for limited D1 and D2 receptor coexpression and colocalization within the dorsal striatum of the neonatal mouse. *The Journal of comparative neurology*, **523**, 1175-1189.

Birket-Smith, E. (1975) Abnormal involuntary movements in relation to anticholinergics and levodopa therapy. *Acta neurologica Scandinavica*, **52**, 158-160.

Birkmayer, W. & Birkmayer, J.D. (1987) Dopamine action and disorders of neurotransmitter balance. *Gerontology*, **33**, 168-171.

Birkmayer, W. & Hornykiewicz, O. (1962) Der L-Dioxyphenylalanin (= L-DOPA)-Effekt beim Parkinson-Syndrom des Menschen: Zur Pathogenese und Behandlung der Parkinson-Akinese. *European Archives of Psychiatry and Clinical Neuroscience*, **203**, 560-574.

Bishop, C., Krolewski, D.M., Eskow, K.L., Barnum, C.J., Dupre, K.B., Deak, T. & Walker, P.D. (2009) Contribution of the striatum to the effects of 5-HT1A receptor stimulation in L-DOPA-treated hemiparkinsonian rats. *J Neurosci Res*, **87**, 1645-1658.

Björklund, A. & Dunnett, S.B. (2007) Dopamine neuron systems in the brain: an update. *Trends in neurosciences*, **30**, 194-202.

Bjorklund, A. & Lindvall, O. (1975) Dopamine in dendrites of substantia nigra neurons: suggestions for a role in dendritic terminals. *Brain Res*, **83**, 531-537.

Björklund, A. & Lindvall, O. (1984) Dopamine-containing systems in the CNS: In: Björklund A and Hökfelt T (eds.) Handbook of chemical neuroanatomy, Vol 2: Classical transmitters in the CNS, part 1. Elsevier, Amsterdam.

Blier, P. & Ward, N.M. (2003) Is there a role for 5-HT 1A agonists in the treatment of depression? *Biological psychiatry*, **53**, 193-203.

Blue, M.E., Yagaloff, K.A., Mamounas, L.A., Hartig, P.R. & Molliver, M.E. (1988) Correspondence between 5-HT 2 receptors and serotonergic axons in rat neocortex. *Brain research*, **453**, 315-328.

Boileau, I., Warsh, J.J., Guttman, M., Saint-Cyr, J.A., McCluskey, T., Rusjan, P., Houle, S., Wilson, A.A., Meyer, J.H. & Kish, S.J. (2008) Elevated serotonin transporter binding in depressed patients with Parkinson's disease: a preliminary PET study with [11C] DASB. *Movement disorders*, **23**, 1776-1780.

Bolam, J. & Smith, Y. (1990) The GABA and substance P input to dopaminergic neurones in the substantia nigra of the rat. *Brain research*, **529**, 57-78.

Bolam, J., Wainer, B. & Smith, A. (1984) Characterization of cholinergic neurons in the rat neostriatum. A combination of choline acetyltransferase immunocytochemistry, Golgi-impregnation and electron microscopy. *Neuroscience*, **12**, 711-718.

Bolam, J.P. & Pissadaki, E.K. (2012a) Living on the edge with too many mouths to feed: why dopamine neurons die. *Mov Disord*, **27**, 1478-1483.

Bolam, J.P. & Pissadaki, E.K. (2012b) Living on the edge with too many mouths to feed: why dopamine neurons die. *Movement Disorders*, **27**, 1478-1483.

Bonaventure, P., Hall, H., Gommeren, W., Cras, P., Langlois, X., Jurzak, M. & Leysen, J.E. (2000) Mapping of serotonin 5-HT4 receptor mRNA and ligand binding sites in the post-mortem human brain. *Synapse*, **36**, 35-46.

Bonaventure, P., Langlois, X. & Leysen, J. (1998a) Co-localization of 5-HT 1B-and 5-HT 1D receptor mRNA in serotonergic cell bodies in guinea pig dorsal raphe nucleus: a double labeling in situ hybridization histochemistry study. *Neurosci Lett*, **254**, 113-116.

Bonaventure, P., Voorn, P., Luyten, W., Jurzak, M., Schotte, A. & Leysen, J. (1997) Detailed mapping of serotonin 5-HT 1B and 5-HT 1D receptor messenger RNA and ligand binding sites in guinea-pig brain and trigeminal ganglion: clues for function. *Neuroscience*, **82**, 469-484.

Bonaventure, P., Voorn, P., Luyten, W.H., Jurzak, M., Schotte, A. & Leysen, J.E. (1998b) Detailed mapping of serotonin 5-HT1B and 5-HT1D receptor messenger RNA and ligand binding sites in guinea-pig brain and trigeminal ganglion: clues for function. *Neuroscience*, **82**, 469-484.

Bordia, T., Campos, C., McIntosh, J.M. & Quik, M. (2010) Nicotinic receptor-mediated reduction in L-DOPA-induced dyskinesias may occur via desensitization. *The Journal of pharmacology and experimental therapeutics*, **333**, 929-938.

Bories, C., Husson, Z., Guitton, M.J. & De Koninck, Y. (2013) Differential balance of prefrontal synaptic activity in successful versus unsuccessful cognitive aging. *The Journal of neuroscience : the official journal of the Society for Neuroscience*, **33**, 1344-1356.

Boulet, S., Mounayar, S., Poupard, A., Bertrand, A., Jan, C., Pessiglione, M., Hirsch, E.C., Feuerstein, C., Francois, C., Feger, J., Savasta, M. & Tremblay, L. (2008) Behavioral recovery in MPTP-treated monkeys: neurochemical mechanisms studied by intrastriatal microdialysis. *The Journal of neuroscience : the official journal of the Society for Neuroscience*, **28**, 9575-9584.

Boulland, J.L., Qureshi, T., Seal, R.P., Rafiki, A., Gundersen, V., Bergersen, L.H., Fremeau, R.T., Edwards, R.H., Storm-Mathisen, J. & Chaudhry, F.A. (2004) Expression of the vesicular glutamate transporters during development indicates the widespread corelease of multiple neurotransmitters. *Journal of Comparative Neurology*, **480**, 264-280.

Bourque, M., Morissette, M. & Di Paolo, T. (2015) Neuroprotection in Parkinsonian-treated mice via estrogen receptor alpha activation requires G protein-coupled estrogen receptor 1. *Neuropharmacology*, **95**, 343-352.

Bowden, D.M. & Martin, R.F. (2000a) *Primate brain maps : structure of the macaque brain*. Elsevier, Amsterdam.

Bowden, D.M. & Martin, R.F. (2000b) Primate brain maps : structure of the macaque brain. Elsevier,, Amsterdam ; New York, pp. viii, 160 p. ill. 129 cm. + 161 computer optical disc (164 163/164 in.).

Braak, H., Del Tredici, K., Rüb, U., de Vos, R.A., Steur, E.N.J. & Braak, E. (2003a) Staging of brain pathology related to sporadic Parkinson's disease. *Neurobiology of aging*, **24**, 197-211.

Braak, H., Ghebremedhin, E., Rüb, U., Bratzke, H. & Del Tredici, K. (2004) Stages in the development of Parkinson's disease-related pathology. *Cell and tissue research*, **318**, 121-134.

Braak, H., Rub, U., Gai, W.P. & Del Tredici, K. (2003b) Idiopathic Parkinson's disease: possible routes by which vulnerable neuronal types may be subject to neuroinvasion by an unknown pathogen. *J Neural Transm*, **110**, 517-536.

Braak, H., Rüb, U., Steur, E.J., Del Tredici, K. & De Vos, R. (2005) Cognitive status correlates with neuropathologic stage in Parkinson disease. *Neurology*, **64**, 1404-1410.

Breese, G.R., Baumeister, A.A., McCOWN, T.J., Emerick, S.G., Frye, G.D., Crotty, K. & Mueller, R.A. (1984) Behavioral differences between neonatal and adult 6-hydroxydopamine-treated rats to dopamine agonists: relevance to neurological symptoms in clinical syndromes with reduced brain dopamine. *Journal of Pharmacology and Experimental Therapeutics*, **231**, 343-354.

Breier, A. (1995) Serotonin, schizophrenia and antipsychotic drug action. *Schizophrenia research*, **14**, 187-202.

Brooks, D., Ibanez, V., Sawle, G., Quinn, N., Lees, A., Mathias, C., Bannister, R., Marsden, C. & Frackowiak, R. (1990) Differing patterns of striatal 18F-dopa uptake in Parkinson's disease, multiple system atrophy, and progressive supranuclear palsy. *Ann Neurol*, **28**, 547-555.

Brown, R.E., Sergeeva, O., Eriksson, K.S. & Haas, H.L. (2001) Orexin A excites serotonergic neurons in the dorsal raphe nucleus of the rat. *Neuropharmacology*, **40**, 457-459.

Brust, P., Hesse, S., Muller, U. & Szabo, Z. (2006) Neuroimaging of the serotonin transporter: possibilities and pitfalls. *Current psychiatry reviews*, **2**, 111-149.

Bubser, M., Backstrom, J.R., Sanders-Bush, E., Roth, B.L. & Deutch, A.Y. (2001) Distribution of serotonin 5-HT2A receptors in afferents of the rat striatum. *Synapse*, **39**, 297-304.

Buhl, E.H. & Lubke, J. (1989) Intracellular lucifer yellow injection in fixed brain slices combined with retrograde tracing, light and electron microscopy. *Neuroscience*, **28**, 3-16.

Bunin, M.A. & Wightman, R.M. (1998) Quantitative evaluation of 5-hydroxytryptamine (serotonin) neuronal release and uptake: an investigation of extrasynaptic transmission. *The Journal of neuroscience : the official journal of the Society for Neuroscience*, **18**, 4854-4860.

Bunney, B.S., Walters, J.R., Roth, R.H. & Aghajanian, G.K. (1973) Dopaminergic neurons: effect of antipsychotic drugs and amphetamine on single cell activity. *The Journal of pharmacology and experimental therapeutics*, **185**, 560-571.

Burke, R.E., Dauer, W.T. & Vonsattel, J.P.G. (2008) A critical evaluation of the Braak staging scheme for Parkinson's disease. *Ann Neurol*, **64**, 485-491.

Burnet, P.W., Eastwood, S.L. & Harrison, P.J. (1996) 5-HT 1A and 5-HT 2A receptor mRNAs and binding site densities are differentially altered in schizophrenia. *Neuropsychopharmacology : official publication of the American College of Neuropsychopharmacology*, **15**, 442-455.

Burns, R.S., Chiueh, C.C., Markey, S.P., Ebert, M.H., Jacobowitz, D.M. & Kopin, I.J. (1983) A primate model of parkinsonism: selective destruction of dopaminergic neurons in the pars compacta of the substantia nigra by N-methyl-4-phenyl-1, 2, 3, 6-tetrahydropyridine. *Proceedings of the National Academy of Sciences*, **80**, 4546-4550.

Cajal, S.R. (1904) *Textura del Sistema Nervioso del Hombre y los Vertebrados*, Madrid.

Cajal, S.R. (1909, 1911) *Histologie du système nerveux de l'Homme et des Vertébrés*, Azoulay L, translator. Maloine. Reprinted CSdIC, Madrid: Institutio Ramón y Cajal, 1972., editor. Paris.

Calabresi, P., Ghiglieri, V., Mazzocchetti, P., Corbelli, I. & Picconi, B. (2015) Levodopa-induced plasticity: a double-edged sword in Parkinson's disease? *Philosophical transactions of the Royal Society of London. Series B, Biological sciences*, **370**.

Calas, A., Besson, M.J., Gaughy, C., Alonso, G., Glowinski, J. & Cheramy, A. (1976) Radioautographic study of in vivo incorporation of 3H-monoamines in the cat caudate nucleus: identification of serotoninergic fibers. *Brain Res*, **118**, 1-13.

Calon, F., Morissette, M., Rajput, A.H., Hornykiewicz, O., Bedard, P.J. & Di Paolo, T. (2003) Changes of GABA receptors and dopamine turnover in the postmortem brains of parkinsonians with levodopa-induced motor complications. *Movement disorders : official journal of the Movement Disorder Society*, **18**, 241-253.

Campbell, G.A., Eckardt, M.J. & Weight, F.F. (1985) Dopaminergic mechanisms in subthalamic nucleus of rat: analysis using horseradish peroxidase and microiontophoresis. *Brain research*, **333**, 261-270.

Canteras, N., Simerly, R. & Swanson, L. (1995) Organization of projections from the medial nucleus of the amygdala: a PHAL study in the rat. *Journal of Comparative Neurology*, **360**, 213-245.

Canteras, N.S., Shammah-Lagnado, S.J., Silva, B.A. & Ricardo, J.A. (1990) Afferent connections of the subthalamic nucleus: a combined retrograde and anterograde horseradish peroxidase study in the rat. *Brain research*, **513**, 43-59.

Carlsson, T., Carta, M., Winkler, C., Björklund, A. & Kirik, D. (2007) Serotonin neuron transplants exacerbate L-DOPA-induced dyskinesias in a rat model of Parkinson's disease. *Journal of Neuroscience*, **27**, 8011-8022.

Carpenter, M.B., Carleton, S.C., Keller, J.T. & Conte, P. (1981) Connections of the subthalamic nucleus in the monkey. *Brain research*, **224**, 1-29.

Carpenter, M.B., Fraser, R.A. & Shriver, J.E. (1968) The organization of pallidosubthalamic fibers in the monkey. *Brain research*, **11**, 522-559.

Carta, M., Carlsson, T., Kirik, D. & Bjorklund, A. (2007a) Dopamine released from 5-HT terminals is the cause of L-DOPA-induced dyskinesia in parkinsonian rats. *Brain : a journal of neurology*, **130**, 1819-1833.

Carta, M., Carlsson, T., Kirik, D. & Björklund, A. (2007b) Dopamine released from 5-HT terminals is the cause of L-DOPA-induced dyskinesia in parkinsonian rats. *Brain : a journal of neurology*, **130**, 1819-1833.

Carta, M., Carlsson, T., Munoz, A., Kirik, D. & Bjorklund, A. (2008a) Involvement of the serotonin system in L-dopa-induced dyskinesias. *Parkinsonism & related disorders*, **14 Suppl 2**, S154-158.

Carta, M., Carlsson, T., Munoz, A., Kirik, D. & Bjorklund, A. (2008b) Serotonin-dopamine interaction in the induction and maintenance of L-DOPA-induced dyskinesias. *Prog Brain Res*, **172**, 465-478.

Carta, M. & Tronci, E. (2014) Serotonin System Implication in l-DOPA-Induced Dyskinesia: From Animal Models to Clinical Investigations. *Front Neurol*, **5**, 78.

Carter, C. (1982) Topographical distribution of possible glutamatergic pathways from the frontal cortex to the striatum and substantia nigra in rats. *Neuropharmacology*, **21**, 379-383.

Carter, D. & Fibiger, H. (1978) The projections of the entopeduncular nucleus and globus pallidus in rat as demonstrated by autoradiography and horseradish peroxidase histochemistry. *Journal of Comparative Neurology*, **177**, 113-123.

Cash, R., Raisman, R., Ploska, A. & Agid, Y. (1985) High and low affinity [3 H] imipramine binding sites in control and Parkinsonian brains. *European journal of pharmacology*, **117**, 71-80.

Castro, M.E., Pascual, J., Romon, T., Berciano, J., Figols, J. & Pazos, A. (1998) 5-HT1B receptor binding in degenerative movement disorders. *Brain Res*, **790**, 323-328.

Chan, P., DeLanney, L.E., Irwin, I., Langston, J.W. & Monte, D. (1991) Rapid ATP Loss Caused by 1-Methyl-4-Phenyl-1, 2, 3, 6-Tetrahydropyridine in Mouse Brain. *Journal of neurochemistry*, **57**, 348-351.

Charara, A. & Parent, A. (1994) Brainstem dopaminergic, cholinergic and serotoninergic afferents to the pallidum in the squirrel monkey. *Brain Res*, **640**, 155-170.

Charara, A. & Parent, A. (1998) Chemoarchitecture of the primate dorsal raphe nucleus. *J Chem Neuroanat*, **15**, 111-127.

Charcot, J.-M. & Vulpian, A. (1862) *De la paralysie agitante*. V. Masson et fils, Paris.

Chen, C.P.L.H., Alder, J.T., Bray, L., Kingsbury, A.E., Francis, P.T. & Foster, O.J.F. (1998) Post-Synaptic 5-HT1A and 5-HT2A Receptors Are Increased in Parkinson's Disease Neocortex. *Annals of the New York Academy of Sciences*, **861**, 288-289.

Cheramy, A., Leviel, V. & Glowinski, J. (1981) Dendritic release of dopamine in the substantia nigra. *Nature*, **289**, 537-543.

Cheshire, P., Ayton, S., Bertram, K.L., Ling, H., Li, A., McLean, C., Halliday, G.M., O'Sullivan, S.S., Revesz, T., Finkelstein, D.I., Storey, E. & Williams, D.R. (2015) Serotonergic markers in Parkinson's disease and levodopa-induced dyskinesias. *Movement disorders : official journal of the Movement Disorder Society*, **30**, 796-804.

Chevalier, G., Vacher, S., Deniau, J. & Desban, M. (1985) Disinhibition as a basic process in the expression of striatal functions. I. The striato-nigral influence on tecto-spinal/tecto-diencephalic neurons. *Brain research*, **334**, 215-226.

Chinaglia, G., Landwehrmeyer, B., Probst, A. & Palacios, J.M. (1993) Serotoninergic terminal transporters are differentially affected in Parkinson's disease and progressive supranuclear palsy: an autoradiographic study with [^{3}H]citalopram. *Neuroscience*, **54**, 691-699.

Chua, J.J., Kindler, S., Boyken, J. & Jahn, R. (2010) The architecture of an excitatory synapse. *J Cell Sci*, **123**, 819-823.

Cilia, R., Akpalu, A., Sarfo, F.S., Cham, M., Amboni, M., Cereda, E., Fabbri, M., Adjei, P., Akassi, J. & Bonetti, A. (2014) The modern pre-levodopa era of Parkinson's disease: insights into motor complications from sub-Saharan Africa. *Brain*, **137**, 2731-2742.

Clarke, P., Hommer, D., Pert, A. & Skirboll, L. (1987) Innervation of substantia nigra neurons by cholinergic afferents from pedunculopontine nucleus in the rat: neuroanatomical and electrophysiological evidence. *Neuroscience*, **23**, 1011-1019.

Cloud, L.J. & Greene, J.G. (2011) Gastrointestinal features of Parkinson's disease. *Current neurology and neuroscience reports*, **11**, 379-384.

Commons, K.G. (2009) Locally collateralizing glutamate neurons in the dorsal raphe nucleus responsive to substance P contain vesicular glutamate transporter 3 (VGLUT3). *J Chem Neuroanat*, **38**, 273-281.

Compan, V., Daszuta, A., Salin, P., Sebben, M., Bockaert, J. & Dumuis, A. (1996) Lesion Study of the Distribution of Serotonin 5-HT4 Receptors in Rat Basal Ganglia and Hippocampus. *European Journal of Neuroscience*, **8**, 2591-2598.

Compan, V., Zhou, M., Grailhe, R., Gazzara, R.A., Martin, R., Gingrich, J., Dumuis, A., Brunner, D., Bockaert, J. & Hen, R. (2004) Attenuated response to stress and novelty and hypersensitivity to seizures in 5-HT4 receptor knock-out mice. *Journal of Neuroscience*, **24**, 412-419.

Condes-Lara, M., Omana Zapata, I., Leon-Olea, M. & Sanchez-Alvarez, M. (1989) Dorsal raphe neuronal responses to thalamic centralis lateralis and medial prefrontal cortex electrical stimulation. *Brain Res*, **499**, 141-144.

Cools, R., Roberts, A.C. & Robbins, T.W. (2008) Serotoninergic regulation of emotional and behavioural control processes. *Trends Cogn Sci*, **12**, 31-40.

Coons, A.H., Creech, H.J. & Jones, R.N. (1941) Immunological Properties of an Antibody Containing a Fluorescent Group. *Proceedings of the Society for Experimental Biology and Medicine*, **47**, 200-202.

Cooper, I.S. & Bravo, G. (1958) Chemopallidectomy and chemothalamectomy. *Journal of neurosurgery*, **15**, 244-250.

Cornea-Hébert, V., Riad, M., Wu, C., Singh, S.K. & Descarries, L. (1999) Cellular and subcellular distribution of the serotonin 5-HT2A receptor in the central nervous system of adult rat. *Journal of Comparative Neurology*, **409**, 187-209.

Cossette, M., Lévesque, M. & Parent, A. (1999) Extrastriatal dopaminergic innervation of human basal ganglia. *Neuroscience research*, **34**, 51-54.

Cotzias, G.C., Papavasiliou, P.S. & Gellene, R. (1969) Modification of Parkinsonism—chronic treatment with L-dopa. *New England Journal of Medicine*, **280**, 337-345.

Cotzias, G.C., Van Woert, M.H. & Schiffer, L.M. (1967) Aromatic amino acids and modification of parkinsonism. *New England Journal of Medicine*, **276**, 374-379.

Crissman, R.S., Arce, E.A., Bennett-Clarke, C.A., Mooney, R.D. & Rhoades, R.W. (1993) Reduction in the percentage of serotoninergic axons making synapses during the development of the superficial layers of the hamster's superior colliculus. *Brain Res Dev Brain Res*, **75**, 131-135.

Crosby, N.J., Deane, K. & Clarke, C.E. (2003) Amantadine in Parkinson's disease. *The Cochrane Library*.

Cross, A.J. & Joseph, M.H. (1981) The concurrent estimation of the major monoamine metabolites in human and non-human primate brain by HPLC with fluorescence and electrochemical detection. *Life Sci*, **28**, 499-505.

Cuello, A.C., Milstein, C., Couture, R., Wright, B., Priestley, J.V. & Jarvis, J. (1984) Characterization and immunocytochemical application of monoclonal antibodies against enkephalins. *J Histochem Cytochem*, **32**, 947-957.

Cui, G., Jun, S.B., Jin, X., Pham, M.D., Vogel, S.S., Lovinger, D.M. & Costa, R.M. (2013) Concurrent activation of striatal direct and indirect pathways during action initiation. *Nature*, **494**, 238-242.

Dahlstroem, A. & Fuxe, K. (1964a) Evidence for the Existence of Monoamine-Containing Neurons in the Central Nervous System. I. Demonstration of Monoamines in the Cell Bodies of Brain Stem Neurons. *Acta physiologica Scandinavica. Supplementum*, SUPPL 232:231-255.

Dahlstroem, A. & Fuxe, K. (1964b) Localization of monoamines in the lower brain stem. *Experientia*, **20**, 398-399.

Damier, P., Hirsch, E.C., Agid, Y. & Graybiel, A.M. (1999) The substantia nigra of the human brainI. Nigrosomes and the nigral matrix, a compartmental organization based on calbindin D28K immunohistochemistry. *Brain : a journal of neurology*, **122**, 1421-1436.

Davie, C.A. (2008) A review of Parkinson's disease. *British medical bulletin*, **86**, 109-127.

Day, H.E., Greenwood, B.N., Hammack, S.E., Watkins, L.R., Fleshner, M., Maier, S.F. & Campeau, S. (2004) Differential expression of 5HT-1A, α1b adrenergic, CRF-R1, and CRF-R2 receptor mRNA in serotonergic, γ-aminobutyric acidergic, and catecholaminergic cells of the rat dorsal raphe nucleus. *Journal of Comparative Neurology*, **474**, 364-378.

Day, M., Wang, Z., Ding, J., An, X., Ingham, C.A., Shering, A.F., Wokosin, D., Ilijic, E., Sun, Z., Sampson, A.R., Mugnaini, E., Deutch, A.Y., Sesack, S.R., Arbuthnott, G.W. & Surmeier, D.J. (2006) Selective elimination of glutamatergic synapses on striatopallidal neurons in Parkinson disease models. *Nat Neurosci*, **9**, 251-259.

de Quervain, D.J., Henke, K., Aerni, A., Coluccia, D., Wollmer, M.A., Hock, C., Nitsch, R.M. & Papassotiropoulos, A. (2003) A functional genetic variation of the 5-HT2a receptor affects human memory. *Nature neuroscience*, **6**, 1141.

Debeir, T., Ginestet, L., Francois, C., Laurens, S., Martel, J.C., Chopin, P., Marien, M., Colpaert, F. & Raisman-Vozari, R. (2005) Effect of intrastriatal 6-OHDA lesion on dopaminergic innervation of the rat cortex and globus pallidus. *Exp Neurol*, **193**, 444-454.

Dejerine, J.J. & Dejerine-Klumpke, A. (1895) *Anatomie des centres nerveux*. Rueff.

Deng, Y.P., Lei, W.L. & Reiner, A. (2006) Differential perikaryal localization in rats of D1 and D2 dopamine receptors on striatal projection neuron types identified by retrograde labeling. *J Chem Neuroanat*, **32**, 101-116.

Deniau, J. & Chevalier, G. (1985) Disinhibition as a basic process in the expression of striatal functions. II. The striato-nigral influence on thalamocortical cells of the ventromedial thalamic nucleus. *Brain research*, **334**, 227-233.

Deniau, J. & Chevalier, G. (1992) The lamellar organization of the rat substantia nigra pars reticulata: distribution of projection neurons. *Neuroscience*, **46**, 361-377.

Deniau, J., Feger, J. & Le Guyader, C. (1976) Striatal evoked inhibition of identified nigro-thalamic neurons. *Brain Research*, **104**, 152-156.

Descarries, L., Beaudet, A. & Watkins, K.C. (1975) Serotonin nerve terminals in adult rat neocortex. *Brain Res*, **100**, 563-588.

Descarries, L., Berthelet, F., Garcia, S. & Beaudet, A. (1986) Dopaminergic projection from nucleus raphe dorsalis to neostriatum in the rat. *The Journal of comparative neurology*, **249**, 511-520, 484-515.

Descarries, L., Bérubé-Carrière, N., Riad, M., Bo, G.D., Mendez, J.A. & Trudeau, L.E. (2008) Glutamate in dopamine neurons: synaptic versus diffuse transmission. *Brain research reviews*, **58**, 290-302.

Descarries, L., Gisiger, V. & Steriade, M. (1997) Diffuse transmission by acetylcholine in the CNS. *Progress in neurobiology*, **53**, 603-625.

Descarries, L. & Mechawar, N. (2000) Ultrastructural evidence for diffuse transmission by monoamine and acetylcholine neurons of the central nervous system. *Prog Brain Res*, **125**, 27-47.

Descarries, L. & Mechawar, N. (2008) Structural organization of monoamine and acetylcholine neuron systems in the rat CNS. In Vizi, E.S., Lajtha, A. (eds) *Handbook of neurochemistry and molecular neurobiology*. Springer US, New York, pp. 1-20.

Descarries, L., Riad, M. & Parent, M. (2010a) Ultrastructure of the serotonin innervation in mammalian CNS. In Müller, C.P., Jacobs, B.L. (eds) *Handbook of the Behavioural Neurobiology of Serotonin*. Academic Press, London, Unated Kindom, pp. 65-102.

Descarries, L., Riad, M. & Parent, M. (2010b) Ultrastructure of the serotonin innervation in the mammalian central nervous system. In Müller, C., Jacobs, B. (eds) *Handbook of the behavioral neurobiology of serotonin*. Elsevier, Amsterdam, pp. 65-102.

Descarries, L., Soghomonian, J.J., Garcia, S., Doucet, G. & Bruno, J.P. (1992) Ultrastructural analysis of the serotonin hyperinnervation in adult rat neostriatum following neonatal dopamine denervation with 6-hydroxydopamine. *Brain Res*, **569**, 1-13.

Descarries, L., Watkins, K.C., Garcia, S. & Beaudet, A. (1982) The serotonin neurons in nucleus raphe dorsalis of adult rat: a light and electron microscope radioautographic study. *Journal of Comparative Neurology*, **207**, 239-254.

Descarries, L., Watkins, K.C., Garcia, S., Bosler, O. & Doucet, G. (1996) Dual character, asynaptic and synaptic, of the dopamine innervation in adult rat neostriatum: a quantitative autoradiographic and immunocytochemical analysis. *Journal of Comparative Neurology*, **375**, 167-186.

Deschênes, M., Bourassa, J., Doan, V.D. & Parent, A. (1996) A Single-cell Study of the Axonal Projections Arising from the Posterior Intralaminar Thalamic Nuclei in the Rat. *European Journal of Neuroscience*, **8**, 329-343.

Deutch, A.Y., Colbran, R.J. & Winder, D.J. (2007) Striatal plasticity and medium spiny neuron dendritic remodeling in parkinsonism. *Parkinsonism & related disorders*, **13 Suppl 3**, S251-258.

DeVito, J. & Anderson, M. (1982) An autoradiographic study of efferent connections of the globus pallidus in Macaca mulatta. *Exp Brain Res*, **46**, 107-117.

DeVito, J., Anderson, M. & Walsh, K. (1980) A horseradish peroxidase study of afferent connections of the globus pallidus in Macaca mulatta. *Exp Brain Res*, **38**, 65-73.

Dewar, K., Soghomonian, J.-J., Bruno, J., Descarries, L. & Reader, T. (1990) Elevation of dopamine D 2 but not D 1 receptors in adult rat neostriatum after neonatal 6-hydroxydopamine denervation. *Brain research*, **536**, 287-296.

Dewey, R.B. & Jankovic, J. (1989) Hemiballism-hemichorea: clinical and pharmacologic findings in 21 patients. *Archives of Neurology*, **46**, 862-867.

Di Chiara, G., Porceddu, M., Morelli, M., Mulas, M. & Gessa, G. (1979) Evidence for a GABAergic projection from the substantia nigra to the ventromedial thalamus and to the superior colliculus of the rat. *Brain research*, **176**, 273-284.

Di Matteo, V., Pierucci, M., Esposito, E., Crescimanno, G., Benigno, A. & Di Giovanni, G. (2008) Serotonin modulation of the basal ganglia circuitry: therapeutic implication for Parkinson's disease and other motor disorders. *Prog Brain Res*, **172**, 423-463.

Di Paolo, T., Bedard, P., Daigle, M. & Boucher, R. (1986) Long-term effects of MPTP on central and peripheral catecholamine and indoleamine concentrations in monkeys. *Brain Res*, **379**, 286-293.

DiFiglia, M. & Carey, J. (1986) Large neurons in the primate neostriatum examined with the combined Golgi-electron microscopic method. *Journal of Comparative Neurology*, **244**, 36-52.

DiFiglia, M., Pasik, P. & Pasik, T. (1976) A Golgi study of neuronal types in the neostriatum of monkeys. *Brain research*, **114**, 245-256.

DiFiglia, M., Pasik, P. & Pasik, T. (1982) A Golgi and ultrastructural study of the monkey globus pallidus. *Journal of Comparative Neurology*, **212**, 53-75.

Dimova, R., Vuillet, J., Nieoullon, A. & Kerkerian-Le Goff, L. (1993) Ultrastructural features of the choline acetyltransferase-containing neurons and relationships with nigral dopaminergic and cortical afferent pathways in the rat striatum. *Neuroscience*, **53**, 1059-1071.

Ding, Y., Won, L., Britt, J.P., Lim, S.A., McGehee, D.S. & Kang, U.J. (2011) Enhanced striatal cholinergic neuronal activity mediates L-DOPA-induced dyskinesia in parkinsonian mice. *Proceedings of the National Academy of Sciences of the United States of America*, **108**, 840-845.

Doder, M., Rabiner, E.A., Turjanski, N., Lees, A.J. & Brooks, D.J. (2003) Tremor in Parkinson's disease and serotonergic dysfunction: an 11C-WAY 100635 PET study. *Neurology*, **60**, 601-605.

Doig, N.M., Magill, P.J., Apicella, P., Bolam, J.P. & Sharott, A. (2014) Cortical and thalamic excitation mediate the multiphasic responses of striatal cholinergic interneurons to motivationally salient stimuli. *Journal of Neuroscience*, **34**, 3101-3117.

Dong, H.W. & Swanson, L.W. (2006a) Projections from bed nuclei of the stria terminalis, anteromedial area: cerebral hemisphere integration of neuroendocrine, autonomic, and behavioral aspects of energy balance. *Journal of Comparative Neurology*, **494**, 142-178.

Dong, H.W. & Swanson, L.W. (2006b) Projections from bed nuclei of the stria terminalis, dorsomedial nucleus: implications for cerebral hemisphere integration of neuroendocrine, autonomic, and drinking responses. *Journal of Comparative Neurology*, **494**, 75-107.

Dopeso-Reyes, I.G., Rico, A.J., Roda, E., Sierra, S., Pignataro, D., Lanz, M., Sucunza, D., Chang-Azancot, L. & Lanciego, J.L. (2014) Calbindin content and differential vulnerability of midbrain efferent dopaminergic neurons in macaques. *Front Neuroanat*, **8**, 146.

Drevets, W.C., Frank, E., Price, J.C., Kupfer, D.J., Holt, D., Greer, P.J., Huang, Y., Gautier, C. & Mathis, C. (1999) PET imaging of serotonin 1A receptor binding in depression. *Biological psychiatry*, **46**, 1375-1387.

Dumitriu, D., Rodriguez, A. & Morrison, J.H. (2011) High-throughput, detailed, cell-specific neuroanatomy of dendritic spines using microinjection and confocal microscopy. *Nature protocols*, **6**, 1391-1411.

Dumuis, A., Bouhelal, R., Sebben, M., Cory, R. & Bockaert, J. (1988) A nonclassical 5-hydroxytryptamine receptor positively coupled with adenylate cyclase in the central nervous system. *Molecular Pharmacology*, **34**, 880-887.

Eid, L., Champigny, M.F., Parent, A. & Parent, M. (2013) Quantitative and ultrastructural study of serotonin innervation of the globus pallidus in squirrel monkeys. *Eur J Neurosci*, **37**, 1659-1668.

Eid, L. & Parent, M. (2015a) Morphological evidence for dopamine interactions with pallidal neurons in primates. *Front Neuroanat*, **9**.

Eid, L. & Parent, M. (2015b) Morphological evidence for dopamine interactions with pallidal neurons in primates. *Front Neuroanat*, **9**, 111.

Eid, L. & Parent, M. (2016) Chemical anatomy of pallidal afferents in primates. *Brain structure & function*, **221**, 4291-4317.

Eid, L. & Parent, M. (2017) Preparation of Non-human Primate Brain Tissue for Pre-embedding Immunohistochemistry and Electron Microscopy. *J Vis Exp*.

El Mestikawy, S., Wallén-Mackenzie, Å., Fortin, G.M., Descarries, L. & Trudeau, L.-E. (2011) From glutamate co-release to vesicular synergy: vesicular glutamate transporters. *Nature reviews. Neuroscience*, **12**, 204.

Engel, G., Göthert, M., Hoyer, D., Schlicker, E. & Hillenbrand, K. (1986) Identity of inhibitory presynaptic 5-hydroxytryptamine (5-HT) autoreceptors in the rat brain cortex with 5-HT 1B binding sites. *Naunyn-Schmiedeberg's archives of pharmacology*, **332**, 1-7.

Engeln, M., Bastide, M.F., Toulmé, E., Dehay, B., Bourdenx, M., Doudnikoff, E., Li, Q., Gross, C.E., Boué-Grabot, E. & Pisani, A. (2016) Selective inactivation of striatal FosB/ΔFosB-expressing neurons alleviates L-DOPA–induced dyskinesia. *Biological psychiatry*, **79**, 354-361.

Erinoff, L. & Snodgrass, S. (1986) Effects of adult or neonatal treatment with 6-hydroxydopamine or 5, 7-dihydroxytryptamine on locomotor activity, monoamine levels, and response to caffeine. *Pharmacology Biochemistry and Behavior*, **24**, 1039-1045.

Erspamer, V. & Asero, B. (1952) Identification of enteramine, the specific hormone of the enterochromaffin cell system, as 5-hydroxytryptamine. *Nature*, **169**, 800-801.

Escande, M.V., Taravini, I.R., Zold, C.L., Belforte, J.E. & Murer, M.G. (2016) Loss of Homeostasis in the Direct Pathway in a Mouse Model of Asymptomatic Parkinson's Disease. *The Journal of neuroscience : the official journal of the Society for Neuroscience*, **36**, 5686-5698.

Eskow, K.L., Dupre, K.B., Barnum, C.J., Dickinson, S.O., Park, J.Y. & Bishop, C. (2009) The role of the dorsal raphe nucleus in the development, expression, and treatment of L-dopa-induced dyskinesia in hemiparkinsonian rats. *Synapse*, **63**, 610-620.

Eskow, K.L., Gupta, V., Alam, S., Park, J.Y. & Bishop, C. (2007) The partial 5-HT 1A agonist buspirone reduces the expression and development of L-DOPA-induced dyskinesia in rats and improves L-DOPA efficacy. *Pharmacology Biochemistry and Behavior*, **87**, 306-314.

Everett, G.M. & Borcherding, J.W. (1970) L-dopa: effect on concentrations of dopamine, norepinephrine, and serotonin in brains of mice. *Science*, **168**, 849-850.

Fabre, E., Monserrat, J., Herrero, A., Barja, G. & Leret, M. (1999) Effect of MPTP on brain mitochondrial H2O2 and ATP production and on dopamine and DOPAC in the striatum. *Journal of physiology and biochemistry*, **55**, 325-331.

Fahn, S., Libsch, L. & Cutler, R. (1971) Monoamines in the human neostriatum: topographic distribution in normals and in Parkinson's disease and their role in akinesia, rigidity, chorea, and tremor. *Journal of the neurological sciences*, **14**, 427-455.

Fearnley, J.M. & Lees, A.J. (1991) Ageing and Parkinson's disease: substantia nigra regional selectivity. *Brain : a journal of neurology*, **114**, 2283-2301.

Fenelon, F. (Year) Essais de traitement neurochirurgical du syndrôme parkinsonien par intervention directe sur les voies extrapyramidales immédiatement sous-striopallidales. Vol. 83, Rev Neurol (Paris). Masson, City. p. 437-440.

Fénelon, G., Mahieux, F., Huon, R. & Ziégler, M. (2000) Hallucinations in Parkinson's disease: Prevalence, phenomenology and risk factors. *Brain : a journal of neurology*, **123**, 733-745.

Ferraro, G., Montalbano, M.E., Sardo, P. & La Grutta, V. (1996) Lateral habenular influence on dorsal raphe neurons. *Brain research bulletin*, **41**, 47-52.

Fieblinger, T. & Cenci, M.A. (2015) Zooming in on the small: the plasticity of striatal dendritic spines in L-DOPA-induced dyskinesia. *Movement disorders : official journal of the Movement Disorder Society*, **30**, 484-493.

Fieblinger, T., Graves, S.M., Sebel, L.E., Alcacer, C., Plotkin, J.L., Gertler, T.S., Chan, C.S., Heiman, M., Greengard, P., Cenci, M.A. & Surmeier, D.J. (2014) Cell type-specific plasticity of striatal projection neurons in parkinsonism and L-DOPA-induced dyskinesia. *Nature communications*, **5**, 5316.

Filion, M. & Tremblay, L. (1991) Abnormal spontaneous activity of globus pallidus neurons in monkeys with MPTP-induced parkinsonism. *Brain Res*, **547**, 142-151.

Fino, E., Glowinski, J. & Venance, L. (2007) Effects of acute dopamine depletion on the electrophysiological properties of striatal neurons. *Neuroscience research*, **58**, 305-316.

Flores, G., Rosales, M.G., Hernández, S., Sierra, A. & Aceves, J. (1995) 5-Hydroxytryptamine increases spontaneous activity of subthalamic neurons in the rat. *Neurosci Lett*, **192**, 17-20.

Foix, C. & Nicolesco, J. (1925) *Anatomie cérébrale: les noyaux gris centraux et la région mésencéphalo-sous-optique*. Masson.

Foley, J.M. & Banter, D. (1958) On the nature of pigment granules in the cells of the locus coeruleus and substantia nigra. *Journal of Neuropathology & Experimental Neurology*, **17**, 586-598.

Forster, G.L. & Blaha, C.D. (2003) Pedunculopontine tegmental stimulation evokes striatal dopamine efflux by activation of acetylcholine and glutamate receptors in the midbrain and pons of the rat. *European Journal of Neuroscience*, **17**, 751-762.

Fox, S.H., Chuang, R. & Brotchie, J.M. (2009) Serotonin and Parkinson's disease: On movement, mood, and madness. *Movement Disorders*, **24**, 1255-1266.

Francois, C., Percheron, G., Parent, A., Sadikot, A., Fenelon, G. & Yelnik, J. (1991) Topography of the projection from the central complex of the thalamus to the sensorimotor striatal territory in monkeys. *Journal of comparative neurology*, **305**, 17-34.

François, C., Savy, C., Jan, C., Tande, D., Hirsch, E.C. & Yelnik, J. (2000) Dopaminergic innervation of the subthalamic nucleus in the normal state, in MPTP-treated monkeys, and in Parkinson's disease patients. *Journal of Comparative Neurology*, **425**, 121-129.

François, C., Yelnik, J. & Percheron, G. (1987) Golgi study of the primate substantia nigra. II. Spatial organization of dendritic arborizations in relation to the cytoarchitectonic boundaries and to the striatonigral bundle. *Journal of Comparative Neurology*, **265**, 473-493.

Franklin, K.B.J. & Paxinos, G. (1997) *The mouse brain in stereotaxic coordinates*. Academic Press, San Diego.

Frechilla, D., Cobreros, A., Saldise, L., Moratalla, R., Insausti, R., Luquin, M. & Del Rio, J. (2001) Serotonin 5-HT(1A) receptor expression is selectively enhanced in the striosomal compartment of chronic parkinsonian monkeys. *Synapse*, **39**, 288-296.

Frederick, A.L., Yano, H., Trifilieff, P., Vishwasrao, H.D., Biezonski, D., Meszaros, J., Urizar, E., Sibley, D.R., Kellendonk, C., Sonntag, K.C., Graham, D.L., Colbran, R.J., Stanwood, G.D. & Javitch, J.A. (2015) Evidence against dopamine D1/D2 receptor heteromers. *Molecular psychiatry*, **20**, 1373-1385.

Fremeau, R.T., Jr., Burman, J., Qureshi, T., Tran, C.H., Proctor, J., Johnson, J., Zhang, H., Sulzer, D., Copenhagen, D.R., Storm-Mathisen, J., Reimer, R.J., Chaudhry, F.A. & Edwards, R.H. (2002) The identification of vesicular glutamate transporter 3 suggests novel modes of signaling by glutamate. *Proceedings of the National Academy of Sciences of the United States of America*, **99**, 14488-14493.

Freund, T.F., Powell, J.F. & Smith, A.D. (1984) Tyrosine hydroxylase-immunoreactive boutons in synaptic contact with identified striatonigral neurons, with particular reference to dendritic spines. *Neuroscience*, **13**, 1189-1215.

Friedman, L.K. & Mytilineou, C. (1990) Neurochemical and toxic effects of 1-methyl-4-phenyl-1, 2, 3, 6-tetrahydropyridine and 1-methyl-4-phenylpyridine to rat serotonin neurons in dissociated cell cultures. *Journal of Pharmacology and Experimental Therapeutics*, **253**, 892-898.

Frisina, P.G., Haroutunian, V. & Libow, L.S. (2009) The neuropathological basis for depression in Parkinson's disease. *Parkinsonism Relat Disord*, **15**, 144-148.

Fu, W., Le Maître, E., Fabre, V., Bernard, J.F., David Xu, Z.Q. & Hökfelt, T. (2010) Chemical neuroanatomy of the dorsal raphe nucleus and adjacent structures of the mouse brain. *Journal of Comparative Neurology*, **518**, 3464-3494.

Fuchs, H. & Hauber, W. (2004) Dopaminergic innervation of the rat globus pallidus characterized by microdialysis and immunohistochemistry. *Exp Brain Res*, **154**, 66-75.

Fujiyama, F., Kuramoto, E., Okamoto, K., Hioki, H., Furuta, T., Zhou, L., Nomura, S. & Kaneko, T. (2004) Presynaptic localization of an AMPA-type glutamate receptor in corticostriatal and thalamostriatal axon terminals. *European Journal of Neuroscience*, **20**, 3322-3330.

Futami, T., Takakusaki, K. & Kitai, S. (1995) Glutamatergic and cholinergic inputs from the pedunculopontine tegmental nucleus to dopamine neurons in the substantia nigra pars compacta. *Neuroscience research*, **21**, 331-342.

Fuxe, K. & Jonsson, G. (1967) A modification of the histochemical fluorescence method for the improved localization of 5-hydroxytryptamine. *Histochemie. Histochemistry. Histochimie*, **11**, 161-166.

Gabbott, P.L., Warner, T.A., Jays, P.R., Salway, P. & Busby, S.J. (2005) Prefrontal cortex in the rat: projections to subcortical autonomic, motor, and limbic centers. *Journal of Comparative Neurology*, **492**, 145-177.

Gagnon, D., Gregoire, L., Di Paolo, T. & Parent, M. (2016) Serotonin hyperinnervation of the striatum with high synaptic incidence in parkinsonian monkeys. *Brain Struct Funct*, **221**, 3675-3691.

Gagnon, D. & Parent, M. (2014) Distribution of VGLUT3 in highly collateralized axons from the rat dorsal raphe nucleus as revealed by single-neuron reconstructions. *PLoS One*, **9**, e87709.

Gai, W.P., Halliday, G.M., Blumbergs, P.C., Geffen, L.B. & Blessing, W.W. (1991) Substance P-containing neurons in the mesopontine tegmentum are severely affected in Parkinson's disease. *Brain : a journal of neurology*, **114 (Pt 5)**, 2253-2267.

Gangarossa, G., Espallergues, J., de Kerchove d'Exaerde, A., El Mestikawy, S., Gerfen, C.R., Herve, D., Girault, J.A. & Valjent, E. (2013a) Distribution and compartmental organization of GABAergic medium-sized spiny neurons in the mouse nucleus accumbens. *Frontiers in neural circuits*, **7**, 22.

Gangarossa, G., Espallergues, J., Mailly, P., De Bundel, D., de Kerchove d'Exaerde, A., Herve, D., Girault, J.A., Valjent, E. & Krieger, P. (2013b) Spatial distribution of D1R- and D2R-expressing medium-sized spiny neurons differs along the rostro-caudal axis of the mouse dorsal striatum. *Frontiers in neural circuits*, **7**, 124.

Gao, K. & Mason, P. (1997) Somatodendritic and axonal anatomy of intracellularly labeled serotonergic neurons in the rat medulla. *The Journal of comparative neurology*, **389**, 309-328.

Gariano, R. & Groves, P. (1988) Burst firing induced in midbrain dopamine neurons by stimulation of the medial prefrontal and anterior cingulate cortices. *Brain research*, **462**, 194-198.

Gash, D.M., Zhang, Z., Ovadia, A. & Cass, W.A. (1996a) Functional recovery in parkinsonian monkeys treated with GDNF. *Nature*, **380**, 252.

Gash, D.M., Zhang, Z., Ovadia, A., Cass, W.A., Yi, A., Simmerman, L., Russell, D., Martin, D., Lapchak, P.A., Collins, F., Hoffer, B.J. & Gerhardt, G.A. (1996b) Functional recovery in parkinsonian monkeys treated with GDNF. *Nature*, **380**, 252-255.

Gaspar, P., Febvret, A. & Colombo, J. (1993a) Serotonergic sprouting in primate MTP-induced hemiparkinsonism. *Exp Brain Res*, **96**, 100-106.

Gaspar, P., Febvret, A. & Colombo, J. (1993b) Serotonergic sprouting in primate MTP-induced hemiparkinsonism. *Exp Brain Res*, **96**, 100-106.

Gaspar, P. & Lillesaar, C. (2012) Probing the diversity of serotonin neurons. *Philosophical transactions of the Royal Society of London. Series B, Biological sciences*, **367**, 2382-2394.

Gauthier, J., Parent, M., Lévesque, M. & Parent, A. (1999) The axonal arborization of single nigrostriatal neurons in rats. *Brain research*, **834**, 228-232.

Gerfen, C.R. (2000) Molecular effects of dopamine on striatal-projection pathways. *Trends in neurosciences*, **23**, S64-70.

Gerfen, C.R., Engber, T.M., Mahan, L.C., Susel, Z., Chase, T.N., Monsma, F.J., Jr. & Sibley, D.R. (1990) D1 and D2 dopamine receptor-regulated gene expression of striatonigral and striatopallidal neurons. *Science*, **250**, 1429-1432.

Gerfen, C.R., Herkenham, M. & Thibault, J. (1987) The neostriatal mosaic: II. Patch-and matrix-directed mesostriatal dopaminergic and non-dopaminergic systems. *Journal of Neuroscience*, **7**, 3915-3934.

Gerfen, C.R., Staines, W.A., Fibiger, H.C. & Arbuthnott, G.W. (1982) Crossed connections of the substantia nigra in the rat. *Journal of Comparative Neurology*, **207**, 283-303.

Gerlach, M., Gsell, W., Kornhuber, J., Jellinger, K., Krieger, V., Pantucek, F., Vock, R. & Riederer, P. (1996) A post mortem study on neurochemical markers of dopaminergic, GABA-ergic and glutamatergic neurons in basal ganglia-thalamocortical circuits in Parkinson syndrome. *Brain research*, **741**, 142-152.

German, D.C., Dubach, M., Askari, S., Speciale, S.G. & Bowden, D.M. (1988) 1-Methyl-4-phenyl-1,2,3,6-tetrahydropyridine-induced parkinsonian syndrome in Macaca fascicularis: which midbrain dopaminergic neurons are lost? *Neuroscience*, **24**, 161-174.

German, D.C., Manaye, K., Smith, W.K., Woodward, D.J. & Saper, C.B. (1989) Midbrain dopaminergic cell loss in Parkinson's disease: computer visualization. *Ann Neurol*, **26**, 507-514.

German, D.C., Manaye, K.F., Sonsalla, P.K. & Brooks, B.A. (1992a) Midbrain dopaminergic cell loss in Parkinson's disease and MPTP-induced parkinsonism: sparing of calbindin-D28k-containing cells. *Ann N Y Acad Sci*, **648**, 42-62.

German, D.C., Manaye, K.F., Sonsalla, P.K. & Brooks, B.A. (1992b) Midbrain Dopaminergic Cell Loss in Parkinson's Disease and MPTP-Induced Parkinsonism: Sparing of Calbindin-D25k—Containing Cellsa. *Annals of the New York Academy of Sciences*, **648**, 42-62.

Gershon, M.D. (2005) Nerves, reflexes, and the enteric nervous system: pathogenesis of the irritable bowel syndrome. *Journal of clinical gastroenterology*, **39**, S184-S193.

Gertler, T.S., Chan, C.S. & Surmeier, D.J. (2008) Dichotomous anatomical properties of adult striatal medium spiny neurons. *The Journal of neuroscience : the official journal of the Society for Neuroscience*, **28**, 10814-10824.

Gibb, W. & Lees, A. (1988) The relevance of the Lewy body to the pathogenesis of idiopathic Parkinson's disease. *Journal of Neurology, Neurosurgery & Psychiatry*, **51**, 745-752.

Glennon, R.A. (1987) Central serotonin receptors as targets for drug research. *Journal of medicinal chemistry*, **30**, 1-12.

Gong, S., Zheng, C., Doughty, M.L., Losos, K., Didkovsky, N., Schambra, U.B., Nowak, N.J., Joyner, A., Leblanc, G., Hatten, M.E. & Heintz, N. (2003) A gene expression atlas of the central nervous system based on bacterial artificial chromosomes. *Nature*, **425**, 917-925.

Gonon, F. (1997) Prolonged and extrasynaptic excitatory action of dopamine mediated by D1 receptors in the rat striatum in vivo. *Journal of Neuroscience*, **17**, 5972-5978.

Gonzales, K.K., Pare, J.F., Wichmann, T. & Smith, Y. (2013) GABAergic inputs from direct and indirect striatal projection neurons onto cholinergic interneurons in the primate putamen. *Journal of Comparative Neurology*, **521**, 2502-2522.

Grace, A. & Bunney, B. (1983) Intracellular and extracellular electrophysiology of nigral dopaminergic neurons—1. Identification and characterization. *Neuroscience*, **10**, 301-315.

Grace, A.A. & Bunney, B.S. (1984) The control of firing pattern in nigral dopamine neurons: single spike firing. *The Journal of neuroscience : the official journal of the Society for Neuroscience*, **4**, 2866-2876.

Grace, A.A. & Onn, S.-P. (1989) Morphology and electrophysiological properties of immunocytochemically identified rat dopamine neurons recorded in vitro. *Journal of Neuroscience*, **9**, 3463-3481.

Gradinaru, V., Mogri, M., Thompson, K.R., Henderson, J.M. & Deisseroth, K. (2009) Optical deconstruction of parkinsonian neural circuitry. *Science*, **324**, 354-359.

Granerus, A.-K., Magnusson, T., Roos, B.-E. & Svanborg, A. (1974) Relationship of age and mood to monoamine metabolites in cerebrospinal fluid in parkinsonism. *European journal of clinical pharmacology*, **7**, 105-109.

Gras, C., Amilhon, B., Lepicard, E.M., Poirel, O., Vinatier, J., Herbin, M., Dumas, S., Tzavara, E.T., Wade, M.R., Nomikos, G.G., Hanoun, N., Saurini, F., Kemel, M.L., Gasnier, B., Giros, B. & El Mestikawy, S. (2008) The vesicular glutamate transporter VGLUT3 synergizes striatal acetylcholine tone. *Nat Neurosci*, **11**, 292-300.

Gras, C., Herzog, E., Bellenchi, G.C., Bernard, V., Ravassard, P., Pohl, M., Gasnier, B., Giros, B. & El Mestikawy, S. (2002) A third vesicular glutamate transporter expressed by cholinergic and serotoninergic neurons. *The Journal of neuroscience : the official journal of the Society for Neuroscience*, **22**, 5442-5451.

Graveland, G.A. & DiFiglia, M. (1985) The frequency and distribution of medium-sized neurons with indented nuclei in the primate and rodent neostriatum. *Brain Res*, **327**, 307-311.

Graybiel, A.M. & Ragsdale, C.W., Jr. (1983) Biochemical anatomy of the striatum. In Emson, P.C. (ed) *Chemical Neuroanatomy*. Raven Press, New York, pp. 427-504.

Grofova, I., Deniau, J. & Kitai, S. (1982) Morphology of the substantia nigra pars reticulata projection neurons intracellularly labeled with HRP. *Journal of Comparative Neurology*, **208**, 352-368.

Grofová, I. & Rinvik, E. (1970) An experimental electron microscopic study on the striatonigral projection in the cat. *Exp Brain Res*, **11**, 249-262.

Groves, P., Linder, J. & Young, S. (1994) 5-hydroxydopamine-labeled dopaminergic axns: Three-dimensional reconstructions of axons, synapses and postsynaptic targets in rat neostriatum. *Neuroscience*, **58**, 593-604.

Guerra, M.J., Liste, I. & Labandeira-Garcia, J.L. (1997) Effects of lesions of the nigrostriatal pathway and of nigral grafts on striatal serotonergic innervation in adult rats. *Neuroreport*, **8**, 3485-3488.

Guiot, G. & Brion, S. (Year) Traitement des mouvements anormaux par la coagulation pallidale-Technique et resultats. Vol. 89, Rev Neurol (Paris). Masson, City. p. 578-580.

Gulley, R.L. & Wood, R.L. (1971) The fine structure of the neurons in the rat substantia nigra. *Tissue & cell*, **3**, 675-690.

Gundersen, H.J. (1986) Stereology of arbitrary particles. A review of unbiased number and size estimators and the presentation of some new ones, in memory of William R. Thompson. *Journal of microscopy*, **143**, 3-45.

Gundersen, H.J., Bagger, P., Bendtsen, T.F., Evans, S.M., Korbo, L., Marcussen, N., Moller, A., Nielsen, K., Nyengaard, J.R., Pakkenberg, B. & et al. (1988) The new stereological tools: disector, fractionator, nucleator and point sampled intercepts and their use in pathological research and diagnosis. *APMIS : acta pathologica, microbiologica, et immunologica Scandinavica*, **96**, 857-881.

Gundersen, H.J. & Jensen, E.B. (1987) The efficiency of systematic sampling in stereology and its prediction. *Journal of microscopy*, **147**, 229-263.

Gupta, M., Felten, D.L. & Gash, D.M. (1984) MPTP alters central catecholamine neurons in addition to the nigrostriatal system. *Brain Res Bull*, **13**, 737-742.

Guttman, M., Boileau, I., Warsh, J., Saint-Cyr, J.A., Ginovart, N., McCluskey, T., Houle, S., Wilson, A., Mundo, E., Rusjan, P., Meyer, J. & Kish, S.J. (2007) Brain serotonin transporter binding in non-depressed patients with Parkinson's disease. *Eur J Neurol*, **14**, 523-528.

Haapaniemi, T.H., Ahonen, A., Torniainen, P., Sotaniemi, K.A. & Myllylä, V.V. (2001) [123I] β-CIT SPECT demonstrates decreased brain dopamine and serotonin transporter levels in untreated parkinsonian patients. *Movement disorders*, **16**, 124-130.

Haber, S.N. & Fudge, J.L. (1997) The primate substantia nigra and VTA: integrative circuitry and function. *Critical Reviews™ in Neurobiology*, **11**.

Hadipour-Niktarash, A., Rommelfanger, K.S., Masilamoni, G.J., Smith, Y. & Wichmann, T. (2012a) Extrastriatal D2-like receptors modulate basal ganglia pathways in normal and Parkinsonian monkeys. *J Neurophysiol*, **107**, 1500-1512.

Hadipour-Niktarash, A., Rommelfanger, K.S., Masilamoni, G.J., Smith, Y. & Wichmann, T. (2012b) Extrastriatal D2-like receptors modulate basal ganglia pathways in normal and Parkinsonian monkeys. *J Neurophysiol*, **107**, 1500-1512.

Hadj Tahar, A., Gregoire, L., Darre, A., Belanger, N., Meltzer, L. & Bedard, P.J. (2004) Effect of a selective glutamate antagonist on L-dopa-induced dyskinesias in drug-naive parkinsonian monkeys. *Neurobiology of disease*, **15**, 171-176.

Hajós, M., Richards, C., Székely, A.D. & Sharp, T. (1998) An electrophysiological and neuroanatomical study of the medial prefrontal cortical projection to the midbrain raphe nuclei in the rat. *Neuroscience*, **87**, 95-108.

Halberstadt, A.L., Van Der Heijden, I., Ruderman, M.A., Risbrough, V.B., Gingrich, J.A., Geyer, M.A. & Powell, S.B. (2009) 5-HT2A and 5-HT2C receptors exert opposing effects on locomotor activity in mice. *Neuropsychopharmacology : official publication of the American College of Neuropsychopharmacology*, **34**, 1958-1967.

Halliday, G., Blumbergs, P., Cotton, R., Blessing, W. & Geffen, L. (1990) Loss of brainstem serotonin-and substance P-containing neurons in Parkinson's disease. *Brain research*, **510**, 104-107.

Hammond, C., Deniau, J., Rizk, A. & Feger, J. (1978) Electrophysiological demonstration of an excitatory subthalamonigral pathway in the rat. *Brain research*, **151**, 235-244.

Hansen, L., Salmon, D., Galasko, D., Masliah, E., Katzman, R., DeTeresa, R., Thal, L., Pay, M., Hofstetter, R. & Klauber, M. (1990) The Lewy body variant of Alzheimer's disease A clinical and pathologic entity. *Neurology*, **40**, 1-1.

Harding, A., Paxinos, G. & Halliday, G. (2004) Serotonin and tachykinin systems. In Paxinos, G. (ed) *The Rat Nervous System (3rd edition)*. Elsevier Academic Press, San Diego, pp. 1203-1256.

Harlan, R.E., Guillot, M. & Garcia, M.M. (2003) Re-evaluation of markers for the patch-matrix organization of the rat striatum. In Graybiel, A.M., DeLong, M.R., Kitai, S.T. (eds) *The Basal Ganglia VI*. Springer US, New York, pp. 393 - 397.

Hasbi, A., Fan, T., Alijaniaram, M., Nguyen, T., Perreault, M.L., O'Dowd, B.F. & George, S.R. (2009) Calcium signaling cascade links dopamine D1-D2 receptor heteromer to striatal BDNF production and neuronal growth. *Proceedings of the National Academy of Sciences of the United States of America*, **106**, 21377-21382.

Hassani, O.-K., François, C., Yelnik, J. & Féger, J. (1997) Evidence for a dopaminergic innervation of the subthalamic nucleus in the rat. *Brain research*, **749**, 88-94.

Hassler, R. (1938) Zur Pathologie der Paralysis agitans und des postenzephalitischen Parkinsonismus. *J Psychol Neurol*, **48**, 387-476.

Hassler, R. & Riechert, T. (1954) Indikationen und Lokalisationsmethode der gezielten Hirnoperationen. *Der Nervenarzt*, **25**, 441-447.

Hassler, R., Riechert, T., Mundinger, F., Umbach, W. & Ganglberger, J.A. (1960) Physiological observations in stereotaxic operations in extrapyramidal motor disturbances. *Brain : a journal of neurology*, **83**, 337-350.

Haycock, J.W., Kumer, S.C., Lewis, D.A., Vrana, K.E. & Stockmeier, C.A. (2002) A monoclonal antibody to tryptophan hydroxylase: applications and identification of the epitope. *J Neurosci Methods*, **114**, 205-212.

Hazrati, L.-N. & Parent, A. (1992a) Convergence of subthalamic and striatal efferents at pallidal level in primates: an anterograde double-labeling study with biocytin and PHA-L. *Brain research*, **569**, 336-340.

Hazrati, L.-N. & Parent, A. (1992b) The striatopallidal projection displays a high degree of anatomical specificity in the primate. *Brain research*, **592**, 213-227.

Hedreen, J.C. (1999) Tyrosine hydroxylase-immunoreactive elements in the human globus pallidus and subthalamic nucleus. *Journal of Comparative Neurology*, **409**, 400-410.

Heisler, L.K., Chu, H.-M., Brennan, T.J., Danao, J.A., Bajwa, P., Parsons, L.H. & Tecott, L.H. (1998) Elevated anxiety and antidepressant-like responses in serotonin 5-HT1A receptor mutant mice. *Proceedings of the National Academy of Sciences*, **95**, 15049-15054.

Hely, M.A., Morris, J.G., Reid, W.G. & Trafficante, R. (2005a) Sydney Multicenter Study of Parkinson's disease: non-L-dopa-responsive problems dominate at 15 years. *Movement disorders : official journal of the Movement Disorder Society*, **20**, 190-199.

Hely, M.A., Morris, J.G., Reid, W.G. & Trafficante, R. (2005b) Sydney multicenter study of Parkinson's disease: Non-L-dopa–responsive problems dominate at 15 years. *Movement Disorders*, **20**, 190-199.

Herkenham, M. & Nauta, W.J. (1979) Efferent connections of the habenular nuclei in the rat. *Journal of Comparative Neurology*, **187**, 19-47.

Hery, F., Faudon, M. & Ternaux, J.-P. (1982) In vivo release of serotonin in two raphe nuclei (raphe dorsalis and magnus) of the cat. *Brain research bulletin*, **8**, 123-129.

Hioki, H., Fujiyama, F., Nakamura, K., Wu, S.X., Matsuda, W. & Kaneko, T. (2004) Chemically specific circuit composed of vesicular glutamate transporter 3- and preprotachykinin B-producing interneurons in the rat neocortex. *Cereb Cortex*, **14**, 1266-1275.

Hioki, H., Nakamura, H., Ma, Y.F., Konno, M., Hayakawa, T., Nakamura, K.C., Fujiyama, F. & Kaneko, T. (2010) Vesicular glutamate transporter 3-expressing nonserotonergic projection neurons constitute a subregion in the rat midbrain raphe nuclei. *The Journal of comparative neurology*, **518**, 668-686.

Hnasko, T.S., Chuhma, N., Zhang, H., Goh, G.Y., Sulzer, D., Palmiter, R.D., Rayport, S. & Edwards, R.H. (2010) Vesicular glutamate transport promotes dopamine storage and glutamate corelease in vivo. *Neuron*, **65**, 643-656.

Hollister, A.S., Breese, G.R. & Mueller, R.A. (1979a) Role of monoamine neural systems in L-dihydroxyphenylalanine-stimulated activity. *The Journal of pharmacology and experimental therapeutics*, **208**, 37-43.

Hollister, A.S., Breese, G.R. & Mueller, R.A. (1979b) Role of monoamine neural systems in L-dihydroxyphenylalanine-stimulated activity. *Journal of Pharmacology and Experimental Therapeutics*, **208**, 37-43.

Holloway, R., Shoulson, I., Fahn, S., Kieburtz, K., Lang, A., Marek, K., McDermott, M., Seibyl, J., Weiner, W. & Musch, B. (2004) Pramipexole vs levodopa as initial treatment for Parkinson disease: a 4-year randomized controlled trial. *Archives of Neurology*, **61**, 1044-1053.

Hornung, J.P. (2003) The human raphe nuclei and the serotonergic system. *J Chem Neuroanat*, **26**, 331-343.

Hornung, J.P., Fritschy, J.M. & Tork, I. (1990) Distribution of two morphologically distinct subsets of serotoninergic axons in the cerebral cortex of the marmoset. *The Journal of comparative neurology*, **297**, 165-181.

Hornykiewicz, O. (1966) Dopamine (3-hydroxytyramine) and brain function. *Pharmacol Rev*, **18**, 925-964.

Hornykiewicz, O. (1998) Biochemical aspects of Parkinson's disease. *Neurology*, **51**, S2-9.

Hoyer, D., Engel, G. & Kalkman, H.O. (1985) Molecular pharmacology of 5-HT1 and 5-HT2 recognition sites in rat and pig brain membranes: radioligand binding studies with [3H] 5-HT,[3H] 8-OH-DPAT,(−)[125I] iodocyanopindolol,[3H] mesulergine and [3H] ketanserin. *European journal of pharmacology*, **118**, 13-23.

Huang, J., Spier, A.D. & Pickel, V.M. (2004) 5-HT3A receptor subunits in the rat medial nucleus of the solitary tract: subcellular distribution and relation to the serotonin transporter. *Brain Res*, **1028**, 156-169.

Huot, P. & Fox, S.H. (2013) The serotonergic system in motor and non-motor manifestations of Parkinson's disease. *Exp Brain Res*, **230**, 463-476.

Huot, P., Fox, S.H. & Brotchie, J.M. (2011a) The serotonergic system in Parkinson's disease. *Progress in neurobiology*, **95**, 163-212.

Huot, P., Fox, S.H., Newman-Tancredi, A. & Brotchie, J.M. (2011b) Anatomically selective serotonergic type 1A and serotonergic type 2A therapies for Parkinson's disease: an approach to reducing dyskinesia without exacerbating parkinsonism? *The Journal of pharmacology and experimental therapeutics*, **339**, 2-8.

Huot, P., Johnston, T.H., Koprich, J.B., Winkelmolen, L., Fox, S.H. & Brotchie, J.M. (2012a) Regulation of cortical and striatal 5-HT 1A receptors in the MPTP-lesioned macaque. *Neurobiology of aging*, **33**, 207. e209-207. e219.

Huot, P., Johnston, T.H., Winkelmolen, L., Fox, S.H. & Brotchie, J.M. (2012b) 5-HT 2A receptor levels increase in MPTP-lesioned macaques treated chronically with L-DOPA. *Neurobiology of aging*, **33**, 194. e195-194. e115.

Huot, P., Levesque, M. & Parent, A. (2007) The fate of striatal dopaminergic neurons in Parkinson's disease and Huntington's chorea. *Brain : a journal of neurology*, **130**, 222-232.

Hurley, K.M., Herbert, H., Moga, M.M. & Saper, C.B. (1991) Efferent projections of the infralimbic cortex of the rat. *Journal of Comparative Neurology*, **308**, 249-276.

Hurley, M.J., Brandon, B., Gentleman, S.M. & Dexter, D.T. (2013) Parkinson's disease is associated with altered expression of CaV1 channels and calcium-binding proteins. *Brain*, **136**, 2077-2097.

Hyman, J.M., Zilli, E.A., Paley, A.M. & Hasselmo, M.E. (2005) Medial prefrontal cortex cells show dynamic modulation with the hippocampal theta rhythm dependent on behavior. *Hippocampus*, **15**, 739-749.

Iacopino, A., Christakos, S., German, D., Sonsalla, P. & Altar, C. (1992) Calbindin-D 28k-containing neurons in animal models of neurodegeneration: possible protection from excitotoxicity. *Molecular Brain Research*, **13**, 251-261.

Ilinsky, I., Jouandet, M. & Goldman-Rakic, P. (1985) Organization of the nigrothalamocortical system in the rhesus monkey. *Journal of Comparative Neurology*, **236**, 315-330.

Imai, H., Steindler, D.A. & Kitai, S.T. (1986) The organization of divergent axonal projections from the midbrain raphe nuclei in the rat. *The Journal of comparative neurology*, **243**, 363-380.

Ingham, C., Hood, S. & Arbuthnott, G. (1989) Spine density on neostriatal neurones changes with 6-hydroxydopamine lesions and with age. *Brain research*, **503**, 334-338.

Ingham, C., Hood, S., Taggart, P. & Arbuthnott, G. (1998) Plasticity of synapses in the rat neostriatum after unilateral lesion of the nigrostriatal dopaminergic pathway. *Journal of Neuroscience*, **18**, 4732-4743.

Ingham, C.A., Hood, S.H., van Maldegem, B., Weenink, A. & Arbuthnott, G.W. (1993) Morphological changes in the rat neostriatum after unilateral 6-hydroxydopamine injections into the nigrostriatal pathway. *Experimental brain research*, **93**, 17-27.

Inui, A., Yoshikawa, T., Nagai, R., Yoshida, N. & Ito, T. (2002) Effects of mosapride citrate, a 5-HT4 receptor agonist, on colonic motility in conscious guinea pigs. *The Japanese Journal of Pharmacology*, **90**, 313-320.

Ito, K., Nagano-Saito, A., Kato, T., Arahata, Y., Nakamura, A., Kawasumi, Y., Hatano, K., Abe, Y., Yamada, T. & Kachi, T. (2002) Striatal and extrastriatal dysfunction in Parkinson's disease with dementia: a 6-[18F] fluoro-L-dopa PET study. *Brain : a journal of neurology*, **125**, 1358-1365.

Jackson, J., Bland, B.H. & Antle, M.C. (2009) Nonserotonergic projection neurons in the midbrain raphe nuclei contain the vesicular glutamate transporter VGLUT3. *Synapse*, **63**, 31-41.

Jan, C., Francois, C., Tande, D., Yelnik, J., Tremblay, L., Agid, Y. & Hirsch, E. (2000a) Dopaminergic innervation of the pallidum in the normal state, in MPTP-treated monkeys and in parkinsonian patients. *Eur J Neurosci*, **12**, 4525-4535.

Jan, C., François, C., Tandé, D., Yelnik, J., Tremblay, L., Agid, Y. & Hirsch, E. (2000b) Dopaminergic innervation of the pallidum in the normal state, in MPTP-treated monkeys and in parkinsonian patients. *European Journal of Neuroscience*, **12**, 4525-4535.

Jankovic, J., Rajput, A.H., McDermott, M.P. & Perl, D.P. (2000) The evolution of diagnosis in early Parkinson disease. *Archives of neurology*, **57**, 369-372.

Jankowski, M.P. & Sesack, S.R. (2004) Prefrontal cortical projections to the rat dorsal raphe nucleus: ultrastructural features and associations with serotonin and gamma-aminobutyric acid neurons. *The Journal of comparative neurology*, **468**, 518-529.

Jasmin, L., Granato, A. & Ohara, P.T. (2004) Rostral agranular insular cortex and pain areas of the central nervous system: A tract-tracing study in the rat. *Journal of Comparative Neurology*, **468**, 425-440.

Jaunarajs, K.E., George, J.A. & Bishop, C. (2012) L-DOPA-induced dysregulation of extrastriatal dopamine and serotonin and affective symptoms in a bilateral rat model of Parkinson's disease. *Neuroscience*, **218**, 243-256.

Jaunarajs, K.L.E., Dupre, K.B., Ostock, C.Y., Button, T., Deak, T. & Bishop, C. (2010) Behavioral and neurochemical effects of chronic L-DOPA treatment on non-motor sequelae in the hemiparkinsonian rat. *Behavioural pharmacology*, **21**, 627.

Javitch, J.A., D'Amato, R.J., Strittmatter, S.M. & Snyder, S.H. (1985) Parkinsonism-inducing neurotoxin, N-methyl-4-phenyl-1, 2, 3, 6-tetrahydropyridine: uptake of the metabolite N-methyl-4-phenylpyridine by dopamine neurons explains selective toxicity. *Proceedings of the National Academy of Sciences*, **82**, 2173-2177.

Jellinger, K. (1989) Pathology of Parkinson's Syndrome. In Calne, D. (ed) *Drugs for the Treatment of Parkinson's Disease*. Springer Berlin Heidelberg, pp. 47-112.

Jellinger, K., Riederer, P., Kleinberger, G., Wuketich, S. & Kothbauer, P. (1978) Brain monoamines in human hepatic encephalopathy. *Acta Neuropathol*, **43**, 63-68.

Jellinger, K.A. (2010) Synucleinopathies *Encyclopedia of Movement Disorders*. Academic Press, Oxford, pp. 203-207.

Johnson, K.A., Conn, P.J. & Niswender, C.M. (2009) Glutamate receptors as therapeutic targets for Parkinson's disease. *CNS & Neurological Disorders-Drug Targets (Formerly Current Drug Targets-CNS & Neurological Disorders)*, **8**, 475-491.

Johnson, M.D. (1994) Synaptic glutamate release by postnatal rat serotonergic neurons in microculture. *Neuron*, **12**, 433-442.

Jones, B.E. (2005) From waking to sleeping: neuronal and chemical substrates. *Trends Pharmacol Sci*, **26**, 578-586.

Jones, C.K., Engers, D.W., Thompson, A.D., Field, J.R., Blobaum, A.L., Lindsley, S.R., Zhou, Y., Gogliotti, R.D., Jadhav, S. & Zamorano, R. (2011) Discovery, synthesis, and structure–activity relationship development of a series of N-4-(2, 5-dioxopyrrolidin-1-yl) phenylpicolinamides (VU0400195, ML182): characterization of a novel positive allosteric modulator of the metabotropic glutamate receptor 4 (mGlu4) with oral efficacy in an antiparkinsonian animal model. *Journal of medicinal chemistry*, **54**, 7639-7647.

Jones, I.W., Bolam, J.P. & Wonnacott, S. (2001) Presynaptic localisation of the nicotinic acetylcholine receptor β2 subunit immunoreactivity in rat nigrostriatal dopaminergic neurones. *Journal of Comparative Neurology*, **439**, 235-247.

Jones, M.W. & Wilson, M.A. (2005) Theta rhythms coordinate hippocampal-prefrontal interactions in a spatial memory task. *PLoS biology*, **3**, e402.

Jost, W. & Schimrigk, K. (1993) Cisapride treatment of constipation in Parkinson's disease. *Movement disorders*, **8**, 339-343.

Jost, W. & Schimrigk, K. (1997) Long-term results with cisapride in Parkinson's disease. *Movement disorders*, **12**, 423-425.

Joyce, J.N., Shane, A., Lexow, N., Winokur, A., Casanova, M.F. & Kleinman, J.E. (1993) Serotonin uptake sites and serotonin receptors are altered in the limbic system of schizophrenics.

Neuropsychopharmacology : official publication of the American College of Neuropsychopharmacology, **8**, 315-336.

Juraska, J.M., Wilson, C.J. & Groves, P.M. (1977) The substantia nigra of the rat: a Golgi study. *Journal of Comparative Neurology*, **172**, 585-599.

Jürgens, U. (1984) The efferent and afferent connections of the supplementary motor area. *Brain research*, **300**, 63-81.

Kalén, P., Karlson, M. & Wiklund, L. (1985) Possible excitatory amino acid afferents to nucleus raphe dorsalis of the rat investigated with retrograde wheat germ agglutinin and D-[3H] aspartate tracing. *Brain research*, **360**, 285-297.

Kannari, K., Shen, H., Arai, A., Tomiyama, M. & Baba, M. (2006) Reuptake of L-DOPA-derived extracellular dopamine in the striatum with dopaminergic denervation via serotonin transporters. *Neurosci Lett*, **402**, 62-65.

Kannari, K., Yamato, H., Shen, H., Tomiyama, M., Suda, T. & Matsunaga, M. (2001) Activation of 5-HT(1A) but not 5-HT(1B) receptors attenuates an increase in extracellular dopamine derived from exogenously administered L-DOPA in the striatum with nigrostriatal denervation. *J Neurochem*, **76**, 1346-1353.

Kawaguchi, Y., Wilson, C.J. & Emson, P.C. (1990) Projection subtypes of rat neostriatal matrix cells revealed by intracellular injection of biocytin. *The Journal of neuroscience : the official journal of the Society for Neuroscience*, **10**, 3421-3438.

Kellar, K.J., Brown, P.A., Madrid, J., Bernstein, M., Vernikos-Danellis, J. & Mehler, W.R. (1977) Origins of serotonin innervation of forebrain structures. *Exp Neurol*, **56**, 52-62.

Kelley, A.E. & Swanson, C.J. (1997) Feeding induced by blockade of AMPA and kainate receptors within the ventral striatum: a microinfusion mapping study. *Behavioural brain research*, **89**, 107-113.

Kemp, J.M. & Powell, T. (1971) The structure of the caudate nucleus of the cat: light and electron microscopy. *Philosophical Transactions of the Royal Society of London B: Biological Sciences*, **262**, 383-401.

Kempster, P., Frankel, J., Bovingdon, M., Webster, R., Lees, A. & Stern, G. (1989) Levodopa peripheral pharmacokinetics and duration of motor response in Parkinson's disease. *Journal of Neurology, Neurosurgery & Psychiatry*, **52**, 718-723.

Kerenyi, L., Ricaurte, G.A., Schretlen, D.J., McCann, U., Varga, J., Mathews, W.B., Ravert, H.T., Dannals, R.F., Hilton, J., Wong, D.F. & Szabo, Z. (2003) Positron emission tomography of striatal serotonin transporters in Parkinson disease. *Arch Neurol*, **60**, 1223-1229.

Kia, H.K., Brisorgueil, M.J., Hamon, M., Calas, A. & Vergé, D. (1996a) Ultrastructural localization of 5-hydroxytryptamine1A receptors in the rat brain. *Journal of neuroscience research*, **46**, 697-708.

Kia, H.K., Miquel, M.C., Brisorgueil, M.J., Daval, G., Riad, M., Mestikawy, S.E., Hamon, M. & Vergé, D. (1996b) Immunocytochemical localization of serotonin1A receptors in the rat central nervous system. *Journal of Comparative Neurology*, **365**, 289-305.

Kim, R., Nakano, K., Jayaraman, A. & Carpenter, M.B. (1976) Projections of the globus pallidus and adjacent structures: an autoradiographic study in the monkey. *Journal of Comparative Neurology*, **169**, 263-289.

Kim, S.E., Choi, J.Y., Choe, Y.S., Choi, Y. & Lee, W.Y. (2003) Serotonin transporters in the midbrain of Parkinson's disease patients: a study with ^{123}I-beta-CIT SPECT. *J Nucl Med*, **44**, 870-876.

Kimura, M. & Matsumoto, N. (1997) Nigrostriatal dopamine system may contribute to behavioral learning through providing reinforcement signals to the striatum. *European neurology*, **38 Suppl 1**, 11-17.

Kincaid, A.E., Penney, J.B., Young, A.B. & Newman, S.W. (1991) The globus pallidus receives a projection from the parafascicular nucleus in the rat. *Brain research*, **553**, 18-26.

Kish, S.J., Tong, J., Hornykiewicz, O., Rajput, A., Chang, L.J., Guttman, M. & Furukawa, Y. (2008) Preferential loss of serotonin markers in caudate versus putamen in Parkinson's disease. *Brain : a journal of neurology*, **131**, 120-131.

Kita, H., Chiken, S., Tachibana, Y. & Nambu, A. (2007) Serotonin modulates pallidal neuronal activity in the awake monkey. *J Neurosci*, **27**, 75-83.

Kita, H. & Kita, T. (2001) Number, origins, and chemical types of rat pallidostriatal projection neurons. *Journal of Comparative Neurology*, **437**, 438-448.

Kita, H. & Kitai, S. (1987) Efferent projections of the subthalamic nucleus in the rat: light and electron microscopic analysis with the PHA-L method. *Journal of Comparative Neurology*, **260**, 435-452.

Kitai, S. & Deniau, J. (1981) Cortical inputs to the subthalamus: intracellular analysis. *Brain research*, **214**, 411-415.

Kiyasova, V., Fernandez, S.P., Laine, J., Stankovski, L., Muzerelle, A., Doly, S. & Gaspar, P. (2011) A genetically defined morphologically and functionally unique subset of 5-HT neurons in the mouse raphe nuclei. *The Journal of neuroscience : the official journal of the Society for Neuroscience*, **31**, 2756-2768.

Klein, C. & Schlossmacher, M.G. (2007) Parkinson disease, 10 years after its genetic revolution: multiple clues to a complex disorder. *Neurology*, **69**, 2093-2104.

Klemm, W.R. (2004) Habenular and interpeduncularis nuclei: shared components in multiple-function networks. *Medical Science Monitor*, **10**, RA261-RA273.

Kliem, M.A., Maidment, N.T., Ackerson, L.C., Chen, S., Smith, Y. & Wichmann, T. (2007a) Activation of nigral and pallidal dopamine D1-like receptors modulates basal ganglia outflow in monkeys. *J Neurophysiol*, **98**, 1489-1500.

Kliem, M.A., Maidment, N.T., Ackerson, L.C., Chen, S., Smith, Y. & Wichmann, T. (2007b) Activation of nigral and pallidal dopamine D1-like receptors modulates basal ganglia outflow in monkeys. *J Neurophysiol*, **98**, 1489-1500.

Kliem, M.A., Pare, J.F., Khan, Z.U., Wichmann, T. & Smith, Y. (2010a) Ultrastructural localization and function of dopamine D1-like receptors in the substantia nigra pars reticulata and the internal segment of the globus pallidus of parkinsonian monkeys. *Eur J Neurosci*, **31**, 836-851.

Kliem, M.A., Pare, J.F., Khan, Z.U., Wichmann, T. & Smith, Y. (2010b) Ultrastructural localization and function of dopamine D1-like receptors in the substantia nigra pars reticulata and the internal segment of the globus pallidus of parkinsonian monkeys. *European Journal of Neuroscience*, **31**, 836-851.

Knobelman, D.A., Kung, H.F. & Lucki, I. (2000) Regulation of extracellular concentrations of 5-hydroxytryptamine (5-HT) in mouse striatum by 5-HT1A and 5-HT1B receptors. *Journal of Pharmacology and Experimental Therapeutics*, **292**, 1111-1117.

Kocsis, B., Varga, V., Dahan, L. & Sik, A. (2006) Serotonergic neuron diversity: identification of raphe neurons with discharges time-locked to the hippocampal theta rhythm. *Proceedings of the National Academy of Sciences of the United States of America*, **103**, 1059-1064.

Kocsis, B. & Vertes, R.P. (1992) Dorsal raphe neurons: synchronous discharge with the theta rhythm of the hippocampus in the freely behaving rat. *Journal of neurophysiology*, **68**, 1463-1467.

Kohler, C., Chan-Palay, V. & Steinbusch, H. (1982) The distribution and origin of serotonin-containing fibers in the septal area: a combined immunohistochemical and fluorescent retrograde tracing study in the rat. *The Journal of comparative neurology*, **209**, 91-111.

Köhler, C., Chan-Palay, V. & Steinbusch, H. (1981) The distribution and orientation of serotonin fibers in the entorhinal and other retrohippocampal areas. *Anatomy and Embryology*, **161**, 237-264.

Köhler, C., Radesäter, A.-C., Lang, W. & Chan-Palay, V. (1986) Distribution of serotonin-1A receptors in the monkey and the postmortem human hippocampal region. A quantitative autoradiographic study using the selective agonist [3 H] 8-OH-DPAT. *Neurosci Lett*, **72**, 43-48.

Kohler, C. & Steinbusch, H. (1982) Identification of serotonin and non-serotonin-containing neurons of the mid-brain raphe projecting to the entorhinal area and the hippocampal formation. A combined immunohistochemical and fluorescent retrograde tracing study in the rat brain. *Neuroscience*, **7**, 951-975.

Kornhuber, J., Kim, J.-S., Kornhuber, M.E. & Kornhuber, H.H. (1984) The cortico-nigral projection: reduced glutamate content in the substantia nigra following frontal cortex ablation in the rat. *Brain research*, **322**, 124-126.

Kosofsky, B.E. & Molliver, M.E. (1987) The serotoninergic innervation of cerebral cortex: different classes of axon terminals arise from dorsal and median raphe nuclei. *Synapse*, **1**, 153-168.

Kreiss, D.S. & Lucki, I. (1994) Differential regulation of serotonin (5-HT) release in the striatum and hippocampus by 5-HT1A autoreceptors of the dorsal and median raphe nuclei. *Journal of Pharmacology and Experimental Therapeutics*, **269**, 1268-1279.

Künzle, H. (1978) An Autoradiographic Analysis of the Efferent Connections from Premotor and Adjacent Prefrontal Regions (Areas 6 and 9) in Macaca fascicularis; pp. 210–234. *Brain, behavior and evolution*, **15**, 210-234.

Künzle, H. & Akert, K. (1977) Efferent connections of cortical, area 8 (frontal eye field) in Macaca fascicularis. A reinvestigation using the autoradiographic technique. *Journal of Comparative Neurology*, **173**, 147-163.

Kuo, J.S. & Carpenter, M.B. (1973) Organization of pallidothalamic projections in the rhesus monkey. *Journal of Comparative Neurology*, **151**, 201-235.

Kupchik, Y.M., Brown, R.M., Heinsbroek, J.A., Lobo, M.K., Schwartz, D.J. & Kalivas, P.W. (2015) Coding the direct/indirect pathways by D1 and D2 receptors is not valid for accumbens projections. *Nat Neurosci*, **18**, 1230-1232.

Lai, M., Tsang, S., Alder, J., Keene, J., Hope, T., Esiri, M., Francis, P. & Chen, C. (2005) Loss of serotonin 5-HT2A receptors in the postmortem temporal cortex correlates with rate of cognitive decline in Alzheimer's disease. *Psychopharmacology*, **179**, 673-677.

Lamirault, L. & Simon, H. (2001) Enhancement of place and object recognition memory in young adult and old rats by RS 67333, a partial agonist of 5-HT 4 receptors. *Neuropharmacology*, **41**, 844-853.

Landolt, H.P. & Wehrle, R. (2009) Antagonism of serotonergic 5-HT2A/2C receptors: mutual improvement of sleep, cognition and mood? *European Journal of Neuroscience*, **29**, 1795-1809.

Langston, J.W. (2017) The MPTP Story. *Journal of Parkinson's Disease*, **7**, S11.

Langston, J.W., Forno, L.S., Rebert, C.S. & Irwin, I. (1984) Selective nigral toxicity after systemic administration of 1-methyl-4-phenyl-1, 2, 5, 6-tetrahydropyrine (MPTP) in the squirrel monkey. *Brain research*, **292**, 390-394.

Lapper, S. & Bolam, J. (1992) Input from the frontal cortex and the parafascicular nucleus to cholinergic interneurons in the dorsal striatum of the rat. *Neuroscience*, **51**, 533-545.

Lavoie, B. & Parent, A. (1990) Immunohistochemical study of the serotoninergic innervation of the basal ganglia in the squirrel monkey. *The Journal of comparative neurology*, **299**, 1-16.

Lavoie, B. & Parent, A. (1991a) Dopaminergic neurons expressing calbindin in normal and parkinsonian monkeys. *Neuroreport*, **2**, 601-604.

Lavoie, B. & Parent, A. (1991b) Dopaminergic neurons expressing calbindin in normal and parkinsonian monkeys. *Neuroreport*, **2**, 601-604.

Lavoie, B. & Parent, A. (1994a) Pedunculopontine nucleus in the squirrel monkey: cholinergic and glutamatergic projections to the substantia nigra. *Journal of Comparative Neurology*, **344**, 232-241.

Lavoie, B. & Parent, A. (1994b) Pedunculopontine nucleus in the squirrel monkey: projections to the basal ganglia as revealed by anterograde tract-tracing methods. *Journal of Comparative Neurology*, **344**, 210-231.

Lavoie, B., Smith, Y. & Parent, A. (1989) Dopaminergic innervation of the basal ganglia in the squirrel monkey as revealed by tyrosine hydroxylase immunohistochemistry. *Journal of Comparative Neurology*, **289**, 36-52.

Le Moine, C. & Bloch, B. (1995) D1 and D2 dopamine receptor gene expression in the rat striatum: sensitive cRNA probes demonstrate prominent segregation of D1 and D2 mRNAs in distinct neuronal populations of the dorsal and ventral striatum. *The Journal of comparative neurology*, **355**, 418-426.

Lee, C.S., Samii, A., Sossi, V., Ruth, T.J., Schulzer, M., Holden, J.E., Wudel, J., Pal, P.K., La Fuente-Fernandez, D. & Calne, D.B. (2000) In vivo positron emission tomographic evidence for compensatory changes in presynaptic dopaminergic nerve terminals in Parkinson's disease. *Ann Neurol*, **47**, 493-503.

Lee, H.S., Kim, M.-A., Valentino, R.J. & Waterhouse, B.D. (2003) Glutamatergic afferent projections to the dorsal raphe nucleus of the rat. *Brain research*, **963**, 57-71.

Lee, H.S., Lee, B.Y. & Waterhouse, B.D. (2005a) Retrograde study of projections from the tuberomammillary nucleus to the dorsal raphe and the locus coeruleus in the rat. *Brain research*, **1043**, 65-75.

Lee, H.S., Park, S.H., Song, W.C. & Waterhouse, B.D. (2005b) Retrograde study of hypocretin-1 (orexin-A) projections to subdivisions of the dorsal raphe nucleus in the rat. *Brain research*, **1059**, 35-45.

Lee, M.D. & Simansky, K.J. (1997) CP-94,253: a selective serotonin1B (5-HT1B) agonist that promotes satiety. *Psychopharmacology*, **131**, 264-270.

Lee, S.P., So, C.H., Rashid, A.J., Varghese, G., Cheng, R., Lanca, A.J., O'Dowd, B.F. & George, S.R. (2004) Dopamine D1 and D2 receptor Co-activation generates a novel phospholipase C-mediated calcium signal. *J Biol Chem*, **279**, 35671-35678.

Leenders, K.L., Salmon, E.P., Tyrrell, P., Perani, D., Brooks, D.J., Sager, H., Jones, T., Marsden, C.D. & Frackowiak, R.S. (1990) The nigrostriatal dopaminergic system assessed in vivo by positron emission tomography in healthy volunteer subjects and patients with Parkinson's disease. *Archives of Neurology*, **47**, 1290-1298.

Leichnetz, G. & Astruc, J. (1977) The course of some prefrontal corticofugals to the pallidum, substantia innominata, and amygdaloid complex in monkeys. *Exp Neurol*, **54**, 104-109.

Lelong, V., Dauphin, F. & Boulouard, M. (2001) RS 67333 and D-cycloserine accelerate learning acquisition in the rat. *Neuropharmacology*, **41**, 517-522.

Lester, J., Fink, S., Aronin, N. & DiFiglia, M. (1993) Colocalization of D1 and D2 dopamine receptor mRNAs in striatal neurons. *Brain Res*, **621**, 106-110.

Levesque, M. & Parent, A. (2005) The striatofugal fiber system in primates: a reevaluation of its organization based on single-axon tracing studies. *Proceedings of the National Academy of Sciences of the United States of America*, **102**, 11888-11893.

Lewis, S.J., Pavese, N., Rivero-Bosch, M., Eggert, K., Oertel, W., Mathias, C.J., Brooks, D.J. & Gerhard, A. (2012) Brain monoamine systems in multiple system atrophy: a positron emission tomography study. *Neurobiol Dis*, **46**, 130-136.

Lewy, F. (1912) Paralysis agitans. I. Pathologische anatomie. *Handbuch der neurologie*, **3**, 920-933.

Li, Y.Q., Kaneko, T. & Mizuno, N. (2001a) Collateral projections of nucleus raphe dorsalis neurones to the caudate-putamen and region around the nucleus raphe magnus and nucleus reticularis gigantocellularis pars alpha in the rat. *Neuroscience letters*, **299**, 33-36.

Li, Y.Q., Li, H., Kaneko, T. & Mizuno, N. (2001b) Morphological features and electrophysiological properties of serotonergic and non-serotonergic projection neurons in the dorsal raphe nucleus. An intracellular recording and labeling study in rat brain slices. *Brain Res*, **900**, 110-118.

Lidov, H., Grzanna, R. & Molliver, M. (1980) The serotonin innervation of the cerebral cortex in the rat—an immunohistochemical analysis. *Neuroscience*, **5**, 207-227.

Lindgren, H.S., Andersson, D.R., Lagerkvist, S., Nissbrandt, H. & Cenci, M.A. (2010) l-DOPA-induced dopamine efflux in the striatum and the substantia nigra in a rat model of Parkinson's disease: temporal and quantitative relationship to the expression of dyskinesia. *J Neurochem*, **112**, 1465-1476.

Lindvall, O. & Björklund, A. (1974) The organization of the ascending catecholamine neuron systems in the rat brain as revealed by the glyoxylic acid fluorescence method. *Acta Physiol Scand Suppl*, **412**, 1.

Lloyd, K.G., Farley, I.J., Deck, J.H. & Hornykiewicz, O. (1974) Serotonin and 5-hydroxyindoleacetic acid in discrete areas of the brainstem of suicide victims and control patients. *Adv Biochem Psychopharmacol*, **11**, 387-397.

Lopes, A.P., da Cunha, I.C., Steffens, S.M., Ferraz, A., Vargas, J.C., de Lima, T.C., Neto, J.M., Faria, M.S. & Paschoalini, M.A. (2007) GABAA and GABAB agonist microinjections into medial accumbens shell increase feeding and induce anxiolysis in an animal model of anxiety. *Behavioural brain research*, **184**, 142-149.

Lopez, A., Munoz, A., Guerra, M.J. & Labandeira-Garcia, J.L. (2001) Mechanisms of the effects of exogenous levodopa on the dopamine-denervated striatum. *Neuroscience*, **103**, 639-651.

Lorens, S.A. & Guldberg, H.C. (1974) Regional 5-hydroxytryptamine following selective midbrain raphe lesions in the rat. *Brain research*, **78**, 45-56.

Luginger, E., Wenning, G., Bösch, S. & Poewe, W. (2000) Beneficial effects of amantadine on L-dopa-induced dyskinesias in Parkinson's disease. *Movement Disorders*, **15**, 873-878.

Luk, K. & Sadikot, A. (2001) GABA promotes survival but not proliferation of parvalbumin-immunoreactive interneurons in rodent neostriatum: an in vivo study with stereology. *Neuroscience*, **104**, 93-103.

Luthman, J., Bolioli, B., Tsutsumi, T., Verhofstad, A. & Jonsson, G. (1987) Sprouting of striatal serotonin nerve terminals following selective lesions of nigro-striatal dopamine neurons in neonatal rat. *Brain research bulletin*, **19**, 269-274.

Luys, J. (1865) *Recherches sur le système nerveux cérébro-spinal: sa structure, ses fonctions et ses maladies*. J.-B. Bailliére et fils.

Mackay, A.V., Yates, C.M., Wright, A., Hamilton, P. & Davies, P. (1978) Regional distribution of monoamines and their metabolites in the human brain. *Journal of neurochemistry*, **30**, 841-848.

Maeda, T., Kannari, K., Shen, H., Arai, A., Tomiyama, M., Matsunaga, M. & Suda, T. (2003) Rapid induction of serotonergic hyperinnervation in the adult rat striatum with extensive dopaminergic denervation. *Neuroscience letters*, **343**, 17-20.

Maeda, T., Nagata, K., Yoshida, Y. & Kannari, K. (2005a) Serotonergic hyperinnervation into the dopaminergic denervated striatum compensates for dopamine conversion from exogenously administered l-DOPA. *Brain Res*, **1046**, 230-233.

Maeda, T., Nagata, K., Yoshida, Y. & Kannari, K. (2005b) Serotonergic hyperinnervation into the dopaminergic denervated striatum compensates for dopamine conversion from exogenously administered l-DOPA. *Brain research*, **1046**, 230-233.

Mai, J.K., Paxinos, G. & Voss, T. (2008) *Atlas of the Human Brain (3rd edition)*. Elsevier Academic Press, San Diego.

Malleret, G., Hen, R., Guillou, J.-L., Segu, L. & Buhot, M.-C. (1999) 5-HT1B receptor knock-out mice exhibit increased exploratory activity and enhanced spatial memory performance in the Morris water maze. *Journal of Neuroscience*, **19**, 6157-6168.

Mamounas, L.A., Mullen, C.A., O'hearn, E. & Molliver, M.E. (1991) Dual serotoninergic projections to forebrain in the rat: Morphologically distinct 5-HT axon terminals exhibit differential vulnerability to neurotoxic amphetamine derivatives. *Journal of Comparative Neurology*, **314**, 558-586.

Mann, D.M. & Yates, P.O. (1983a) Pathological basis for neurotransmitter changes in Parkinson's disease. *Neuropathology and applied neurobiology*, **9**, 3-19.

Mann, D.M. & Yates, P.O. (1983b) Possible role of neuromelanin in the pathogenesis of Parkinson's disease. *Mechanisms of ageing and development*, **21**, 193-203.

Marin, C., Aguilar, E., Rodriguez-Oroz, M.C., Bartoszyk, G.D. & Obeso, J.A. (2009) Local administration of sarizotan into the subthalamic nucleus attenuates levodopa-induced dyskinesias in 6-OHDA-lesioned rats. *Psychopharmacology (Berl)*, **204**, 241-250.

Markesbery, W.R., Jicha, G.A., Liu, H. & Schmitt, F.A. (2009) Lewy body pathology in normal elderly subjects. *Journal of Neuropathology & Experimental Neurology*, **68**, 816-822.

Markey, S., Johannessen, J., Chiueh, C., Burns, R. & Herkenham, M. (1984) Intraneuronal generation of a pyridinium metabolite may cause drug-induced parkinsonism. *Nature*, **311**, 464-467.

Martin, K.A. & Spühler, I.A. (2013) The fine structure of the dopaminergic innervation of area 10 of macaque prefrontal cortex. *European Journal of Neuroscience*, **37**, 1061-1071.

Martin, K.F., Hannon, S., Phillips, I. & Heal, D.J. (1992) Opposing roles for 5-HT1B and 5-HT3 receptors in the control of 5-HT release in rat hippocampus in vivo. *British journal of pharmacology*, **106**, 139-142.

Masilamoni, G., Weinkle, A., Bogenpohl, J., Groover, O., Wichmann, T. & Smith, Y. (2011) A nonhuman primate model of Parkinson's disease associated with cortical and subcortical dopaminergic, noradrenergic and serotonergic neuronal degeneration. *Movement Disorders*, **26**, S23-S24.

Mathur, B.N., Capik, N.A., Alvarez, V.A. & Lovinger, D.M. (2011) Serotonin induces long-term depression at corticostriatal synapses. *Journal of Neuroscience*, **31**, 7402-7411.

Matsuda, W., Furuta, T., Nakamura, K.C., Hioki, H., Fujiyama, F., Arai, R. & Kaneko, T. (2009) Single nigrostriatal dopaminergic neurons form widely spread and highly dense axonal arborizations in the neostriatum. *Journal of Neuroscience*, **29**, 444-453.

Maurice, N., Mercer, J., Chan, C.S., Hernandez-Lopez, S., Held, J., Tkatch, T. & Surmeier, D.J. (2004) D2 dopamine receptor-mediated modulation of voltage-dependent Na+ channels reduces autonomous activity in striatal cholinergic interneurons. *The Journal of neuroscience : the official journal of the Society for Neuroscience*, **24**, 10289-10301.

Mayeux, R. (2003) Epidemiology of neurodegeneration. *Annual review of neuroscience*, **26**, 81-104.

Mayeux, R., Stern, Y., Cote, L. & Williams, J.B. (1984) Altered serotonin metabolism in depressed patients with Parkinson's disease. *Neurology*, **34**, 642-642.

McDowell, F., Lee, J.E., Swift, T., Sweet, R.D., Ogsbury, J.S. & Kessler, J.T. (1970) Treatment of Parkinson's syndrome with L dihydroxyphenylalanine (levodopa). *Annals of internal medicine*, **72**, 29-35.

McGeer, P., McGeer, E., Scherer, U. & Singh, K. (1977a) A glutamatergic corticostriatal path? *Brain research*, **128**, 369-373.

McGeer, P. & Zeldowicz, L. (1964) Administration of dihydroxyphenylalanine to parkinsonian patients. *Can Med Assoc J*, **90**, 463.

McGeer, P.L., Boulding, J.E., Gibson, W.C. & Foulkes, R.G. (1961) Drug-induced extrapyramidal reactions. Treatment with diphenhydramine hydrochloride and dihydroxyphenylalanine. *JAMA*, **177**, 665-670.

McGeer, P.L., Itagaki, S., Akiyama, H. & McGeer, E.G. (1988) Rate of cell death in parkinsonism indicates active neuropathological process. *Ann Neurol*, **24**, 574-576.

McGeer, P.L., McGeer, E.G. & Suzuki, J.S. (1977b) Aging and extrapyramidal function. *Archives of Neurology*, **34**, 33-35.

McMahon, L.R. & Cunningham, K.A. (1999) Antagonism of 5-hydroxytryptamine4 receptors attenuates hyperactivity induced by cocaine: putative role for 5-hydroxytryptamine4 receptors in the nucleus accumbens shell. *Journal of Pharmacology and Experimental Therapeutics*, **291**, 300-307.

McNeill, T.H., Brown, S.A., Rafols, J.A. & Shoulson, I. (1988) Atrophy of medium spiny I striatal dendrites in advanced Parkinson's disease. *Brain Res*, **455**, 148-152.

Meador-Woodruff, J.H., Mansour, A., Healy, D.J., Kuehn, R., Zhou, Q.Y., Bunzow, J.R., Akil, H., Civelli, O. & Watson, S.J., Jr. (1991) Comparison of the distributions of D1 and D2 dopamine receptor mRNAs in rat brain. *Neuropsychopharmacology : official publication of the American College of Neuropsychopharmacology*, **5**, 231-242.

Meissner, W., Prunier, C., Guilloteau, D., Chalon, S., Gross, C.E. & Bezard, E. (2003) Time-course of nigrostriatal degeneration in a progressive MPTP-lesioned macaque model of Parkinson's disease. *Mol Neurobiol*, **28**, 209-218.

Metman, L.V., Del Dotto, P., Van Den Munckhof, P., Fang, J., Mouradian, M. & Chase, T. (1998) Amantadine as treatment for dyskinesias and motor fluctuations in Parkinson's disease. *Neurology*, **50**, 1323-1326.

Meynert, T. (1872) The brain of mammals. *A manual of histology*, 650-766.

Michelsen, K.A., Prickaerts, J. & Steinbusch, H.W. (2008) The dorsal raphe nucleus and serotonin: implications for neuroplasticity linked to major depression and Alzheimer's disease. *Prog Brain Res*, **172**, 233-264.

Middlemiss, D.N. (1984) Stereoselective blockade at [3H] 5-HT binding sites and at the 5-HT autoreceptor by propranolol. *European journal of pharmacology*, **101**, 289-293.

Mignon, L.J. & Wolf, W.A. (2005) 8-hydroxy-2-(di-n-propylamino) tetralin reduces striatal glutamate in an animal model of Parkinson's disease. *Neuroreport*, **16**, 699-703.

Miller, D.W. & Abercrombie, E.D. (1999) Role of High-Affinity Dopamine Uptake and Impulse Activity in the Appearance of Extracellular Dopamine in Striatum After Administration of Exogenous L-DOPA. *J Neurochem*, **72**, 1516-1522.

Miller, W.C. & DeLong, M.R. (1987) Altered Tonic Activity of Neurons in the Globus Pallidus and Subthalamic Nucleus in the Primate MPTP Model of Parkinsonism. In Carpenter, M.B., Jayaraman, A. (eds) *The Basal Ganglia II: Structure and Function—Current Concepts*. Springer US, Boston, MA, pp. 415-427.

Mintz, E.M. & Scott, T.J. (2006) Colocalization of serotonin and vesicular glutamate transporter 3-like immunoreactivity in the midbrain raphe of Syrian hamsters (Mesocricetus auratus). *Neuroscience letters*, **394**, 97-100.

Miyawaki, E., Meah, Y. & Koller, W.C. (1997) Serotonin, dopamine, and motor effects in Parkinson's disease. *Clin Neuropharmacol*, **20**, 300-310.

Monakow, K.H.-v., Akert, K. & Künzle, H. (1978) Projections of the precentral motor cortex and other cortical areas of the frontal lobe to the subthalamic nucleus in the monkey. *Exp Brain Res*, **33**, 395-403.

Monti, J.M. & Jantos, H. (2008) The roles of dopamine and serotonin, and of their receptors, in regulating sleep and waking. *Prog Brain Res*, **172**, 625-646.

Moore, R.Y., Halaris, A.E. & Jones, B.E. (1978) Serotonin neurons of the midbrain raphe: ascending projections. *Journal of Comparative Neurology*, **180**, 417-438.

Moore, R.Y., Whone, A.L. & Brooks, D.J. (2008) Extrastriatal monoamine neuron function in Parkinson's disease: an 18F-dopa PET study. *Neurobiol Dis*, **29**, 381-390.

Mori, S., Matsuura, T., Takino, T. & Sano, Y. (1987) Light and electron microscopic immunohistochemical studies of serotonin nerve fibers in the substantia nigra of the rat, cat and monkey. *Anat Embryol (Berl)*, **176**, 13-18.

Mori, S., Takino, T., Yamada, H. & Sano, Y. (1985a) Immunohistochemical demonstration of serotonin nerve fibers in the subthalamic nucleus of the rat, cat and monkey. *Neurosci Lett*, **62**, 305-309.

Mori, S., Ueda, S., Yamada, H., Takino, T. & Sano, Y. (1985b) Immunohistochemical demonstration of serotonin nerve fibers in the corpus striatum of the rat, cat and monkey. *Anat Embryol (Berl)*, **173**, 1-5.

Morin, L. & Meyer-Bernstein, E. (1999a) The ascending serotonergic system in the hamster: comparison with projections of the dorsal and median raphe nuclei. *Neuroscience*, **91**, 81-105.

Morin, L.P. & Meyer-Bernstein, E.L. (1999b) The ascending serotonergic system in the hamster: comparison with projections of the dorsal and median raphe nuclei. *Neuroscience*, **91**, 81-105.

Morrish, P., Sawle, G. & Brooks, D. (1995) Clinical and [18F] dopa PET findings in early Parkinson's disease. *Journal of Neurology, Neurosurgery & Psychiatry*, **59**, 597-600.

Moss, J. & Bolam, J.P. (2008) A dopaminergic axon lattice in the striatum and its relationship with cortical and thalamic terminals. *The Journal of neuroscience : the official journal of the Society for Neuroscience*, **28**, 11221-11230.

Mostany, R., Pazos, A. & Castro, M.E. (2005a) Autoradiographic characterisation of [35 S] GTPγS binding stimulation mediated by 5-HT 1B receptor in postmortem human brain. *Neuropharmacology*, **48**, 25-33.

Mostany, R., Pazos, A. & Castro, M.E. (2005b) Autoradiographic characterisation of [35S]GTPgammaS binding stimulation mediated by 5-HT1B receptor in postmortem human brain. *Neuropharmacology*, **48**, 25-33.

Moukhles, H., Bosler, O., Bolam, J.P., Vallee, A., Umbriaco, D., Geffard, M. & Doucet, G. (1997) Quantitative and morphometric data indicate precise cellular interactions between serotonin terminals and postsynaptic targets in rat substantia nigra. *Neuroscience*, **76**, 1159-1171.

Mounayar, S., Boulet, S., Tande, D., Jan, C., Pessiglione, M., Hirsch, E.C., Feger, J., Savasta, M., Francois, C. & Tremblay, L. (2007a) A new model to study compensatory mechanisms in MPTP-treated monkeys exhibiting recovery. *Brain*, **130**, 2898-2914.

Mounayar, S., Boulet, S., Tandé, D., Jan, C., Pessiglione, M., Hirsch, E.C., Féger, J., Savasta, M., François, C. & Tremblay, L. (2007b) A new model to study compensatory mechanisms in MPTP-treated monkeys exhibiting recovery. *Brain : a journal of neurology*, **130**, 2898-2914.

Mouton, P.R., Gokhale, A.M., Ward, N.L. & West, M.J. (2002) Stereological length estimation using spherical probes. *Journal of microscopy*, **206**, 54-64.

Mugnaini, E.O.W.H. & Oertel, W.H. (1985) An atlas of the distribution of GABAergic neurons and terminals in the rat CNS as revealed by GAD immunohistochemistry. *Handbook of chemical neuroanatomy*, **4**, 436-608.

Müller, C.P., Carey, R.J., Huston, J.P. & Silva, M.A.D.S. (2007) Serotonin and psychostimulant addiction: focus on 5-HT 1A-receptors. *Prog Neurobiol*, **81**, 133-178.

Mulligan, K.A. & Tork, I. (1988) Serotoninergic innervation of the cat cerebral cortex. *The Journal of comparative neurology*, **270**, 86-110.

Nagatsu, I., Kobayashi, K., Fujii, T., Komori, K., Sekiguchi, K., Titani, K., Fujita, K. & Nagatsu, T. (1990) Antibodies raised against different oligopeptide segments of human dopamine-beta-hydroxylase. *Neuroscience letters*, **120**, 141-145.

Nagatsu, T. & Sawada, M. (2009) L-dopa therapy for Parkinson's disease: past, present, and future. *Parkinsonism & related disorders*, **15**, S3-S8.

Naito, A. & Kita, H. (1994) The cortico-nigral projection in the rat: an anterograde tracing study with biotinylated dextran amine. *Brain research*, **637**, 317-322.

Nakamura, H., Saheki, T., Ichiki, H., Nakata, K. & Nakagawa, S. (1991) Immunocytochemical localization of argininosuccinate synthetase in the rat brain. *Journal of Comparative Neurology*, **312**, 652-679.

Nandhagopal, R., Kuramoto, L., Schulzer, M., Mak, E., Cragg, J., Lee, C.S., McKenzie, J., McCormick, S., Samii, A. & Troiano, A. (2009) Longitudinal progression of sporadic Parkinson's disease: a multi-tracer positron emission tomography study. *Brain : a journal of neurology*, awp209.

Nauta, H.J. & Cole, M. (1978) Efferent projections of the subthalamic nucleus: an autoradiographic study in monkey and cat. *Journal of Comparative Neurology*, **180**, 1-16.

Nauta, W.J.H. & Mehler, W.R. (1966) Projections of the Lentiform Nucleus in the Monkey *Neuroanatomy*. Birkhäuser Boston, Boston, MA, pp. 393-431.

Navailles, S., Bioulac, B., Gross, C. & De Deurwaerdere, P. (2010) Serotonergic neurons mediate ectopic release of dopamine induced by L-DOPA in a rat model of Parkinson's disease. *Neurobiology of disease*, **38**, 136-143.

Navailles, S., Bioulac, B., Gross, C. & De Deurwaerdere, P. (2011) Chronic L-DOPA therapy alters central serotonergic function and L-DOPA-induced dopamine release in a region-dependent manner in a rat model of Parkinson's disease. *Neurobiology of disease*, **41**, 585-590.

Nayyar, T., Bubser, M., Ferguson, M.C., Diana Neely, M., Shawn Goodwin, J., Montine, T.J., Deutch, A.Y. & Ansah, T.A. (2009) Cortical serotonin and norepinephrine denervation in parkinsonism: preferential loss of the beaded serotonin innervation. *European Journal of Neuroscience*, **30**, 207-216.

Nelson, A.B., Bussert, T.G., Kreitzer, A.C. & Seal, R.P. (2014a) Striatal cholinergic neurotransmission requires VGLUT3. *Journal of Neuroscience*, **34**, 8772-8777.

Nelson, A.B., Hammack, N., Yang, C.F., Shah, N.M., Seal, R.P. & Kreitzer, A.C. (2014b) Striatal cholinergic interneurons Drive GABA release from dopamine terminals. *Neuron*, **82**, 63-70.

Neumane, S., Mounayar, S., Jan, C., Epinat, J., Ballanger, B., Costes, N., Feger, J., Thobois, S., Francois, C., Sgambato-Faure, V. & Tremblay, L. (2012) Effects of dopamine and serotonin antagonist injections into the striatopallidal complex of asymptomatic MPTP-treated monkeys. *Neurobiol Dis*, **48**, 27-39.

Ng, K., Chase, T., Colburn, R. & Kopin, I. (1970a) L-Dopa-induced release of cerebral monoamines. *Science*, **170**, 76-77.

Ng, K., Chase, T., Colburn, R. & Kopin, I. (1972) Release of [3 H] dopamine by l-5-hydroxytryptophan. *Brain research*, **45**, 499-505.

Ng, K.Y., Chase, T.N., Colburn, R.W. & Kopin, I.J. (1970b) L-Dopa-induced release of cerebral monoamines. *Science*, **170**, 76-77.

Ng, K.Y., Colburn, R.W. & Kopin, I.J. (1971) Effects of L-dopa on efflux of cerebral monoamines from synaptosomes. *Nature*, **230**, 331-332.

Nichols, D.E. & Nichols, C.D. (2008) Serotonin receptors. *Chemical reviews*, **108**, 1614-1641.

Nickerson Poulin, A., Guerci, A., El Mestikawy, S. & Semba, K. (2006) Vesicular glutamate transporter 3 immunoreactivity is present in cholinergic basal forebrain neurons projecting to the basolateral amygdala in rat. *Journal of Comparative Neurology*, **498**, 690-711.

Nicklas, W., Vyas, I. & Heikkila, R.E. (1985) Inhibition of NADH-linked oxidation in brain mitochondria by 1-methyl-4-phenyl-pyridine, a metabolite of the neurotoxin, 1-methyl-4-phenyl-1, 2, 5, 6-tetrahydropyridine. *Life sciences*, **36**, 2503-2508.

Nilsson, F., Kessing, L. & Bolwig, T. (2001) Increased risk of developing Parkinson's disease for patients with major affective disorder: a register study. *Acta Psychiatrica Scandinavica*, **104**, 380-386.

Nishijima, H., Suzuki, S., Kon, T., Funamizu, Y., Ueno, T., Haga, R., Suzuki, C., Arai, A., Kimura, T., Suzuki, C., Meguro, R., Miki, Y., Yamada, J., Migita, K., Ichinohe, N., Ueno, S., Baba, M. & Tomiyama, M. (2014) Morphologic changes of dendritic spines of striatal neurons in the levodopa-induced dyskinesia model. *Movement disorders : official journal of the Movement Disorder Society*, **29**, 336-343.

Numan, S., Lundgren, K.H., Wright, D.E., Herman, J.P. & Seroogy, K.B. (1995) Increased expression of 5HT 2 receptor mRNA in rat striatum following 6-OHDA lesions of the adult nigrostriatal pathway. *Molecular brain research*, **29**, 391-396.

Nurmi, E., Ruottinen, H.M., Bergman, J., Haaparanta, M., Solin, O., Sonninen, P. & Rinne, J.O. (2001) Rate of progression in Parkinson's disease: A 6-[18F] fluoro-L-dopa PET study. *Movement Disorders*, **16**, 608-615.

Nyholm, D., Remahl, A.N., Dizdar, N., Constantinescu, R., Holmberg, B., Jansson, R., Aquilonius, S.-M. & Askmark, H. (2005) Duodenal levodopa infusion monotherapy vs oral polypharmacy in advanced Parkinson disease. *Neurology*, **64**, 216-223.

Oberlander, C., Blaquière, B. & Pujol, J.-F. (1986) Distinct functions for dopamine and serotonin in locomotor behaviour: evidence using the 5-HT 1 agonist RU 24969 in globus pallidus-lesioned rats. *Neurosci Lett*, **67**, 113-118.

Oberlander, C., Demassey, Y., Verdu, A., Van de Velde, D. & Bardelay, C. (1987) Tolerance to the serotonin 5-HT1 agonist RU 24969 and effects on dopaminergic behaviour. *European journal of pharmacology*, **139**, 205-214.

Obeso, J.A., Olanow, C.W. & Nutt, J.G. (2000a) Levodopa motor complications in Parkinson's disease. *Trends in neurosciences*, **23**, S2-7.

Obeso, J.A., Olanow, C.W. & Nutt, J.G. (2000b) Levodopa motor complications in Parkinson's disease. *Trends in neurosciences*, **23**, S2-7.

Ohama, E. & Ikuta, F. (1976) Parkinson's disease: distribution of Lewy bodies and monoamine neuron system. *Acta neuropathologica*, **34**, 311-319.

Olson, L., Boreus, L.O. & Seiger, A. (1973) Histochemical demonstration and mapping of 5-hydroxytryptamine- and catecholamine-containing neuron systems in the human fetal brain. *Z Anat Entwicklungsgesch*, **139**, 259-282.

Oppenheimer, D. (1992) Disease of the basal ganglia, cerebellum and motor neurons. *Greenfield's neuropathology*.

Overstreet, D.H., Commissaris, R.C., De La Garza 2nd, R., File, S.E., Knapp, D.J. & Seiden, L.S. (2003) Involvement of 5-HT1A receptors in animal tests of anxiety and depression: evidence from genetic models. *Stress (Amsterdam, Netherlands)*, **6**, 101-110.

Owens, M.J. & Nemeroff, C.B. (1994) Role of serotonin in the pathophysiology of depression: focus on the serotonin transporter. *Clin Chem*, **40**, 288-295.

Pacelli, C., Giguère, N., Bourque, M.-J., Lévesque, M., Slack, R.S. & Trudeau, L.-É. (2015) Elevated mitochondrial bioenergetics and axonal arborization size are key contributors to the vulnerability of dopamine neurons. *Current Biology*, **25**, 2349-2360.

Pagano, G., Niccolini, F., Fusar-Poli, P. & Politis, M. (2017) Serotonin transporter in Parkinson's disease: A meta-analysis of positron emission tomography studies. *Ann Neurol*, **81**, 171-180.

Palkovits, M., Brownstein, M. & Saavedra, J.M. (1974) Serotonin content of the brain stem nuclei in the rat. *Brain Res*, **80**, 237-249.

Parent, A. (1986) *Comparative Neurobiology of the Basal Ganglia*. John Wiley, New York.

Parent, A. (1990) Extrinsic connections of the basal ganglia. *Trends in neurosciences*, **13**, 254-258.

Parent, A. (1996) *Carpenter's Human Neuroanatomy (9th edition)*. Williams & Wilkins, Baltimore.

Parent, A., Charara, A. & Pinault, D. (1995) Single striatofugal axons arborizing in both pallidal segments and in the substantia nigra in primates. *Brain Res*, **698**, 280-284.

Parent, A., Descarries, L. & Beaudet, A. (1981) Organization of ascending serotonin systems in the adult rat brain. A radioautographic study after intraventricular administration of [3H]5-hydroxytryptamine. *Neuroscience*, **6**, 115-138.

Parent, A. & Hazrati, L.-N. (1995a) Functional anatomy of the basal ganglia. II. The place of subthalamic nucleus and external pallidium in basal ganglia circuitry. *Brain Res Rev*, **20**, 128-154.

Parent, A. & Hazrati, L.N. (1995b) Functional anatomy of the basal ganglia. I. The cortico-basal ganglia-thalamo-cortical loop. *Brain research. Brain research reviews*, **20**, 91-127.

Parent, A. & Lavoie, B. (1993) The heterogeneity of the mesostriatal dopaminergic system as revealed in normal and parkinsonian monkeys. *Adv Neurol*, **60**, 25-33.

Parent, A., Lavoie, B., Smith, Y. & Bedard, P. (1989) The dopaminergic nigropallidal projection in primates: distinct cellular origin and relative sparing in MPTP-treated monkeys. *Advances in neurology*, **53**, 111-116.

Parent, A., Lavoie, B., Smith, Y. & Bedard, P. (1990) The dopaminergic nigropallidal projection in primates: distinct cellular origin and relative sparing in MPTP-treated monkeys. *Adv Neurol*, **53**, 111-116.

Parent, A., Poitras, D. & Dubé, L. (1984) Comparative anatomy of central monoaminergic systems. In Bjorklund, A., Hokfelt, T. (eds) *Handbook of Chemical Neuroanatomy. Vol.2: Classical Neurotransmitters in the CNS, Part 1, Chap. 9*. Elsevier, Amsterdam, pp. 409-439.

Parent, A., Sato, F., Wu, Y., Gauthier, J., Levesque, M. & Parent, M. (2000) Organization of the basal ganglia: the importance of axonal collateralization. *Trends in neurosciences*, **23**, S20-27.

Parent, A. & Smith, Y. (1987) Differential dopaminergic innervation of the two pallidal segments in the squirrel monkey (Saimiri sciureus). *Brain Res*, **426**, 397-400.

Parent, M., Lévesque, M. & Parent, A. (2001) Two types of projection neurons in the internal pallidum of primates: single-axon tracing and three-dimensional reconstruction. *Journal of Comparative Neurology*, **439**, 162-175.

Parent, M. & Parent, A. (2005) Single-axon tracing and three-dimensional reconstruction of centre médian-parafascicular thalamic neurons in primates. *Journal of Comparative Neurology*, **481**, 127-144.

Parent, M. & Parent, A. (2006a) Relationship between axonal collateralization and neuronal degeneration in basal ganglia. *J Neural Transm Suppl*, 85-88.

Parent, M. & Parent, A. (2006b) Relationship between axonal collateralization and neuronal degeneration in basal ganglia. *J Neural Transm Suppl*, 85-88.

Parent, M., Wallman, M.J. & Descarries, L. (2010) Distribution and ultrastructural features of the serotonin innervation in rat and squirrel monkey subthalamic nucleus. *Eur J Neurosci*, **31**, 1233-1242.

Parent, M., Wallman, M.J., Gagnon, D. & Parent, A. (2011) Serotonin innervation of basal ganglia in monkeys and humans. *J Chem Neuroanat*, **41**, 256-265.

Park, M.R., Imai, H. & Kitai, S.T. (1982) Morphology and intracellular responses of an identified dorsal raphe projection neuron. *Brain Res*, **240**, 321-326.

Parkinson-Study-Group (2004) A controlled, randomized, delayed-start study of rasagiline in early Parkinson disease. *Archives of Neurology*, **61**, 561.

Parkinson, J. (1817) An essay on the shaking palsy (Printed by Whittingham and Rowland for Sherwood, Neely, and Jones). London.

Parkkinen, L., Kauppinen, T., Pirttilä, T., Autere, J.M. & Alafuzoff, I. (2005) α-Synuclein pathology does not predict extrapyramidal symptoms or dementia. *Ann Neurol*, **57**, 82-91.

Parkkinen, L., Pirttilä, T. & Alafuzoff, I. (2008) Applicability of current staging/categorization of α-synuclein pathology and their clinical relevance. *Acta neuropathologica*, **115**, 399-407.

Parkkinen, L., Soininen, H. & Alafuzoff, I. (2003) Regional distribution of α-synuclein pathology in unimpaired aging and Alzheimer disease. *Journal of Neuropathology & Experimental Neurology*, **62**, 363-367.

Pasik, P., Pasik, T., Holstein, G.R. & Saavedra, J.M. (1984a) Serotoninergic innervation of the monkey basal ganglia: an immunocytochemical light and electron microscopic study. In McKenzie, J.S., Kemm,

R.E., Wilcock, L.N. (eds) *The Basal Ganglia: Structure and Function*. Plenum Press, New York, pp. 115-129.

Pasik, P., Pasik, T., Pecci-Saavedra, J., Holstein, G.R. & Yahr, M.D. (1984b) Serotonin in pallidal neuronal circuits: an immunocytochemical study in monkeys. *Adv Neurol*, **40**, 63-76.

Pasik, P., Pasik, T. & Saavedra, J.P. (1982) Immunocytochemical localization of serotonin at the ultrastructural level. *J Histochem Cytochem*, **30**, 760-764.

Pasik, T. & Pasik, P. (1982) Serotoninergic afferents in the monkey neostriatum. *Acta Biol Acad Sci Hung*, **33**, 277-288.

Pasqualotto, B.A., Hope, B.T. & Vincent, S.R. (1991) Citrulline in the rat brain: immunohistochemistry and coexistence with NADPH-diaphorase. *Neurosci Lett*, **128**, 155-160.

Patel, S., Roberts, J., Moorman, J. & Reavill, C. (1995) Localization of serotonin-4 receptors in the striatonigral pathway in rat brain. *Neuroscience*, **69**, 1159-1167.

Paulus, W. & Jellinger, K. (1991) The neuropathologic basis of different clinical subgroups of Parkinson's disease. *Journal of Neuropathology & Experimental Neurology*, **50**, 743-755.

Pavese, N., Metta, V., Bose, S.K., Chaudhuri, K.R. & Brooks, D.J. (2010) Fatigue in Parkinson's disease is linked to striatal and limbic serotonergic dysfunction. *Brain : a journal of neurology*, **133**, 3434-3443.

Pavese, N., Rivero-Bosch, M., Lewis, S.J., Whone, A.L. & Brooks, D.J. (2011) Progression of monoaminergic dysfunction in Parkinson's disease: a longitudinal 18F-dopa PET study. *Neuroimage*, **56**, 1463-1468.

Pavese, N., Simpson, B.S., Metta, V., Ramlackhansingh, A., Chaudhuri, K.R. & Brooks, D.J. (2012) [(1)(8)F]FDOPA uptake in the raphe nuclei complex reflects serotonin transporter availability. A combined [(1)(8)F]FDOPA and [(1)(1)C]DASB PET study in Parkinson's disease. *Neuroimage*, **59**, 1080-1084.

Paxinos, G. & Watson, C. (1986) *The Rat Brain in Stereotaxic Coordinates*. Academic Press, Sidney.

Pazos, A. & Palacios, J. (1985) Quantitative autoradiographic mapping of serotonin receptors in the rat brain. I. Serotonin-1 receptors. *Brain research*, **346**, 205-230.

Pazos, A., Probst, A. & Palacios, J. (1987a) Serotonin receptors in the human brain—IV. Autoradiographic mapping of serotonin-2 receptors. *Neuroscience*, **21**, 123-139.

Pazos, A., Probst, A. & Palacios, J.M. (1987b) Serotonin receptors in the human brain--III. Autoradiographic mapping of serotonin-1 receptors. *Neuroscience*, **21**, 97-122.

Penney, J. & Young, A. (1983) Speculations on the functional anatomy of basal ganglia disorders. *Annual review of neuroscience*, **6**, 73-94.

Perez-Otano, I., Herrero, M.T., Oset, C., De Ceballos, M.L., Luquin, M.R., Obeso, J.A. & Del Rio, J. (1991) Extensive loss of brain dopamine and serotonin induced by chronic administration of MPTP in the marmoset. *Brain Res*, **567**, 127-132.

Perreault, M.L., Fan, T., Alijaniaram, M., O'Dowd, B.F. & George, S.R. (2012) Dopamine D1-D2 receptor heteromer in dual phenotype GABA/glutamate-coexpressing striatal medium spiny neurons: regulation of BDNF, GAD67 and VGLUT1/2. *PloS one*, **7**, e33348.

Perreault, M.L., Hasbi, A., Alijaniaram, M., Fan, T., Varghese, G., Fletcher, P.J., Seeman, P., O'Dowd, B.F. & George, S.R. (2010) The dopamine D1-D2 receptor heteromer localizes in dynorphin/enkephalin neurons: increased high affinity state following amphetamine and in schizophrenia. *J Biol Chem*, **285**, 36625-36634.

Perreault, M.L., Hasbi, A., O'Dowd, B.F. & George, S.R. (2011) The dopamine d1-d2 receptor heteromer in striatal medium spiny neurons: evidence for a third distinct neuronal pathway in Basal Ganglia. *Frontiers in neuroanatomy*, **5**, 31.

Perreault, M.L., Hasbi, A., Shen, M.Y., Fan, T., Navarro, G., Fletcher, P.J., Franco, R., Lanciego, J.L. & George, S.R. (2016) Disruption of a dopamine receptor complex amplifies the actions of cocaine. *European neuropsychopharmacology : the journal of the European College of Neuropsychopharmacology*, **26**, 1366-1377.

Peschanski, M. & Besson, J.M. (1984) Diencephalic connections of the raphe nuclei of the rat brainstem: an anatomical study with reference to the somatosensory system. *Journal of Comparative Neurology*, **224**, 509-534.

Petryszyn, S. (2016) Les interneurones striataux exprimant la calrétinine : comparaison interspécifique et étude neuroanatomopathologique *Faculté de médecine*. Université Laval, Québec.

Peyron, C., Luppi, P.-H., Kitahama, K., Fort, P., Hermann, D.M. & Jouvet, M. (1995) Origin of the dopaminergic innervation of the rat dorsal raphe nucleus. *Neuroreport*, **6**, 2527-2531.

Peyron, C., Luppi, P.H., Fort, P., Rampon, C. & Jouvet, M. (1996) Lower brainstem catecholamine afferents to the rat dorsal raphe nucleus. *Journal of Comparative Neurology*, **364**, 402-413.

Peyron, C., Petit, J.-M., Rampon, C., Jouvet, M. & Luppi, P.-H. (1997) Forebrain afferents to the rat dorsal raphe nucleus demonstrated by retrograde and anterograde tracing methods. *Neuroscience*, **82**, 443-468.

Peyron, C., Tighe, D.K., Van Den Pol, A.N., De Lecea, L., Heller, H.C., Sutcliffe, J.G. & Kilduff, T.S. (1998) Neurons containing hypocretin (orexin) project to multiple neuronal systems. *Journal of Neuroscience*, **18**, 9996-10015.

Piccini, P., Morrish, P., Turjanski, N., Sawle, G., Burn, D., Weeks, R., Mark, M., Maraganore, D., Lees, A.J. & Brooks, D. (1997) Dopaminergic function in familial Parkinson's disease: A clinical and 18F-dopa positron emission tomography study. *Ann Neurol*, **41**, 222-229.

Pickel, V.M. & Chan, J. (1999) Ultrastructural localization of the serotonin transporter in limbic and motor compartments of the nucleus accumbens. *The Journal of neuroscience : the official journal of the Society for Neuroscience*, **19**, 7356-7366.

Pifl, C., Schingnitz, G. & Hornykiewicz, O. (1991) Effect of 1-methyl-4-phenyl-1,2,3,6-tetrahydropyridine on the regional distribution of brain monoamines in the rhesus monkey. *Neuroscience*, **44**, 591-605.

Pifl, C., Schingnitz, G. & Hornykiewicz, O. (1992) Striatal and non-striatal neurotransmitter changes in MPTP-parkinsonism in rhesus monkey: the symptomatic versus the asymptomatic condition. *Neurochem Int*, **20 Suppl**, 295S-297S.

Ploska, A., Taquet, H., Javoy-Agid, F., Gaspar, P., Cesselin, F., Berger, B., Hamon, M., Legrand, J.C. & Agid, Y. (1982) Dopamine and methionine-enkephalin in human brain. *Neurosci Lett*, **33**, 191-196.

Poewe, W. (2008) Non-motor symptoms in Parkinson's disease. *European Journal of Neurology*, **15**, 14-20.

Poewe, W. & Wenning, G.K. (2000) Apomorphine: an underutilized therapy for Parkinson's disease. *Movement Disorders*, **15**, 789-794.

Poirier, L.J., Giguére, M. & Marchand, R. (1983) Comparative morphology of the substantia nigra and ventral tegmental area in the monkey, cat and rat. *Brain research bulletin*, **11**, 371-397.

Politis, M., Wu, K., Loane, C., Brooks, D.J., Kiferle, L., Turkheimer, F.E., Bain, P., Molloy, S. & Piccini, P. (2014) Serotonergic mechanisms responsible for levodopa-induced dyskinesias in Parkinson's disease patients. *The Journal of clinical investigation*, **124**, 1340-1349.

Politis, M., Wu, K., Loane, C., Kiferle, L., Molloy, S., Brooks, D.J. & Piccini, P. (2010a) Staging of serotonergic dysfunction in Parkinson's disease: an in vivo 11 C-DASB PET study. *Neurobiol Dis*, **40**, 216-221.

Politis, M., Wu, K., Loane, C., Turkheimer, F., Molloy, S., Brooks, D. & Piccini, P. (2010b) Depressive symptoms in PD correlate with higher 5-HTT binding in raphe and limbic structures. *Neurology*, **75**, 1920-1927.

Pollak, P., Benabid, A.L., Gross, C., Gao, D.M., Laurent, A., Benazzouz, A., Hoffmann, D., Gentil, M. & Perret, J. (1993) [Effects of the stimulation of the subthalamic nucleus in Parkinson disease]. *Revue neurologique*, **149**, 175-176.

Polymeropoulos, M.H., Lavedan, C., Leroy, E., Ide, S.E., Dehejia, A., Dutra, A., Pike, B., Root, H., Rubenstein, J. & Boyer, R. (1997) Mutation in the α-synuclein gene identified in families with Parkinson's disease. *Science*, **276**, 2045-2047.

Pons, R., Syrengelas, D., Youroukos, S., Orfanou, I., Dinopoulos, A., Cormand, B., Ormazabal, A., Garzía-Cazorla, A., Serrano, M. & Artuch, R. (2013) Levodopa-induced dyskinesias in tyrosine hydroxylase deficiency. *Movement Disorders*, **28**, 1058-1063.

Pourcher, E., Bonnet, A.M., Kefalos, J., Dubois, B. & Agid, Y. (1989) Effects of etybenzatropine and diazepam on levodopa-induced diphasic dyskinesias in Parkinson's disease. *Movement disorders : official journal of the Movement Disorder Society*, **4**, 195-201.

Powell, T. & Cowan, W. (1956) A study of thalamo-striate relations in the monkey. *Brain : a journal of neurology*, **79**, 364-366.

Prensa, L., Cossette, M. & Parent, A. (2000) Dopaminergic innervation of human basal ganglia. *J Chem Neuroanat*, **20**, 207-213.

Prensa, L., Gimenez-Amaya, J.M. & Parent, A. (1999) Chemical heterogeneity of the striosomal compartment in the human striatum. *The Journal of comparative neurology*, **413**, 603-618.

Prensa, L.a. & Parent, A. (2001) The nigrostriatal pathway in the rat: a single-axon study of the relationship between dorsal and ventral tier nigral neurons and the striosome/matrix striatal compartments. *Journal of Neuroscience*, **21**, 7247-7260.

Qamhawi, Z., Towey, D., Shah, B., Pagano, G., Seibyl, J., Marek, K., Borghammer, P., Brooks, D.J. & Pavese, N. (2015) Clinical correlates of raphe serotonergic dysfunction in early Parkinson's disease. *Brain : a journal of neurology*, awv215.

Qian, Y., Melikian, H.E., Rye, D.B., Levey, A.I. & Blakely, R.D. (1995) Identification and characterization of antidepressant-sensitive serotonin transporter proteins using site-specific antibodies. *The Journal of neuroscience : the official journal of the Society for Neuroscience*, **15**, 1261-1274.

Quinn, N.P. (1998) Classification of fluctuations in patients with Parkinson's disease. *Neurology*, **51**, S25-S29.

Quist, J., Barr, C., Schachar, R., Roberts, W., Malone, M., Tannock, R., Basile, V., Beitchman, J. & Kennedy, J. (2000) Evidence for the serotonin HTR2A receptor gene as a susceptibility factor in attention deficit hyperactivity disorder (ADHD). *Molecular psychiatry*, **5**, 537.

Radja, F., Descarries, L., Dewar, K.M. & Reader, T.A. (1993) Serotonin 5-HT 1 and 5-HT 2 receptors in adult rat brain after neonatal destruction of nigrostriatal dopamine neurons: a quantitative autoradiographic study. *Brain research*, **606**, 273-285.

Rafols, J.A. & Fox, C.A. (1976) The neurons in the primate subthalamic nucleus: a Golgi and electron microscopic study. *Journal of Comparative Neurology*, **168**, 75-111.

Raisman, R., Cash, R. & Agid, Y. (1986) Parkinson's disease: decreased density of ^{3}H-imipramine and ^{3}H-paroxetine binding sites in putamen. *Neurology*, **36**, 556-560.

Rajput, A.H., Fenton, M.E., Birdi, S., Macaulay, R., George, D., Rozdilsky, B., Ang, L.C., Senthilselvan, A. & Hornykiewicz, O. (2002a) Clinical-pathological study of levodopa complications. *Movement disorders : official journal of the Movement Disorder Society*, **17**, 289-296.

Rajput, A.H., Fenton, M.E., Birdi, S., Macaulay, R., George, D., Rozdilsky, B., Ang, L.C., Senthilselvan, A. & Hornykiewicz, O. (2002b) Clinical–pathological study of levodopa complications. *Movement disorders*, **17**, 289-296.

Rajput, A.H., Sitte, H.H., Rajput, A., Fenton, M.E., Pifl, C. & Hornykiewicz, O. (2008) Globus pallidus dopamine and Parkinson motor subtypes: clinical and brain biochemical correlation. *Neurology*, **70**, 1403-1410.

Rakshi, J., Uema, T., Ito, K., Bailey, D., Morrish, P., Ashburner, J., Dagher, A., Jenkins, I., Friston, K. & Brooks, D. (1999) Frontal, midbrain and striatal dopaminergic function in early and advanced Parkinson's disease A 3D [18F] dopa-PET study. *Brain : a journal of neurology*, **122**, 1637-1650.

Ramboz, S., Saudou, F., Amara, D.A., Belzung, C., Segu, L., Misslin, R., Buhot, M.-C. & Hen, R. (1995) 5-HT 1B receptor knock out—behavioral consequences. *Behav Brain Res*, **73**, 305-312.

Rapport, M.M., Green, A.A. & Page, I.H. (Year) Purification of the substance which is responsible for the vasoconstrictor activity of serum. Vol. 6, Federation proceedings. City. p. 184-184.

Rapport, M.M., Green, A.A. & Page, I.H. (1948) Serum vasoconstrictor (serotonin) IV. Isolation and characterization. *Journal of Biological Chemistry*, **176**, 1243-1251.

Rascol, O., Brooks, D.J., Korczyn, A.D., De Deyn, P.P., Clarke, C.E. & Lang, A.E. (2000) A five-year study of the incidence of dyskinesia in patients with early Parkinson's disease who were treated with ropinirole or levodopa. *New England Journal of Medicine*, **342**, 1484-1491.

Rav-Acha, M., Bergman, H. & Yarom, Y. (2008) Pre- and postsynaptic serotoninergic excitation of globus pallidus neurons. *Journal of neurophysiology*, **100**, 1053-1066.

Ravina, B., Marder, K., Fernandez, H.H., Friedman, J.H., McDonald, W., Murphy, D., Aarsland, D., Babcock, D., Cummings, J. & Endicott, J. (2007) Diagnostic criteria for psychosis in Parkinson's disease: report of an NINDS, NIMH work group. *Movement Disorders*, **22**, 1061-1068.

Raz, A., Feingold, A., Zelanskaya, V., Vaadia, E. & Bergman, H. (1996) Neuronal synchronization of tonically active neurons in the striatum of normal and parkinsonian primates. *Journal of neurophysiology*, **76**, 2083-2088.

Raz, A., Frechter-Mazar, V., Feingold, A., Abeles, M., Vaadia, E. & Bergman, H. (2001) Activity of pallidal and striatal tonically active neurons is correlated in mptp-treated monkeys but not in normal monkeys. *The Journal of neuroscience : the official journal of the Society for Neuroscience*, **21**, RC128.

Reijnders, J.S., Ehrt, U., Weber, W.E., Aarsland, D. & Leentjens, A.F. (2008) A systematic review of prevalence studies of depression in Parkinson's disease. *Movement Disorders*, **23**, 183-189.

Reisine, T.D., Fields, J.Z. & Yamamura, H.I. (1977) Neurotransmitter receptor alterations in Parkinson's disease. *Life sciences*, **21**, 335-343.

Révy, D., Jaouen, F., Salin, P., Melon, C., Chabbert, D., Tafi, E., Concetta, L., Langa, F., Amalric, M. & Kerkerian-Le Goff, L. (2014) Cellular and behavioral outcomes of dorsal striatonigral neuron ablation: new insights into striatal functions. *Neuropsychopharmacology*, **39**, 2662-2672.

Reynolds, G., Mason, S., Meldrum, A., Keczer, S., Parties, H., Eglen, R. & Wong, E. (1995) 5-Hydroxytryptamine (5-HT) 4 receptors in post mortem human brain tissue: distribution, pharmacology and effects of neurodegenerative diseases. *British journal of pharmacology*, **114**, 993-998.

Riad, M., Garcia, S., Watkins, K.C., Jodoin, N., Doucet, E., Langlois, X., el Mestikawy, S., Hamon, M. & Descarries, L. (2000) Somatodendritic localization of 5-HT1A and preterminal axonal localization of 5-HT1B serotonin receptors in adult rat brain. *The Journal of comparative neurology*, **417**, 181-194.

Riahi, G., Morissette, M., Levesque, D., Rouillard, C., Samadi, P., Parent, M. & Di Paolo, T. (2012) Effect of chronic l-DOPA treatment on 5-HT(1A) receptors in parkinsonian monkey brain. *Neurochem Int*, **61**, 1160-1171.

Riahi, G., Morissette, M., Parent, M. & Di Paolo, T. (2011) Brain 5-HT(2A) receptors in MPTP monkeys and levodopa-induced dyskinesias. *Eur J Neurosci*, **33**, 1823-1831.

Riahi, G., Morissette, M., Samadi, P., Parent, M. & Di Paolo, T. (2013) Basal ganglia serotonin 1B receptors in parkinsonian monkeys with L-DOPA-induced dyskinesia. *Biochem Pharmacol*, **86**, 970-978.

Ribak, C.E., Vaughn, J.E. & Roberts, E. (1980) GABAergic nerve terminals decrease in the substantia nigra following hemitransections of the striatonigral and pallidonigral pathways. *Brain research*, **192**, 413-420.

Rice, M.E. & Cragg, S.J. (2004) Nicotine amplifies reward-related dopamine signals in striatum. *Nature neuroscience*, **7**, 583-584.

Rico, A.J., Dopeso-Reyes, I.G., Martinez-Pinilla, E., Sucunza, D., Pignataro, D., Roda, E., Marin-Ramos, D., Labandeira-Garcia, J.L., George, S.R., Franco, R. & Lanciego, J.L. (2016) Neurochemical evidence supporting dopamine D1-D2 receptor heteromers in the striatum of the long-tailed macaque: changes following dopaminergic manipulation. *Brain structure & function*.

Riederer, P. & Wuketich, S. (1976) Time course of nigrostriatal degeneration in parkinson's disease. A detailed study of influential factors in human brain amine analysis. *J Neural Transm*, **38**, 277-301.

Rinne, U., Bracco, F., Chouza, C., Dupont, E., Gershanik, O., Masso, J.M., Montastruc, J. & Marsden, C. (1998a) Early treatment of Parkinson's disease with cabergoline delays the onset of motor complications. *Drugs*, **55**, 23-30.

Rinne, U., Larsen, J., Siden, Å. & Worm-Petersen, J. (1998b) Entacapone enhances the response to levodopa in parkinsonian patients with motor fluctuations. *Neurology*, **51**, 1309-1314.

Rodrigo, J., Fernandez, P., Bentura, M.L., de Velasco, J.M., Serrano, J., Uttenthal, O. & Martinez-Murillo, R. (1998) Distribution of catecholaminergic afferent fibres in the rat globus pallidus and their relations with cholinergic neurons. *J Chem Neuroanat*, **15**, 1-20.

Roselli, F., Pisciotta, N.M., Pennelli, M., Aniello, M.S., Gigante, A., De Caro, M.F., Ferrannini, E., Tartaglione, B., Niccoli-Asabella, A. & Defazio, G. (2010) Midbrain SERT in degenerative parkinsonisms: a 123I-FP-CIT SPECT study. *Movement Disorders*, **25**, 1853-1859.

Royce, G.J. & Mourey, R.J. (1985) Efferent connections of the centromedian and parafascicular thalamic nuclei: an autoradiographic investigation in the cat. *Journal of comparative Neurology*, **235**, 277-300.

Rozas, G., Liste, I., Guerra, M.J. & Labandeira-Garcia, J.L. (1998) Sprouting of the serotonergic afferents into striatum after selective lesion of the dopaminergic system by MPTP in adult mice. *Neuroscience letters*, **245**, 151-154.

Russ, H., Mihatsch, W., Gerlach, M., Riederer, P. & Przuntek, H. (1991) Neurochemical and behavioural features induced by chronic low dose treatment with 1-methyl-4-phenyl-1,2,3,6-tetrahydropyridine (MPTP) in the common marmoset: implications for Parkinson's disease? *Neuroscience letters*, **123**, 115-118.

Rutz, S., Riegert, C., Rothmaier, A.K., Buhot, M.-C., Cassel, J.-C. & Jackisch, R. (2006) Presynaptic serotonergic modulation of 5-HT and acetylcholine release in the hippocampus and the cortex of 5-HT 1B-receptor knockout mice. *Brain research bulletin*, **70**, 81-93.

Rylander, D., Parent, M., O'Sullivan, S.S., Dovero, S., Lees, A.J., Bezard, E., Descarries, L. & Cenci, M.A. (2010) Maladaptive plasticity of serotonin axon terminals in levodopa-induced dyskinesia. *Annals of neurology*, **68**, 619-628.

Rymar, V.V., Sasseville, R., Luk, K.C. & Sadikot, A.F. (2004) Neurogenesis and stereological morphometry of calretinin-immunoreactive GABAergic interneurons of the neostriatum. *The Journal of comparative neurology*, **469**, 325-339.

Saavedra, J.M. (1977) Distribution of serotonin and synthesizing enzymes in discrete areas of the brain. *Fed Proc*, **36**, 2134-2141.

Sadikot, A., Parent, A. & Francois, C. (1992) Efferent connections of the centromedian and parafascicular thalamic nuclei in the squirrel monkey: a PHA-L study of subcortical projections. *Journal of Comparative Neurology*, **315**, 137-159.

Sanchez, M.G., Estrada-Camarena, E., Belanger, N., Morissette, M. & Di Paolo, T. (2011) Estradiol modulation of cortical, striatal and raphe nucleus 5-HT1A and 5-HT2A receptors of female hemiparkinsonian monkeys after long-term ovariectomy. *Neuropharmacology*, **60**, 642-652.

Saper, C., Swanson, L. & Cowan, W. (1979) An autoradiographic study of the efferent connections of the lateral hypothalamic area in the rat. *Journal of Comparative Neurology*, **183**, 689-706.

Sarhan, H., Grimaldi, B., Hen, R. & Fillion, G. (2000) 5-HT 1B receptors modulate release of [3 H] dopamine from rat striatal synaptosomes: further evidence using 5-HT moduline, polyclonal 5-HT 1B receptor antibodies and 5-HT 1B receptor knock-out mice. *Naunyn-Schmiedeberg's archives of pharmacology*, **361**, 12-18.

Sari, Y. (2004a) Serotonin1B receptors: from protein to physiological function and behavior. *Neurosci Biobehav Rev*, **28**, 565-582.

Sari, Y. (2004b) Serotonin 1B receptors: from protein to physiological function and behavior. *Neuroscience & Biobehavioral Reviews*, **28**, 565-582.

Sari, Y., Miquel, M.-C., Brisorgueil, M.-J., Ruiz, G., Doucet, E., Hamon, M. & Verge, D. (1999) Cellular and subcellular localization of 5-hydroxytryptamine 1B receptors in the rat central nervous system: immunocytochemical, autoradiographic and lesion studies. *Neuroscience*, **88**, 899-915.

Sarter, M. & Markowitsch, H.J. (1984) Collateral innervation of the medial and lateral prefrontal cortex by amygdaloid, thalamic, and brain-stem neurons. *The Journal of comparative neurology*, **224**, 445-460.

Sato, F., Lavallée, P., Lévesque, M. & Parent, A. (2000) Single-axon tracing study of neurons of the external segment of the globus pallidus in primate. *Journal of Comparative Neurology*, **417**, 17-31.

Saudou, F., Amara, D.A., Dierich, A., LeMeur, M., Ramboz, S., Segu, L., Buhot, M.-C. & Hen, R. (1994) Enhanced aggressive behavior in mice lacking 5-HT1B receptor. *Science*, **265**, 1875-1878.

Sawada, M., Nagatsu, T., Nagatsu, I., Ito, K., Iizuka, R., Kondo, T. & Narabayashi, H. (1985) Tryptophan hydroxylase activity in the brains of controls and parkinsonian patients. *J Neural Transm (Vienna)*, **62**, 107-115.

Scatton, B., Javoy-Agid, F., Rouquier, L., Dubois, B. & Agid, Y. (1983) Reduction of cortical dopamine, noradrenaline, serotonin and their metabolites in Parkinson's disease. *Brain research*, **275**, 321-328.

Schafer, M.K., Varoqui, H., Defamie, N., Weihe, E. & Erickson, J.D. (2002) Molecular cloning and functional identification of mouse vesicular glutamate transporter 3 and its expression in subsets of novel excitatory neurons. *J Biol Chem*, **277**, 50734-50748.

Schapira, A., Cooper, J., Dexter, D., Clark, J., Jenner, P. & Marsden, C. (1990) Mitochondrial complex I deficiency in Parkinson's disease. *J Neurochem*, **54**, 823-827.

Schapira, A.H.V., Chaudhuri, K.R. & Jenner, P. (2017) Non-motor features of Parkinson disease. *Nat Rev Neurosci*, **18**, 509.

Schell, G. & Strick, P. (1984) The origin of thalamic inputs to the arcuate premotor and supplementary motor areas. *Journal of Neuroscience*, **4**, 539-560.

Scherman, D., Desnos, C., Darchen, F., Pollak, P., Javoy-Agid, F. & Agid, Y. (1989) Striatal dopamine deficiency in Parkinson's disease: role of aging. *Ann Neurol*, **26**, 551-557.

Schmidt, H. & Rathjen, F.G. (2010) Signalling mechanisms regulating axonal branching in vivo. *Bioessays*, **32**, 977-985.

Schneider, J.S. (1990) Chronic exposure to low doses of MPTP. II. Neurochemical and pathological consequences in cognitively-impaired, motor asymptomatic monkeys. *Brain Res*, **534**, 25-36.

Schneider, J.S. & Dacko, S. (1991) Relative sparing of the dopaminergic innervation of the globus pallidus in monkeys made hemi-parkinsonian by intracarotid MPTP infusion. *Brain Res*, **556**, 292-296.

Schofield, S.P. & Everitt, B.J. (1981) The organization of indoleamine neurons in the brain of the rhesus monkey (Macaca mulatta). *The Journal of comparative neurology*, **197**, 369-383.

Schroder, K. (1975) Morphometrisch-statistische Strukturanalysen des Striatum, Pallidum und Nucleus Subthalamicus beim Menschen. *J Hirnforsch*, **16**, 333-350.

Schultz, W., Romo, R., Ljungberg, T., Mirenowicz, J., Hollerman, J.R. & Dickinson, A. (1995) Reward-related signals carried by dopamine neurons.

Schuurman, A., Van Den Akker, M., Ensinck, K., Metsemakers, J., Knottnerus, J., Leentjens, A. & Buntinx, F. (2002) Increased risk of Parkinson's disease after depression A retrospective cohort study. *Neurology*, **58**, 1501-1504.

Schwarz, G.A. & Fahn, S. (1970) Newer medical treatment in parkinsonism. *The Medical clinics of North America*, **54**, 773.

Seguela, P., Watkins, K.C. & Descarries, L. (1989) Ultrastructural relationships of serotonin axon terminals in the cerebral cortex of the adult rat. *The Journal of comparative neurology*, **289**, 129-142.

Sempere, A., Duarte, J., Cabezas, C., Claveria, L. & Coria, F. (1995) Aggravation of parkinsonian tremor by cisapride. *Clinical neuropharmacology*, **18**, 76-78.

Sesack, S.R., Deutch, A.Y., Roth, R.H. & Bunney, B.S. (1989a) Topographical organization of the efferent projections of the medial prefrontal cortex in the rat: an anterograde tract-tracing study with Phaseolus vulgaris leucoagglutinin. *The Journal of comparative neurology*, **290**, 213-242.

Sesack, S.R., Deutch, A.Y., Roth, R.H. & Bunney, B.S. (1989b) Topographical organization of the efferent projections of the medial prefrontal cortex in the rat: an anterograde tract-tracing study with Phaseolus vulgaris leucoagglutinin. *Journal of Comparative Neurology*, **290**, 213-242.

Sethy, V.H. & Van Woert, M.H. (1973) Antimuscarinic drugs--effect on brain acetylcholine and tremors in rats. *Biochem Pharmacol*, **22**, 2685-2691.

Shannak, K., Rajput, A., Rozdilsky, B., Kish, S., Gilbert, J. & Hornykiewicz, O. (1994) Noradrenaline, dopamine and serotonin levels and metabolism in the human hypothalamus: observations in Parkinson's disease and normal subjects. *Brain research*, **639**, 33-41.

Shannak, K.S. & Hornykiewicz, O. (1980) Brain monoamines in the rhesus monkey during long-term neuroleptic administration. *Adv Biochem Psychopharmacol*, **24**, 315-323.

Sharp, S.I., Ballard, C.G., Ziabreva, I., Piggott, M.A., Perry, R.H., Perry, E.K., Aarsland, D., Ehrt, U., Larsen, J.P. & Francis, P.T. (2008) Cortical serotonin 1A receptor levels are associated with depression in patients with dementia with Lewy bodies and Parkinson's disease dementia. *Dement Geriatr Cogn Disord*, **26**, 330-338.

Shen, K.Z. & Johnson, S.W. (2008) 5-HT inhibits synaptic transmission in rat subthalamic nucleus neurons in vitro. *Neuroscience*, **151**, 1029-1033.

Shen, M.Y., Perreault, M.L., Bambico, F.R., Jones-Tabah, J., Cheung, M., Fan, T., Nobrega, J.N. & George, S.R. (2015) Rapid anti-depressant and anxiolytic actions following dopamine D1-D2 receptor heteromer inactivation. *European neuropsychopharmacology : the journal of the European College of Neuropsychopharmacology*, **25**, 2437-2448.

Shen, W., Tian, X., Day, M., Ulrich, S., Tkatch, T., Nathanson, N.M. & Surmeier, D.J. (2007) Cholinergic modulation of Kir2 channels selectively elevates dendritic excitability in striatopallidal neurons. *Nat Neurosci*, **10**, 1458-1466.

Shepard, P.D. & Bunney, B.S. (1988) Effects of apamin on the discharge properties of putative dopamine-containing neurons in vitro. *Brain Res*, **463**, 380-384.

Sherer, T.B., Richardson, J.R., Testa, C.M., Seo, B.B., Panov, A.V., Yagi, T., Matsuno-Yagi, A., Miller, G.W. & Greenamyre, J.T. (2007) Mechanism of toxicity of pesticides acting at complex I: relevance to environmental etiologies of Parkinson's disease. *J Neurochem*, **100**, 1469-1479.

Shetreat, M.E., Lin, L., Wong, A.C. & Rayport, S. (1996) Visualization of D1 dopamine receptors on living nucleus accumbens neurons and their colocalization with D2 receptors. *Journal of neurochemistry*, **66**, 1475-1482.

Shink, E., Bevan, M., Bolam, J. & Smith, Y. (1996) The subthalamic nucleus and the external pallidum: two tightly interconnected structures that control the output of the basal ganglia in the monkey. *Neuroscience*, **73**, 335-357.

Shuen, J.A., Chen, M., Gloss, B. & Calakos, N. (2008) Drd1a-tdTomato BAC transgenic mice for simultaneous visualization of medium spiny neurons in the direct and indirect pathways of the basal ganglia. *The Journal of neuroscience : the official journal of the Society for Neuroscience*, **28**, 2681-2685.

Shumake, J., Edwards, E. & Gonzalez-Lima, F. (2003) Opposite metabolic changes in the habenula and ventral tegmental area of a genetic model of helpless behavior. *Brain research*, **963**, 274-281.

Shutoh, F., Ina, A., Yoshida, S., Konno, J. & Hisano, S. (2008) Two distinct subtypes of serotonergic fibers classified by co-expression with vesicular glutamate transporter 3 in rat forebrain. *Neuroscience letters*, **432**, 132-136.

Siegfried, J. & Lippitz, B. (1994) Bilateral chronic electrostimulation of ventroposterolateral pallidum: a new therapeutic approach for alleviating all parkinsonian symptoms. *Neurosurgery*, **35**, 1126-1129; discussion 1129-1130.

Sjoerdsma, A. & Palfreyman, M.G. (1990) History of serotonin and serotonin disorders. *Annals of the New York Academy of Sciences*, **600**, 1-8.

Smiley, J.F. & Goldman-Rakic, P.S. (1996) Serotonergic axons in monkey prefrontal cerebral cortex synapse predominantly on interneurons as demonstrated by serial section electron microscopy. *The Journal of comparative neurology*, **367**, 431-443.

Smith, A.D. & Bolam, J.P. (1990a) The neural network of the basal ganglia as revealed by the study of synaptic connections of identified neurones. *Trends in neurosciences*, **13**, 259-265.

Smith, I.D. & Grace, A.A. (1992) Role of the subthalamic nucleus in the regulation of nigral dopamine neuron activity. *Synapse*, **12**, 287-303.

Smith, R., Wu, K., Hart, T., Loane, C., Brooks, D.J., Björklund, A., Odin, P., Piccini, P. & Politis, M. (2015) The role of pallidal serotonergic function in Parkinson's disease dyskinesias: a positron emission tomography study. *Neurobiol Aging*, **36**, 1736-1742.

Smith, Y. & Bolam, J. (1990b) The output neurones and the dopaminergic neurones of the substantia nigra receive a GABA-Containing input from the globus pallidus in the rat. *Journal of Comparative Neurology*, **296**, 47-64.

Smith, Y. & Bolam, J. (1991) Convergence of synaptic inputs from the striatum and the globus pallidus onto identified nigrocollicular cells in the rat: a double anterograde labelling study. *Neuroscience*, **44**, 45-73.

Smith, Y. & Bolam, J.P. (1989) Neurons of the substantia nigra reticulata receive a dense GABA-containing input from the globus pallidus in the rat. *Brain research*, **493**, 160-167.

Smith, Y., Hazrati, L.N. & Parent, A. (1990) Efferent projections of the subthalamic nucleus in the squirrel monkey as studied by the PHA-L anterograde tracing method. *Journal of Comparative Neurology*, **294**, 306-323.

Smith, Y. & Kieval, J.Z. (2000) Anatomy of the dopamine system in the basal ganglia. *Trends in neurosciences*, **23**, S28-S33.

Smith, Y., Lavoie, B., Dumas, J. & Parent, A. (1989) Evidence for a distinct nigropallidal dopaminergic projection in the squirrel monkey. *Brain Res*, **482**, 381-386.

Smith, Y. & Villalba, R. (2008) Striatal and extrastriatal dopamine in the basal ganglia: an overview of its anatomical organization in normal and Parkinsonian brains. *Movement disorders : official journal of the Movement Disorder Society*, **23 Suppl 3**, S534-547.

Smith, Y., Wichmann, T., Factor, S.A. & DeLong, M.R. (2012) Parkinson's disease therapeutics: new developments and challenges since the introduction of levodopa. *Neuropsychopharmacology : official publication of the American College of Neuropsychopharmacology*, **37**, 213.

Smits, S.M., Noorlander, C.W., Kas, M.J., Ramakers, G.M. & Smidt, M.P. (2008) Alterations in serotonin signalling are involved in the hyperactivity of Pitx3-deficient mice. *Eur J Neurosci*, **27**, 388-395.

Snyder, A.M., Zigmond, M.J. & Lund, R.D. (1986) Sprouting of serotoninergic afferents into striatum after dopamine-depleting lesions in infant rats: A retrograde transport and immunocytochemical study. *Journal of Comparative Neurology*, **245**, 274-281.

Soghomonian, J.J., Descarries, L. & Watkins, K.C. (1989) Serotonin innervation in adult rat neostriatum. II. Ultrastructural features: a radioautographic and immunocytochemical study. *Brain Res*, **481**, 67-86.

Sommer, C. (2004) Serotonin in pain and analgesia: actions in the periphery. *Mol Neurobiol*, **30**, 117-125.

Somogyi, J., Baude, A., Omori, Y., Shimizu, H., El Mestikawy, S., Fukaya, M., Shigemoto, R., Watanabe, M. & Somogyi, P. (2004) GABAergic basket cells expressing cholecystokinin contain vesicular glutamate transporter type 3 (VGLUT3) in their synaptic terminals in hippocampus and isocortex of the rat. *Eur J Neurosci*, **19**, 552-569.

Sotelo, C., Cholley, B., El Mestikawy, S., Gozlan, H. & Hamon, M. (1990) Direct immunohistochemical evidence of the existence of 5-HT1A autoreceptors on serotoninergic neurons in the midbrain raphe nuclei. *European Journal of Neuroscience*, **2**, 1144-1154.

Spann, B.M. & Grofova, I. (1992) Cholinergic and non-cholinergic neurons in the rat pedunculopontine tegmental nucleus. *Anatomy and embryology*, **186**, 215-227.

Spencer, H.J. (1976) Antagonism of cortical excitation of striatal neurons by glutamic acid diethyl ester: evidence for glutamic acid as an excitatory transmitter in the rat striatum. *Brain research*, **102**, 91-101.

Spillantini, M.G., Schmidt, M.L., Lee, V.M.-Y., Trojanowski, J.Q., Jakes, R. & Goedert, M. (1997) α-Synuclein in Lewy bodies. *Nature*, **388**, 839-840.

Sprouse, J. & Aghajanian, G. (1988) Responses of hippocampal pyramidal cells to putative serotonin 5-HT 1A and 5-HT 1B agonists: a comparative study with dorsal raphe neurons. *Neuropharmacology*, **27**, 707-715.

Sprouse, J.S. & Aghajanian, G.K. (1987) Electrophysiological responses of serotoninergic dorsal raphe neurons to 5-HT1A and 5-HT1B agonists. *Synapse*, **1**, 3-9.

Stachowiak, M.K., Bruno, J.P., Snyder, A.M., Stricker, E.M. & Zigmond, M.J. (1984) Apparent sprouting of striatal serotonergic terminals after dopamine-depleting brain lesions in neonatal rats. *Brain research*, **291**, 164-167.

Stamp, J.A. & Semba, K. (1995) Extent of colocalization of serotonin and GABA in the neurons of the rat raphe nuclei. *Brain research*, **677**, 39-49.

Stanford, I.M., Kantaria, M.A., Chahal, H.S., Loucif, K.C. & Wilson, C.L. (2005) 5-Hydroxytryptamine induced excitation and inhibition in the subthalamic nucleus: action at 5-HT(2C), 5-HT(4) and 5-HT(1A) receptors. *Neuropharmacology*, **49**, 1228-1234.

Stansley, B.J. & Yamamoto, B.K. (2014) Chronic L-dopa decreases serotonin neurons in a subregion of the dorsal raphe nucleus. *Journal of Pharmacology and Experimental Therapeutics*, **351**, 440-447.

Steinbusch, H.W. (1981) Distribution of serotonin-immunoreactivity in the central nervous system of the rat-cell bodies and terminals. *Neuroscience*, **6**, 557-618.

Steiner, H. & Gerfen, C.R. (1998) Role of dynorphin and enkephalin in the regulation of striatal output pathways and behavior. *Experimental brain research*, **123**, 60-76.

Steininger, T.L., Gong, H., Mcginty, D. & Szymusiak, R. (2001) Subregional organization of preoptic area/anterior hypothalamic projections to arousal-related monoaminergic cell groups. *Journal of Comparative Neurology*, **429**, 638-653.

Stephens, B., Mueller, A.J., Shering, A.F., Hood, S.H., Taggart, P., Arbuthnott, G.W., Bell, J.E., Kilford, L., Kingsbury, A.E., Daniel, S.E. & Ingham, C.A. (2005) Evidence of a breakdown of corticostriatal connections in Parkinson's disease. *Neuroscience*, **132**, 741-754.

Steriade, M. (2004) Slow-wave sleep: serotonin, neuronal plasticity, and seizures. *Arch Ital Biol*, **142**, 359-367.

Stowe, R., Ives, N., Clarke, C., Van Hilten, J., Ferreira, J., Hawker, R., Shah, L., Wheatley, K. & Gray, R. (2008) Dopamine agonist therapy in early Parkinson's disease. *Cochrane Database of Systematic Reviews*.

Stratford, T.R. & Kelley, A.E. (1997) GABA in the nucleus accumbens shell participates in the central regulation of feeding behavior. *The Journal of neuroscience : the official journal of the Society for Neuroscience*, **17**, 4434-4440.

Strecker, K., Wegner, F., Hesse, S., Becker, G.A., Patt, M., Meyer, P.M., Lobsien, D., Schwarz, J. & Sabri, O. (2011) Preserved serotonin transporter binding in de novo Parkinson's disease: negative correlation with the dopamine transporter. *Journal of neurology*, **258**, 19-26.

Stuart, A.M., Mitchell, I.J., Slater, P., Unwin, H.L. & Crossman, A.R. (1986) A semi-quantitative atlas of 5-hydroxytryptamine-1 receptors in the primate brain. *Neuroscience*, **18**, 619-639.

Suarez, L.M., Solis, O., Carames, J.M., Taravini, I.R., Solis, J.M., Murer, M.G. & Moratalla, R. (2014) L-DOPA treatment selectively restores spine density in dopamine receptor D2-expressing projection neurons in dyskinetic mice. *Biological psychiatry*, **75**, 711-722.

Sugimoto, T. & Hattori, T. (1983) Confirmation of thalamosubthalamic projections by electron microscopic autoradiography. *Brain research*, **267**, 335-339.

Sugimoto, T., Hattori, T., Mizuno, N., Itoh, K. & Sato, M. (1983) Direct projections from the centre median-parafascicular complex to the subthalamic nucleus in the cat and rat. *Journal of Comparative Neurology*, **214**, 209-216.

Surmeier, D.J., Ding, J., Day, M., Wang, Z. & Shen, W. (2007) D1 and D2 dopamine-receptor modulation of striatal glutamatergic signaling in striatal medium spiny neurons. *Trends in neurosciences*, **30**, 228-235.

Surmeier, D.J., Obeso, J.A. & Halliday, G.M. (2017) Parkinson's disease is not simply a prion disorder. *Journal of Neuroscience*, **37**, 9799-9807.

Surmeier, D.J., Song, W.J. & Yan, Z. (1996) Coordinated expression of dopamine receptors in neostriatal medium spiny neurons. *The Journal of neuroscience : the official journal of the Society for Neuroscience*, **16**, 6579-6591.

Surmeier, D.J., Yan, Z. & Song, W.J. (1998) Coordinated expression of dopamine receptors in neostriatal medium spiny neurons. *Advances in pharmacology*, **42**, 1020-1023.

Takagishi, M. & Chiba, T. (1991) Efferent projections of the infralimbic (area 25) region of the medial prefrontal cortex in the rat: an anterograde tracer PHA-L study. *Brain research*, **566**, 26-39.

Takahashi, K., Wang, Q.-P., Guan, J.-L., Kayama, Y., Shioda, S. & Koyama, Y. (2005) State-dependent effects of orexins on the serotonergic dorsal raphe neurons in the rat. *Regulatory peptides*, **126**, 43-47.

Takamori, S., Malherbe, P., Broger, C. & Jahn, R. (2002) Molecular cloning and functional characterization of human vesicular glutamate transporter 3. *EMBO Rep*, **3**, 798-803.

Takeuchi, Y. & Sano, Y. (1983) Immunohistochemical demonstration of serotonin nerve fibers in the neocortex of the monkey (Macaca fuscata). *Anat Embryol (Berl)*, **166**, 155-168.

Tanaka, E. & North, R. (1993) Actions of 5-hydroxytryptamine on neurons of the rat cingulate cortex. *J Neurophysiol*, **69**, 1749-1757.

Tanaka, H., Kannari, K., Maeda, T., Tomiyama, M., Suda, T. & Matsunaga, M. (1999a) Role of serotonergic neurons in L-DOPA-derived extracellular dopamine in the striatum of 6-OHDA-lesioned rats. *Neuroreport*, **10**, 631-634.

Tanaka, H., Kannari, K., Maeda, T., Tomiyama, M., Suda, T. & Matsunaga, M. (1999b) Role of serotonergic neurons in L-DOPA-derived extracellular dopamine in the striatum of 6-OHDA-lesioned rats. *Neuroreport*, **10**, 631-634.

Tao, R., Ma, Z., McKenna, J., Thakkar, M., Winston, S., Strecker, R. & McCarley, R. (2006) Differential effect of orexins (hypocretins) on serotonin release in the dorsal and median raphe nuclei of freely behaving rats. *Neuroscience*, **141**, 1101-1105.

Tassone, A., Madeo, G., Schirinzi, T., Vita, D., Puglisi, F., Ponterio, G., Borsini, F., Pisani, A. & Bonsi, P. (2011) Activation of 5-HT6 receptors inhibits corticostriatal glutamatergic transmission. *Neuropharmacology*, **61**, 632-637.

Tepper, J.M. & Bolam, J.P. (2004) Functional diversity and specificity of neostriatal interneurons. *Current opinion in neurobiology*, **14**, 685-692.

Tepper, J.M., Sawyer, S.F. & Groves, P.M. (1987) Electrophysiologically identified nigral dopaminergic neurons intracellularly labeled with HRP: light-microscopic analysis. *Journal of Neuroscience*, **7**, 2794-2806.

Tepper, J.M., Tecuapetla, F., Koós, T. & Ibáñez-Sandoval, O. (2010) Heterogeneity and diversity of striatal GABAergic interneurons. *Front Neuroanat*, **4**.

Terry Jr, A., Buccafusco, J.J., Jackson, W.J., Prendergast, M.A., Fontana, D.J., Wong, E.H., Bonhaus, D.W., Weller, P. & Eglen, R.M. (1998) Enhanced delayed matching performance in younger and older macaques administered the 5-HT4 receptor agonist, RS 17017. *Psychopharmacology*, **135**, 407-415.

Thibault, D., Loustalot, F., Fortin, G.M., Bourque, M.J. & Trudeau, L.E. (2013) Evaluation of D1 and D2 dopamine receptor segregation in the developing striatum using BAC transgenic mice. *PloS one*, **8**, e67219.

Thompson, R., Canteras, N. & Swanson, L. (1996) Organization of projections from the dorsomedial nucleus of the hypothalamus: A PHA-L study in the rat. *Journal of comparative Neurology*, **376**, 143-173.

Threlfell, S., Clements, M.A., Khodai, T., Pienaar, I.S., Exley, R., Wess, J. & Cragg, S.J. (2010) Striatal muscarinic receptors promote activity dependence of dopamine transmission via distinct receptor subtypes on cholinergic interneurons in ventral versus dorsal striatum. *Journal of Neuroscience*, **30**, 3398-3408.

Tischler, R.C. & Morin, L. (2003) Reciprocal serotonergic connections between the hamster median and dorsal raphe nuclei. *Brain research*, **981**, 126-132.

Tohgi, H., Abe, T., Takahashi, S., Takahashi, J. & Hamato, H. (1993) Concentrations of serotonin and its related substances in the cerebrospinal fluid of parkinsonian patients and their relations to the severity of symptoms. *Neurosci Lett*, **150**, 71-74.

Tong, Z.Y., Overton, P. & Clark, D. (1996) Stimulation of the prefrontal cortex in the rat induces patterns of activity in midbrain dopaminergic neurons which resemble natural burst events. *Synapse*, **22**, 195-208.

Tork, I. (1990) Anatomy of the serotonergic system. *Ann N Y Acad Sci*, **600**, 9-34; discussion 34-35.

Tork, I., Halliday, G.M. & Cotton, R.G. (1992) Application of antiphenylalanine hydroxylase antibodies to the study of the serotonergic system in the human brain. *J Chem Neuroanat*, **5**, 311-313.

Toth, M. (2003) 5-HT 1A receptor knockout mouse as a genetic model of anxiety. *European journal of pharmacology*, **463**, 177-184.

Towle, A., Criswell, H., Maynard, E., Lauder, J., Joh, T., Mueller, R. & Breese, G. (1989) Serotonergic innervation of the rat caudate following a neonatal 6-hydroxydopamine lesion: an anatomical, biochemical and pharmacological study. *Pharmacology Biochemistry and Behavior*, **34**, 367-374.

Toy, W.A., Petzinger, G.M., Leyshon, B.J., Akopian, G.K., Walsh, J.P., Hoffman, M.V., Vuckovic, M.G. & Jakowec, M.W. (2014) Treadmill exercise reverses dendritic spine loss in direct and indirect striatal medium spiny neurons in the 1-methyl-4-phenyl-1,2,3,6-tetrahydropyridine (MPTP) mouse model of Parkinson's disease. *Neurobiology of disease*, **63**, 201-209.

Tretiakoff, C. (1919) Contribution à l'étude de l'anatomie du locus niger de Soemmering avec quelques déductions relatives à la pathogenie des troubles du tonus musculaire et de la maladie de Parkinson. *Paris: Thèse de*.

Tronci, E., Napolitano, F., Muñoz, A., Fidalgo, C., Rossi, F., Björklund, A., Usiello, A. & Carta, M. (2017) BDNF over-expression induces striatal serotonin fiber sprouting and increases the susceptibility to l-DOPA-induced dyskinesia in 6-OHDA-lesioned rats. *Exp Neurol*, **297**, 73-81.

Trulson, M.E., Cannon, M.S. & Raese, J.D. (1985) Identification of dopamine-containing cell bodies in the dorsal and median raphe nuclei of the rat brain using tyrosine hydroxylase immunochemistry. *Brain research bulletin*, **15**, 229-234.

Twarog, B.M. & Page, I.H. (1953) Serotonin content of some mammalian tissues and urine and a method for its determination. *American Journal of Physiology--Legacy Content*, **175**, 157-161.

Uhl, G.R., Hedreen, J.C. & Price, D.L. (1985) Parkinson's disease Loss of ineurons from the ventral tegmental area contralateral to therapeutic surgical lesions. *Neurology*, **35**, 1215-1215.

Ullmer, C., Engels, P., Abdel'Al, S. & Lübbert, H. (1996) Distribution of 5-HT 4 receptor mRNA in the rat brain. *Naunyn-Schmiedeberg's archives of pharmacology*, **354**, 210-212.

Umbriaco, D., Watkins, K.C., Descarries, L., Cozzari, C. & Hartman, B.K. (1994) Ultrastructural and morphometric features of the acetylcholine innervation in adult rat parietal cortex: an electron microscopic study in serial sections. *The Journal of comparative neurology*, **348**, 351-373.

Ursin, R. (2002) Serotonin and sleep. *Sleep Med Rev*, **6**, 55-67.

Van Bockstaele, E.J., Chan, J. & Pickel, V.M. (1996) Pre- and postsynaptic sites for serotonin modulation of GABA-containing neurons in the shell region of the rat nucleus accumbens. *The Journal of comparative neurology*, **371**, 116-128.

Van Bockstaele, E.J. & Pickel, V.M. (1993) Ultrastructure of serotonin-immunoreactive terminals in the core and shell of the rat nucleus accumbens: cellular substrates for interactions with catecholamine afferents. *The Journal of comparative neurology*, **334**, 603-617.

Van Der Kooy, D. & Hattori, T. (1980) Dorsal raphe cells with collateral projections to the caudate-putamen and substantia nigra: a fluorescent retrograde double labeling study in the rat. *Brain Res*, **186**, 1-7.

Van Der Kooy, D., Hattori, T., Shannak, K. & Hornykiewicz, O. (1981) The pallido-subthalamic projection in rat: anatomical and biochemical studies. *Brain research*, **204**, 253-268.

Van der Maelen, C.P., Matheson, G.K., Wilderman, R.C. & Patterson, L.A. (1986) Inhibition of serotonergic dorsal raphe neurons by systemic and iontophoretic administration of buspirone, a non-benzodiazepine anxiolytic drug. *European journal of pharmacology*, **129**, 123-130.

Van Vliet, S.A., Vanwersch, R.A., Jongsma, M.J., Van der Gugten, J., Olivier, B. & Philippens, I.H. (2006) Neuroprotective effects of modafinil in a marmoset Parkinson model: behavioral and neurochemical aspects. *Behavioural pharmacology*, **17**, 453-462.

Van Woert, M.H. & Ambani, L.M. (1974) Biochemistry of neuromelanin. *Advances in neurology*, **5**, 215.

Varga, V., Losonczy, A., Zemelman, B.V., Borhegyi, Z., Nyiri, G., Domonkos, A., Hangya, B., Holderith, N., Magee, J.C. & Freund, T.F. (2009) Fast synaptic subcortical control of hippocampal circuits. *Science*, **326**, 449-453.

Varnäs, K., Hall, H., Bonaventure, P. & Sedvall, G. (2001) Autoradiographic mapping of 5-HT 1B and 5-HT 1D receptors in the post mortem human brain using [3 H] GR 125743. *Brain research*, **915**, 47-57.

Varnäs, K., Halldin, C. & Hall, H. (2004) Autoradiographic distribution of serotonin transporters and receptor subtypes in human brain. *Human brain mapping*, **22**, 246-260.

Varnäs, K., Nyberg, S., Halldin, C., Varrone, A., Takano, A., Karlsson, P., Andersson, J., McCarthy, D., Smith, M. & Pierson, M.E. (2011) Quantitative analysis of [11C] AZ10419369 binding to 5-HT1B receptors in human brain. *Journal of Cerebral Blood Flow & Metabolism*, **31**, 113-123.

Vergé, D., Daval, G., Marcinkiewicz, M., Patey, A., El Mestikawy, S., Gozlan, H. & Hamon, M. (1986) Quantitative autoradiography of multiple 5-HT1 receptor subtypes in the brain of control or 5, 7-dihydroxytryptamine-treated rats. *Journal of Neuroscience*, **6**, 3474-3482.

Verge, D., Daval, G., Patey, A., Gozlan, H., El Mestikawy, S. & Hamon, M. (1985) Presynaptic 5-HT autoreceptors on serotonergic cell bodies and/or dendrites but not terminals are of the 5-HT1A subtype. *European journal of pharmacology*, **113**, 463-464.

Vertes, R.P. (1991a) A PHA-L analysis of ascending projections of the dorsal raphe nucleus in the rat. *The Journal of comparative neurology*, **313**, 643-668.

Vertes, R.P. (1991b) A PHA-L analysis of ascending projections of the dorsal raphe nucleus in the rat. *Journal of Comparative Neurology*, **313**, 643-668.

Vertes, R.P. (2004) Differential projections of the infralimbic and prelimbic cortex in the rat. *Synapse*, **51**, 32-58.

Vertes, R.P., Fortin, W.J. & Crane, A.M. (1999a) Projections of the median raphe nucleus in the rat. *Journal of Comparative Neurology*, **407**, 555-582.

Vertes, R.P., Fortin, W.J. & Crane, A.M. (1999b) Projections of the median raphe nucleus in the rat. *The Journal of comparative neurology*, **407**, 555-582.

Vertes, R.P. & Kocsis, B. (1994) Projections of the dorsal raphe nucleus to the brainstem: PHA-L analysis in the rat. *Journal of Comparative Neurology*, **340**, 11-26.

Vilaró, M.T., Cortés, R., Gerald, C., Branchek, T.A., Palacios, J.M. & Mengod, G. (1996) Localization of 5-HT 4 receptor mRNA in rat brain by in situ hybridization histochemistry. *Molecular Brain Research*, **43**, 356-360.

Villalba, R.M., Lee, H., Raju, D. & Smith, Y. (2009a) Striatal dopaminergic denervation and spine loss in MPTP-treated monkeys *The Basal Ganglia IX*. Springer, pp. 361-375.

Villalba, R.M., Lee, H. & Smith, Y. (2009b) Dopaminergic denervation and spine loss in the striatum of MPTP-treated monkeys. *Experimental neurology*, **215**, 220-227.

Vitek, J.L. (2008) Deep brain stimulation: how does it work? *Cleveland Clinic journal of medicine*, **75**, S59.

Vogt, C. (1911) Quelques considérations générales à propos du syndrome du corps strié. *Journal für Psychologie und Neurologie*, **18**, 479-488.

Vogt, C. & Vogt, O. (1919) *Zur Kenntnis der pathologischen Veränderungen des Striatum und des Pallidum und zur Pathophysiologie der dabei auftretenden Krankheitserscheinungen*.

Vogt, C. & Vogt, O. (1920) *Zur Lehre der Erkrankungen des striären systems*. JA Barth.

Waeber, C., Hoyer, D. & Palacios, J. (1989) 5. HT 1 receptors in the vertebrate brain. *Naunyn-Schmiedeberg's archives of pharmacology*, **340**, 486-494.

Wakabayashi, K., Takahashi, H., Ohama, E. & Ikuta, F. (1990) Parkinson's disease: an immunohistochemical study of Lewy body-containing neurons in the enteric nervous system. *Acta neuropathologica*, **79**, 581-583.

Wallman, M.J., Gagnon, D. & Parent, M. (2011) Serotonin innervation of human basal ganglia. *Eur J Neurosci*, **33**, 1519-1532.

Walsh, F.X., Bird, E.D. & Stevens, T.J. (1982) Monoamine transmitters and their metabolites in the basal ganglia of Huntington's disease and control postmortem brain. *Adv Neurol*, **35**, 165-169.

Wang, Q.-P., Koyama, Y., Guan, J.-L., Takahashi, K., Kayama, Y. & Shioda, S. (2005) The orexinergic synaptic innervation of serotonin-and orexin 1-receptor-containing neurons in the dorsal raphe nucleus. *Regulatory peptides*, **126**, 35-42.

Wang, S., Zhang, Q., Liu, J., Wu, Z., Wang, T., Gui, Z., Chen, L. & Wang, Y. (2009) Unilateral lesion of the nigrostriatal pathway induces an increase of neuronal firing of the midbrain raphe nuclei 5-HT neurons and a decrease of their response to 5-HT 1A receptor stimulation in the rat. *Neuroscience*, **159**, 850-861.

Waselus, M., Valentino, R.J. & Van Bockstaele, E.J. (2011) Collateralized dorsal raphe nucleus projections: a mechanism for the integration of diverse functions during stress. *J Chem Neuroanat*, **41**, 266-280.

Weiner, D.M., Levey, A.I., Sunahara, R.K., Niznik, H.B., O'Dowd, B.F., Seeman, P. & Brann, M.R. (1991) D1 and D2 dopamine receptor mRNA in rat brain. *Proceedings of the National Academy of Sciences of the United States of America*, **88**, 1859-1863.

Weintraub, D., Morales, K.H., Moberg, P.J., Bilker, W.B., Balderston, C., Duda, J.E., Katz, I.R. & Stern, M.B. (2005) Antidepressant studies in Parkinson's disease: A review and meta-analysis. *Movement Disorders*, **20**, 1161-1169.

Weisstaub, N.V., Zhou, M., Lira, A., Lambe, E., González-Maeso, J., Hornung, J.-P., Sibille, E., Underwood, M., Itohara, S. & Dauer, W.T. (2006) Cortical 5-HT2A receptor signaling modulates anxiety-like behaviors in mice. *Science*, **313**, 536-540.

West, M.J., Slomianka, L. & Gundersen, H.J. (1991) Unbiased stereological estimation of the total number of neurons in thesubdivisions of the rat hippocampus using the optical fractionator. *Anat Rec*, **231**, 482-497.

Whittier, J. (1947) Ballism and the subthalamic nucleus (nucleus hypothalamicus; corpus Luysi): review of the literature and study of thirty cases. *Archives of Neurology & Psychiatry*, **58**, 672-692.

Whone, A.L., Moore, R.Y., Piccini, P.P. & Brooks, D.J. (2003a) Plasticity of the nigropallidal pathway in Parkinson's disease. *Ann Neurol*, **53**, 206-213.

Whone, A.L., Moore, R.Y., Piccini, P.P. & Brooks, D.J. (2003b) Plasticity of the nigropallidal pathway in Parkinson's disease. *Ann Neurol*, **53**, 206-213.

Whone, A.L., Watts, R.L., Stoessl, A.J., Davis, M., Reske, S., Nahmias, C., Lang, A.E., Rascol, O., Ribeiro, M.J. & Remy, P. (2003c) Slower progression of Parkinson's disease with ropinirole versus levodopa: The REAL-PET study. *Ann Neurol*, **54**, 93-101.

Wichmann, T., Bergman, H., Starr, P.A., Subramanian, T., Watts, R.L. & DeLong, M.R. (1999) Comparison of MPTP-induced changes in spontaneous neuronal discharge in the internal pallidal segment and in the substantia nigra pars reticulata in primates. *Exp Brain Res*, **125**, 397-409.

Wichmann, T. & DeLong, M.R. (1998) Models of basal ganglia function and pathophysiology of movement disorders. *Neurosurgery clinics of North America*, **9**, 223-236.

Wile, D.J., Agarwal, P.A., Schulzer, M., Mak, E., Dinelle, K., Shahinfard, E., Vafai, N., Hasegawa, K., Zhang, J. & McKenzie, J. (2017) Serotonin and dopamine transporter PET changes in the premotor phase of LRRK2 parkinsonism: cross-sectional studies. *The Lancet Neurology*.

Wilson, J., Levey, A., Rajput, A., Ang, L., Guttman, M., Shannak, K., Niznik, H., Hornykiewicz, O., Pifl, C. & Kish, S. (1996) Differential changes in neurochemical markers of striatal dopamine nerve terminals in idiopathic Parkinson's disease. *Neurology*, **47**, 718-726.

Wilson, M., Ricaurte, G. & Molliver, M. (1989) Distinct morphologic classes of serotonergic axons in primates exhibit differential vulnerability to the psychotropic drug 3, 4-methylenedioxymethamphetamine. *Neuroscience*, **28**, 121-137.

Wilson, S.K. (1912) Progressive lenticular degeneration: a familial nervous disease associated with cirrhosis of the liver. *The Lancet*, **179**, 1115-1119.

Wilson, S.K. (1914) An experimental research into the anatomy and physiology of the corpus striatum. *Brain : a journal of neurology*, **36**, 427-492.

Won, L., Ding, Y., Singh, P. & Kang, U.J. (2014) Striatal Cholinergic Cell Ablation Attenuates L-DOPA Induced Dyskinesia in Parkinsonian Mice. *The Journal of neuroscience : the official journal of the Society for Neuroscience*, **34**, 3090-3094.

Wong-Riley, M. (1979) Changes in the visual system of monocularly sutured or enucleated cats demonstrable with cytochrome oxidase histochemistry. *Brain Res*, **171**, 11-28.

Wong, D.F., Lever, J.R., Hartig, P.R., Dannals, R.F., Villemagne, V., Hoffman, B.J., Wilson, A.A., Ravert, H.T., Links, J.M. & Scheffel, U. (1987) Localization of serotonin 5-HT2 receptors in living human brain by positron emission tomography using N1-([11C]-methyl)-2-BR-LSD. *Synapse*, **1**, 393-398.

Wong, E.H., Reynolds, G.P., Bonhaus, D.W., Hsu, S. & Eglen, R.M. (1995) Characterization of [3 H] GR 113808 binding to 5-HT 4 receptors in brain tissues from patients with neurodegenerative disorders. *Behav Brain Res*, **73**, 249-252.

Woolf, N.J. & Butcher, L.L. (1986) Cholinergic systems in the rat brain: III. Projections from the pontomesencephalic tegmentum to the thalamus, tectum, basal ganglia, and basal forebrain. *Brain research bulletin*, **16**, 603-637.

Wouterlood, F.G., Hartig, W., Groenewegen, H.J. & Voorn, P. (2012) Density gradients of vesicular glutamate- and GABA transporter-immunoreactive boutons in calbindinand mu-opioid receptor-defined compartments in the rat striatum. *The Journal of comparative neurology*, **520**, 2123-2142.

Wu, Y., Richard, S. & Parent, A. (2000) The organization of the striatal output system: a single-cell juxtacellular labeling study in the rat. *Neuroscience research*, **38**, 49-62.

Xiang, Z., Wang, L. & Kitai, S.T. (2005) Modulation of spontaneous firing in rat subthalamic neurons by 5-HT receptor subtypes. *J Neurophysiol*, **93**, 1145-1157.

Yahr, M.D. (1972) The treatment of parkinsonism. Current concepts. *Med Clin North Am*, **56**, 1377-1392.

Yahr, M.D., Duvoisin, R.C., Schear, M.J., Barrett, R.E. & Hoehn, M.M. (1969) Treatment of parkinsonism with levodopa. *Archives of Neurology*, **21**, 343-354.

Yamada, T., McGeer, P.L., Baimbridge, K.G. & McGeer, E.G. (1990) Relative sparing in Parkinson's disease of substantia nigra dopamine neurons containing calbindin-D28K. *Brain Res*, **526**, 303-307.

Yamazoe, I., Takeuchi, Y., Matsushita, H., Kawano, H. & Sawada, T. (2001) Serotonergic heterotypic sprouting in the unilaterally dopamine-depleted mouse neostriatum. *Dev Neurosci*, **23**, 78-83.

Yang, L.-M., Hu, B., Xia, Y.-H., Zhang, B.-L. & Zhao, H. (2008) Lateral habenula lesions improve the behavioral response in depressed rats via increasing the serotonin level in dorsal raphe nucleus. *Behavioural brain research*, **188**, 84-90.

Yelnik, J., Percheron, G. & François, C. (1984) A Golgi analysis of the primate globus pallidus. II. Quantitative morphology and spatial orientation of dendritic arborizations. *Journal of Comparative Neurology*, **227**, 200-213.

Young, S.N. (2013) Acute tryptophan depletion in humans: a review of theoretical, practical and ethical aspects. *Journal of psychiatry & neuroscience: JPN*, **38**, 294.

Yung, K.K., Bolam, J.P., Smith, A.D., Hersch, S.M., Ciliax, B.J. & Levey, A.I. (1995) Immunocytochemical localization of D1 and D2 dopamine receptors in the basal ganglia of the rat: light and electron microscopy. *Neuroscience*, **65**, 709-730.

Zaja-Milatovic, S., Milatovic, D., Schantz, A.M., Zhang, J., Montine, K.S., Samii, A., Deutch, A.Y. & Montine, T.J. (2005) Dendritic degeneration in neostriatal medium spiny neurons in Parkinson disease. *Neurology*, **64**, 545-547.

Zeng, B.Y., Iravani, M.M., Jackson, M.J., Rose, S., Parent, A. & Jenner, P. (2010) Morphological changes in serotoninergic neurites in the striatum and globus pallidus in levodopa primed MPTP treated common marmosets with dyskinesia. *Neurobiology of disease*, **40**, 599-607.

Zhang, H. & Sulzer, D. (2004) Frequency-dependent modulation of dopamine release by nicotine. *Nature neuroscience*, **7**, 581-582.

Zhang, Q., Gao, R., Liu, J., Liu, Y. & Wang, S. (2007) Changes in the firing activity of serotonergic neurons in the dorsal raphe nucleus in a rat model of Parkinson's disease. *ACTA PHYSIOLOGICA SINICA-CHINESE EDITION-*, **59**, 183.

Zhang, X., Andren, P.E., Greengard, P. & Svenningsson, P. (2008) Evidence for a role of the 5-HT1B receptor and its adaptor protein, p11, in L-DOPA treatment of an animal model of Parkinsonism. *Proceedings of the National Academy of Sciences of the United States of America*, **105**, 2163-2168.

Zhang, Y., Meredith, G.E., Mendoza-Elias, N., Rademacher, D.J., Tseng, K.Y. & Steece-Collier, K. (2013) Aberrant restoration of spines and their synapses in L-DOPA-induced dyskinesia: involvement of corticostriatal but not thalamostriatal synapses. *The Journal of neuroscience : the official journal of the Society for Neuroscience*, **33**, 11655-11667.

Zhao, H., Zhang, B.-L., Yang, S.-J. & Rusak, B. (2015) The role of lateral habenula–dorsal raphe nucleus circuits in higher brain functions and psychiatric illness. *Behavioural brain research*, **277**, 89-98.

Zhou, F.-M., Liang, Y. & Dani, J.A. (2001) Endogenous nicotinic cholinergic activity regulates dopamine release in the striatum. *Nature neuroscience*, **4**, 1224-1229.

Zhou, F.C., Bledsoe, S. & Murphy, J. (1991) Serotonergic sprouting is induced by dopamine-lesion in substantia nigra of adult rat brain. *Brain Res*, **556**, 108-116.

Zhou, F.C., Xu, Y., Bledsoe, S., Lin, R. & Kelley, M.R. (1996) Serotonin transporter antibodies: production, characterization, and localization in the brain. *Brain Res Mol Brain Res*, **43**, 267-278.